A PROTEOMIC INVESTIGATION OF THE IMMUNE RESPONSE OF THE SOUTH AFRICAN ABALONE, *HALIOTIS MIDAE*

By Caroline G.G. Beltran

Thesis submitted in fulfilment of the requirements for the degree of

Doctor of Philosophy

Department of Molecular and Cell Biology
Faculty of Science
University of Cape Town

June 2015

DECLARATION

I hereby declare that this thesis, submitted in fulfilment of the requirements for the degree of Doctor of Philosophy in the Department of Molecular and Cell Biology at the University of Cape Town, is the result of my own investigations, apart from the referenced work of others.

_____

Caroline Beltran
University of Cape Town
June 2015

ACKNOWLEDGEMENTS

I wish to acknowledge the financial assistance provided by the University of Cape Town, Harry Crossley Foundation and the National Research Foundation, without which this thesis would not have been possible.

I would like to extend my deepest gratitude to my supervisor Associate Professor Vernon Coyne, for his constant support, patience and guidance throughout this project. Who always took the time to discuss ideas and whose humour kept me sane towards the end. Thank you for reading my thesis and for your invaluable input in completing this research. I have learnt so much from this process and I thank you for the opportunity to grow as a scientist.

I would also like to thank everyone in the Molecular and Cell Biology Department, particularly my lab mates in lab 201. Thank you especially to Bridget, Karis, Amy and Taryn for the laughs, motivation, advice and general support throughout this endeavour. It's been a tough journey but your friendships kept me going. A special thanks to my friend, Dr Dave Choveaux, whose advice and encouragement during the writing of my thesis helped me immensely. I would also like to extend my thanks to Dr Zac McDonald for his assistance during mass spectrometry and Assoc. Prof Dirk Lang for his valuable expertise in confocal imaging.

Finally, to my family and friends, thank you for the love and encouragement throughout the years. A special thank you to my parents Danielle and Alain, who have supported and believed in me from the beginning and provided me with the opportunities to pursue my goals. To my sisters Marine and Anne, thank you for being there for me even when we were far apart and to Michael, for your support and patience over the years. I love you all very much and I could not have done this without you.

TABLE OF CONTENTS

A PROTEOMIC INVESTIGATION OF THE IMMUNE RESPONSE OF THE SOUTH AFRICAN ABALONE, *HALIOTIS MIDAE*

By
Caroline G. G. Beltran

June 2015

Department of Molecular and Cell Biology, University of Cape Town, Private Bag, Rondebosch, South Africa, 7701, South Africa

ABSTRACT

Haliotis midae is a commercially important abalone in South Africa, previously harvested from a stable, quota-managed fishery. However, the combined effects of overharvesting, increased illegal catches and negative environmental factors led to a collapse in wild populations in the mid-90s. Consequently, land-based aquaculture of *H. midae* has grown significantly in South Africa, to satisfy the global demand for abalone and alleviate pressure on wild stocks. Unfortunately, disease outbreaks have had a severe impact on the abalone aquaculture industry internationally and remain one of the single biggest factors contributing to economic loss. Understanding the effects of pathogen infection of abalone is therefore crucial to mitigating and controlling infection outbreaks on farms. Despite this, the molecular mechanisms underlying the immune response of *H. midae* remain obscure. High-throughput proteomics, a powerful tool to analyse global protein expression changes, can provide an integrated view of the immune system. Thus, this study aimed to elucidate the haemocyte proteome of *H. midae* and gain insight into regulatory molecular pathways underlying innate immunity.

In this study, a comparative shotgun proteomics approach using isobaric tagging for relative and absolute quantification (iTRAQ) coupled with LC-MS/MS was employed to investigate *H. midae* proteome changes in response to *Vibrio anguillarum* challenge. A preliminary iTRAQ challenge trial was conducted which identified a putative early (1 and 2 hours post-injection) and late (48 hours post-injection) proteome response to bacterial-challenge. Using these time points, four independent challenge trials were conducted and analysed by iTRAQ and the results combined to produce a high-confidence dataset with good quantitative reproducibility for statistical analysis. A parallel set of experiments was conducted using mock-infected samples. In

total, 118 non-redundant unique haemocyte proteins were simultaneously identified and quantified in response to bacterial-challenge, with 16 found to be significantly regulated relative to the unchallenged and mock-infected controls.

To gain insight into the biological processes temporally regulated in response to bacterial-challenge, hierarchical cluster analysis was employed to group the differentially expressed proteins according to expression profile similarities. As many of the identified proteins lacked functional characterisation in abalone, functional annotation, data mining and network modelling was conducted on the individual protein clusters. This uncovered a complex and multifaceted response to bacterial challenge in *H. midae,* implicating the coordinated response of multiple signalling pathways. Calcium and cAMP signalling control the majority of signalling pathways regulated in *H. midae* and exert immune responses via activation of MAPK signalling cascades. Based on these functions, molecular pathways were integrated into a pathway model to generate a more complete picture of the regulatory processes underlying innate immunity in *H. midae*. Distinct biological processes were shown to be temporally regulated in response to bacterial challenge. This includes early up-regulation of proteins involved in phagocytosis, nitric oxide production and ATP-synthesis, whilst down-regulated responses were predominantly involved in the regulation of apoptosis. The late up-regulated response primarily involved protein kinase activity and detoxification processes. Validation of significant differential expression of allograft inflammatory factor-1, calreticulin and NADP-dependent isocitrate dehydrogenase by immunoblotting confirmed their overexpression in response to bacterial-challenge.

A putative allograft inflammatory factor-1 protein was selected as a potential molecular indicator of health and further characterised to establish its functional molecular and biological role in *H. midae*. Through immunoblotting, inhibitory assays and confocal imaging, allograft inflammatory factor-1 was confirmed to be significantly overexpressed upon immune stimulation and shown to regulate phagocytosis in cultured *H. midae* haemocytes via a functional interaction with filamentous actin.

This is the first time a high-throughput proteomics approach has been used to investigate the immune response of *H. midae*. Data generated from this study provided further insight into the mechanisms of immune regulation in *H. midae* and demonstrated the utility of proteome profiling as a means of discovering proteins in non-model organisms. These results contribute to the broader knowledge of innate immunity in marine molluscs and provide a platform for future investigations in the search for biomarkers for aquacultured abalone.

ABBREVIATIONS

1^0	primary
2^0	secondary
1D	one dimensional
2D	two dimensional
α	alpha
β	beta
µA	microamp (s)
µg	microgram (s)
µL	microliter (s)
µm	micrometre
^0C	degrees Celsius
%	percentage
®	trademark
A	
ACTH	adrenocorticotrophic hormone
ADP	adenosine diphosphate
AIF-1	allograft inflammatory factor-1
AMPs	anti-microbial peptides
AMPS	ammonium persulfate
ANOVA	analysis of variance
ATP	adenosine triphosphate
B	
B2G	Blast2GO
BCA	bicinchoninic acid assay
BLAST	basic local alignment search tool
BP	band pass
BSA	bovine serum albumin

C

Ca	calcium
Ca^{2+}	calcium ions
CaM	calmodulin
CAMKII	calmodulin-dependent protein kinase
cAMP	cyclic adenosine monophosphate
CHAPS	3-[(3-Cholamidopropyl)dimethylammonio]-1-propanesulfonate hydrate
CREB	cAMP response element-binding protein
CRH	corticotropin releasing hormone
CRT	calreticulin

D

DISC	death inducing signalling complex
dH_20	distilled water+
dpi	dots per inch
DTT	dithiothreitol

E

EDTA	ethylenediaminetetraacetic acid
ELISA	enzyme-linked immunosorbent assay
ER	endoplasmic reticulum
ERK	extracellular signal-regulated kinase
ESI	electrospray ionization
et al.	et alia
EtBr	ethidium bromide

F

F-actin	filamentous actin
FAO	Food and Agriculture Organization
FASP	filter aided sample preparation
FcRs	Fc receptors
FDR	false discovery rate

FITC	fluorescein isothiocyanate
G	
G6PDH	glucose-6-phosphate dehydrogenase
g	gram (s)
G-actin	globular actin
GAPDH	glyceraldehyde-3-phosphate dehydrogenase
GE	gel electrophoresis
GHz	gigahertz
GO	gene ontology
GPCRs	G protein coupled receptors
GST	glutathione-S-transferase
GTP	guanine triphosphate
GTPases	small nucleotide binding proteins
H	
h	hour (s)
HCA	hierarchical cluster analysis
HCl	hydrochloric acid
H_2O	water
HPLC	high-performance liquid chromatography
HSP	heat shock protein
HSPs	heat shock protein multigene families
I	
I.D	identification
IDH	NADP-dependent isocitrate dehydrogenase
IEF	isoelectric focussing
IFN	interferon
Ig	Immunoglobulin
IgSF	immunoglobulin super family
IL	Interleukin

IPG	immobilized pH gradient
iTRAQ	isobaric tagging for relative and absolute quantification
J	
JNK	c-jun N-terminal kinase
K	
kDa	kilodalton (s)
KEGG	Kyoto Encyclopedia of Genes and Genomes
kVh	kilovolthour (s)
L	
L	litre (s)
LC-MS/MS	liquid chromatography tandem mass spectrometry
LPS	lipopolysaccharide
Ltd	limited
M	
M	molar (s)
MAPK	mitogen-activated protein kinase
MAPKK	mitogen-activated protein kinase kinase
mg	milligram (s)
MIF	migration inhibitory factor
min	minute (s)
ml	millilitre (s)
mM	millimolar (s)
MMTS	s-methylmethanethiosulfonate
MS	mass spectrometry
Mw	molecular weight
m/z	mass to charge ratio
N	
$NADP^+$	β-Nicotinamide adenine dinucleotide phosphate sodium salt

NADPH	β-Nicotinamide adenine dinucleotide 2'- phosphate reduced tetrasodium salt
NCBI	National Centre for Biotechnology Information
NDP	nucleoside diaphosphate
NF-κB	nuclear factor-kappaB
N-FMLP	N-formyl-methionyl-leucyl-phenyalanine
ng	nanogram (s)
NO	nitric oxide
NOS	nitric oxide synthase
nL	nanolitre (s)
nm	nanometre (s)
P	
PAGE	polyacrylamide gel electrophoresis
PAMPs	pathogen-associated molecular patterns
PBS	phosphate-buffered saline
pH	potential of hydrogen
pI	isoelectric point
p.i	post-injection
PKA	cAMP-dependent protein kinase
PKC	protein kinase C
PMSF	phenylmethanesulfonyl fluoride
proPO	prophenoloxidase
PRR	pattern recognition proteins
PTM	post translational modification
Q	
Q-TOF	quadrupole time of flight mass analyzer
R	
RNI	reactive nitrogen intermediates
ROI	reactive oxygen intermediates

ROS	reactive oxygen species
RT	room temperature
S	
SAB	sample application buffer
SDS	sodium dodecyl sulphate
spp.	species
SRM	selected reaction monitoring
SSS	sterile sea salts
T	
TBS	tris-buffered saline
TBST	tris-buffered saline with Tween 20
TCEP	tris(2-carboxyethyl)phosphine
TEAB	triethylammonium bicarbonate
TEMED	N,N,N',N'-Tetramethylethylenediamine
TLRs	Toll-like receptors
™	trademark
TNF	tumour necrosis factor
TPx	thioredoxin peroxidase
Tris	tris(hydroxymethyl)aminomethane
TSA	tryptone soy agar
TSB	tryptone soy broth
TSP	total soluble protein
U	
UPGMA	unweighted pair group method with arithmetic mean
V	
V	volt
VSMCs	vascular smooth muscle cells

CHAPTER 1
LITERATURE REVIEW
CONTENTS

1.1 Introduction

The global population is projected to exceed 9 billion by 2050 (United Nations, 2004) and with it, a growing demand for food. It is estimated that world agricultural production needs to increase by 60% to meet this demand, requiring new strategies if this goal is to be achieved (Alexandratos & Bruinsma, 2012). Food shortage is already a worldwide problem since most arable land has been lost to urbanization, desertification and environmental degradation, while depleting resources and a changing climate further contribute to the challenges of production. Aquaculture, the cultivation of aquatic organisms such as fish and shellfish, has emerged as a strong contender for a high production strategy. As wild fisheries have become overexploited and depleted, the aquaculture industry has seen significant growth worldwide, expanding at an annual rate of 8% and contributing to 142 million tonnes in 2008 (FAO, 2010). Aquaculture is therefore an important socio-economic sector providing jobs, local farming development and domestic and international trade (FAO, 2001). The sub-Saharan African region, rich in natural resources and space, is gradually developing its aquaculture industry with South Africa leading as an emerging market. Specifically, abalone cultivation has developed rapidly in South Africa which is currently one of the largest producers of abalone outside of Asia (FAO, 2010).

1.1.1 *Haliotis midae* aquaculture

Abalone are marine gastropod molluscs belonging to the Haliotidae family that are cultivated for their large, muscular foot and their mother-of-pearl shells. In South Africa, *Haliotis midae* is the only commercially exploited abalone species, owing to its larger size and abundance along the South African coastlines (Sales & Britz, 2001; Raemaekers et al., 2011). Originally harvested from wild fisheries, the collapse of wild *H. midae* populations due to unregulated harvesting, soaring market prices and a rise in black market trade led to a significant growth in land-based aquaculture systems (Hauck & Sweijd, 1999; Raemaekers et al., 2011). Commercial aquaculture of *H. midae* has been ongoing for about 33 years and as of 2011, there were 14 operating abalone farms in South Africa contributing to R379 million, representing 94% of the entire aquaculture

revenue (South Africa Aquaculture yearbook, 2012). Abalone farming is therefore an important economic sector for South Africa. However, the occurrence of infectious diseases is considered a severe limitation factor to production (Mialhe et al., 1995; Murray & Peeler, 2005).

1.1.2 Disease in abalone aquaculture

Disease outbreaks are one of the single biggest cause of economic loss in abalone aquaculture and remain a significant challenge to mitigate (Nicolas et al., 2002;Bondad-Reantaso et al., 2005; Gordon and Cook, 2013; Lafferty et al., 2014). Many of the rearing conditions necessary for intensive farming have a direct influence on infection rates in abalone. Overcrowding, low oxygen levels, diet, as well as water temperature and salinity fluctuations contribute to increased stress levels in animals, which has been shown to directly affect infection susceptibility (Hooper et al., 2011; Malham et al., 2003; Stone et al., 2013; Stone et al., 2014). A wide range of pathogens have been described in both wild and reared abalone species including bacteria, viruses, fungi and protozoan and metazoan parasites (Bower et al., 1994; Paillard et al., 2004). Amongst these, bacterial diseases remain the leading cause of mass mortalities in abalone aquaculture with estimated mortality rates as high as 90% (Hooper et al., 2007; Nicolas et al., 2002; Sawabe et al., 2007). For example in 1999, following mass mortalities of endemic abalone populations along the French coastline, the land-based abalone farm SMEL in Normandy suffered 50% loss within 2 weeks of *Vibrio* infection, reaching 85% mortality in 2 months without any major symptoms evident before death (Nicolas et al., 2002). Similarly, mass mortalities in cultured *H. diversicolor* have been observed in Taiwan since 1998, resulting in the loss of 400 million TWD to their abalone industry (Bondad-Reantaso et al., 2005; Liu et al., 2001). Mass mortalities of wild and farmed abalone populations have also been described in America, Japan, China, France and Australia (Huang et al., 2001;Lee et al., 2003; Bondad-Reantaso et al., 2005; Lafferty & Kuris, 1993; Lafferty et al., 2014). In South Africa, abalone infection by *Vibrio* and *Clostridium* bacteria have been described, as well as evidence of the accumulation of paralytic shellfish poisoning toxins caused by *Alexandrium catenella* blooms (Dixon et al., 1991; Pitcher et al., 2001).

The high mortality rates observed may be attributed to the rapid spread of disease once infection sets in, as decreased immunity in animals renders them highly susceptible to infection and close contact amongst animals favours the spread of pathogens. These are optimal conditions for opportunistic bacteria such as *Pseudomonas*, *Aeromonas*, *Pasteurella* and more notably, *Vibrio* species (Sindermann, 1984). *Vibrio* spp. are considered the most serious pathogen in fish and shellfish aquaculture worldwide due to their pervasive presence in marine and estuarine ecosystems (Bricknell et al., 2000; Cheng et al., 2004b; Nicolas et al., 2002). Vibriosis, caused by *Vibrio* spp. infection, is the most common fish and shellfish disease and is widely responsible for mortalities in aquaculture-reared organisms (Chatterjee & Haldar, 2012).

Another vector for disease propagation is the pathogenic cycling that may occur between cultured and wild populations of abalone (Arechavala-Lopez et al., 2013; Lafferty et al., 2014). Since most abalone farms are situated along the coastline and pump effluents back into the ocean, the possibility of wild stocks becoming infected (and vice versa) is high and could have devastating consequences for the already over-exploited wild populations. Furthermore, many South African abalone farms harvest kelp directly from the ocean to feed abalone stocks. These may harbour pathogenic organisms which could further increase the risk of bidirectional pathogen transfer within and among the farm stocks (Mouton & Gummow, 2011).

1.1.3 Health management and disease control

Disease prevention is the primary goal of abalone farmers and as such, a number of strategies exist. Ideally, optimal water quality, diet and moderate stocking densities can prevent opportunistic infection, but this is not often feasible. Although therapeutic agents such as antibiotics have proven successful in treating animals infected with bacteria, the emergence of drug resistant strains has raised concern regarding the hazards of antibiotic overuse (Schwarz et al., 2001). Probiotic treatments are becoming increasingly favourable as an alternative to antibiotics and their use in aquaculture is gaining momentum (Balcázar et al., 2006; Kesarcodi-Watson et al., 2008). One mechanism of action of probiotics is the enhancement of the immune response which is stimulated by the beneficial bacteria (Balcázar et al., 2006). A comprehensive

understanding of the mechanisms underlying the immune response would thus be highly beneficial to fully exploit this option.

Despite recent progress with the preventative measures highlighted above, disease outbreaks continue to plague the abalone industry. Current diagnostic methods involve *in vitro* testing of parameters such as haemocyte counts, haemocyte morphology, phagocytic capability and respiratory burst assays (Hooper et al., 2007). However, there is a concern that single parameter biomarkers are sensitive to biotic and abiotic stressors and may not reflect disease-specific markers (Song et al., 2003). The long term goal of disease management on farms would involve a test-based kit as a monitor for health, which will require the identification and characterization of appropriate biomarker candidates. To fulfil their role as biomarkers, certain criteria are to be met such as repeatability, rapid response and relevance to the stress involved (Schiess et al., 2009). Ideally, the combination of several biomarkers as a test-based kit would provide an extensive health monitoring system, capable of detecting early signs of stress, disease and other alterations to the biological status of farmed abalone.

The invertebrate immune response however, is a complex and dynamic system which functions through convoluted, coordinated molecular and cellular interactions. Consequently, it is not sufficient to understand a single component of this response. In order to develop a holistic and predictive approach to disease prevention in abalone aquaculture, a comprehensive understanding of all the molecular constituents responsible for immune system processes is required (Zak et al., 2014). Our current understanding of the immune and stress response in abalone is limited and mostly based on work conducted on other marine invertebrates (Hooper et al., 2007). There is a need for a comprehensive exploration of the innate immune response of *H. midae* which could provide insight into previously unknown molecular mechanisms of the innate immune response. These could pave the way for the development of preventative measures, early detection and novel therapeutic treatments in abalone aquaculture and ultimately reduce disease-related mortalities.

1.2 The molluscan innate immune system

Pathogen infection disrupts cellular homeostasis and consequently, an arsenal of host responses are required to both detect and destroy the invading pathogen (Nappi & Ottaviani, 2000; Travers et al., 2010; Cardinaud et al., 2015., Shiel et al., 2015). Unlike vertebrate species, invertebrates lack adaptive immunity and rely entirely on a non-specific innate immune system as a first line of inducible defence against pathogens (Mogensen, 2009). The innate immune response is comprised of a collection of subsystems, principally of humoral and cellular components, that function simultaneously to exert various functions to eliminate foreign microorganisms (Tiscar & Mosca, 2004; Ellis et al., 2011). Knowledge of the abalone innate immune response is based on limited work conducted in abalone, focussed work on a few gastropods and bivalves, considerable work conducted in invertebrates and a large body of work in vertebrates (Hooper et al., 2007). Although the immune and stress response system of molluscs and invertebrates do share similarities, major divergences between groups of invertebrate phyla have been uncovered (Hooper et al., 2007). Thus, invertebrate immune responses cannot be generalised and there is a fundamental need for investigations into the immune response of different molluscan phyla. As such, the mechanisms by which *H. midae* regulates the immune response are largely unknown. Nevertheless, results from the aforementioned studies provide a composite view into the complex nature of the innate immune response in marine invertebrates. An overview of the available literature characterising the innate immune response of marine molluscs is presented below.

1.2.1 Cellular response

The cellular response is mediated primarily through circulating cells in the haemolymph known as haemocytes (or immunocytes), which are responsible for carrying out immune functions mainly involving phagocytosis, agglutination, encapsulation as well as the production of cytotoxic reactive intermediates of oxygen (ROI) and nitrogen (RNI), and certain enzymes (Canesi et al., 2002a; Travers et al., 2008). Although characterisation of molluscan haemocytes remains contentious, two

basic cell types are generally recognised; namely hyalinocytes and granulocytes (Donaghy et al., 2010; Sahaphong et al., 2001; Travers et al., 2008). Granulocytes contain granules within the cytoplasm, making up the majority of the total haemocyte population, whereas hyalinocytes are smaller, oval shaped cells containing little to no granules (Donaghy et al., 2010; Travers et al., 2008). Functionally, both hyalinocytes and granulocytes can form pseudopodia, phagocytose particles and produce reactive oxygen species (ROS) (Donaghy et al., 2009). However, kinetic differences in phagocytic and oxidative activities are also apparent between these cell types (Donaghy et al., 2010).

Considering the central role phagocytosis plays in the cellular response, it is not surprising that it has received considerable attention in invertebrate studies. Phagocytosis is a critical component of innate immunity whereby infected or damaged cells are removed (Greenberg, 1995; Aderem & Underhill, 1999). Although phagocytosis has not been characterised extensively in abalone, it is well understood in other marine invertebrate species. The process is characterised by discreet stages: recognition, chemotaxis, attachment, ingestion and destruction of foreign particles (Hooper et al., 2007).

The detection and recognition of foreign particles is a crucial step in executing immune responses. Phagocytosis is induced when haemocyte surface receptors are activated by pattern recognition proteins, agglutinins or opsonins, collectively known as lectins, in a process called recognition of non-self (Hooper et al., 2007). The ability to recognize self from non-self is an integral system in immune cells. Lectins circulating in the haemolymph recognise non-self motifs, also known as pathogen-associated molecular patterns (PAMPs), and bind to the carbohydrate determinants of membrane glycoproteins (Pipe & Coles, 1995). Upon binding, a conformational change occurs, allowing binding sites on the lectin to become available to haemocyte receptors. Haemocytes migrate towards the site of infection in a process termed chemotaxis that is driven by chemotaxin molecules. A number of chemotaxins have been identified in molluscs, including interleukin-8 (IL-8), lipopolysaccharide (LPS) and N-formyl-methionyl-leucyl-phenyalanine (N-FMLP) which are released by both Gram-positive and Gram-negative bacteria (Canesi et al., 2002b; Lopez-Cotes et al., 1999).

The movement of haemocytes is orchestrated via a remodelling of the actin-myosin network which involves many signalling cascades and effector molecules (May & Machesky, 2001). Some of the most extensively studied signalling molecules utilised by mammalian immunocytes during phagocytic events are also involved in the phagocytic response of invertebrates. The participation of pattern recognition proteins, Toll-like receptors, pro-inflammatory cytokines, tumour necrosis factor (TNF)-like molecules, activation of the mitogen activated protein kinase (MAPK) family, tyrosine kinase phosphorylation, cAMP-dependent protein kinase (PKA), protein kinase C (PKC) as well as nitric oxide (NO) and calcium signalling have been identified as key players in the modulation of phagocytosis in numerous marine invertebrate haemocytes (Canesi et al., 2006; De Vico & Carella, 2012; Winter et al., 2007; Plows et al., 2004, 2006; Walker & Plows, 2003), mirroring their mammalian counterparts.

The role of different MAPKs, such as p38 MAPK and extracellular signal-regulated kinase (ERK), in haemocyte phagocytosis has been investigated and confirmed in the mussel *M. galloprovincialis* (Canesi et al., 2002b), trematode larvae (Zelck et al., 2007), the Mediterranean fruit fly *Ceratitis capitata* (Mavrouli et al., 2005), *Littorina littorina* (Iakovleva et al., 2006) and *Biomphalaria glabrata* (Humphries & Yoshino, 2003). By using different MAPK inhibitors, the authors were able to demonstrate the involvement of these MAPKS in phagocytosis, encapsulation and ROS production suggesting MAPK-induced oxidative burst. In abalone, p38-MAPK mediated phagocytosis has been confirmed in *H. tuberculata*, showing rapid activation within an hour of *Vibrio* infection (Travers et al., 2009). Although much of the work conducted in the field of invertebrate MAPK signalling shows primarily P38-MAPK involvement in phagocytosis (Davies et al., 2000), the involvement of other MAPKs in regulating immune responses in marine invertebrates remains to be established.

In abalone, regulation of IFN-inducible gene products in response to an immune challenge in *H. discus discus* supports receptor-mediated recognition (De Zoysa et al., 2009ab; De Zoysa et al., 2012). Haemocyte adhesion via adenosine receptors has been shown in *H. diversicolor* and appears to be regulated mainly via PKC signalling pathways (Chen & Chen, 2007). The cAMP/PKA dependent pathway was also demonstrated to be active although only a mild regulation was observed, suggesting it may not be a major pathway (Chen & Chen, 2007). PKC-dependent activation of phagocytosis is supported

by some marine invertebrate studies although there remains conflicted reports on the role of PKA in this regulation (Bardales et al., 2004; Ottaviani et al., 2000; Plows et al., 2006). Further investigations into the signalling pathways regulating abalone phagocytosis are thus required.

One cytokine molecule that has been shown to directly influence and activate mammalian immune cells, the inflammatory response and cytokine secretion is the calcium-binding cytokine allograft inflammatory factor-1 (AIF-1) (Autieri, 1996; Yang et al., 2005). Transcriptional regulation of AIF-1 has been shown to occur in response to bacterial challenge in the oysters *Pinctada martensii* (Li et al., 2013), *C. gigas* (Zhang et al., 2013) and *C. ariakensis* (Xu et al., 2014), the scallop *Chlamys farreri* (Wang et al., 2013), carpet shell clam *Venerupis philippinarum* (Zhang et al., 2011), sea cucumber *Apostichopus japonicus* (Ji et al., 2014) and in the abalone *H. discus discus* (De Zoysa et al., 2010a). This molecule appears to function as a pro-inflammatory cytokine in marine invertebrates. Recombinant AIF in *C. ariakensis* and *C. gigas* significantly upregulated the mRNA levels of inflammatory-related factors such as MIF, TNF and IL-17, IL-1α and IFNγ (Xu et al., 2014; Zhang et al., 2013). AIF has also been shown to activate mammalian macrophages (Yang et al., 2005) and this effect is reflected in *C. gigas* haemocytes (Zhang et al., 2013).

Upon attachment, foreign particles are enclosed in a primary phagosome which fuses with lysosomes to form a mature phagolysosome (Luzio et al., 2007). Finally, foreign particles are destroyed in either an oxygen-dependent (respiratory burst) or oxygen-independent manner (Ellis et al., 2011).

1.2.2 Oxidative mechanisms

The mechanisms whereby phagocytosed cells are killed involve the production of cytotoxic compounds such as reactive oxygen species (ROS), nitric oxide (NO), microbicidal agents and certain cytokine molecules (Apel & Hirt, 2004; Beutler, 2004). Some of the most important ROS that are produced include superoxide, singlet oxygen, hydrogen peroxide, hypohalides and halidamines, which are all extremely potent oxidants (Tiscar & Mosca, 2004). Oxidative mechanisms have been shown to be induced in response to pathogen infection in many bivalve species including oysters, clams,

scallop and mussels (Donaghy et al., 2009; Goedken & De Guise, 2004; Hooper et al., 2007; Maldonado-Aguayo et al., 2015). In abalone, similar increased oxidative activity has been reported in *H. cracherodii, H. rufescens*, *H. tuberculata, H. diversicolor, H. discus discus, H. laevigata* and *H. rubra* in response to chemical, thermal and disease stresses (Cardinaud et al., 2015; Cheng et al., 2004; Dang et al., 2013; De Zoysa et al., 2011ab; Donaghy et al., 2010; Martello & Tjeerdema, 2001; Travers et al., 2008).

Nitric oxide (NO) represents another significant free radical since it has been shown to also regulate various important physiological functions such as phagocytosis and apoptosis, in addition to its oxidative activity (Colasanti & Venturini, 1998). The production of NO following stimulation with a pathogen has been observed in *Mytilus galloprovincialis* and *Ruditapes decussates* haemocytes (Costa et al., 2009). In abalone, this has been demonstrated in the species *H. diversicolor* following xenobiotic exposure (Gopalakrishnan et al., 2011).

The production of highly oxidising compounds can lead to lipid peroxidation as well as protein and DNA oxidation in the host, resulting in oxidative stress (Matés, 2000). Eukaryotes possess highly coordinated antioxidant systems, which include enzymatic and non-enzymatic antioxidants, which function to protect the cells from oxidative damage (Devasagayam et al., 2004). Antioxidants may be induced at different stages of the immune response and function either by blocking the initial production of oxidants or scavenging and converting oxidants to less harmful compounds (Devasagayam et al., 2004). Differential expression of antioxidant enzymes in response to bacterial challenge has been reported in numerous invertebrate species (Bao et al., 2009; Canesi et al., 2010; Labreuche et al., 2006; Liu et al., 2007; Yang et al., 2004), including the disc abalone (De Zoysa et al., 2011a; De Zoysa et al., 2008). Although classical antioxidant systems appear to be conserved across invertebrates, remarkably different oxidative activities and antioxidant responses have been reported in different species depending on the tissue type and pathogen used to elicit a response (Martello & Tjeerdema, 2001; Torreilles et al., 1996).

Even though oxidative mechanisms and antioxidant systems represent important mechanisms of innate immunity, which are clearly active in abalone, there remain uncertainties regarding these systems in marine invertebrates. Many currently used *in*

vitro tests for detection of immune stimulation, such as superoxide production, often yield mixed results in immune studies of abalone (Hooper et al., 2007). This highlights the need for an investigation into oxidative responses in different molluscan species so as to generate a deeper understanding of the regulation of these mechanisms. Specifically, it would be beneficial to establish the inducing pathways of ROS production and the resulting antioxidant system (Rivero, 2006). Many cytotoxic compounds are produced as part of the humoral immune response and have also been shown to modulate vital physiological processes in certain vertebrate and invertebrate organisms (Fialkow et al., 2007; Apel & Hirt, 2004) and this modulatory role needs to be explored further in marine molluscs.

1.2.3 Humoral response

The humoral response involves the induction of enzymatic cascades that regulate the production and release of humoral factors secreted by haemocytes, including lysosomal enzymes, lectins, ROIs, cytokines and antimicrobial peptides (AMPs) (Marmaras & Lampropoulou, 2009; Nappi & Ottaviani, 2000; Koutsogiannaki & Kaloyianni, 2010). AMPs are the main effectors of the humoral component of the innate immune response and are highly conserved across all phyla (Mitta et al., 2000; Sperstad et al., 2011). Over 700 different AMPs have been described in plants, invertebrate and vertebrate species that display a diversity of biological functions in these organisms (Bachère et al., 2004; Mitta et al., 2000).

In marine invertebrates, a wide array of AMPs are produced that are thought to complement each other in order to respond to a wider range of pathogenic organisms (Sperstad et al., 2011). Upon microbial stimulation, these peptides are rapidly induced to both interact directly with infectious agents and modulate immunoreactions in the host (Otero-González et al., 2010). Although most AMPs are derived from larger inactive proteins, recent evidence suggests that some biologically active proteins, such as haemocyanin, may be altered to produce peptides with microbicidal properties (Lee et al., 2003; Zhuang et al., 2015). Although very few AMPs have been characterised in abalone (Li et al., 2011), novel antimicrobial peptide regions have recently been

identified in *H. discus discus*, *H. laevigata* and *H. tuberculata* (Dang et al., 2011; De Zoysa et al., 2010a; De Zoysa et al., 2009b; Zhuang et al., 2015).

Endogenous AMPs provide an exciting avenue for the development of novel antimicrobial agents owing to their broad antimicrobial spectra and highly selective toxicities (Boman, 1998; Hancock & Scott, 2000). It would therefore be highly beneficial to explore the range of AMPs present in abalone which may permit the development of therapeutic strategies targeted specifically to abalone bacterial pathogens.

1.2.4 Apoptosis

Apoptosis, or programmed cell death, is a fundamental biological process of innate immunity that is critical for the clearance of damaged, senescent or infected cells, without inducing inflammation (Sokolova, 2009; Birge & Ucker, 2008). Characterisation of the molecular mechanisms regulating apoptosis in vertebrate and invertebrate immunity has demonstrated that apoptosis is a highly regulated and multifunctional process that may be initiated via several different mechanisms (Kannan & Jain, 2000). Apoptosis may be triggered either through intrinsic or extrinsic pathways, although evidence suggests that these pathways are not mutually exclusive and that substantial cross-talk may occur between them (Behar et al., 2011;Lee et al., 2011). In mammals, the extrinsic pathway is initiated via the ligation of death receptors (members of the tumour necrosis factor (TNF) receptor superfamily) with their cognate ligands such as Fas, resulting in the formation of the death inducing signalling complex (DISC). Caspase-8 is then activated through dimerization which initiates apoptosis by cleaving and activating effector caspase cascades (Wilson, 1998). The intrinsic pathway, on the other hand, is mediated through non-receptor mediated stimuli which produce intracellular signals leading to apoptosis. Such signals include cellular stresses such as the production of ROS and the resulting oxidative stress (Kannan & Jain, 2000).

Data regarding the molecular mechanisms underlying molluscan apoptosis suggests that there is functional similarity to those of vertebrates. Comparable signalling cascades have been identified in *C. gigas* and *M. galloprovincialis* including MAPK signalling, GTPases of the Ras family, PKA, NO, noradrenaline and cyclic AMP (Canesi et

al., 2006; Hooper et al., 2007; Lacoste et al., 2002; Sokolova, 2009). However, much of this data has been acquired through indirect observations and the inducing factors of these pathways and their modulatory role as either pro- or anti-apoptotic requires clarification (Canesi et al., 2006). In abalone, a few genes relating to extrinsic pathways of apoptosis have been identified and cloned from *H. discus discus* and *H. diversicolor* haemocytes, including a Fas ligand, a caspase gene resembling human caspase-8 and death effector domain (DED)-containing caspase-8 (De Zoysa et al., 2009a; Huang et al., 2010; Lee et al., 2011). The transcription factors, tumour necrosis factor (TNFα) and nuclear factor-kappaB (NF-κB) have also been shown to be induced in *H. diversicolor* haemocytes in response to bacterial infection (De Zoysa et al., 2010c).

An interesting feature of apoptosis regulation that has been revealed in mammals is that apoptotic cells are actively involved in immunosuppression. These have been shown to inhibit inflammatory cytokines and chemokines, triggering an anti-inflammatory response (Birge & Ucker, 2008). Apoptosis clearly plays vital functional roles within the innate immune response as both a mechanism for the maintenance of homeostasis and as a regulator of inflammation. Much of the work that has been conducted on apoptosis-regulated mechanisms is based on vertebrate studies and the invertebrate model organisms *C. elegans* and *Drosophila* (Sokolova, 2009). The molecular mechanisms underlying abalone apoptosis remain to be clarified to fully understand this critical molecular constituent. The fundamental concepts that require attention include the characterisation of apoptotic receptors and the relevant molecules involved in the induction and regulation of these pathways. These could provide a deeper understanding into the relationship between cell death and the pathophysiology of disease in *H. midae*.

1.3 Stress and immunosuppression

A contributing factor that directly influences the immune system of marine invertebrates is the exposure of organisms to stressors, including elevated temperature, water pollutants, anaesthesia treatment, movement and infection (Hooper et al., 2011; Adamo, 2012; Hooper et al., 2014). Stress may be defined as any change in homeostasis and these effects are typically immunosuppressive (Adamo, 2012). In vertebrates, the stress response is primarily modulated via the release of neuroendocrine factors such as catecholamines and glucocorticoids (Ottaviani & Franceschi, 1996). These messengers function by diverting energy from processes such as growth and reproduction, to energy-requiring processes that help the animal adjust and overcome the stress (Malham et al., 2003). Invertebrates possess neuroendocrine systems comparable to that of vertebrates in that similar endocrine factors such as corticotropin releasing hormone (CRH), adrenocorticotrophic hormone (ACTH), cortisol-like molecules, biogenic amines and cytokine-like molecules have been identified in bivalve and gastropod haemocytes (Ottaviani et al., 2007). The basic mechanism of these molecules displays a typical CRH-ACTH-biogenic amine cascade in gastropods, although this has not been demonstrated in abalone.

There appears to be a distinct interconnected relationship between the immune response and endocrine system, as both have been shown to modulate and influence the response of the other. Immune-related molecules and growth factors have been shown to modulate CRH release by haemocytes (Hooper et al., 2007; Ottaviani et al., 1998) and the subsequent activation of the endocrine system has been shown to influence expression of inflammatory cytokines, NOS, heat shock proteins, as well as affect phagocytosis through modification of the cytoskeleton (Ottaviani & Franceschi, 1997; Salzet, 2000; Stefano et al., 1989). In abalone, the effect of stressors such as shaking, elevated temperature, oxygen depletion and altered salinity on immune parameters such as phagocytic rate and respiratory burst activity has been investigated and shows similar immunosuppressive action (Chen et al., 2005; Hooper et al., 2014; Malham et al., 2003). Stress-induced immunomodulation clearly has dramatic consequences for abalone health and survival and whilst the link between the endocrine and immune

system is understood, many of the underlying biochemical processes and effectors modulating these responses remain to be clarified.

1.4 High-throughput proteomics

Given the dynamic complexity and interconnected nature of the innate immune response, revealing the inner working mechanisms of immune cells remains a challenging and key aspect of cell biology. Developing molecular interventions for the prevention or treatment of disease requires an overall understanding of the relationships between the constituents making up the innate immune response, in addition to how they are regulated in response to pathogens. Studying single immunological parameters may not be sufficient to unlock the dynamics of the immune system but rather, a whole-system approach is required for a comprehensive understanding. This is the goal of systems biology, which aims to define the genetic, protein and ultimately, biochemical reactions of cellular and organismal functions and to characterise the networks that link these components (Garcia-Reyero & Perkins, 2011). In the past, stress response studies characterising the innate immune response have focussed primarily on genomic and transcriptomic investigations (Dang et al., 2012; Travers et al., 2010., Cardinaud et al., 2015; Shiel et al., 2015). However, mounting evidence highlighting discordance between transcript levels and protein abundance has led to a rise in the field of proteomics (Ghazalpour et al., 2011; Lundberg et al., 2010; Cox & Mann, 2007).

Since most cellular processes are facilitated through protein-protein interactions, investigating changes at the protein level is crucial to deconvoluting the molecular mechanisms involved in the immune and stress response. Proteomics is the large scale study of proteins expressed in a given system, including information about abundance, posttranslational modifications and protein-protein interactions (Tomanek, 2014; Zhou et al., 2010). This offers compelling and attractive prospects from a research standpoint since a variety of research questions may be answered through this approach. Regulatory mechanisms exhibit distinct temporal and spatial phases and evaluating this change may capture the dynamic composition of the molecular workings of cells in time

and space (Pontén et al., 2009). More specifically, quantitative protein profiling enables large-scale measurement of proteins and their changes in perturbed systems (Cox & Mann, 2007). Traditionally, quantitative proteomics employed targeted approaches such as two-dimensional gel electrophoresis (2-D GE) analysis to compare protein expression in different biological states (i.e. stressed vs. unstressed). Although quite successful, inherent limitations of gel-based techniques necessitated migration to novel mass spectrometry-based methods for relative and absolute quantification (Wright et al., 2012). Advancements in liquid chromatography and high-resolution mass spectrometry have facilitated high-throughput quantitative proteomics, capable of detecting vast numbers of peptides in complex mixtures (Meissner & Mann, 2014). Indeed, MS-based shotgun proteomics is currently the most widely used approach in large scale studies. The simultaneous identification and quantification of a couple hundred proteins offers exciting prospects as a biomarker discovery tool in aquaculture research (Rodrigues et al., 2012). Furthermore, global analysis of different cellular states can relay information from changes in protein expression, activation status, interacting networks and protein modifications that may be used to determine important pathways and networks that are modulated as a response to different conditions (Wright et al., 2012).

Two main tactics may be employed in a high-throughput quantitative proteomic study, which are broadly categorised as bottom-up or top-down, depending on whether intact or digested proteins are used for measurements (Becker & Bern, 2011). The bottom-up approach, also known as shotgun or discovery based proteomics, does not focus on specific targets and allows for a "hypothesis free" and proteome wide exploration (Meissner & Mann, 2014). As such, numerous MS-based quantitation strategies are available based upon metabolic labelling, chemical labelling or label-free (Aebersold & Mann, 2003). One such labelling strategy is isobaric tagging for relative and absolute quantification (iTRAQ), which allows parallel proteome analysis of up to eight samples (Aggarwal et al., 2006).

1.4.1 Abalone proteomic studies

To date, a large cohort of transcriptomic studies have been conducted in abalone (De Zoysa et al., 2008; Travers et al., 2010; Cardinaud et al., 2015), yet similar proteomic investigations are largely absent. There is a need for a more complete description of the proteomic response of abalone, which can both corroborate earlier genomic and transcriptomic results, but also uncover novel molecular pathways of the innate immune response. Of all the marine invertebrate proteomic studies conducted to date, only five have been performed on abalone (Slattery et al., 2012). Shell formation (Marie et al., 2010; Bédouet et al., 2012) and aquatic toxicology (Liu et al., 2011; Zhou et al., 2010) remain the leading focus of protein stress response studies in abalone. More recently, shotgun proteomics was applied to investigate the sperm proteome *of H. rufescens*, resulting in the identification of several novel peptides previously unknown in abalone fertilization (Palmer et al., 2013). Thus far, no large-scale, whole proteome investigations into the innate immune response of abalone have been conducted.

The comparative proteomic investigations of immune perturbations that have been conducted in marine invertebrates have been mainly focussed on shrimp immunity. This includes haemocytes and the stomach of *Penaeus vannamei* (Chongsatja et al., 2007; Wang et al., 2007), subcuticular epithelium and haemocytes of *P. monodon* (Somboonwiwat et al., 2010; Wu et al., 2007) and the lymphoid organ of *Fenneropenaeus chinensis* (Zhang et al., 2010). Differential protein expression of coelomocytes from the sea cucumber *Apostichopus japonicas* (Zhang et al., 2014), coelomic fluid from the purple sea urchin *Heliocidaris erythrogramma* (Dheilly et al., 2011; Dheilly et al., 2013) and haemocytes from the scallop *Chlamys farreri* (Chen et al., 2011; Huan et al., 2011) have also been investigated following immune challenge. These studies observed differential expression of novel proteins involved in critical roles in the innate immune response such as defence response proteins, proteins involved in oxidative burst, signal transduction molecules, proteins involved in energy metabolism, cytoskeletal proteins and proteins involved in the endoplasmic reticulum (ER) stress response. Results from these studies demonstrate the capacity of shotgun proteomics to uncover how cells respond to cellular challenges in different cell types and organisms. It would thus be highly beneficial to conduct a similar, whole proteome analysis

investigating the immune response *H. midae* haemocytes. Such a study would contribute to the broader knowledge of molluscan innate immunity and specifically further our understanding of the molecular mechanisms underlying the abalone immune response.

1.5 Research objectives of this study

Cultivation of the abalone *Haliotis midae* is an important and valuable economic sector for South Africa, which is currently one of the largest producers of abalone outside of Asia (Troell et al., 2006). One of the major constraints of abalone aquaculture is the reoccurrence of pathogens and disease outbreaks, particularly *Vibrio* species. These have plagued the abalone industry worldwide and resulted in major financial loss in the past. Furthermore, typical animal husbandry practises, such as high stocking densities, exacerbate and contribute directly to disease susceptibility and infection intensity (Hooper et al., 2007). Our ability to detect and predict infection outbreaks, as well as implement disease control strategies, relies on an intricate understanding of the complex cellular and molecular interactions of the constituents making up the innate immune response. Thus far, a large body of work has been conducted to characterise and decipher the innate immune response in other marine organisms. Although the stress and immune response appears to be very similar to that of other invertebrate models, there is an abundance of evidence that suggests that a high level of species-specific regulatory mechanisms exist, even amongst members of the same invertebrate order (Hooper et al., 2007; Ghosh et al., 2011). Our current understanding of the abalone immune response is based on genomic (Wang et al., 2008; Travers et al., 2010) and transcriptomic studies (De Zoysa et al., 2011a; De Zoysa et al., 2012) and a few targeted proteomic investigations conducted in different abalone species (Slattery et al., 2012). Consequently, our understanding of the immune response in *H. midae* is severely lacking. Given the complexity of the innate immune system, it is becoming increasingly imperative to comprehensively characterise the immunoproteome of these commercially valuable molluscs. Recent developments in MS-based proteomics have made large-scale investigations into the proteome of cells and organisms possible.

Thus, this study will focus on the proteomic immune response of *H. midae* following exposure to a bacterial pathogen using a high-throughput, quantitative shotgun proteomic strategy. Together with existing genomic and proteomic data from other marine invertebrate studies, the differential proteome of challenged *H. midae* haemocytes will be used to construct global expression profiles of protein groups with analogous expression. Through functional bioinformatic analysis, these protein groups will be mapped to consolidate and integrate the dataset into molecular pathways that are responsible for the innate immune response. Ultimately this investigation will be used to model the biological processes that respond to immune stimulation in abalone. This information may provide a more integrated view of the coordinated immune functions of abalone haemocytes, which will not only further our understanding of the molecular processes underlying the abalone immune system, but could also provide a platform for further characterisation of potential biomarkers of health and disease in abalone aquaculture. In so doing, the three main aims of this study were to:

i. Quantitatively profile the protein expression of *H. midae* haemocytes and identify proteins that are differentially regulated following immune stimulation using isobaric tagging for relative and absolute quantification (iTRAQ)-based LC-MS/MS proteomics.
ii. Elucidate and gain insight into the molecular pathways modulating the immune response of *H. midae* and establish the pathophysiological mechanisms underlying the temporal regulation of innate immune systems in abalone.
iii. Validate and functionally characterise a potential molecular indicator of health in *H. midae* haemocytes to establish its relevance as a suitable biomarker candidate in abalone aquaculture.

CHAPTER 2

PROTEOME PROFILING USING ISOBARIC TAGGING FOR RELATIVE AND ABSOLUTE QUANTIFICATION (iTRAQ)

CONTENTS

2.1 Introduction

Infection and disease results in complex, multifactorial responses in the host and consequently, improved management and diagnosis can only be achieved through a complete understanding of the host's immune response. As proteins are the cellular effectors of almost all biological functions, characterising the proteomic changes associated with disease will not only increase our understanding of the immune response, but may also reveal novel targets for therapeutic strategies (Meissner & Mann, 2014). Shotgun proteomics aims to achieve a systems-wide analysis of the proteome via a "bottom-up" technique which identifies proteins from a complex mixture. By combining liquid chromatography-tandem mass spectrometry (LC-MS/MS) with a labelling technique, a high-throughput analysis of the proteome can be carried out that may elucidate important molecular pathways associated with the immune response.

One such labelling technique makes use of an isobaric label known as isobaric tagging for relative and absolute quantification (iTRAQ) which, when coupled with mass spectrometry (MS), enables the simultaneous identification and quantification of large protein sets under specific conditions (i.e. diseased vs. control) (Boehm et al., 2007). The isobaric nature of the label allows for the simultaneous, multiplexed analysis of up to eight samples in a single MS experiment. This multiplex ability provides numerous options for experimental design and in-depth statistical validation as more replicates can be included in one experiment (Zieske, 2006).

Despite its advantages, studies employing the 8-plex iTRAQ system still remain limited in non-model organisms (Wright et al., 2012). Nevertheless, the use of iTRAQ for whole proteome analysis and biomarker discovery is growing and has successfully been used in numerous studies (Schiess et al., 2009; Martyniuk et al., 2012; Ernoult et al., 2010). Unsurprisingly, human studies dominate the current iTRAQ-based literature followed closely by mouse, rat and plants. The use of iTRAQ as a shotgun proteomics tool has more recently been applied to marine organisms, particularly in the area of aquatic toxicology (Martyniuk et al., 2012; Fong et al., 2014). iTRAQ studies investigating host-pathogen interactions and the immune response are fairly limited in marine species,

with only a few having been reported (Li et al., 2007b; Chen et al., 2008; Lü et al., 2014). Although these studies identified interesting alterations in the protein expression pattern of the host innate immune response following challenge with an infectious organism, they were conducted specifically on shrimp white spot virus and the zebrafish immune response. Large-scale proteomic investigations of the immune response of marine gastropods are still lacking and there are currently no abalone infection studies using iTRAQ as a quantitative tool.

A typical iTRAQ workflow begins with the reduction, alkylation and enzymatic digestion of each protein sample (Meissner & Mann, 2014). The iTRAQ reagents are used to label the individual samples which can then be pooled and subsequently analysed via mass spectrometry to identify and quantify proteins. The tags are designed to react with all primary amines of peptides, including the N-terminus and the ε-amino group of the lysine side chain, which not only enhances proteome coverage, but still retains important structural information such as post-translational modifications (PTMs) (Aggarwal et al., 2006). Each label is made up of three components: a peptide reactive group, a unique charge reporter group, and a neutral balanced group to maintain an overall mass of 145 Da (Figure 2.1).

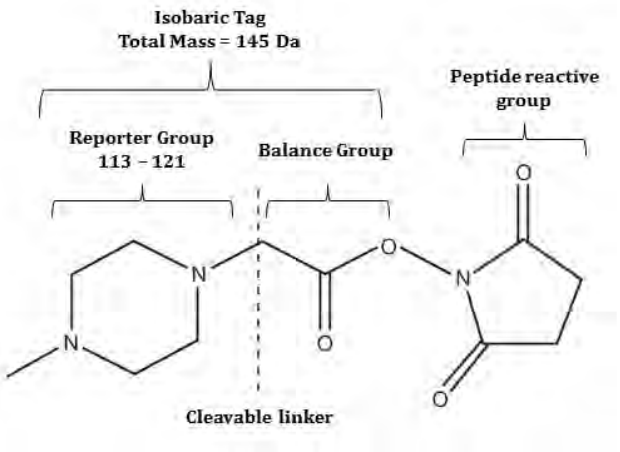

Figure 2.1 Chemical structure of the iTRAQ label consisting of a charged reporter group attached to a mass balance group and a peptide reactive group. The reporter groups range in mass from 113 – 121 and the isobaric tag is kept at a constant mass of 145 Da by pairing heavier reporters with lighter balance regions.

During LC-MS/MS analysis (Figure 2.2), the mass spectrometer collects 3 sets of information from each peptide; its mass, its ion intensity and a list of its fragments (Meissner & Mann, 2014). During the first MS, ionized peptides are sampled to produce the precursor ion spectra which relates information about the peptide masses. The balancing of the isobaric tag ensures that peptides from different samples derived during this step, will have the same mass to charge ratio on the mass spectrum. Individual ions are then selected for collision induced dissociation (CID) and upon MS/MS fragmentation, the reporters are broken off, producing distinct ions (m/z = 114-121) unique to each sample that can be measured for relative quantification. The fragment ions (consisting of b- and y- ions) are employed to calculate fragment masses which are used together with the peptide masses collected in MS1 for peptide and protein identification. An advantage of MS/MS quantification is that the signal to noise ratio is significantly reduced during fragment scans (Evans et al., 2012).

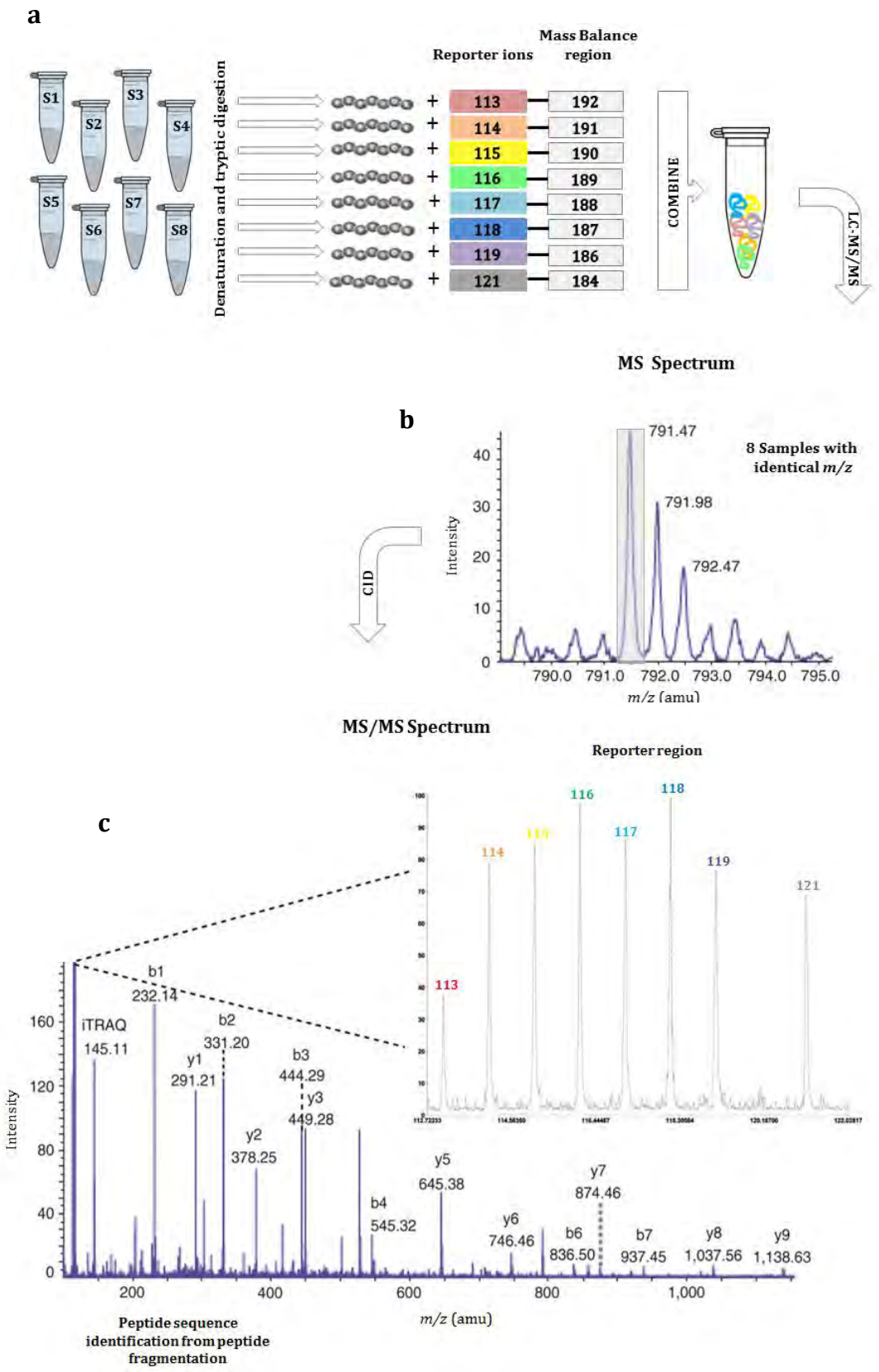

Figure 2.2 General workflow of an 8-plex iTRAQ experiment. (a) Samples are extracted, digested into peptides and labelled with the iTRAQ labels (113 – 121) before combining the samples and analysing via LC-MS/MS. (b) In the MS analysis, each identical peptide from the 8 samples appears as a single precursor ion. (c) During MS/MS fragmentation each of the 8 peptides fragments in the same way giving rise to b- and y- ions for peptide and protein identification. iTRAQ reporter ions break off and the relative intensities are used for quantification.

Accurate peptide and protein identification is fundamental to the outcome of a proteomic study and relies heavily on the availability of an appropriate database to search against in order to identify peptides from MS spectra information. Non-model organisms pose a challenge with regard to identifying proteins comprehensively as many will have unsequenced genomes. Although the use of sequence information from closely related organisms is a way to circumvent this (Shevchenko et al., 2001), caution must be exercised when assessing results as the data may include a high number of false negatives (Habermann et al., 2004). Protein identification by sequence similarity relies on evolutionary conservation between analysed proteins and their homologues in the database. If the queried peptide does not coincide within the region of similarity then it will remain unidentified. Phylogenetic distance is therefore an important determinant for successful identification and 60% shared sequence identity is required to identify more than half the queries (Habermann et al., 2004).

Combining direct database searching with *de novo* sequencing is an effective tool for generating maximal information from MS data (Shevchenko et al., 2001). Direct database searching makes use of theoretical peptide masses obtained from *in silico* enzymatic digestion of a queried database to try and find the "best match" for the observed peptide masses (Cottrell, 2011). Conversely, *de novo* sequencing derives the peptide sequence directly from the MS/MS spectrum using a "universal" database which contains all linear amino acid combinations (Zhang et al., 2012). This approach is much more complicated than database searching and is further exasperated by incomplete series of b-and y-ions (arising from missed cleavages) and different amino acid combinations that may have the same mass. The software must then scan other ion types and lower intensity peaks to fill in the missing pieces (Xu & Ma, 2006). Although requiring more computational ability, the advantages of *de novo* sequencing, such as the ability to identify peptides without a database as well as peptide homologues and modifications (Standing, 2003), make it a powerful tool. Low identification rates and high false discovery rates can be improved by coupling both strategies (Zhang et al., 2012).

A number of software packages are currently available for peptide and protein identification and the most widely used are SEQUEST, MASCOT and PEAKS (Xu & Ma, 2006). Specific features are required from the software in order to perform database

searches whilst still retaining the ability to quantify the iTRAQ ratios. These include the ability to exclude the iTRAQ reporter ion masses from the search for peptide and protein identification, identify spectra with fixed iTRAQ modifications and apply appropriate correction factors to account for any deviation in iTRAQ ratios that may arise from unequal protein concentrations or impurities present in the tags themselves (Fuller & Morris, 2012).

PEAKS software employs a combination of *de novo* sequencing and database searching using a sophisticated computing algorithm (Ma et al., 2003). PEAKS computing begins with a data refining step where raw MS/MS data is processed to remove noise and perform peak centering. This pre-processing step is particularly important for *de novo* sequencing as higher success rates have been achieved using this approach (Ma et al., 2003). The best 10 000 sequences of possible amino acids for a precursor mass are then calculated during candidate computing. A reward/penalty system is assigned to either b- or y-ions in order to find the best match for that particular ion and account for factors such as peak abundance, mass errors and the co-existence of other peaks. A more stringent scoring system is then applied which refines the selected 10 000 sequences with a stricter ion mass tolerance, as well as taking into account the immonium and internal cleavage ions. Finally, global and positional confidence scoring is employed which assigns a confidence score to the highest ranking peptide sequences (Ma et al., 2003; Xu & Ma, 2006; Zhang et al., 2012). The overall probability of successful sequencing can be measured by the score distribution.

The study described in this chapter employed an iTRAQ-based proteomic profiling approach coupled with LC-MS/MS to investigate the protein expression profiles of *Haliotis midae* haemocytes when exposed to heat-killed *Vibrio anguillarum*. The results obtained from this study will provide insight into the proteomic response of *H. midae* haemocytes by generating protein expression profiles for extensive bioinformatics analysis (Chapter 3).

2.1.1 Aims of this chapter

Infection outbreaks on abalone farms can lead to significant financial loss, seriously jeopardising the aquaculture industry in South Africa. The development of preventative strategies and health monitoring systems relies on an intricate understanding of molecular mechanisms of the abalone disease response. Proteomics is an ideal tool for elucidating the cellular processes associated with the innate immune response. Specifically, high throughput profiling of the haemocyte proteome using labelling strategies can provide qualitative and quantitative data to identify altered protein expression levels in infected samples.

The aim of this chapter was to characterise the immune response proteins in haemocytes of the South African abalone *H. midae* by employing iTRAQ-coupled LC-MS/MS. In order to assay immune response stimulation, *H. midae* were challenged with a bacterial pathogen and total haemocyte counts monitored for significant changes. A preliminary iTRAQ challenge trial was conducted to establish a haemocyte proteome response time interval for further investigation. This was achieved by challenging animals over a broad-range time frame and monitoring global protein expression changes by cluster analysis. Four independent challenge trials were conducted and analysed by iTRAQ and the results combined to produce a high-confidence dataset with good quantitative reproducibility for statistical analysis. In order to exclude proteins that may be responding to the infection protocol rather than the injected pathogen, a parallel set of experiments was conducted using mock-infected samples.

2.2 Materials and methods

All media and solutions used in this study are listed in Appendix A.

2.2.1 Maintenance of animals

H. midae (approximately 7.0 ±2 cm shell length) was acquired from a commercial South African abalone farm and kept at the Department of Agriculture, Forestry and Fisheries Research Aquarium at Sea Point, Cape Town, South Africa. Animals were housed in plastic, meshed baskets suspended in polyethylene tanks containing approximately 98 L of continuously flowing, aerated, natural sea water between 13 and 16^0C. Animals were fed a weekly diet of brown seaweed (*Ecklonia maxima*) collected from the shore line at Sea Point, Cape Town. Tanks and mesh baskets were cleaned thoroughly once a week. The average stocking density was approximately 20 animals per basket.

2.2.2 Preparation of heat-killed *Vibrio anguillarum*

V. anguillarum 5676 was grown to exponential phase in 50 ml Tryptone Soy Broth (TSB; Appendix A.1.2) containing 0.5% (*w/v*) NaCl for 16 hours at 22^0C on an orbital shaker (100 rpm). The bacterial culture was heat inactivated, (sterilization tested by incubating an aliquot of heat-killed culture on TSA plates), in a 65^0C waterbath for five minutes. Bacterial cells were pelleted by centrifugation at 13000 × *g* for 10 minutes and washed twice using 1 × phosphate buffered saline (PBS) (137mM NaCl, 2.7mM KCl, 10mM Na_2HPO_4, 1.8 mM KH_2PO_4) prepared from a 10 × PBS stock (Appendix A.2.1.2). Cells were resuspended in sterile sea salts (SSS; Appendix A.1.1) ((*w/v*) 3% NaCl, 0.23% $MgCl_2$, 0.03% KCl) and the concentration of the bacterial suspension determined using a haemocytometer at 1000 X magnification under a microscope (Olympus CX 21).

Cell concentration was calculated using the following equation:

Cells/ml = [(# of cells/0.1)/A] × 1000 × dilution factor
Where A = 0.0025 mm^2 × number of squares counted

The bacterial suspension was diluted to a concentration of 1×10^9 cells/ml and stored at -20^0C.

2.2.3 Bacterial challenge and haemocyte sampling

Animals were divided randomly into experimental groups namely, control, bacterial-challenged and mock-infected groups and placed into separate tanks. The bacterial-challenged group was injected with 100 µL heat killed *V. anguillarum* 5676 suspension (1×10^9 cells/ml) into the anterior right side of the foot of each animal using a 25 G X 5/8" sterile hypodermic needle attached to a 1ml syringe. A mock-infected group was included to account for the wounding response to the injection. These animals were injected with 100 µL SSS (Appendix A.1.1) in the same manner as the bacterial-challenged animals. The third group (control) was left untouched. For each time point, 6 animals were included and the haemolymph from each animal pooled.

Haemolymph (500µL/animal) was collected and pooled via the pedal sinus of each animal using a 21 G X $1^{1/2"}$ hypodermic needle attached to a 1.5 ml syringe. Independent animals were sampled at various times (as stipulated for each experiment) post-injection (p.i.) for both bacterial-challenged and mock-infected groups. Control animals were sampled at the start of each experiment. A 10µL aliquot of the pooled haemolymph was placed in a microfuge tube for total haemocyte count (section 2.2.4). Extracted haemolymph was aliquoted into 1 ml volumes and haemocytes were collected by centrifugation at 8000 × *g* for 10 minutes. The supernatant was discarded and the concentrated haemocytes were immediately flash frozen in liquid nitrogen and stored at -80^0C.

2.2.4 Total haemocyte count

Total number of circulating haemocytes was determined immediately after haemolymph collection. One part haemolymph from each experimental time point was added to two parts Alsever's fixative solution ((*w/v*) 0.1M $C_6H_{12}O_6$, 0.03M $C_6H_5Na_3O_7.2H_2O$, 0.5M EDTA, 2.2% NaCl, 4.4% HCHO, pH7.5; Appendix A.2.1.1) to prevent haemocyte coagulation. Ten microliters of this solution was placed on a haemocytometer (Neubauer Improved Brightline Haemocytometer, Superior) and haemocytes were counted under a microscope (Olympus CX 21) at 40 X magnification. Each sample was counted three times using an eight block count to determine the

concentration in cells/ml. Total haemocyte count was determined using the equation shown in section 2.2.2.

2.2.5 Induction of an immune response in *H. midae*

To establish whether heat-killed bacterial injection induces an immune response in *H. midae*, three independent challenge experiments were conducted. For each experiment, animals were divided into three experimental groups (n = 6) (section 2.2.3). Bacterial-challenged and mock-infected groups were sampled at 24, 48 and 96 hours p.i. (n = 6/time point) and total haemocyte counts were performed for each sample (section 2.2.4). The control group (unchallenged animals) and a mock-infected group were sampled at the start of the experiment in order to establish a basal total haemocyte count. One-way ANOVA with pairwise post-hoc analysis was performed to determine statistical significance between control, bacterial-challenged and mock-infected groups using Sigma Stat version 3.10 (Systat Software Inc.) with statistical significance set at $P \leq 0.05$.

2.2.6 iTRAQ-based proteomic profiling: experimental design

In this study, five individual iTRAQ experiments were conducted. Experiment 1 was conducted to identify time points of interest for further investigation. Experiments 2 and 3 were conducted in order to identify differentially expressed abalone haemocyte proteins following challenge with *V. anguillarum* (bacterial-challenge iTRAQ). Experiments 4 and 5 served as a mock-infected control to account for the wounding response during the infection protocol (mock-infection iTRAQ).

2.2.6.1 Initial iTRAQ time course

A bacterial challenge experiment was performed using a broad time frame in order to identify changes in the proteome that warrant further investigation. The bacterial-challenge abalone group was injected with *V. anguillarum* (section 2.2.3) and haemocytes were sampled at 1, 2, 3, 6, 24 and 48 hours p.i. (n = 6/time point). Two control groups (unchallenged animals) were included as comparative controls in order to ensure reproducibility. The samples were prepared for iTRAQ analysis (section 2.2.7)

and labelled as follows; 0a: 113, 0b: 114, 1: 115, 2: 116, 3: 117, 6: 118, 24: 119 and 48: 121. MS files were searched against a mollusc protein database for peptide and protein identification using PEAKS studio 6.0 (section 2.2.8). Expression analysis was performed using CLC main workbench to establish groups of co-expressed proteins by hierarchical clustering (section 2.2.6.2).

2.2.6.2 Hierarchical clustering

CLC main workbench (CLC Bio, Aarhus, Denmark) allows feature clustering to be performed in order to group proteins based on similar expression profiles. In this way, global protein expression analysis can be assessed and interpreted quickly through graphical visualisation. Following peptide and protein identification using PEAKS (section 2.2.8), protein IDs and their expression values were imported into CLC main workbench. Expression values were quantile normalised and log2 transformed prior to feature clustering analysis. Hierarchical clustering was performed on the normalised, transformed expression values using a Euclidian distance metric and single cluster linkage.

2.2.6.3 Bacterial challenge iTRAQ analysis

Having monitored changes in protein expression over a broad time frame, three time points were chosen based on the hierarchical clustering analysis (section 2.2.6.2) that would enable investigation of a putative early and late immune response in *H. midae*. It has been established that the combination of multiple biological replicates reduces deviation from biological variance during iTRAQ analysis (Gan et al., 2007). Thus, four bacterial challenge trials were conducted in order to combine data results and produce high quality quantitative data and ensure reproducibility. To accomplish this, two iTRAQ 8-plex experiments were performed where one iTRAQ 8-plex experiment included two independent biological replicates (Figure 2.3). Each biological replicate consisted of four experimental samples namely, control (unchallenged animals), 1, 2 and 48 hours p.i. (post-injection).

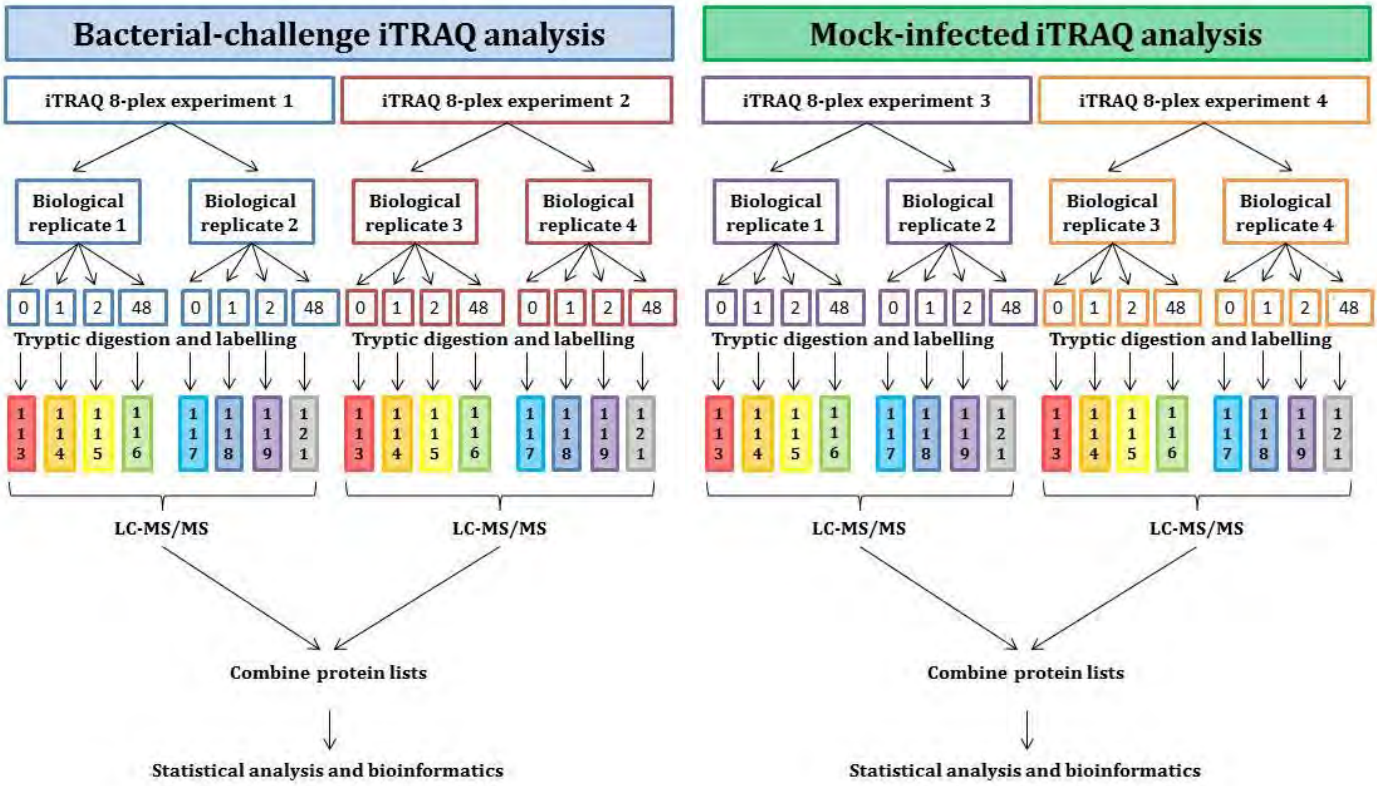

Figure 2.3). Biological samples were prepared for iTRAQ analysis (section 2.2.7) and analysed with PEAKS studio 6.0 (section 2.2.8) before statistical analysis using CLC main workbench (section 2.2.9).

Figure 2.3 Schematic representation of the iTRAQ analysis experimental design workflow for identification and quantitation of differentially expressed *H. midae* haemocyte proteins following a bacterial-challenge and mock-infection. Each iTRAQ 8-plex experiment was split into two biological replicates consisting of pooled *H. midae* haemocytes sampled at 0, 1, 2 and 48 hours post-injection.

2.2.6.4 Mock-infection iTRAQ analysis

Mock-infection experiments were conducted to eliminate haemocyte proteins that may have been expressed in response to the infection protocol, rather than the pathogen in the bacterial-challenge group. The iTRAQ experiments were conducted in the exact same manner as for the bacterial-challenge group (section 2.2.6.3) where animals were injected with sterile sea salts and haemocytes sampled at 0, 1, 2 and 48 hours p.i. (section 2.2.3).

2.2.7 iTRAQ methodology

2.2.7.1 Filter aided sample preparation (FASP) for in-solution digest

MS-based analysis requires the preparation of clean, low complexity peptide samples which can be achieved through in-solution digestion. Isolated protein samples are denatured and subject to disulfide reduction and alkylation of cysteine residues, followed by enzymatic protein digestion to fragment proteins into peptides. The method used for in-solution digest for MS-based proteome analysis is adapted from Wisniewski *et al*. (Wiśniewski et al., 2009) with modifications to reduce contaminating substances and enhance iTRAQ labelling.

2.2.7.1.1 Tissue and cell solubilisation

Haemocyte pellets (section 2.2.3) were thawed on ice and lysed using 100 µL lysis buffer (1% (*w/v*) sodium dodecyl sulphate (SDS) in 0.5 M (*v/v*) triethylammonium bicarbonate (TEAB); Appendix A.2.2.1) by incubating at room temperature for 5 minutes. Haemocyte pellets were resuspended by pipetting up and down and vortexing gently for 20 minutes at 4^0C. The homogenate was centrifuged at 10 000 × g for 30 minutes at 4^0C to collect cell debris. The supernatant was transferred to a clean low-bind, microfuge tube (Eppendorf, Germany) and protein concentration was determined using a Pierce BCA protein assay kit (Thermo Scientific, USA) according to the manufacturer's instructions. A dilution series of bovine serum albumin (BSA, Pierce, USA) (Appendix A.2.3.1) was used to construct a protein standard curve.

2.2.7.1.2 Reduction, denaturation and blocking of cysteine residues

Aliquots of each time point sample, corresponding to 300 µg protein, were reduced with 5mM (*w/v*) Tris (2-carboxyethyl) phosphine (TCEP; Appendix A.2.2.2) for 1 h at 60°C. Reduced total protein was transferred to a 30 kDa MWCO Amicon Ultra centrifugal filter (#UFC503024, Millipore©) and concentrated by centrifugation at 10,000 × *g* for 20 min at 20^{0}C to a final volume of 30 µL. The retentate was alkylated with 100 µL 8 M urea in 0.5M TEAB (UT buffer; Appendix A.2.2.3) containing 15mM s-methylmethane thiosulfonate (MMTS, Sigma-Aldrich) prepared from a 200mM stock (Appendix A.2.2.4) at room temperature for 10 min. Subsequently, 300 µL UT buffer (Appendix A.2.2.3) was added to the spin filter retentate and centrifuged at 10,000 × *g* for 30 min at 20^{0}C to remove the SDS (repeated a total of three times). The urea concentration was reduced by diluting the spin filter retentate with 60 µL 0.5 M TEAB and centrifuging at 10,000 × *g* for 30 min at 20^{0}C (repeated a total of two times) leaving a final reaction volume of 30 µL.

2.2.7.1.3 Protein digestion using trypsin

The protein retentate was collected by centrifugation of the inverted Amicon filters at 1000 × *g* for 10 min at 20^{0}C. The filter device was rinsed with an additional 10 µL 1 M TEAB and centrifuged to collect any residual proteins left on the column. Mass spectrometry grade Trypsin Gold (Promega, USA) was reconstituted in 50 mM acetic acid (*v/v*) to yield a stock solution at 2 µg/µL concentration (Appendix A.2.2.5). Trypsin was added to the protein samples to yield a final protein:trypsin ratio of 100:1. Since trypsin has an optimal operating pH in the range of pH 7.5-9, the pH of the final solution was adjusted accordingly using 0.5M TEAB. Samples were wrapped in Parafilm® (Sigma-Aldrich) to prevent evaporation and incubated at 37^{0}C for a minimum of 18 hours.

2.2.7.2 Labelling of protein digests with iTRAQ reagents

The digested samples were labelled with the iTRAQ reagents following the protocol provided by the vendor (Applied Biosystems). Briefly, one vial of iTRAQ labelling reagent was used for every 300 µg of protein. The iTRAQ reagents were brought to room temperature and solubilised using mass-spectrometry grade isopropanol (Sigma-Aldrich) prior to adding the labels to the peptide sample ensuring a final organic concentration of at least 60% (*v/v*). Samples were vortexed briefly, pulsed and left to incubate for 1 hour at room temperature. Following labelling, samples were combined into one low-bind microfuge tube prior to off-gel fractionation and LC-MS/MS analysis.

2.2.7.3 Isoelectric focussing (IEF) of peptides

Since a number of contaminating substances commonly present in biological samples hinder efficient isoelectric focussing (IEF) and interfere with LC-MS/MS, it is necessary to remove them with the use of reverse-phase C18 resin. Thus, the combined samples were desalted prior to IEF using C18 Spin columns (Pierce) according to the manufacturer's instructions with the modifications specified for ESI, to yield a total of 240 µg peptide sample. The samples were concentrated in a centrifugal vacuum concentrator to less than 5 µL but not to dryness, and separated into 12 fractions using a 12-well 3100 OFFGEL Fractionator (Agilent Technologies) following the manufacturer's instructions for peptide fractionation. Briefly, immobilized pH gradient strips (Immobiline Dry-strip pH 4-7, 13 cm) (GE Healthcare) were rehydrated with 40 µL per well of IPG strip Rehydration Solution (GE Healthcare) for 15 min. Peptides were solubilised in Peptide OFFGEL Stock Solution (GE Healthcare) and 150 µL of this solution was loaded into each well. The wells were sealed and mineral oil was added to each end of the strip. Focussing was performed at 20^0C for a total of 20 kVh with a limited maximum current set to 50 µA and maximum voltage at 8000V.

2.2.7.4 LC-MS/MS analysis

In order to remove contaminants from the OFFGEL fractionation solutions and prevent clogging of the trapping column, each focussed fraction was desalted prior to LC-MS/MS using Pierce C18 Spin columns (section 2.2.7.3). The iTRAQ labelled samples were analysed on an Agilent 1200 series HPLC-Chip/MS system interfaced to an Agilent 6530 Accurate-Mass Q-TOF LC/MS. The HPLC–chip configuration consisted of a 160 nL enrichment column and a 150 mm × 75 µm analytical column. Mobile phases employed were: A) 0.1% (*v/v*) formic acid in water and B) 90% (*v/v*) acetonitrile with 0.1% (*v/v*) formic acid. An 84 minute long gradient method was used for the LC separation. Sample loading onto the enrichment column was done at 1%B. The gradient used for the analytical column began at 1%B, was raised to 8%B at 1 minute, maintained at 8%B until 4 minutes, raised to 16%B at 18 minutes, 28%B at 50 minutes, 42%B at 70 minutes, 70%B at 80 minutes, maintained at 70%B until 82 minutes and then brought back to 1%B at 84 minutes. Samples were loaded at 2 µL/minute flow rate and eluted at 0.4 µL/minute flow rate. An Agilent 6530 Accurate-Mass Q-TOF LC/MS operating in high resolution (4GHz) positive ion mode was used for all experiments.

The MS source conditions were:

Source temperature: 350^{0}C

Capillary voltage: 1955 V

Fragmentor voltage: 175 V

Drying gas flow rate: 4.3 L/min

The mass spectrometer was set to perform data acquisition with a selected mass range of 200-1700 *m/z* and an acquisition rate of 6 spectra/second in MS mode and *m/z* region of 90-1700 and an acquisition rate of 3 spectra/second in MS/MS mode. Isolation width for MS/MS mode was set to 4 amu. Ramped collision energy slope was 3.9 and offset at 4.2.

2.2.8 Peak list generation and database searching for peptide and protein identification using PEAKS studio 6.0

Raw MS files (.d format) acquired through MassHunter were converted into .mzML files using the MSconvert tool in the ProteoWizard suite. These were uploaded to PEAKS studio 6.0 and processed for peptide and protein identification as well as quantification. Database search parameters were set as follows:

Mass error tolerance :

Precursor mass: 20 ppm

Fragment ion: 0.1 Da

Enzyme: Trypsin

Non-specific cleavage: 1

Maximum missed cleavage: 2

PTM:

Fixed:

Carbamidomethylation, 8-plex (K, N)

Variable:

Oxidation of methionine, 8-plex (Y)

Ion source: ESI (nanospray)

Fragmentation mode: CID

MS Scan mode: Quadrupole

MS/MS Scan mode: Time of flight (TOF)

Database:

The Uniprot SwissProt/TrEMBL database (uniprot.org) was accessed on the 20th August 2013 to download all molluscan protein sequences.

A concatenated, target-decoy database (containing forward and reverse entries) was used to estimate false discovery rate using a decoy fusion algorithm in PEAKS studio 6.0.

Quantification:

Quantification workflow was performed using the reporter ion quantification tool in PEAKS studio 6.0 with the sample type set up for an iTRAQ 8-plex experiment.

2.2.9 Data processing on CLC main workbench and statistical analysis

Exported expression values generated in PEAKS studio 6.0 (auto normalised) from each iTRAQ experiment were quantile normalised and log2 transformed using CLC main workbench prior to processing in Excel. Filtering was performed in order to remove redundant, duplicated protein entries as well as proteins with insufficient scores to yield quantifiable information. Proteins were retained using the following criteria: Unique number of peptides ≥ 2, -10lgp score ≥ 20. Multiple entries with the same quantity information were condensed to one entry by choosing the protein with the highest score. Protein IDs with multiple hits (homologous proteins, fragments and isoforms) were processed by performing a multiple sequence alignment (uniprot.org) and grouping proteins with highly significant alignment scores. In situations where only fragments were obtained, entries with the highest scores were retained. A final protein list with quantity information for each protein ID was created by merging iTRAQ 1 and 2 experiments (and iTRAQ 3 and 4) by matching identical protein entries in each experiment. Relative expression was performed by normalising expression values to the control group in each experiment thus indicating either a down- or up-regulated pattern. Statistical analysis was performed using the Excel add-on Analysis Toolpak. The difference between the relative expression values of the control group (unchallenged animals) and experimental groups was compared by one-way ANOVA with Tukey's pairwise comparison and significance set at $P < 0.05$. A second analysis was performed on proteins exhibiting similar expression values in three of the four biological replicates

2.3 Results

2.3.1 Total haemocyte count as an indicator of immune induction

H. midae total haemocyte counts (THC) were used as an indicator of immune induction and to determine the period of immune activation in mock-infected and bacterial-challenged animals (Figure 2.4). Haemocyte samples were collected at 24, 48 and 96 hours p.i. Mock-infected animals accounted for the wounding response as a result of the infection protocol. In comparison to the zero hour control sample, the THC decreased in both the bacterial-challenged and mock-infected groups over the 96-hour time-course experiment. The THC decrease did, however, appear greater for the bacterial-challenged group (Figure 2.4). The decrease observed for the bacterial-challenged group at 48 hours p.i. was found to be statistically significant ($P \leq 0.05$) when compared to the zero hour control.

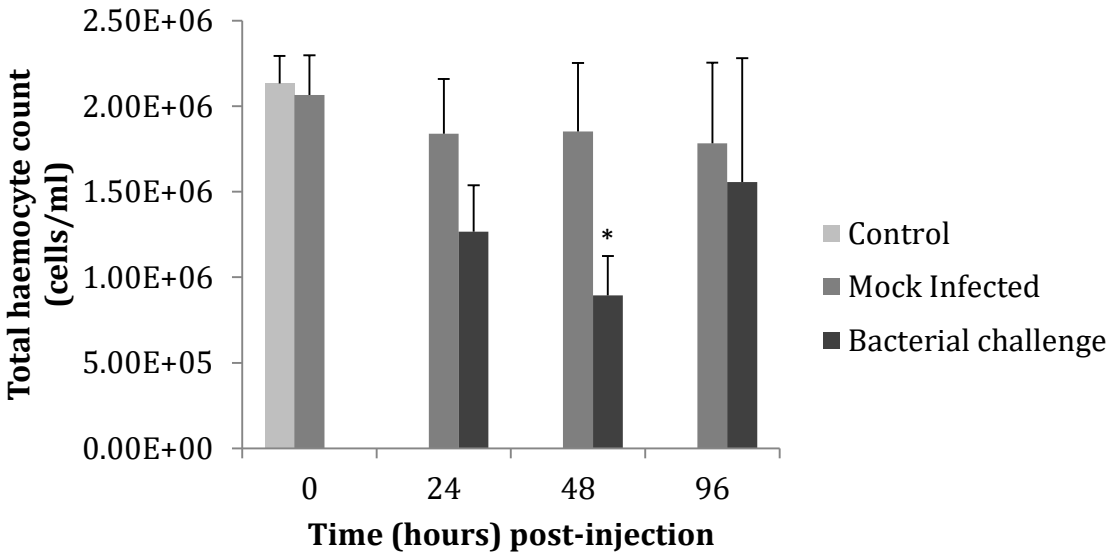

Figure 2.4 Total *H. midae* haemocyte counts (cells/ml) following immune stimulation with *V. anguillarum* (bacterial-challenged), mock-infection and in uninfected animals (control). Bacterial-challenged and mock-infected groups were sampled at 24, 48 and 96 hours p.i.. The control group and a mock-infected group were sampled at the start of the experiment (0 hours p.i.). Error bars represent the ± standard error of the means from three biological replicates. A one-way ANOVA with pairwise post-hoc comaprison was performed to compare data between groups. Asterisk (*) indicates a significant statistical difference ($P \leq 0.05$) as determined by Student's t-test.

2.3.2 Establishing time points of interest for further analysis of the *H. midae* immune response

In order to investigate the general change in protein expression and choose time points for further investigation, a preliminary investigation of the *H. midae* immune response was conducted over a broad time frame where haemocytes samples were collected at 1, 2, 3, 6, 24 and 48 hours p.i. and changes in the proteome investigated by iTRAQ LC-MS/MS and cluster analysis.

2.3.2.1 Feature clustering using CLC main workbench

Hierarchical clustering provides a fast, heuristic method for grouping proteins based on their ratio profiles and provides clear, interpretable results in the form of a heat-map tree. The heat-map showed distinct down-regulated patterns for labels 115 (1 hour p.i.) and 121 (48 hours p.i.) (Figure 2.5). All the other time points examined did not show significant changes in expression levels, although some differences were apparent between the two replicate controls (label 113 and 114).

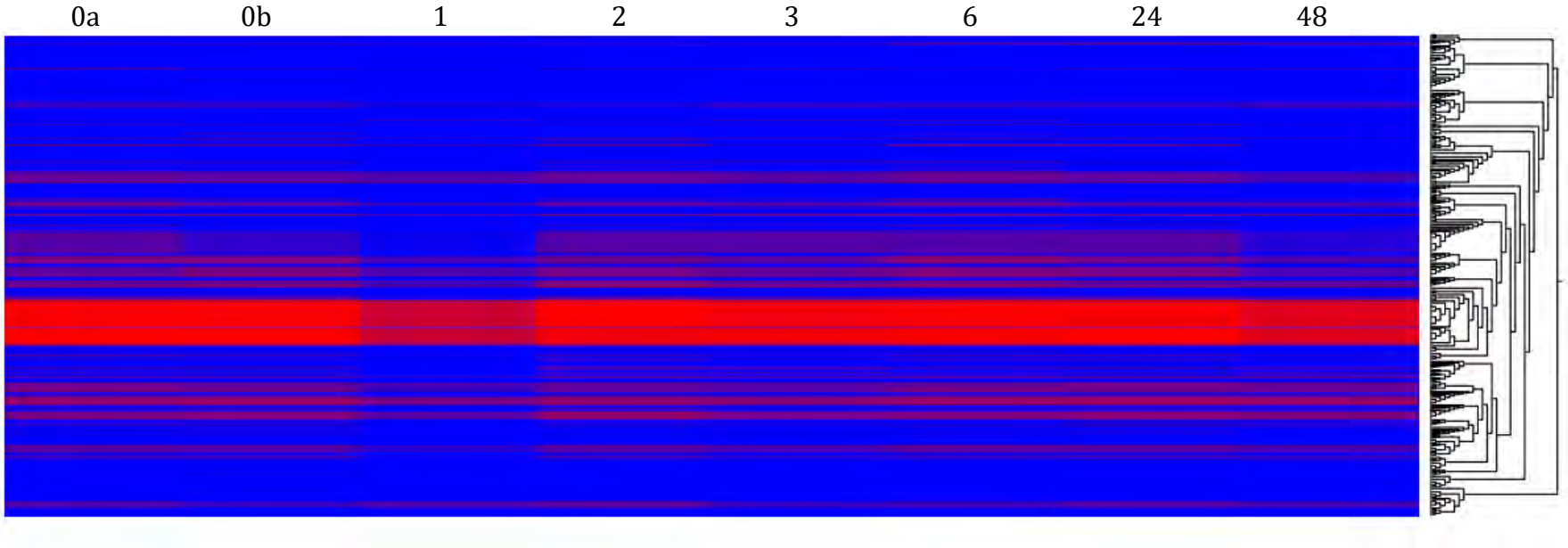

Figure 2.5 Hierarchical cluster analysis of protein expression levels in bacterial-challenged *H. midae* haemocytes. Protein expression was determined using iTRAQ analysis of samples collected at 0a (label 113), 0b (114), 1 (115), 2 (116), 3 (117), 6 (118), 24 (119) and 48 (121) hours p.i. to determine time points of interest. Blue indicates down-regulation and red indicates up-regulation.

2.3.3 iTRAQ-based proteomic profiling

Preliminary profiling of the haemocyte proteome from bacterial-challenged *H. midae* indicated differential protein expression at 1 and 48 hours p.i. (Figure 2.5). These two time points were therefore selected to further investigate and characterise a putative early and late immune response to bacterial-challenge in *H. midae*.

MS-scan information was fairly consistent throughout the four iTRAQ 8-plex experiments (Table 2.1), with iTRAQ 1 containing the most number of MS, MS/MS scans and peptide spectrum matches (PSM), thus resulting in the most number of protein identity matches prior to merging. Following merging, a total of 118 and 144 proteins were identified to be common to both iTRAQ 8-plex experiments in the bacterial-challenged group and the mock-infected group, respectively.

Table 2.1 Summary of LC-MS/MS analysis of the haemocyte proteome from bacterial-challenged (iTRAQ 1 and 2) and mock-infected (iTRAQ 3 and 4) *H. midae*.

	Bacterial-challenged		**Mock-infected**	
	iTRAQ 1	**iTRAQ 2**	**iTRAQ 3**	**iTRAQ 4**
MS scans [a]	468751	110738	78542	75725
MS/MS scans [a]	130739	104547	121666	122736
PSM [b]	3369	1751	1551	2023
Protein IDs before merge [c]	319	218	286	263
Protein IDs after merge [c]	118		144	

[a] The number of MS and MS/MS scans following LC-MS/MS analysis.

[b] The number of peptide spectrum matches (PSM) following peptide and protein identification.

[c] The number of protein identity entries before and after merging following filtering of redundant and multiple protein entries.

2.3.3.1 Bacterial challenge and mock-infection iTRAQ analysis

Haemocyte proteome profiling of bacterial-challenged and mock-infected *H. midae* at 1, 2 and 48 hours post-injection was investigated using iTRAQ analysis from four independent biological replicates for each condition (bacterial-challenged and mock-infected). A control group (0 hours p.i.) was included in each experiment and used as the reference sample to normalise expression values. The 118 and 144 proteins identified in the bacterial-challenged and mock-infected animals respectively (Table 2.1) had quantifiable information with a sufficient -10lgP score and a minimum number of 2 unique peptides. The proteins identified in the bacterial-challenged group (Table 2.2) and the mock-infected group (Table 2.3) are presented in greater detail for comparative purposes. The majority of protein identities appear to have been acquired from the TrEMBL portion of the SwissProt database as indicated by the tr| prefacing the accession number.

Table 2.2 Proteins identified in *H. midae* haemocytes following exposure to heat-killed *V. anguillarum* in four independent experiments. Fold changes were expressed as an average of the ratios of bacterial-challenged groups at 1, 2 and 48 hours p.i. to the untreated control following quantile normalisation and log2 transformation in CLC main workbench.

Accession number [a]	Description [b]	-10lgP [c]	Peptides [d]	Unique [e]	Coverage [f]	Average ratios			
						Control	1	2	48
tr|G8A4W9|G8A4W9_9BIVA	14-3-3 protein	104.21	17	14	56	0	-4.124E-01	-5.304E-01	-2.953E-01
tr|B6RB81|B6RB81_HALDI	40S ribosomal protein S18	75.71	7	7	35	0	2.552E-01	1.163E-01	1.018E-01
tr|B3TK66|B3TK66_HALDV	40S ribosomal protein S8	116.96	9	8	60	0	-2.157E-01	-3.734E-01	-2.488E-01
tr|B3TK58|B3TK58_HALDV	60S acidic ribosomal protein P0 (Frag)	125.5	13	12	56	0	-2.026E-01	2.138E-02	3.825E-02
tr|B3TK87|B3TK87_HALDV	60S acidic ribosomal protein P2	114.6	9	8	36	0	-4.49E+307	-1.26E-01	-4.49E+307
tr|Q75W49|Q75W49_CRAGI	78kDa glucose regulated protein	204.26	54	19	45	0	-9.318E-01	-7.760E-01	-3.146E-01
tr|Q17UC2|Q17UC2_HALTU	84kDa heat shock protein	271.62	214	132	59	0	-2.013E-02	-2.720E-01	-2.316E-01
tr|B3SND4|B3SND4_HALDV	Actin	329.75	178	9	24	0	-3.369E-01	-4.205E-01	-1.957E-01
tr|Q9Y0D6|Q9Y0D6_MYTGA	Actin depolymerisation factor/cofilin	92.38	6	6	99	0	-1.411E-02	4.811E-02	5.074E-01
tr|G8XUN4|G8XUN4_CRAAR	Adenosylhomocysteinase	75.67	10	9	26	0	2.451E-02	9.705E-02	-2.288E-01
tr|Q5MAL1|Q5MAL1_APLCA	Adenylate cyclase	47.26	5	2	6	0	-1.063E-01	-6.981E-01	-8.872E-01
tr|B3TK64|B3TK64_HALDV	ADP/ATP carrier protein (Frag)	103.71	11	8	24	0	-3.782E-03	-9.629E-02	1.554E-01
tr|B6RB72|B6RB72_HALDI	ADP-ribosylation factor 2	194.76	18	18	79	0	-3.153E-01	-3.463E-01	-1.232E-01
tr|B6RB93|B6RB93_HALDI	Alcohol dehydrogenase (Frag)	40.39	3	2	9	0	3.556E-01	-3.910E-01	6.597E-02
tr|Q9NJH2|Q9NJH2_PLAMG	Aldehyde dehydrogenase	67.66	6	4	8	0	-1.201E-01	-2.731E-01	-2.668E-01
tr|B3SN77|B3SN77_HALDV	Allograft inflammatory factor (Frag)	94.13	7	6	53	0	6.806E-02	-1.946E-01	1.955E+00
tr|Q5NT89|Q5NT89_CRAGI	Alpha-tubulin	254.98	52	3	83	0	-8.848E-01	-4.045E-01	-3.363E-01
tr|H6BD08|H6BD08_OSTED	Anexin 11a (Frag)	45.32	6	5	16	0	1.199E-01	-6.942E-01	-3.508E-01

Table 2.2 (Continued)

Accession number [a]	Description [b]	-10lgP [c]	Peptides [d]	Unique [e]	Coverage [f]	Average ratios			
						Control	1	2	48
tr|E3TMG6|E3TMG6_9CAEN	Arginine kinase	141.21	29	11	18	0	-3.675E-02	2.280E-02	4.553E-02
tr|Q8MWR8|Q8MWR8_9BIVA	Arginine kinase	96.73	28	16	5	0	-4.49E+307	-4.49E+307	-4.49E+307
O15989|KARG_TURCO	Arginine kinase	51.31	13	4	35	0	7.231E-01	9.968E-01	1.487E-01
tr|Q000T7|Q000T7_PINFU	ATP synthase subunit alpha	113.93	18	14	31	0	-1.748E-02	1.447E-03	-3.224E-03
tr|Q2WEC5|Q2WEC5_PECMA	ATP-binding cassette transporter sub-fam A	28.83	5	4	8	0	9.960E-01	3.333E-01	7.505E-02
tr|E5F064|E5F064_APLCA	ATP-dependent RNA helicase DDX5	100.21	10	6	47	0	5.742E-02	-4.512E-01	-1.428E-01
tr|Q8MPR0|Q8MPR0_CRAGI	Bone morphogenic protein type 2 receptor	34.76	5	3	4	0	-3.627E-01	-4.168E-01	1.358E-01
tr|B3TK26|B3TK26_HALDV	Calmodulin	207.42	17	12	33	0	4.686E-01	2.901E-01	1.438E+00
P02595|CALM_PATSP	Calmodulin 2	119.62	15	4	36	0	-1.558E-01	-4.946E-01	0.000E+00
tr|B3TK60|B3TK60_HALDV	Calmodulin-dependent protein kinase (Frag)	107.09	10	8	53	0	-6.840E-01	-9.226E-01	1.138E+00
tr|Q26268|Q26268_APLCA	Calreticulin	127.69	37	18	36	0	-4.104E-01	-7.098E-02	1.084E-01
tr|A5LGG9|A5LGG9_CRAGI	Calreticulin	119.05	45	25	49	0	-8.653E-02	-4.918E-01	-1.474E-01
tr|A6YIE3|A6YIE3_PINFU	Calreticulin	137.2	29	16	58	0	-2.805E-01	-7.135E-02	1.072E-01
P31319|KAPR_APLCA	cAMP-dependent protein kinase regulatory sbu	50.56	5	3	17	0	6.302E-01	-6.447E-01	1.086E+00
tr|Q86DH9|Q86DH9_APLCA	Cdc42	118.19	9	7	37	0	-9.733E-03	-2.893E-01	6.546E-02
tr|H9AWU2|H9AWU2_HALDH	Chaperonin containing T-complex polypep sbu Z	165.27	26	19	35	0	-1.882E-01	-1.656E-01	2.312E-01
tr|B6RB18|B6RB18_HALDI	Chaperonin containing tcp1	197.89	43	41	57	0	1.681E-01	1.161E-01	8.884E-02
tr|D1H0L8|D1H0L8_HALTU	Elongation factor 1- α	237.29	51	5	65	0	5.670E-01	4.414E-01	3.480E-01
tr|Q9BNW3|Q9BNW3_CHAAP	Elongation factor-2 (Frag)	73.09	13	8	13	0	2.931E-02	2.403E-02	1.580E-01
tr|B3TK44|B3TK44_HALDV	Fascin (Frag)	152.04	31	28	24	0	-2.265E-01	-1.350E-01	6.860E-02
tr|E2QDA6|E2QDA6_APLCA	Fragile X mental retardation protein	42.68	5	5	8	0	-5.368E-01	-1.351E-01	-8.393E-01
tr|B6RB70|B6RB70_HALDI	Fructose-bisphosphate aldolase (Frag)	182.83	19	4	57	0	-7.228E-02	-3.502E-03	-8.251E-03

Table 2.2 (Continued)

Accession number [a]	Description [b]	-10lgP [c]	Peptides [d]	Unique [e]	Coverage [f]	Average ratios			
						Control	1	2	48
tr|B6RB97|B6RB97_HALDI	Gelsolin	207.57	26	24	77	0	-1.851E-01	-3.345E-01	6.093E-02
tr|Q0KHB8|Q0KHB8_CRAGI	Glucose-6-phosphate 1-dehydrogenase	114.96	37	33	22	0	-5.761E-01	-4.433E-01	-2.274E-01
tr|A5LGG7|A5LGG7_CRAGI	Glucose-regulated protein 94	198.92	88	72	22	0	5.261E-03	-1.068E-02	-2.942E-01
tr|G0WX16|G0WX16_TEGGR	Glutamine synthetase	37.76	7	3	15	0	1.252E-01	-1.160E-01	-5.624E-01
tr|Q19BK2|Q19BK2_HALDI	Glutathione-S-transferase isoform 1	60.56	4	4	13	0	-5.826E-01	-6.158E-01	8.796E-01
tr|B3TK24|B3TK24_HALDV	Glutathione-S-transferase isoform	84.81	9	9	16	0	-3.609E-01	-1.517E-01	1.007E-01
tr|E4W3F6|E4W3F6_HALDV	Glutathione-S-transferase isoform 1	128.24	13	12	34	0	-9.369E-02	-2.810E-01	5.655E-02
tr|A8DX85|A8DX85_9MOLL	Glyceraldehyde-3-phosphate dehydrogenase	23.28	20	11	46	0	7.302E-01	7.971E-01	5.006E-01
tr|B6RB30|B6RB30_HALDI	Glyceraldehyde-3-phosphate dehydrogenase (Frg)	295.35	72	67	92	0	-1.356E-01	4.447E-03	-2.851E-01
tr|Q70MM9|Q70MM9_CRAGI	Guanine nucleotide-binding protein G alpha sbu	136.88	16	8	51	0	4.306E-01	-1.099E+00	-6.239E-01
P30683|GNAO_LYMST	Guanine nucleotide-binding protein G(o) sbu α	128.71	25	16	55	0	-6.287E-02	-1.282E-01	-2.847E-01
O15976|GNAO_MIZYE	Guanine nucleotide-binding protein G(o) sbu α	125.65	21	9	45	0	-4.414E-01	6.761E-01	6.063E-01
P30684|GNAS_LYMST	Guanine nucleotide-binding protein G(s) sbu α	124.29	17	6	45	0	-5.732E-01	-3.353E-01	9.380E-02
tr|Q8I0U4|Q8I0U4_HALTU	H2 protein (Frag)	388.07	464	141	63	0	6.433E-01	7.032E-01	2.012E-02
tr|Q564J1|Q564J1_APLCA	Haemocyanin	146.76	89	65	27	0	4.190E-01	-1.700E-01	1.018E-01
tr|C1KC83|C1KC83_HALDV	Heat shock cognate protein 70	277.74	155	89	63	0	-5.502E-01	-4.797E-01	-3.484E-01
tr|C1KC84|C1KC84_HALDV	Heat shock inducible protein 70	174.53	46	22	55	0	1.182E-01	7.081E-01	2.994E-01
tr|B8Y4I8|B8Y4I8_BIOGL	Heat shock protein 60	79.38	18	15	25	0	1.693E-01	-3.263E-01	-3.541E-02
tr|A5Y8F9|A5Y8F9_PERVI	Heat shock protein 71	206.76	57	7	49	0	-8.729E-01	-6.222E-01	-4.099E-01
tr|C0Z203|C0Z203_MYTGA	Heat shock protein 90	202.54	71	19	50	0	3.908E-01	5.667E-01	1.194E-02
tr|Q9GP18|Q9GP18_HALTU	Hemocyanin (Frag)	463.84	802	158	74	0	3.641E-01	5.791E-01	1.341E-01
P81732|HC2C_MEGCR	Hemocyanin 2-c chain	104.73	14	7	40	0	-3.434E-01	-8.974E-01	-2.940E-01

Table 2.2 (Continued)

Accession number [a]	Description [b]	-10lgP [c]	Peptides [d]	Unique [e]	Coverage [f]	Average ratios			
						Control	1	2	48
tr|G3FPE5|G3FPE5_HELLU	Hemocyanin beta-sbu	135.75	56	35	25	0	1.972E-01	6.658E-01	6.497E-02
tr|B5RHR0|B5RHR0_9MOLL	Hemocyanin fg (Frag)	123.43	34	23	45	0	2.829E-01	7.473E-01	3.119E-01
tr|C7FEG7|C7FEG7_HALDV	Hemocyanin isoform 1 (Frag)	384.28	610	395	71	0	4.729E-01	7.588E-01	8.720E-02
tr|Q27Q57|Q27Q57_SEPOF	Hemocyanin sbu 1	164.17	154	72	25	0	-1.376E-01	-4.922E-01	-2.243E-01
tr|Q9U5P3|Q9U5P3_HALTU	Hemocyanin type 2 protein (Frag)	331.22	292	23	64	0	6.121E-01	9.156E-01	3.189E-01
tr|H6T4K5|H6T4K5_MYTGA	Histone variant H2A.X	119.72	6	6	60	0	5.648E-01	-1.756E-02	-5.820E-02
tr|Q5QGY7|Q5QGY7_CRAGI	Isocitrate dehydrogenase [NADP]	82.29	8	3	8	0	-6.417E-01	6.660E-03	-2.556E-02
tr|F2Q7T6|F2Q7T6_APLCA	Leucine-rich repeat receptor tyrosine kinase	44.84	10	5	7	0	-2.307E-01	-2.665E-02	-3.642E-01
tr|H6UNQ0|H6UNQ0_9CAEN	Mitochondrial ATP synthase beta sbu (Frag)	215.34	19	2	39	0	6.923E-01	5.839E-01	2.764E-01
tr|Q4PLU5|Q4PLU5_9BIVA	Myosin VI (Fragment)	60.43	67	59	13	0	-4.49E+307	-1.2E+308	-2.494E-01
tr|Q45R40|Q45R40_APLCA	Nonmuscle myosin II (Fragment)	331.77	572	494	57	0	8.959E-02	-2.476E-01	-8.397E-02
tr|Q8SWQ7|Q8SWQ7_LOLPE	Non-muscle myosin II heavy chain	256.31	192	121	53	0	2.948E-01	5.051E-01	-1.209E-03
tr|B6RB47|B6RB47_HALDI	Nucleoside diphosphate kinase	124.51	8	6	34	0	-1.784E-01	1.013E-01	1.346E-01
tr|B6RAZ8|B6RAZ8_HALDI	Omega class glutathione-s-transferase 1	75.84	8	6	12	0	-2.087E-01	-2.471E-01	-2.256E-02
tr|D3WFS3|D3WFS3_9CAEN	Peptidyl-prolyl cis-trans isomerase	105.91	9	5	55	0	1.521E-01	7.833E-01	3.125E-01
tr|H2A0M7|H2A0M7_PINMG	Peroxidase	62.26	4	2	4	0	-2.274E-01	-7.996E-02	-6.995E-02
tr|C7EAA2|C7EAA2_HALAI	PL10-like protein	188.49	45	31	53	0	-2.010E-01	-3.456E-01	3.842E-02
tr|B6RB41|B6RB41_HALDI	Proteasome subunit alpha type	97.14	7	4	29	0	-2.907E-01	3.702E-01	-3.111E-01
tr|B6RB63|B6RB63_HALDI	Protein disulfide isomerase	245.19	46	35	67	0	6.291E-02	4.290E-02	1.894E-01
tr|B6RB65|B6RB65_HALDI	Psmc6 protein	90.33	5	3	14	0	6.533E-02	4.815E-01	2.607E-01
tr|G9K380|G9K380_HALDV	Putative 60S ribosomal protein L3	192.7	43	41	39	0	2.840E-01	-8.520E-02	-1.524E-03
B3A0R0|PPI_LOTGI	Putative peptidyl-prolyl cis-trans isomerase	38.67	6	5	14	0	-2.661E-01	-8.226E-01	-2.205E-01

Table 2.2 (Continued)

Accession number [a]	Description [b]	-10lgP [c]	Peptides [d]	Unique [e]	Coverage [f]	Average ratios			
						Control	1	2	48
tr|G9K385|G9K385_HALDV	Putative polyadenylate-binding protein 1 (Frag)	139.24	16	15	15	0	-4.121E-02	6.111E-02	5.760E-01
tr|G9K384|G9K384_HALDV	Putative procollagen type VI alpha 4	65.01	4	2	10	0	5.419E-01	6.229E-01	-6.849E-04
tr|B3TK70|B3TK70_HALDV	Putative RNA-binding protein	52.49	2	2	26	0	-5.395E-01	-4.557E-01	-2.418E-01
tr|G9K382|G9K382_HALDV	Putative tubulin beta chain	282.19	89	5	61	0	6.612E-01	-4.49E+307	7.143E-01
tr|Q0KHB6|Q0KHB6_CRAGI	Pyruvate kinase	38.82	7	6	10	0	-1.735E-01	-5.001E-01	-1.018E-01
tr|B6RB76|B6RB76_HALDI	RAB protein	206.99	25	21	82	0	-1.845E-01	-1.173E-01	-9.925E-02
tr|C1KBI9|C1KBI9_9BIVA	Rab7-like protein	110.99	8	7	50	0	1.288E-01	2.694E-01	-4.891E-02
tr|B6RB17|B6RB17_HALDI	Raminin receptor	132.78	16	14	56	0	-1.216E-01	-2.505E-01	-2.553E-01
tr|B6RB29|B6RB29_HALDI	Ran-1-prov protein	133.33	12	9	53	0	-2.056E-01	1.476E-01	-4.443E-02
tr|B6RB23|B6RB23_HALDI	Ras-related protein Rab-1A	195.95	20	16	73	0	-3.904E-01	-2.441E-01	-1.064E-01
Q05975|RAB2_LYMST	Ras-related protein Rab-2	123.64	8	6	62	0	-5.907E-03	1.861E-01	2.725E-01
tr|O61472|O61472_APLCA	Reductase-related protein	41.16	5	4	6	0	5.106E-01	2.106E-01	6.274E-01
tr|B6RB82|B6RB82_HALDI	Ribosomal protein l	56.78	8	4	17	0	4.286E-01	4.313E-02	-2.772E-01
tr|Q8ITC2|Q8ITC2_AEQIR	Ribosomal protein L11	62.3	4	2	23	0	2.603E-01	3.567E-01	1.620E-01
tr|Q8IT99|Q8IT99_AEQIR	Ribosomal protein L17A (Frag)	111.88	13	12	59	0	-6.590E-02	-3.207E-02	1.373E-01
tr|B6RB78|B6RB78_HALDI	Ribosomal protein S14	45.76	4	3	29	0	-2.463E-01	-9.732E-02	-9.663E-02
tr|Q70MN4|Q70MN4_CRAGI	Ribosomal protein S20	68.93	5	4	25	0	-2.212E-02	-1.520E-01	2.297E-02
tr|E3P7H5|E3P7H5_9MOLL	Ribosomal protein S25	70.86	5	4	25	0	2.196E-01	1.188E-01	-2.664E-02
tr|Q4H451|Q4H451_CRAGI	Ribosomal protein S5	116.34	4	3	17	0	-3.989E-01	2.674E-01	-1.152E-02
tr|A9LMJ6|A9LMJ6_HALDI	Ribosomal protein S9	80.87	9	5	42	0	-3.646E-01	3.898E-02	-3.556E-01
tr|B0L0Y3|B0L0Y3_PINFU	RNA-binding protein	82.96	18	12	9	0	9.617E-02	3.948E-01	2.982E-01
tr|B6RB22|B6RB22_HALDI	Serine/threonine-protein phosphatase	129.62	16	3	14	0	-1.277E-01	-3.863E-01	-8.666E-03

Table 2.2 (Continued)

Accession number [a]	Description [b]	-10lgP [c]	Peptides [d]	Unique [e]	Coverage [f]	Average ratios			
						Control	1	2	48
tr|Q8MUE3|Q8MUE3_9BIVA	Small nuclear ribonucleoprotein D2-like protein	55.13	3	2	29	0	-2.939E-01	1.010E-01	3.766E-01
tr|E6Y2Z7|E6Y2Z7_HALDV	Splicing factor arginine/serine-rich 4	88.35	5	4	49	0	-1.742E-01	-5.050E-01	-3.592E-02
tr|B1N693|B1N693_HALDI	Thioredoxin peroxidase 1	82.93	8	7	16	0	-6.496E-02	2.727E-01	2.769E-01
tr|B6RB35|B6RB35_HALDI	Transgelin	107.88	7	7	31	0	-3.532E-01	-2.768E-01	-8.685E-02
tr|H6UNP5|H6UNP5_9BIVA	Triosephosphate isomerase (Frag)	104.74	11	5	54	0	3.066E-02	-1.068E-01	-8.128E-02
tr|Q7YT99|Q7YT99_MYTGA	Twitchin	77.13	21	10	4	0	-3.810E-01	-3.955E-01	2.257E-02
tr|B0B031|B0B031_LITLI	Ubiquitin	134.53	9	6	47	0	9.148E-02	1.303E-01	-2.736E-01
tr|D2XEB0|D2XEB0_CRAHO	Ubiquitin (Frag)	169.98	15	9	51	0	-1.118E-01	-1.362E-01	-1.161E-02
tr|O96703|O96703_9CAEN	Vacuolar H+-ATPase (Frag)	69.76	5	4	19	0	3.799E-01	4.250E-01	-3.691E-01
tr|D7RP02|D7RP02_HALDV	Voltage-dependent anion channel 2-like protein	169.97	25	20	71	0	1.605E-01	2.096E-01	2.403E-02

[a] Uniprot SwissProt/Trembl accession number; [b] Description name assigned by Uniprot; [c] PEAKS studio search identification protein score; [d] Number of assigned peptides for protein identification; [e] Number of unique peptides for protein identification; [f] Percentage coverage.

Table 2.3 Proteins identified in *H. midae* haemocytes following sterile sea salt injection in four independent experiments. Fold changes were expressed as a ratio of bacterial challenge to the untreated control at 1, 2 and 48 hours p.i. following quantile normalisation and log2 transformation in CLC main workbench.

Accession number [a]	Description [b]	-10lgP [c]	Peptides [d]	Unique [e]	Coverage [f]	Average ratios			
						Control	1	2	48
G8A4W9|G8A4W9_9BIVA	14-3-3 protein	78.8	17	17	33	0	-0.037	-0.002	-0.096
H9LIY1|H9LIY1_CRAAR	26S protease regulatory subunit 6B (Frag)	49.17	6	4	16	0	0.038	-0.250	0.188
B6RB81|B6RB81_HALDI	40S ribosomal protein S18	51.99	7	6	33	0	0.073	-0.042	-0.006
B3TK56|B3TK56_HALDV	40S ribosomal protein S3a (Frag)	104.4	12	10	48	0	-0.049	-0.131	-0.190
B3TK66|B3TK66_HALDV	40S ribosomal protein S8	108	12	7	51	0	0.181	0.245	0.204
B3TK58|B3TK58_HALDV	60S acidic ribosomal protein P0	89.08	17	9	46	0	-0.038	0.037	0.035
B3TK87|B3TK87_HALDV	60S acidic ribosomal protein P2	71.57	4	4	33	0	0.116	0.019	-0.012
Q17UC2|Q17UC2_HALTU	84kDa heat shock protein	226	99	5	67	0	-0.322	-0.317	-0.076
B3SND4|B3SND4_HALDV	Actin depolymerisation factor/cofilin	73.2	7	5	28	0	0.185	-0.035	-0.008
B6RB19|B6RB19_HALDI	Actin	104.3	34	26	47	0	0.126	0.318	0.248
Q6U1K1|Q6U1K1_HALDH	Actin	273.5	112	2	96	0	-0.217	0.090	0.933
G8XUN4|G8XUN4_CRAAR	Adenosylhomocysteinase	41.88	4	2	6	0	0.221	0.189	-0.042
B3TK64|B3TK64_HALDV	ADP/ATP carrier protein (Fragment)	77.39	6	5	32	0	-0.103	0.083	0.147
B6RB72|B6RB72_HALDI	ADP-ribosylation factor 2	143.2	22	19	60	0	-0.016	-0.083	0.079
B3SN77|B3SN77_HALDV	Allograft inflammatory factor (Frag)	84.15	4	3	33	0	0.023	0.116	0.190
Q8ITH0|Q8ITH0_BIOGL	Alpha-actinin (Frag)	195.6	67	60	51	0	0.052	-0.011	-0.037
B6RB28|B6RB28_HALDI	Apoptosis-linked protein	34.49	3	3	13	0	-0.033	-0.146	0.088
Q000T7|Q000T7_PINFU	ATP synthase subunit alpha	162	55	31	60	0	-0.034	0.000	-0.140
B6RB43|B6RB43_HALDI	ATP synthase_ H+ transporting_ mitochondrial F1 cmplx	66.53	7	5	22	0	0.193	0.017	0.154
E5F064|E5F064_APLCA	ATP-dependent RNA helicase DDX5	117.9	23	18	26	0	0.139	0.021	0.274
I0JGU7|I0JGU7_SEPOF	Beta tubulin 1	190.5	46	4	68	0	0.076	0.098	-0.106
Q8MPR0|Q8MPR0_CRAGI	Bone morphogenic protein type 2 receptor	27.94	6	4	4	0	-0.393	-0.605	-0.580

Table 2.3 (Continued)

Accession number [a]	Description [b]	-10lgP [c]	Peptides [d]	Unique [e]	Coverage [f]	Average ratios			
						Control	1	2	48
B6RB21|B6RB21_HALDI	Calcineurin B	102	6	5	36	0	-0.126	-0.195	-0.146
B3TK60|B3TK60_HALDV	Calmodulin-dependent protein kinase (Frag)	99.76	6	6	20	0	-0.289	-0.421	-0.261
Q26268|Q26268_APLCA	Calreticulin	59.74	21	10	31	0	-0.256	0.081	0.031
A5LGG9|A5LGG9_CRAGI	Calreticulin	90.97	38	20	51	0	-0.008	-0.220	0.002
Q16958|Q16958_APLCA	Catalytic subunit of protein kinase A	71.05	8	8	22	0	-0.126	-0.423	-0.046
E6Y9P6|E6Y9P6_BIOGL	Cdc24-like protein	113.4	10	7	34	0	-0.232	0.010	0.083
B6RB18|B6RB18_HALDI	Chaperonin containing tcp1	158.4	55	51	59	0	-0.067	-0.234	-0.159
D1H0L8|D1H0L8_HALTU	Elongation factor 1-alpha	199.3	59	12	59	0	0.001	0.250	0.168
Q9BNW3|Q9BNW3_CHAAP	Elongation factor-2 (Frag)	70.14	16	12	17	0	-0.108	0.068	0.049
sp|O02654|ENO_LOLPE	Enolase	146.6	46	27	55	0	-0.053	-0.062	-0.026
B3TK44|B3TK44_HALDV	Fascin (Frag)	104.6	17	17	35	0	0.025	-0.200	0.003
Q8ITG6|Q8ITG6_BIOGL	Focal adhesion kinase (Frag)	70.3	9	8	46	0	0.620	0.038	-0.378
A3FKF6|A3FKF6_HALDH	Galectin 4-like protein transcript variant	62.67	3	3	10	0	0.167	0.524	0.250
B6RB97|B6RB97_HALDI	Gelsolin	122.1	20	19	58	0	0.075	-0.106	-0.124
Q0KHB8|Q0KHB8_CRAGI	Glucose-6-phosphate 1-dehydrogenase	127.2	34	26	52	0	-0.050	0.091	-0.024
A5LGG7|A5LGG7_CRAGI	Glucose-regulated protein 94	168.5	101	87	62	0	0.133	0.057	0.094
B3TK24|B3TK24_HALDV	Glutathione-S-transferase isoform	63.55	6	5	22	0	0.046	-0.043	-0.184
E4W3F6|E4W3F6_HALDV	Glutathione-S-transferase	80.71	5	5	29	0	-0.003	0.216	0.350
B6RB30|B6RB30_HALDI	Glyceraldehyde-3-phosphate dehydrogenase	221.4	32	25	68	0	0.121	0.161	0.085
Q6TP31|Q6TP31_PINFU	G-protein a-subunit s class	125.5	20	6	33	0	-0.088	0.178	0.295
E6Y2Z1|E6Y2Z1_HALDV	GTP-binding nuclear protein Ran	111.4	7	7	30	0	0.093	0.122	0.237
Q27J09|Q27J09_APLCA	Guanine nucleotide-binding protein G(Q)_ alpha subunit	138.2	30	9	56	0	-0.263	0.068	-0.345
Q8I0U4|Q8I0U4_HALTU	H2 protein (Frag)	290	176	39	36	0	0.048	0.215	-0.002
Q564J1|Q564J1_APLCA	Haemocyanin	325.5	242	34	43	0	0.145	-0.154	-0.153
C1KC83|C1KC83_HALDV	Heat shock cognate protein 70	210.7	86	27	70	0	0.535	0.312	0.577
C1KC84|C1KC84_HALDV	Heat shock inducible protein 70	145.9	33	13	35	0	0.157	0.070	0.141

Table 2.3 (Continued)

Accession number [a]	Description [b]	-10lgP [c]	Peptides [d]	Unique [e]	Coverage [f]	Average ratios			
						Control	1	2	48
B8Y4I8|B8Y4I8_BIOGL	Heat shock protein 60	84.12	22	18	30	0	-0.026	-0.128	-0.046
A2TF45|A2TF45_9BIVA	Heat shock protein 70	168.1	74	15	55	0	-0.228	0.029	-0.207
Q9GP18|Q9GP18_HALTU	Hemocyanin (Frag)	325.5	242	34	43	0	-0.060	0.102	0.009
Q53IP9|Q53IP9_MEGCR	Hemocyanin 1	161.3	199	145	35	0	0.057	0.196	-0.078
Q1MVA1|Q1MVA1_MEGCR	Hemocyanin 2	218.9	179	116	32	0	0.030	0.200	0.125
G3FPE6|G3FPE6_HELLU	Hemocyanin alphaD-subunit	168.3	193	140	34	0	0.154	0.151	-0.082
G3FPE7|G3FPE7_HELLU	Hemocyanin alphaN-subunit (Frag)	144.4	141	96	31	0	-0.085	0.003	-0.171
G3FPE5|G3FPE5_HELLU	Hemocyanin beta-subunit	148.4	153	109	28	0	-0.187	-0.115	-0.356
B5RHQ6|B5RHQ6_9MOLL	Hemocyanin fgh (Frag)	101.2	30	13	22	0	-0.040	0.668	1.001
C7FEG7|C7FEG7_HALDV	Hemocyanin isoform 1 (Frag)	285.7	215	110	38	0	0.170	0.282	0.182
Q27Q57|Q27Q57_SEPOF	Hemocyanin subunit 1	182.1	189	85	30	0	0.214	0.065	-0.168
Q27Q56|Q27Q56_SEPOF	Hemocyanin subunit 2 (Frag)	163.7	188	92	32	0	0.040	-0.070	-0.392
Q2Z0F4|Q2Z0F4_HALAI	Hemocyanin type 2 (Frag)	106.6	10	3	50	0	0.079	0.411	-0.003
Q9U5P3|Q9U5P3_HALTU	Hemocyanin type 2 protein (Frag)	247.4	112	5	38	0	0.015	-0.127	0.033
H6T4K5|H6T4K5_MYTGA	Histone H2A	107.8	11	3	61	0	0.005	0.168	0.076
H9LTR9|H9LTR9_CRAAR	HMGB-like protein	81.39	15	13	30	0	-0.632	-0.388	-0.145
Q6KC56|Q6KC56_MEGCR	Keyhole limpet hemocyanin1	158.4	179	131	34	0	-0.012	0.124	-0.135
Q6KC55|Q6KC55_MEGCR	Keyhole limpet hemocyanin2	218.9	179	116	32	0	0.026	0.193	0.117
B6RB90|B6RB90_HALDI	Malate dehydrogenase (Frag)	145.8	17	10	56	0	-0.032	0.008	0.104
Q86DP1|Q86DP1_9VEST	Malate dehydrogenase (Frag)	114.4	26	14	55	0	-0.026	0.411	-0.013
B6RB86|B6RB86_HALDI	Map kinase (Frag)	92.43	8	4	44	0	-0.144	-0.146	-0.021
A6MD73|A6MD73_HALDI	Mx	60.22	6	5	11	0	-0.298	-0.799	-0.487
Q4PLU5|Q4PLU5_9BIVA	Myosin VI (Frag)	85.7	112	91	61	0	-0.376	-0.218	-0.005
A1ILZ8|A1ILZ8_MIZYE	Non muscle myosin (Frag)	143.2	94	37	55	0	-0.441	0.048	-0.186
Q45R40|Q45R40_APLCA	Nonmuscle myosin II (Frag)	247.9	224	148	61	0	0.180	0.023	-0.056
Q8SWQ7|Q8SWQ7_LOLPE	Non-muscle myosin II heavy chain	200.8	237	165	64	0	-0.104	-0.041	-0.246

Table 2.3 (Continued)

Accession number [a]	Description [b]	-10lgP [c]	Peptides [d]	Unique [e]	Coverage [f]	Average ratios			
						Control	1	2	48
B6RB47|B6RB47_HALDI	Nucleoside diphosphate kinase	95.24	8	6	30	0	-0.159	-0.087	-0.107
B6RAZ8|B6RAZ8_HALDI	Omega class glutathione-s-transferase 1	85.39	5	5	17	0	-0.289	-0.131	-0.025
Q8ITG7|Q8ITG7_BIOGL	P38 mitogen activated protein kinase	94.65	26	15	51	0	-0.016	0.417	-0.056
D3WFS3|D3WFS3_9CAEN	Peptidyl-prolyl cis-trans isomerase	86.31	14	7	46	0	0.039	0.290	0.261
sp|H2A0M7|PLSP_PINMG	Peroxidase-like protein	52.16	9	6	8	0	-0.107	0.075	-0.050
D3K380|D3K380_PINFU	Peroxiredoxin	110.1	14	5	34	0	0.096	-0.113	-0.363
sp|O61471|PGK_APLCA	Phosphoglycerate kinase	52.16	5	4	11	0	0.288	0.301	-0.175
Q596I0|Q596I0_CRAGI	Phosphorylase	95.41	84	79	47	0	-0.187	-0.093	-0.286
C7EAA2|C7EAA2_HALAI	PL10-like protein	193.7	50	31	43	0	-0.071	-0.303	-0.073
Q9NGA1|Q9NGA1_SPISO	Poly(A)-binding protein (Frag)	49.38	8	4	20	0	0.499	1.171	0.422
Q8I9P5|Q8I9P5_BIOGL	Poly-ubiquitin	81.79	6	2	13	0	-0.237	-0.445	-0.130
G9BBC5|G9BBC5_AEQIR	Programmed cell death 4	30.11	6	5	9	0	0.035	-0.959	-0.020
B6RB41|B6RB41_HALDI	Proteasome subunit alpha type	108.4	8	7	36	0	0.171	0.124	0.169
B6RB63|B6RB63_HALDI	Protein disulfide isomerase	205.7	56	41	60	0	0.014	0.148	0.100
G9HQ39|G9HQ39_9BIVA	Protein phosphatase 1 (Frag)	113.7	7	6	47	0	0.023	0.197	0.196
B6RB65|B6RB65_HALDI	Psmc6 protein	79.76	5	4	21	0	-0.104	0.090	0.192
G9K381|G9K381_HALDV	Putative 40S ribosomal protein S18	51.99	7	6	33	0	0.085	-0.046	0.003
G9K385|G9K385_HALDV	Putative polyadenylate-binding protein 1 (Frag)	82.43	13	9	20	0	0.231	-0.056	-0.055
I3VFQ9|I3VFQ9_9EUPU	Putative ribosomal protein	81.79	9	3	34	0	-0.268	-0.442	-0.157
B3TK70|B3TK70_HALDV	Putative RNA-binding protein	57.11	7	5	36	0	0.463	0.184	-0.238
B3TK33|B3TK33_HALDV	Putative uncharacterized protein (Frag)	68.74	4	3	14	0	-0.037	-0.055	-0.270
Q0KHB6|Q0KHB6_CRAGI	Pyruvate kinase	36.04	3	2	4	0	0.055	0.192	0.008
B8XW76|B8XW76_HALDV	QM-like protein	85.05	25	8	57	0	0.034	-0.070	-0.078
B6RB76|B6RB76_HALDI	RAB protein	153	25	21	81	0	0.179	0.339	0.064
A7L3I9|A7L3I9_HALCR	RAB1 (Frag)	145.4	19	7	85	0	-0.114	-0.149	-0.204
B6RB17|B6RB17_HALDI	Raminin receptor	107.8	11	5	44	0	0.212	0.341	0.028

Table 2.3 (Continued)

Accession number [a]	Description [b]	-10lgP [c]	Peptides [d]	Unique [e]	Coverage [f]	Average ratios			
						Control	1	2	48
B6RB29|B6RB29_HALDI	Ran-1-prov protein	111.4	7	7	30	0	0.091	0.121	0.234
H9LHX4|H9LHX4_CRAAR	Ras-like GTP-binding protein Rho1 isoform 1	91.49	5	5	27	0	0.220	0.096	0.018
B6RB23|B6RB23_HALDI	Ras-related protein Rab-1A	175.7	23	7	74	0	-0.101	-0.143	-0.200
H6WB72|H6WB72_PINFU	Relish	33.44	8	4	5	0	-0.186	-0.082	-0.048
E6Y9P8|E6Y9P8_BIOGL	Rho-like protein	102.7	7	7	26	0	0.055	-0.082	-0.048
B6RB82|B6RB82_HALDI	Ribosomal protein l	45.68	5	2	14	0	-0.163	-0.171	-0.225
Q8ITA1|Q8ITA1_AEQIR	Ribosomal protein L12	68.61	5	2	19	0	0.022	0.271	0.637
Q8IT99|Q8IT99_AEQIR	Ribosomal protein L17A (Frag)	59.6	12	12	72	0	0.066	-0.050	-0.027
E3P7F5|E3P7F5_9MOLL	Ribosomal protein L23 (Frag)	25.6	8	7	50	0	0.108	-0.166	-0.064
Q8ITC5|Q8ITC5_AEQIR	Ribosomal protein L30	33.65	2	2	11	0	0.320	0.029	-0.124
Q8ITA0|Q8ITA0_AEQIR	Ribosomal protein L32	38.69	2	2	15	0	0.156	0.056	0.179
B6RB96|B6RB96_HALDI	Ribosomal protein l5 (Frag)	124.7	27	27	58	0	0.133	0.179	0.032
B6RB78|B6RB78_HALDI	Ribosomal protein S14	66.03	3	3	34	0	-0.120	0.170	0.000
E3P7H1|E3P7H1_9MOLL	Ribosomal protein S16 (Frag)	48.24	4	3	15	0	0.173	0.330	0.286
E3P7G3|E3P7G3_9MOLL	Ribosomal protein S2 (Frag)	57.52	9	5	29	0	-0.314	-0.660	-0.360
Q8MUE5|Q8MUE5_9BIVA	Ribosomal protein S20	47.52	3	3	24	0	-0.054	-0.005	-0.079
E3P7G4|E3P7G4_9MOLL	Ribosomal protein S3 (Frag)	99.82	7	4	34	0	0.151	-0.183	0.205
B6RB83|B6RB83_HALDI	Ribosomal protein S4 (Frag)	116.4	13	12	44	0	0.023	0.027	0.097
Q70ML8|Q70ML8_CRAGI	Ribosomal protein S5 (Frag)	54.34	3	3	12	0	-0.015	0.201	-0.361
E3P7G7|E3P7G7_9MOLL	Ribosomal protein S5 (Frag)	65.04	5	4	21	0	-0.326	-0.392	-0.400
Q8ITA9|Q8ITA9_AEQIR	Ribosomal protein S7	52.22	17	15	56	0	0.081	-0.030	0.240
H6UNR0|H6UNR0_9BIVA	S-adenosylmethionine synthase (Frag)	108.9	17	6	32	0	0.023	0.181	0.161
B2KKR0|B2KKR0_PINFU	Sarco/endoplasmic reticulum calcium ATPase isoform A	48.52	9	3	8	0	-0.043	-0.249	-0.126
B6RB22|B6RB22_HALDI	Serine/threonine-protein phosphatase	142.3	26	10	44	0	0.076	-0.216	0.057
B6RB01|B6RB01_HALDI	Sigma class glutathione-s-transferase 2	20.17	7	7	22	0	0.167	-0.204	-0.003
B6RB52|B6RB52_HALDI	Signal sequence receptor beta-like protein	55.41	2	2	10	0	0.101	-0.027	-0.239

Table 2.3 (Continued)

Accession number [a]	Description [b]	-10lgP [c]	Peptides [d]	Unique [e]	Coverage [f]	Average ratios			
						Control	1	2	48
A7U8D3|A7U8D3_APLCA	Small G-protein	64.33	5	4	21	0	-0.004	-0.147	0.242
Q6W955|Q6W955_9VEST	Sodium/potassium ATPase alpha subunit (Frag)	123.5	16	5	44	0	-0.088	0.240	-0.070
E6Y2Z7|E6Y2Z7_HALDV	Splicing factor arginine/serine-rich 4	81.61	3	3	22	0	0.191	-0.036	-0.192
B6DVV3|B6DVV3_APLCA	Src tyrosine kinase 1	39.54	5	2	7	0	0.155	-0.091	0.112
E3P7H4|E3P7H4_9MOLL	Ribosomal protein S20	46.01	2	2	19	0	0.268	-0.124	0.311
B1N693|B1N693_HALDI	Thioredoxin peroxidase 1	128.3	20	13	43	0	0.144	0.163	0.249
B1N694|B1N694_HALDI	Thioredoxin peroxidase 2	117.1	17	6	49	0	0.040	-0.226	0.017
E1B300|E1B300_9BIVA	Thioredoxin peroxidase	113	12	4	31	0	0.130	-0.113	-0.371
B6RB35|B6RB35_HALDI	Transgelin	104.7	8	6	28	0	0.042	-0.030	-0.224
H9LJ32|H9LJ32_CRAAR	Triosephosphate isomerase	94.93	22	13	53	0	0.022	0.156	-0.671
Q7YZR1|Q7YZR1_HALAI	Tropomyosin 4 (Frag)	115.5	16	8	59	0	0.105	0.081	0.000
B6RB46|B6RB46_HALDI	Troponin	42	2	2	11	0	0.682	0.437	0.822
H9LIG1|H9LIG1_CRAAR	Tubulin beta-2B chain-like protein (Frag)	144.7	28	8	67	0	0.398	-0.029	0.190
Q7YT99|Q7YT99_MYTGA	Twitchin	60.75	57	40	8	0	0.698	0.381	0.246
A8DRV0|A8DRV0_9MOLL	Vacuolar ATP synthase subunit B (Frag)	70.35	12	9	41	0	-0.038	0.215	0.081
C7EAA1|C7EAA1_HALAI	Vasa-like protein	72.83	9	3	9	0	-0.181	-0.113	0.398
B0RZD4|B0RZD4_PECMA	Vitellogenin	63.3	35	22	11	0	-0.028	0.362	0.607
D7RP02|D7RP02_HALDV	Voltage-dependent anion channel 2-like protein	139	19	18	50	0	0.233	0.161	0.180

[a] Uniprot SwissProt/Trembl accession number; [b] Description name assigned by Uniprot; [c] PEAKS studio search identification protein score; [d] Number of assigned peptides for protein identification; [e] Number of unique peptides for protein identification; [f] Percentage coverage.

2.3.4 Differentially expressed proteins identified in bacterial-challenged and mock-infected *H. midae* haemocytes

In order to identify haemocyte proteins that were differentially expressed in response to a bacterial-challenge, one-way ANOVA was used to compare the relative expression values between the control (unchallenged animals) and the experimental groups. A similar analysis was performed on the mock-infected list of proteins to account for the wounding response. Thus, 11 proteins were identified as statistically significantly (P<0.05) changed in four biological replicates, and five in three biological replicates (Table 2.4). The mock-infected experiment identified seven statistically significant proteins in four replicates and three proteins from three biological replicates (Table 2.5).

Calmodulin 2, haemocyanin alphaD-subunit, ATP-binding cassette transporter sub-family A, H2 protein and haemocyanin type 2 protein were up-regulated whilst calreticulin, isocitrate dehydrogenase (NADP), ribosomal protein S9, putative RNA-binding protein, splicing factor arginine/serine-rich 4 and glucose-6-phosphate 1-dehydrogenase were down-regulated in haemocytes sampled from the bacterial-challenged group (Table 2.4). Calmodulin-dependent protein kinase, glutathione-S-transferase and allograft inflammatory factor showed initial down-regulation (1 and 2 hours p.i.) followed by up-regulation at 48 hours p.i., whilst Rab-7-like protein was initially up-regulated and subsequently down-regulated at 48 hours p.i. The average relative protein expression of cAMP-dependent protein kinase was up-regulated at 1 hour p.i., down-regulated at 2 hours p.i. and again up-regulated at 48 hours p.i.

The mock-infected group showed up-regulation for poly(A)-binding protein and troponin and a down-regulated pattern for ribosomal protein S5 and haemocyanin subunit 2 (Table 2.5). Nonmuscle myosin II, haemocyanin and H2 protein were initially up-regulated, but were down-regulated at 48 hours p.i. Malate dehydrogenase was down-regulated at 1 hour p.i., up-regulated at 2 hours p.i. and again down-regulated at 48 hours p.i. Src tyrosine kinase 1 and ribosomal protein S20 were both up-regulated at 1 hour p.i., down-regulated at 2 hours p.i. and up-regulated at 48 hours p.i.

Table 2.4 Differentially expressed proteins in *H. midae* haemocytes following bacterial-challenge at 1, 2 and 48 hours post-injection. Fold changes are expressed as log_2 transformed, normalised ratios to the control sample (treatment – control). The data represent average fold-change from four independent biological replicates. One-way ANOVA with Tukey's pairwise comparison was used to calculate statistical significance (P<0.05) from four biological replicates. Three replicates were used for statistical analysis (indicated by asterisk *) in instances where one replicate was discordant.

Accession number	Protein identified	P-value	Mean fold change			
			0	1	2	48
P31319|KAPR_APLCA	cAMP-dependent protein kinase regulatory subunit	0.005	0	0.630	-0.645	1.086
tr|A5LGG9|A5LGG9_CRAGI	Calreticulin	0.003	0	-0.087	-0.492	-0.147
tr|B3SN77|B3SN77_HALDV	Allograft inflammatory factor	0.012	0	0.068	-0.195	1.955
tr|B3TK26|B3TK26_HALDV	Calmodulin 2	0.00935	0	0.469	0.290	1.438
tr|B3TK60|B3TK60_HALDV	Calmodulin-dependent protein kinase	0.00003	0	-0.684	-0.923	1.138
tr|C1KBI9|C1KBI9_9BIVA	Rab7-like protein	0.02	0	0.129	0.269	-0.049
tr|G3FPE6|G3FPE6_HELLU	Haemocyanin alphaD-subunit	0.009	0	0.899	0.934	0.381
tr|Q2WEC5|Q2WEC5_PECMA	ATP-binding cassette transporter sub-family A	0.04107	0	0.996	0.333	0.075
tr|Q5QGY7|Q5QGY7_CRAGI	Isocitrate dehydrogenase [NADP]	0.018	0	-0.642	0.007	-0.026
tr|Q8I0U4|Q8I0U4_HALTU	H2 protein	0.03046	0	0.643	0.703	0.020
tr|Q9U5P3|Q9U5P3_HALTU	Haemocyanin type 2 protein	0.018	0	0.612	0.916	0.319
tr|A9LMJ6|A9LMJ6_HALDI	*Ribosomal protein S9	0.0169	0	-0.572	-0.122	-0.467
tr|B3TK70|B3TK70_HALDV	*Putative RNA-binding protein	0.0052	0	-0.754	-0.729	-0.357
tr|E6Y2Z7|E6Y2Z7_HALDV	*Splicing factor arginine/serine-rich 4	0.0066	0	-0.307	-0.748	-0.186
tr|Q0KHB8|Q0KHB8_CRAGI	*Glucose-6-phosphate 1-dehydrogenase	0.0299	0	-0.708	-0.591	-0.325
tr|Q19BK2|Q19BK2_HALDI	*Glutathione-S-transferase isoform 1	0.0417	0	-0.945	-1.118	0.702

Table 2.5 Differentially expressed proteins identified in *H. midae* haemocytes following mock-infection at 1, 2 and 48 hours post-injection. Fold changes are expressed as log_2 transformed, normalised ratios to the control sample (treatment – control). The data represent average fold change from four independent biological replicates. One-way ANOVA with Tukey's pairwise comparison was used to calculate statistical significance ($P<0.05$) from four biological replicates. Three replicates were used for statistical analysis (indicated by asterisk) in instances where one replicate was discordant.

Accession number	Protein identified	P-value	Mean fold change			
			0	1	2	48
E3P7G7|E3P7G7_9MOLL	Ribosomal protein S5	0.0430	0	-0.326	-0.392	-0.4
Q27Q56|Q27Q56_SEPOF	Haemocyanin subunit 2	0.0379	0	0.04	-0.07	-0.392
Q45R40|Q45R40_APLCA	Nonmuscle myosin II	0.0158	0	0.1804	0.0227	-0.056
Q564J1|Q564J1_APLCA	Haemocyanin	0.0352	0	0.1454	-0.154	-0.153
Q86DP1|Q86DP1_9VEST	Malate dehydrogenase	0.0201	0	-0.026	0.4111	-0.013
Q8I0U4|Q8I0U4_HALTU	H2 protein	0.0158	0	0.0475	0.2146	-0.002
Q9NGA1|Q9NGA1_SPISO	Poly(A)-binding protein	0.0268	0	0.4994	1.171	0.4219
B6DVV3|B6DVV3_APLCA	*Src tyrosine kinase 1	0.0090	0	0.153	-0.2	0.1391
B6RB46|B6RB46_HALDI	*Troponin	0.0074	0	1.0849	0.9076	0.8322
E3P7H4|E3P7H4_9MOLL	*Ribosomal protein S20	0.0044	0	0.3115	-0.339	0.2909

2.4 Discussion

Minimising the huge economic loss associated with disease outbreaks on abalone farms (Braid et al., 2005; Chang et al., 2005; Sawabe et al., 2007) necessitates an improvement of our knowledge of abalone immunity. Proteome characterisation of the immune response elicited by *H. midae* could reveal important pathways and proteins applicable to biomarker development for the early and rapid detection of bacterial infection. To date, proteomic research investigating the immune response in abalone has mainly focussed on 2-D PAGE analysis (Slattery et al., 2012) which has its limitations and may overlook proteins of interest. There are currently no infection proteomic studies conducted in *H. midae*. In this study, MS and iTRAQ analysis were employed to identify differentially expressed proteins in *H. midae* haemocytes following challenge with *V. anguillarum*. This provided a more in-depth analysis than what has been achieved with 2D-PAGE and led to the identification of 16 proteins that were statistically significantly changed in response to bacterial challenge.

A transient drop in circulating haemocyte numbers, also known as haemacytopenia, has been well documented in stressed and infected abalone (Malham et al., 2003; Hooper et al., 2007; Cheng et al., 2004; Hooper et al., 2012) and in pacific white shrimp (Song et al., 2003; Pan et al., 2008). This cellular parameter can thus be used as an effective and simple way to monitor the physiological state and immune response of *H. midae*. The decreased THC observed in the bacterial challenged group at 48 hours p.i. was absent in the mock-infected and unchallenged groups (Figure 2.4), suggesting that the bacterial pathogen induced an immune response in *H. midae*. These results correlated well with previous bacterial challenge trials (Kemp & Coyne, 2011).

Having established immune stimulation in *H. midae*, iTRAQ experimentation and hierarchical cluster analysis were used to establish a timeline for further analysis of changes in the abalone haemocyte proteome. Two control groups (unchallenged animals) were included to ensure reproducibility. Differences in the expression patterns of the control haemocyte samples were observed in the resulting heat-map tree (Figure 2.5), suggesting some disparity. Variation across identical samples has been reported in iTRAQ studies (Chong et al., 2006) and further explored in a study comparing DIGE,

cICAT and iTRAQ (Wu et al., 2006). Although more sensitive, iTRAQ suffers from errors in precursor ion isolation which can lead to reduced reliability. Another disadvantage is that samples are processed separately prior to the combining step, potentially introducing errors such as variable tryptic digestion (Wu et al., 2006). Finally, inherent biological variation that exists between individual organisms is another source of sample difference (Molloy et al., 2003). A number of experimental design strategies that circumvent these problems (Song et al., 2008) were considered in the design of all subsequent iTRAQ experiments. Nevertheless, both an early and late immune response to bacterial-challenge was observed in *H. midae*, resulting in the selection of time points 1, 2 and 48 hours p.i. for further analysis.

Total protein expression profile experiments require full disclosure of assigned scores, set threshold values, queried database and accompanying algorithm used, sequence coverage, unique number of peptides assigned to the protein match and the filtering of redundant entries of multiple protein hits within the same family (Carr et al., 2004). These guidelines are a consequence of early shotgun proteomic experiments which suffered from high false positive rates (Carr et al., 2004). The number of MS and MS/MS scans is an important factor for obtaining high quality spectra and is critical to identifying proteins accurately. Increasing the MS/MS ion injection time has been shown to significantly increase the number of identified peptides and further improve spectra quality (Wenner & Lynn, 2004). A high number of MS and MS/MS spectra (Table 2.1) were obtained in all four iTRAQ experiments assessing haemocyte protein expression profiles in the early and late immune response of *H. midae*. This indicates the spectra used for subsequent peptide and protein identification were of a sufficiently high quality.

Although the abalone genome is yet to be sequenced, proteome characterisation can be achieved using sequences from related organisms (Shevchenko et al., 2001). Using a database that is taxonomically too narrow could exclude homologous proteins from other species, resulting in unassigned peptides. In order to broaden the identification rate and limit protein omission, an “all molluscan” species protein database was used for screening the abalone haemocyte proteome.

Since the number of protein entries identified was initially fairly high, a stringent filtering method was applied to minimise the number of false positives and thus identify proteins of interest with greater confidence. Upon merging and filtering the respective iTRAQ experiments (Table 1.1), 118 proteins (bacterial-challenged) and 144 proteins (mock-infected) were identified with a confidence cut-off ≥95%. A decoy database was used to estimate a false discovery rate (FDR) of 1%. FDR has been defined as the number of falsely identified peaks divided by the total number of peaks found by the algorithm (Yang et al., 2009). It is recommended that large-scale proteomic studies make use of a target-decoy strategy to validate search results (Elias & Gygi, 2010). The scoring system used by PEAKS studio is denoted by a -10lgP score, calculated from P-values on an increasing scale. The PEAKS studio manual describes the three steps of how this is calculated; first a linear discriminative function (LDF) score is used to measure the quality of the peptide spectrum matches (PSM). This score is then converted to a more traditional P-value score where the smaller a P-value score is, the less likely the PSM is due to a random match. Finally this score is converted to the displayed score of -10lgP, where significant matches will have a higher -10lgP score. As an example, a P-value of 1% will have a -10lgP of 20. Filtering protein entries with a -10lgP score greater than 20 may be regarded as a relatively high confidence threshold. Following peptide and protein identification using PEAKS studio, protein entries were filtered according to the guidelines provided by Carr et al. (2004). Protein entries with a -10lgP score of 20 or higher were retained and at least 2 unique peptides were considered necessary to identify a protein. Multiple protein hits from the same family were condensed by retaining the protein entry with the highest -10lgP score.

The importance of including multiple repeat experiments to improve the reliability of iTRAQ-derived data has previously been explored (Gan et al., 2007). Technical replicates, whereby the same biological sample is analysed multiple times, provide the least amount of variation within experiments. Biological replicates, on the other hand, can be more advantageous to a successful iTRAQ study, since these consider variations between animals (Gan et al., 2007). Thus, six animals were sampled at each time point and the haemolymph pooled to reduce inherent biological variation. iTRAQ experiments were merged to ensure a high level of reproducibility, at the expense of proteins being excluded if not identified in both experiments. It is important to note that proteins

identified in this study are biased toward soluble cytosolic proteins, owing to the lysis buffer and the pH strips used for fractionation (pH 4-7), which would have resulted in the loss of cationic peptides such as antimicrobial peptides. Thus, only a partial description of the *H. midae* haemocyte proteome is described. However, since most immune proteins are not likely to be membrane-bound but rather, humoral or present within the cell cytoplasm, this bias was not considered to significantly influence the proteins identified.

To obtain relative fold change expression values, the quantification values from each experimental sample was normalised to the respective control and expressed as a $\log_2$ ratio. There have been reports that iTRAQ suffers from ratio compression which underestimates fold changes (Karp et al., 2010; Ow et al., 2009; Savitski et al., 2013). It has however been shown that extensive sample fractionation can both enhance proteome coverage and alleviate the issue of ratio compression (Warren et al., 2010; Ow et al., 2011). In this study, off-gel fractionation was performed to reduce sample complexity by resolving samples into 12 fractions according to their isoelectric point within a liquid medium.

Identifying differential expression in iTRAQ data remains a contentious issue. Early expression studies used ratio thresholds as determinants of differential expression (Karp & Lilley, 2007). However, the criteria for thresholds are inconsistent and vary from study to study (Hill et al., 2008). Traditional statistical tests using one way analysis of variance (ANOVA), although time-consuming, have the advantage of using the combined data from multiple experiments and determining the significance of the results (Oberg et al., 2008). Although ANOVA models have been designed to automate this analysis (Hill et al., 2008; Oberg et al., 2008), the choice of model used depends on the research question. Manual calculation of ANOVA has been successfully used in a number of iTRAQ studies (Unwin et al., 2006; Keshamouni et al., 2006; Jagtap et al., 2006) and provides applicable *P*-values for differential analysis without the use of a "black-box" system. Statistically significant changes were identified in 16 proteins in response to bacterial-challenge (Table 2.4) and 10 proteins in the mock-infected group (Table 2.5). The differentially expressed proteins identified in the bacterial-challenge experiments appear to have immune response-related functions and shall be discussed within this context.

Allograft inflammatory factor-1

Upon pathogen recognition, proinflammatory cytokines and chemokines are secreted by immune cells (Janeway & Medzhitov, 2002) to modulate the immune response, activate cell signalling pathways, release nitric oxide (NO) and enhance phagocytosis (Barcia et al., 2008; Ottaviani et al., 2000). Allograft inflammatory factor-1 (AIF-1) is a calcium binding EF-hand cytokine which has been shown to be associated with immune cell activation and the inflammatory response (Zhao et al., 2013; Yang et al., 2005; Liu et al., 2007). Analysis of the immune response in *H. midae* following bacterial-challenge indicated AIF-1 expression was initially down-regulated and then up-regulated. Similar regulatory patterns for AIF-1 have been identified in other molluscs, including: *Venerupis philippinarum* (Zhang et al., 2011), *Pinctada martensii* (Li et al., 2013), *Crassostrea gigas* (Zhang et al., 2013), *C. ariakensis* (Xu et al., 2014) and *Haliotis discus discus* (De Zoysa et al., 2010). Recombinant AIF-1 in *C. gigas* stimulated the phagocytic activity of granulocytes and enhanced the expression of several cytokine mRNA levels (Zhang et al., 2013). Expression of AIF-1 in *H. midae* is predicted to exert a similar effect on haemocyte phagocytic activity and cytokine expression.

cAMP-dependent protein kinase regulatory subunit

A cAMP-dependent protein kinase regulatory subunit was found to be significantly up-regulated at 1 and 48 hours p.i. (Table 2.4). cAMP dependent protein kinase, also known as protein kinase A (PKA), forms part of a family of enzymes whose activity is regulated by fluctuating levels of cyclic AMP and regulates a number of cellular processes via the cyclic AMP signalling pathway. PKA is a heterotetramer comprised of two catalytic subunits and two regulatory subunits (Johnson et al., 2001). Increased levels of cAMP bind to the regulatory subunits causing allosteric changes which release the catalytic subunits. Inhibition of PKA in *M. galloprovincialis* haemocytes resulted in a decrease in noradrenaline (Cao et al., 2004) and nitric oxide (Novas et al., 2004) production by haemocytes. Noradrenaline has been shown to exert a dose-dependent inhibitory effect on phagocytosis in *C. gigas* via the cAMP protein kinase pathway (Lacoste et al., 2001), emphasising the function PKA plays in haemocyte activation. Although its role in *H. midae* haemocyte function has yet to be determined, the identification of a differentially

expressed regulatory subunit in this study may provide the first evidence of its role in the abalone immune response.

Calmodulin and calmodulin-dependent protein kinase

Significant changes in expression of both calmodulin (CaM) and calmodulin-dependent protein kinase were detected. The role CaM plays in immune cells is complex and multi-layered as it modulates a number of immune-related pathways (Racioppi & Means, 2008; Racioppi & Means, 2012), as well as regulating cellular contraction (Cheresh et al., 1999). Myosin II has been shown to promote contraction in cells by forming an association with actin which is modulated by a Ca^{2+}/calmodulin-dependent myosin light chain kinase (Kolega & Taylor, 1993). Microarray analysis of *Haliotis discus discus* following a viral haemorrhagic septicaemia virus challenge identified the calmodulin gene as being up-regulated at 24 hours p.i. Similar studies of gene expression in response to a bacterial-challenge in *Haliotis diversicolor* identified the calmodulin gene in haemocytes, although its expression was not found to change significantly at 36-40 hours post-challenge (Wang et al., 2008). This study showed that calmodulin was significantly up-regulated in *H. midae* haemocytes, particularly at 48 hours p.i. (1.438 log2 fold-change) (Table 2.4). Similarly, the expression pattern of calmodulin-dependent protein kinase indicated that the protein was up-regulated at 48 hours p.i. CaM contains four Ca^{2+} binding motifs which, upon binding, increase its affinity for target enzymes such as calmodulin-dependent protein kinase (Racioppi et al., 2012). Calmodulin-dependent protein kinase forms part of the larger multifunctional Ca^{2+}/CaM-dependent Ser-Thr kinase (CaMK) family which phosphorylate a number of target substrates. There is increasing evidence that the CaMK family regulate important immune functions of the innate immune response (Racioppi & Means, 2008; X. Zhang et al., 2011). Experimental evidence for these enzymes playing a similar role in the immune response of *H. midae* has not been previously reported.

Ribosomal proteins S9, S5 and S20

Ribosomal protein S9 and ribosomal proteins S5 and S20 were down-regulated in the bacterial-challenged and mock-infected groups, respectively (Table 2.4 and 2.5). These proteins form part of the 40S ribosomal protein which is involved in protein synthesis through binding of the free 5' end of mRNA molecules, thus initiating protein translation (Berthelot et al., 2004). Differential expression of ribosomal proteins may indicate regulation of protein synthesis in response to bacterial-challenge or wounding (Lindstro & Zhang, 2008; Fukushi et al., 2001). The host response to physical stressors is known to induce changes in gene translation and protein synthesis, while altered translation rates have been reported in certain marine organisms following injury, infection, heat shock and exposure to toxic compounds (Snyder et al., 2001; Li et al., 2007a; Jurgen et al., 2011; Ji et al., 2013; Rufino-Palomares et al., 2011; Tomanek, 2014; Muralidharan et al., 2012). The 40S ribosomal gene has been found to be differentially expressed in bacterial-challenged *H. diversicolor* haemocytes (Wang et al., 2008), *P. stylirostris* hepatopancreas tissue infected with White spot syndrome virus (Dhar et al., 2003) and LPS-challenged coelomocytes of the purple sea urchin *Strongylocentrotus purpuratus* (Nair et al., 2005). More recently, shotgun proteomic studies indicate differential expression of the 40S ribosomal protein in infected gill protein from *Danio renio* (Lü et al., 2014), *Eriocheir sinensis* haemocytes infected with *Spiroplasma eriocheiris* (Meng et al., 2014) and LPS-challenged coelomic fluid from *S. purpuratus* (Dheilly et al., 2013).

RNA binding protein and splicing factor arginine/serine-rich 4

The importance of transcriptional regulation in the bacterial-challenged group may be reflected by the observed decrease in expression of a putative RNA-binding protein and splicing factor arginine/serine-rich 4 (Table 2.4). Serine/arginine-rich splicing factors (SF) are essential in splicing pre-mRNA molecules and are important in mRNA metabolism (Haynes & Iakoucheva, 2006). RNA-binding protein is responsible for the regulation of gene expression at both the transcriptional and translational levels (Lee & Schedl, 2006).

Calreticulin

A calreticulin protein identified in this study was significantly down-regulated (Table 2.4). Calreticulin is a Ca^{2+} binding chaperone protein residing in the endoplasmic reticulum (ER) (Michalak et al., 1999) and is involved in Ca^{2+} homeostasis and the folding of newly synthesized glycoproteins and misfolded proteins (Kawabe & Yokoyama, 2010). The protein folding process is sensitive to increased ROS production, activation of inflammation pathways, Ca^{2+} depletion and metabolic stimulation (Cao & Kaufman, 2012; McDonagh et al., 2006), all of which have been reported to be associated with the immune response. Up-regulation of calreticulin expression was observed in the coelomic fluid of the sea urchin *Heliocidaris erythrogramma* 20 hours post-injection with bacterial LPS (Dheilly et al., 2011). Differential expression of this chaperone protein in this study may suggest degradation and/or synthesis of new proteins and may indicate the involvement of the ER in the stress response. Furthermore, the involvement of calcium signalling in *H. midae* immune regulation, as suggested above, is further emphasised by the involvement of calreticulin.

Rab 7-like protein

A Rab 7-like protein was found to be up-regulated in bacterial-challenged *H. midae* haemocytes at 1 and 2 hours p.i. (Table 2.4). Sequence analysis indicated that this protein has close homology to human Rab 7 protein. Rab 7 belongs to the large GTPase family and has been shown to be associated with endosome trafficking, lysosome biogenesis and phagosomal trafficking events (Feng et al., 1995; Welter et al., 2002; Poteryaev et al., 2007; Bucci et al., 2000). Down-regulation of the Rab 7 gene has been reported in the deep sea mussel *Bathymodiolus thermophilus* upon thermal challenge although a function was not established (Boutet et al., 2009). Up-regulation of this protein in *H. midae* may reflect its role in regulating endocytosis in abalone haemocytes during the early abalone immune response to bacterial-challenge.

Isocitrate dehydrogenase (NADP), glucose-6-phosphate 1-dehydrogenase and glutathione-S-transferase

NADP-dependent isocitrate dehydrogenase, glucose-6-phosphate 1-dehydrogenase and glutathione-S-transferase isoform 1 were identified as differentially expressed in the bacterial-challenged abalone group (Table 2.4). These proteins have been linked to reactive oxygen species (ROS) scavenging activity and detoxification in the cell. The production of ROS in response to a pathogen is well documented in both vertebrate and invertebrate species, and forms part of the initial cellular defence to infection (Soderhall, 1999; Devasagayam et al., 2004; Torres et al., 2006). It is important for cells to be able to detoxify harmful oxidative environments following degradation of invading organisms (McDonagh & Sheehan, 2006) and this is accomplished through the use of nonenzymatic and enzymatic systems. The nonenzymatic system includes reduced glutathione (GSH) which is an important antioxidant that acts as an electron acceptor for glutathione peroxidase and also reacts directly with ROS, becoming oxidized to glutathione disulphide (Lee et al., 2002). Regeneration of reduced GSH is dependent on the supply of the essential cofactor NADPH (Izawa et al., 1998), which is replenished by the action of glucose-6-phosphate dehydrogenase and isocitrate dehydrogenase. Glutathione-S-transferase (GST) is also an important detoxification enzyme which catalyzes the conjugation of reduced GSH to endogenous and exogenous electrophiles (Hayes et al., 2005; Ivarsson et al., 2003). The proteomic description of GST expression in response to a bacterial pathogen has been demonstrated in *Mytilus galloprovincialis* (Ji et al., 2013) and *Chlamys farreri* (Huan et al., 2011). Although GST was up-regulated in both *M. galloprovincialis* and *C. farreri*, its function remains to be characterised in abalone. Overall, differential expression of these proteins in haemocytes from bacterial-challenged abalone may reflect ROS production and subsequent detoxification.

Haemocyanin

In this study, haemocyanin proteins were found to be differentially expressed in both the bacterial-challenged (Table 2.4) and mock-infected (Table 2.5) abalone groups. Haemocyanin type 2 protein, haemocyanin alphaD-subunit and an H2 protein fragment showed significant up-regulation in the bacterial-challenged group, whilst haemocyanin and haemocyanin subunit 2 were initially up-regulated and subsequently down-regulated in the mock-infected group. Although haemocyanin expression was similar in both experimental groups of abalone, the sustained up-regulation of haemocyanin expression in the bacterial-challenged group suggests a possible role in the immune response. Haemocyanin is a copper-containing respiratory protein involved in oxygen transport in haemolymph (Chongsatja et al., 2007). There is mounting evidence that haemocyanin may exhibit multiple functionalities in addition to its oxygen transport role (Coates & Nairn, 2014). Haemocyanin is a multi-subunit complex, with each subunit possessing different activities. The C-terminus of haemocyanin has been shown to exhibit antimicrobial activity (Lei et al., 2008; Destoumieux-Garzón et al., 2001; Lee et al., 2003), whilst the N-terminus appears to be involved in regulating haemocyanin activity (Lei et al., 2008). The observation that haemocyanin type 2 protein and haemocyanin alphaD-subunit were significantly up-regulated in haemocytes from bacterial-challenged abalone may reflect anti-microbial activity of haemocyanin in *H. midae*, although further characterisation is needed.

ATP-binding cassette transporter protein

ATP-binding cassette (ABC) transporter sub-family A was found to be significantly up-regulated in the bacterial-challenged group (Table 2.4). The ABC transport proteins are transmembrane proteins that utilise the energy generated by ATP hydrolysis to transport a wide array of substrates across membranes (Kingtong et al., 2007). ABC transport proteins have been identified in marine invertebrates in toxicology studies and are thought to provide protection from the accumulation of toxic compounds in the cell (Kingtong et al., 2007). The focus of research has however been on ABC multidrug proteins, with the result that there is very little information regarding the ABC transporter families in marine invertebrates. Characterisation of ABC transporter 1 in *Caenorhabditis elegans* demonstrated its involvement in the engulfment and clearance

of apoptotic cells in macrophages (Luciani & Chimini, 1996). Further characterisation of ABC transporter proteins in *H. midae* would be required to determine a functional role in abalone haemocytes.

Mock-infection vs bacterial-challenge

A parallel iTRAQ analysis was conducted using mock-infected *H. midae* to account for the wounding response during the infection protocol and eliminate statistically significantly changing proteins common to both groups. It is reasonable to expect that since both experimental groups include the same stressor (wounding by injection), there may be proteins identified as statistically significantly changing common to both groups. The identification rates for both treatment groups indicate comparable results, with the mock-infected group having a slightly higher count of protein identifications following filtering (Table 2.1). In total, there were 81 protein identifications common to both groups and 36 and 63 unique proteins belonging to the challenged and mock-infected groups respectively (Appendix B.1.1). A list of the unique protein identities is provided in Appendix B.1.2. The discrepancy of protein entries from each group may be attributed to the nature of MS-based analysis, such as missed peptides during MS/MS acquisition or the removal of protein entries during the filtering portion of the study. It is well documented that the reproducibility of protein identification is affected in shotgun proteomics (Li et al., 2007b; Gan et al., 2007) and this inherent problem is difficult to avoid.

The list of statistically significantly changing proteins did not contain any identical protein entries common to both treatments aside from the metal ion binding H2 protein (Table 2.4 and 2.5). However, the presence of haemocyanin and ribosomal proteins in both treatment groups, although not possessing identical accession numbers, may be seen as common protein families responding in a similar manner. Closer inspection of the proteins identified as statistically significantly changing in the mock-infected group indicate functions related to translation (ribosomal protein S5, poly(A)-binding protein, ribosomal protein S20), cytoskeletal rearrangement (non-muscle myosin II, troponin, Src tyrosine kinase 1), metabolic processes (malate dehydrogenase) and a number of haemocyanin proteins. Contrastingly, the literature relating to the statistically significantly changing proteins from the bacterial-challenged group indicates that these

proteins have immune-related functions. This suggests that the injection of heat-killed *V. anguillarum* significantly stimulated the immune response of *H. midae* and that translation and haemocyanin proteins may be a common response to wounding. However, the significantly different expression profiles of these proteins in the two treatment groups, such as that of H2 and haemocyanin which exhibited sustained up-regulation in the bacterial-challenged group, may indeed reflect their functional importance in the abalone immune response. These results are supported by the sustained haemacytopenia that was observed in the bacterial-challenged group during the induction of an immune response (section 2.3.1), which was not reflected in the mock-infected group (Figure 2.4). Thus, it seems that the iTRAQ data acquired from this analysis may be used to confidently analyse the immune response of *H. midae* haemocytes.

2.4.1 Concluding remarks and future work

iTRAQ-based proteome profiling is a powerful tool for characterising proteome changes. The technique was used to identify and quantify a total of 262 haemocyte proteins in bacterial-challenged and mock-infected *H. midae*. The challenges of proteome characterisation in a non-model organism necessitated careful experimental design and stringent post-analysis filtering strategies. The combination of iTRAQ experiments resulted in the elimination of low-quality matches to produce the highest quality dataset at the expense of increased protein identifications. Nonetheless, 16 significantly expressed haemocyte proteins were identified in the bacterial-challenged abalone groups that are possibly involved in cytokine secretion, cell signalling pathways, reactive oxygen species detoxification, endocytosis, protein folding and phagocytosis. These findings are supported by transcriptional studies conducted in other molluscs. The mock-infection control group demonstrated that the injection protocol elicited a wounding response, as is demonstrated by the differential expression of protein synthesis, cytoskeletal proteins and haemocyanin proteins. However, the differences in protein expression between the two treatment groups and the unique immune-related proteins identified in the bacterial-challenge group indicate that an immune response was indeed elicited in the abalone exposed to *V. anguillarum*. One of the limitations of

this study, which may have affected the outcome of the results, is the stringent filtering that was applied to the data. However, since abalone is considered a non-model organism, a cautious approach was adopted in this study. Additionally, MS-based proteomics may suffer from missing protein entries due to the intrinsic method of peptide acquisition and peptide spectrum matches during peptide and protein identification.

Although the identification of the proteins detected in this study suggests that they function in the *H. midae* immune system, validation of their expression profile using alternate experimental methods would provide conclusive evidence of their involvement. The comprehensive dataset generated by iTRAQ analysis of the *H. midae* haemocyte proteome will be an important resource that will result in new insights into the molecular mechanism of the haemocyte infection response in *H. midae*.

CHAPTER 3

FUNCTIONAL ANALYSIS AND VALIDATION OF *H. MIDAE* HAEMOCYTE PROTEOME PROFILING

CONTENTS

3.1 Introduction

In order to understand the pathophysiology of disease in *H. midae*, it is important to elucidate the underlying molecular mechanisms associated with the immune response. The innate immune system is responsible for a host of regulatory mechanisms orchestrated via a highly interlaced signalling network of interacting proteins and pathways (Mallick & Kuster, 2010). Dissecting the dynamics of cell signalling and multi-protein complexes remains challenging due to the complexity of the system under observation (Wright et al., 2012). It is becoming increasingly clear that to achieve a comprehensive understanding of these intertwined networks, it is necessary to examine all interactions concurrently.

The advances made in proteomic technologies now allow for large-scale investigations into the proteome of cells and organisms both qualitatively and quantitatively (Aggarwal et al., 2006). Through this approach, large datasets of protein expression can be generated, offering a powerful tool for studying complex biological systems. Moreover, investigating the proteomic immune system following network perturbations, particularly from a temporal perspective, can provide important information on regulated signalling pathways and identify molecular signatures of the innate immune response (Rhoet al., 2008). It is thus important to provide a conceptual framework to consolidate and decipher the extensive information generated from this kind of analysis. The final objective of high-throughput proteomics is to integrate global protein expression data into network models of biological processes (Meunier et al., 2007; Sabidó et al., 2011).

Although published iTRAQ studies investigating the immune response of marine molluscs is still lacking, similar studies conducted in other marine organisms demonstrate the ability of shotgun proteomic analysis to reveal previously uncharacterised proteins involved in the immune response (Lü et al., 2014; Meng et al., 2014; Zhang et al., 2014). For example, iTRAQ-based proteome profiling of the immune response of *Apostichopus japonicus* (sea cucumber) over a 96 hour time course following a pathogen challenge demonstrated the involvement of different protein groups at certain times during the challenge. At 24 hours post-infection, deemed early phase by the investigators, the differentially expressed proteins functioned

predominantly in cytoskeletal organization. Proteins involved in metal ion binding and metabolic processes were predominant at 48 hours, followed by a shift at 96 hours to processes governing catabolic processes as well as protein folding and translation (Zhang et al., 2014). There is a clear time-dependent regulation on protein expression that occurs during the induction of immune responses. Thus, temporal proteomic data analysis provides an insight into the kinetics of biological processes and is able elucidate common patterns of regulation.

Data mining and functional analysis of global protein expression profiles constitutes an important, yet challenging step in any proteomic investigation (Kumar & Mann, 2009). Due to the large amount of data collected from high-throughput proteomic experiments, integrating complex proteomic data into functional biological networks by manual means is almost impossible. This has necessitated the development of computer-aided software capable of mapping proteome data with annotational databases and constructing network models to infer systems level differences in the modulation of molecular pathways and as a consequence, biological processes (Kumar & Mann, 2009). A number of existing bioinformatic tools, previously used for functional genomic research, have been modified to process quantitative proteomics data (Bensmail & Haoudi, 2005).

Transforming large protein expression datasets into functional networks first requires global analysis of protein expression profiles. This provides a "preliminary exploration" of proteomic data and groups proteins into a hierarchy of co-expressing clusters. Hierarchical cluster analysis (HCA) is a powerful global analysis tool which has been used extensively in proteomic studies (Meunier et al., 2007). Individual protein groups can then be examined for related biological functions through integration of protein sequences with functional annotation terms (Conesa et al., 2005). The Gene Ontology (GO) project provides an extensive framework for this analysis and aims to assign consistent vocabulary (GO terms) to describe the molecular function, biological process and cellular component of a queried sequence based on homology with proteins from other organisms. This standardised functional annotation allows for proteins from different species to be compared, which greatly facilitates the level of biological inference that can be achieved (Götz et al., 2008). The use of GO terms, protein domains (Interpro) and pathway databases (KEGG) have been widely used as descriptive

strategies in proteomic studies (Chan et al., 2006; Dimmer et al., 2008). The final step of functional analysis is to generate an organised molecular network of the identified cluster sets and examine the key biological processes arising from perturbations, as well as their dynamic transition throughout the investigation. Not only will functional analysis generate a higher level of biological insight into the molecular mechanisms underlying the innate immune response of *H. midae,* but testable hypotheses regarding disease initiation and progression may be generated to identify novel molecular targets for health monitoring on farms.

Validating iTRAQ data

As with many high throughput experimental strategies (such as microarray gene screening), post-analysis and the validation of iTRAQ-derived data remains an important component of proteome profiling studies (Aebersold et al., 2013; Cong et al., 2006). Although the reliability of high-throughput proteomics is becoming increasingly consistent, validation can provide robust scientific validity to a particular finding (Chuaqui et al., 2002). The validation of quantitative proteomic data has been discussed extensively and numerous approaches have been suggested (Karp & Lilley, 2007; Mallick & Kuster, 2010; Fuller & Morris, 2012). Filtering proteins using cut-off values can be used to validate findings (Fuller and Morris, 2012) however, orthogonal validation, which utilizes a different method to the one that resulted in the original findings, provides a more reliable validation strategy (Karp & Lilley, 2007; Mehta et al., 2006). Laboratory-based validation, such as western blotting, ELISA or immunohistochemistry, can be used to provide independent experimental verification of iTRAQ-predicted changes in protein expression. Oftentimes, the genes or proteins with the highest differential expression ratios are selected for validation since such differences are likely to be valid. However, a limiting factor is often the unavailability of appropriate probes or antibodies (Chuaqui et al., 2002).

3.1.1 Aims of this chapter

Rapid progress in the field of proteomics has allowed for large-scale investigations of complex proteome changes in response to changing biotic/abiotic conditions, thus providing a system-wide analysis of the subject. In this study, iTRAQ coupled with LC-MS/MS was used to qualitatively and quantitatively investigate the proteome of *H. midae* haemocytes sampled from abalone challenged with a heat-killed bacterial pathogen, resulting in the simultaneous identification and quantification of over 100 proteins (Chapter 2). Thus, the aim of this chapter was to gain insight into the underlying molecular mechanisms associated with the proteomic immune response of *H. midae* haemocytes through computerised functional data analysis.

The first objective of this study was to functionally characterise the protein expression data acquired in Chapter 2 so as to provide a framework to uncover and investigate the biological functions regulated in response to a bacterial-challenge. Since a putative early (1 and 2 hours p.i.) and late (48 hours p.i.) response was investigated, global mapping was first used to group and classify individual proteins according to similarities in their expression profiles over the time course of the challenge trial. Functional annotation, data mining and network modelling was conducted on the individual protein clusters to identify molecular signatures of the innate immune response. These could be used to establish molecular targets for further investigation to be used as biomarkers of health.

The second objective of this study was to validate and confirm iTRAQ-derived protein expression data through orthogonal validation. *H. midae* were subjected to the same bacterial-challenge experimental conditions used during the iTRAQ experiments and the relative expression of specifically chosen proteins was monitored by western blot analysis. Four proteins identified as significantly changing in statistical analysis in Chapter 2 were chosen to evaluate their temporal expression in *H. midae* haemocytes. A broad time-range was used so as to include both the experimental time points investigated during iTRAQ-profiling and additional time points that provide a more comprehensive and dynamic view of the kinetics of protein expression in response to a bacterial-challenge.

3.2 Materials and methods

All media and solutions used in this study are listed in Appendix A.

3.2.1 Hierarchical clustering of protein expression profiles

Hierarchical clustering analysis (HCA) has been identified as a powerful data mining tool for exploring and visualising global protein expression data (Meunier et al., 2007). HCA was applied to the haemocyte protein expression profiles from the bacterial-challenge iTRAQ experiments (Table 2.2) using the average linkage method based on the unweighted means of all pairwise distances (UPGMA) as implemented in the program HemI (version 1.0.1) (Deng et al., 2014). The similarity distance matrix used was Euclidian distance and the clustering results viewed as a dendrogram. Clusters were defined from the first long stem of the dendrogram into three separate clusters and processed for functional annotation mapping.

3.2.2 Functional annotation of protein clusters

Proteins from each cluster identified during HCA (Figure 3.2) were functionally annotated to derive biological processes unique to each cluster set. Go terms were assigned to each protein from the respective clusters using Blast2GO (B2G) (Conesa et al., 2005). BlastP (NCBI) was used to identify homologous proteins in the database and default parameters as set by B2G were used for GO term assignment and annotation. KEGG pathway and Interpro scans were used to predict molecular pathways of the proteins. To consolidate the list of GO terms and identify immune-related biological processes, the GO term data set from each cluster was further classified in terms of the immune GO classes they represent (Shiel et al., 2014). Thus, higher-level immune response GO terms were determined using CateGOrizer (Hu et al., 2008). GO terms from each cluster were separately imported into CateGOrizer as a .txt file and higher-level immune response GO terms assigned using Immune System Gene classes GO classification. Go term classification by “consolidated single occurrence count” was chosen as it resulted in the least number of “odd terms” over the three clusters. The “odd terms” refers to terms that do not belong to any classes in the given classification

method. Since the classification method that produces the least number of "odd terms" may be considered the best fit for the dataset, both methods were tested prior to choosing. The REViGO resource (Supek et al., 2011) was employed to summarise and visualise the higher-level immune response GO terms assigned to each cluster in an interactive graph. These annotations, expressed in xgmml format, were loaded into Cytoscape (Smoot et al., 2011) for interaction map visualisation. The network map for cluster B and C contained a few redundant terms or terms not pertaining to abalone immunity which were removed to establish the final network. Since the network for cluster B was too large to incorporate into a single figure, all network nodes related to metabolism and protein synthesis were removed. A list of the deleted GO terms and the removed metabolism and protein synthesis networks can be found in Appendix B.2.

3.2.3 Validation of differentially expressed proteins by western blot analysis

The differential expression levels of proteins identified by iTRAQ as statistically significantly changing were validated by western blot analysis. Since *H. midae*-specific antibodies were not available, polyclonal antibodies were selected based on the best sequence similarity between the immunogen and the protein sequence identified by iTRAQ. Thus, allograft inflammatory factor-1 (AIF), calreticulin (CRT), NADP-dependent isocitrate dehydrogenase (IDH) and glutathione-s-transferase (GST) were chosen for further analysis. For the assessment of each protein, total soluble protein was isolated from haemocytes sampled from bacterial-challenged *H. midae* and probed using commercial antibodies as described below.

3.2.3.1 Bacterial-challenge and protein isolation

Three independent bacterial-challenge trial experiments were conducted as described in Chapter 2, section 2.2.3, except that haemocytes were sampled at 0, 1, 2, 6, 16, 24 and 48 hours p.i. (n=4/time point). Haemocyte total soluble protein was isolated and total protein concentration determined (section 2.2.7.1.1). Samples were divided into 20 µg aliquots and stored at -80 ^{0}C pending western blot analysis.

3.2.3.2 SDS PAGE

Total haemocyte protein isolated from bacterial-challenged *H. midae* (section 3.2.1.1) was separated according to size by SDS-PAGE. Stacking gels were prepared as follows: 4% (*v/v*) acrylamide, 0.375M Tris-Cl/0.1% SDS pH 6.8, 0.05% (*w/v*) ammonium persulfate (AMPS), 0.01% (*v/v*) N,N,N',N'-Tetramethylethylenediamine (TEMED) and resolving gels prepared as follows: 10% (*v/v*) acrylamide, 0.125M Tris-Cl/0.1% SDS pH 8.8, 0.2% (*w/v*) AMPS, 0.04% (*v/v*) TEMED), prepared from stock solutions (Appendix A.2.4.1). Protein samples for the AIF western blots were separated on a 15% resolving acrylamide gel. Protein samples were prepared by mixing 5x sample application buffer (SAB; 250 mM Tris-Cl pH 6.8, 500 mM (*w/v*) dithiothreitol (DTT), 10% (*w/v*) SDS, 0.5% (*w/v*) bromophenol blue, 67% (*v/v*) glycerol; Appendix A.2.4.1.5) with the protein sample to yield a final 1x SAB concentration and boiled at 95 ^{0}C for 5 minutes. Protein samples were electrophoresed in SDS PAGE running buffer (Appendix A.2.4.1.7) using a mini-PROTEAN Tetra cell system (Bio-Rad) at 100V at 4^{0}C until the dye front present in the SAB reached the bottom of the gel. Gels were then prepared for western blot analysis.

3.2.3.3 Western blotting

SDS-PAGE gels were rinsed in cold Towbin buffer (25 mM (*w/v*) Tris, 192 (*w/v*) mM glycine, 20% (*v/v*) methanol; Appendix A.2.4.2.1) following electrophoresis. The proteins were transferred onto nitrocellulose membrane (0.2 µM pore size, Biotrace™ NT, Pall Corporation) at 100V at 4^{0}C for 1 hour using a Mini Trans-Blot cell (Bio-Rad). Equal loading and transfer efficiency of the samples was determined by reversible Ponceau S staining (0.1% (*w/v*) Ponceau S, 5% (*v/v*) ethanol; Appendix A.2.4.2.2). Ponceau S-stained membranes were visualised colorimetrically using the Molecular Imager ChemiDoc XRS+ system (Bio-Rad) as per the manufacturer's instructions. Ponceau S stain was subsequently removed by two consecutive washes in Tris-buffered saline solution (TBS; 50 mM (*w/v*) Tris, 150 mM (*w/v*) NaCl, pH 7.4; Appendix A.2.4.2.3). Membranes were blocked in blocking buffer (5% (*w/v*) skim milk powder in 1 x TBS; Appendix A.2.4.2.4) for 1 hour at room temperature whilst shaking gently on an orbital shaker. Primary and secondary antibody dilutions were prepared in blocking

buffer. Protein concentrations and primary and secondary antibody concentrations are shown in Table 3.1.

Table 3.1 Antibody code and manufacturer, antigen, primary and secondary antibody concentrations used for western blot analysis.

Protein Probed	Antibody code & manufacturer	Protein concentration (µg)	1^0 antibody concentration	2^0 antibody concentration
AIF	PA527436, Pierce	30	1:500	1:5000
CRT	ab2907, Abcam	10	1:1 000	1:10 000
IDH	HPA035248, Sigma	20	1:500	1:10 000
GST	HPA037604, Sigma	15	1:1 000	1:10 000

Membranes were incubated individually with primary antibody at 4^0C overnight (O/N) whilst shaking. The membranes were subsequently washed three times in TBS (Appendix 2.4.2.3) containing 0.1% (*v/v*) Tween-20 (TBST) for 15 minutes each followed by a final 15 minute wash in TBS. Membranes were incubated with secondary antibody at RT for 2 hours and then washed a further four times. Chemiluminescent signals were detected using the Pierce ECL western blotting substrate (Thermo Scientific) as per the manufacturer's instructions by adding 1 ml of freshly prepared developing substrate solution onto each membrane and allowing colour development for five minutes. Chemiluminescent signal detection was accomplished with the Molecular Imager ChemiDoc XRS+ system (Bio-Rad), and the images acquired with sequential exposure for 100 seconds with ten seconds between exposures.

3.2.3.4 Densitometric analysis of western blots

For the quantitative analysis of western blots, Image Lab™ (Bio-Rad) software was used to determine the density of each background-subtracted chemiluminescent signal. The Band Analysis tools were used to select and determine the density of the bands in each blot. An area lacking signal was defined for background subtraction. The relative density of the bands was normalized to the respective β-actin signals.

3.2.3.5 Statistical analysis

The adjusted signal intensity value of each band was exported into MS Excel in .csv format and each signal normalised to the respective unchallenged control. Replicate values were used to calculate the average relative expression of each protein. Statistical analysis was conducted by one-way ANOVA ($P < 0.05$) using the Excel add-on Analysis Toolpak. Where data sets were not normally distributed or exhibited unequal variances a non-parametric ANOVA on ranks (Kruskal-Wallis) test was used.

3.3 Results

3.3.1 Hierarchical clustering of protein expression profiles

To investigate the overall dynamics of protein expression changes in bacterial-challenged *H. midae* haemocytes, a hierarchical cluster analysis (HCA) of the 118 proteins identified by iTRAQ analysis was performed using the graphical analysis program HemI (Deng et al. 2014). The HCA plot generated in this study consisted of three major clusters (A-C, Figure 3.1) as defined by the first long stem of the dendrogram. Clear temporal changes in global protein expression were evident: an early up-regulated response (cluster A), a late up-regulated response (cluster C) and a third, large cluster of "moderately changing" proteins (cluster B). These results reflect the induction of different protein expression responses at different times following bacterial-challenge. Closer analysis of the early up-regulated cluster shows a number of co-clustered haemocyanin proteins, as well as heat shock protein (HSP) 90 and inducible HSP 70 (Figure 3.1, cluster A). The late up-regulated cluster is comprised only of proteins that were identified as significantly changing, including the co-regulated kinases, calmodulin 2 and calmodulin-dependent protein kinase (Figure 3.1, cluster C). Cluster B is comprised of both moderate down- and up-regulated sub-clusters (Figure 3.1, cluster B) where calreticulin, putative RNA-binding protein, glucose-6-phosphate 1-dehydrogenase and ribosomal protein S9 are significantly down-regulated and isocitrate dehydrogenase (NADP) and Rab7-like protein occur in the significantly up-regulated cluster.

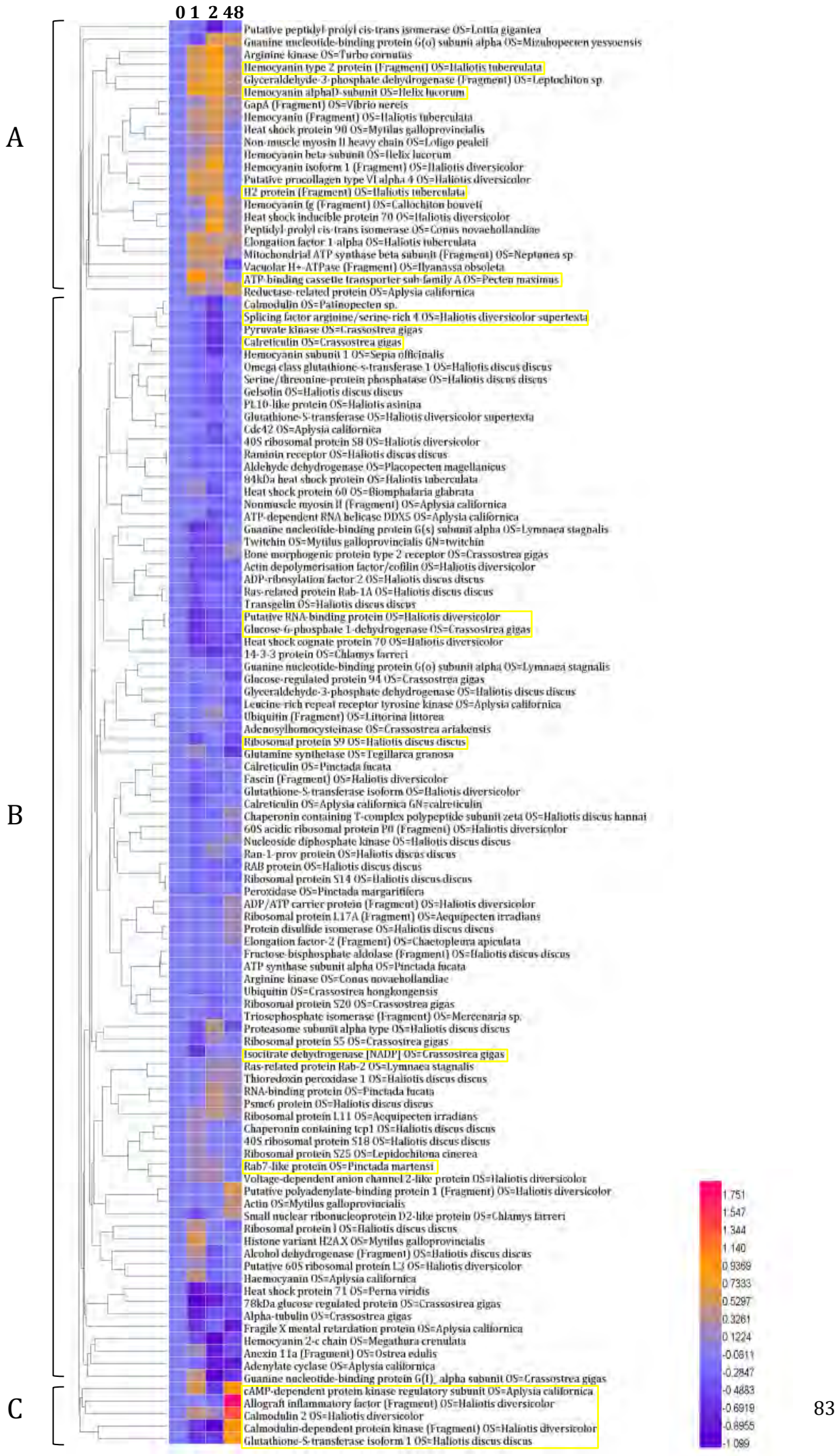

83

Figure legend- refer to the following page

Figure 3.1 Hierarchical clustering analysis heat map of the average relative expression levels (log_2 ratio) of 118 *H. midae* haemocyte proteins quantified by iTRAQ at 0, 1, 2 and 48 hours post-injection with *V. anguillarum*. The dendrogram was constructed using average linkage method and Euclidian similarity distance matrix. Three main clusters (A-C) were identified and selected for further analysis. Bar colour represents average log_2 fold change from 1.751 to -1.099. Yellow boxes indicate the proteins that were identified as having statistically significant changes in their expression profiles in Chapter 2.

3.3.2 Functional annotation of protein clusters

Functional mapping and classification was performed to provide a framework for uncovering immune-related biological processes pertaining to each identified cluster (Figure 3.1). Blast2GO was used to functionally annotate and assign multiple GO terms to the protein sequences comprising each cluster set. This list was further condensed by assigning higher-level immune response GO terms using *Immune System Gene Classes* GO classification (Tables 3.2-3.4). Redundant GO terms (arising from closely related sibling terms and related parent/child terms) were summarised using ReviGO and an interaction network for each cluster (Figures 3.2-3.4) was visualised using Cytoscape.

In total, 1669 GO terms for cluster A were mapped to 108 "immune_class" ancestor terms by single count (Table 3.2). There were 29 unique terms associated with this data set that belonged to at least one of the 12 "immune_class" GO terms and 96 "odd terms" not found to belong to any "immune_class" GO term. Proteins related to metabolism, the immune and stress response, protein synthesis and regulation of nitric-oxide synthase activity were the most abundant immune-related categories in the early-up regulated cluster (Figure 3.2).

Cluster B contained 5559 GO terms of which 175 unique terms were found to belong to at least one of the 36"immune_class" GO terms (Table 3.3). There were 382 "odd terms" in this data set that did not belong to any "immune_class". The most abundant immune-related categories of this cluster set relate to cytokine production, response to oxidative stress, induction of the MAPKK cascade and regulation of apoptosis (Figure 3.3).

Cluster C represents the smallest cluster and is indicative of the late response (48 hours p.i). In total, 75 GO terms were mapped of which 8 unique terms were found to belong to at least one of the four "immune_class" GO terms (Table 3.4). There were 16 "odd

terms" present in this dataset. Signal transduction via protein kinase signalling, ROS detoxification and metabolism are the immune-related categories that dominate this cluster set (Figure 3.4).

Table 3.2 Functional mapping of the 1669 GO terms assigned to *H. midae* haemocyte proteins identified in cluster A to 108 of the "immune class" ancestor terms by single count occurrence.

GO Term	Definition	No of counts	Fraction
GO:0008152	Metabolism	21	45.65%
GO:0006950	Stress response	8	17.39%
GO:0019538	Protein metabolism	5	10.87%
GO:0009605	Response to external stimulus	2	4.35%
GO:0006955	Immunology, immune response	2	4.35%
GO:0009056	Catabolism	2	4.35%
GO:0007155	Cell adhesion	1	2.17%
GO:0006897	Endocytosis	1	2.17%
GO:0005975	Carbohydrate metabolism	1	2.17%
GO:0005739	Mitochondrion	1	2.17%
GO:0006909	Phagocytosis	1	2.17%
GO:0006629	Lipid metabolism	1	2.17%
	Total	46	100%

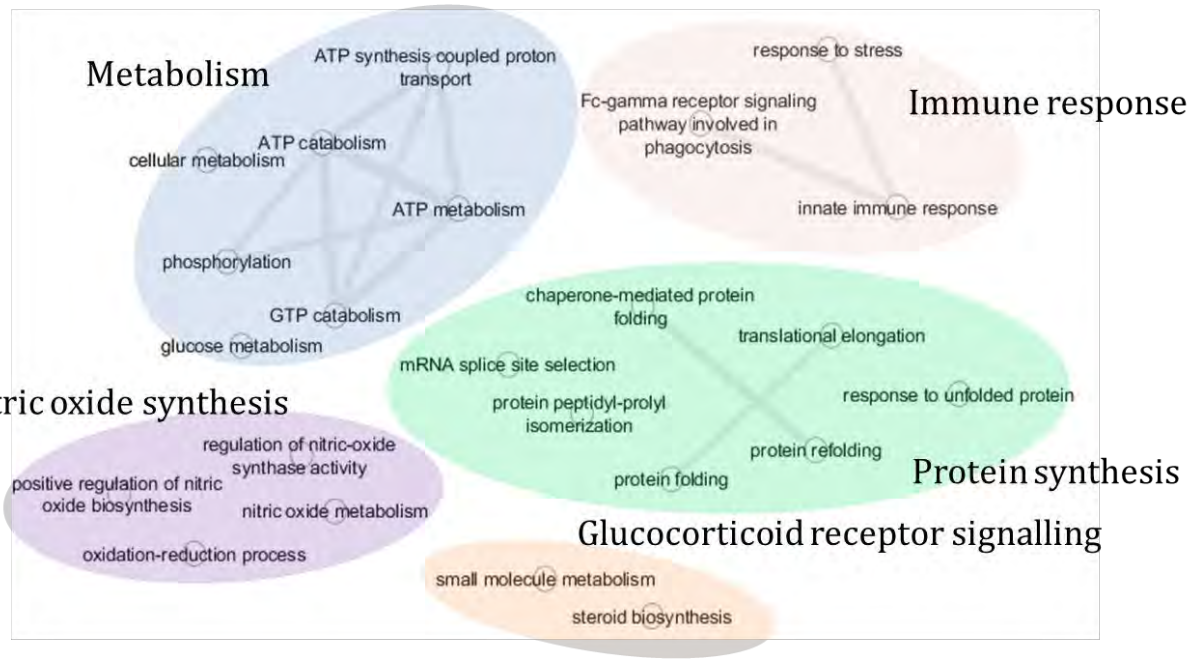

Figure 3.2 Functional network map of the cluster-representative GO terms retrieved following immune-related GO classification of the co-expressed *H. midae* haemocyte proteins identified in cluster A. Each node corresponds to a summarised, single representative GO term for all related sibling and child terms. Highly similar GO terms are linked by edges in the graph where the line width indicates the degree of similarity. Significant and related regions have been marked with background colours and labels to describe the main functions pertaining to that group.

Table 3.3 Functional mapping of the 5559 GO terms assigned to *H. midae* haemocyte proteins identified in cluster B to 108 of the "immune class" ancestor terms by single count occurrence.

GO Term	Definition	No of counts	Fraction
GO:0008152	Metabolism	101	32.58%
GO:0019538	Protein metabolism	30	9.68%
GO:0006950	Stress response	30	9.68%
GO:0006915	Apoptosis	22	7.10%
GO:0016265	Death	22	7.10%
GO:0009719	Response to endogenous stimulus	12	3.87%
GO:0009056	Catabolism	10	3.23%
GO:0042981	Regulation of apoptosis	10	3.23%
GO:0001816	Cytokine production	9	2.90%
GO:0005975	Carbohydrate metabolism	7	2.26%
GO:0005739	Mitochondrion	7	2.26%
GO:0006955	Immunology, immune response	7	2.26%
GO:0000165	MAPKKK cascade	6	1.94%
GO:0009605	Response to external stimulus	5	1.61%
GO:0043408	Regulation of MAPKKK cascade	5	1.61%
GO:0046649	Lymphocyte activation	5	1.61%
GO:0016032	Viral life cycle	4	1.29%
GO:0009607	Response to biotic stimulus	3	0.97%
GO:0042113	B cell activation	3	0.97%
GO:0009628	Response to abiotic stimulus	2	0.65%
GO:0019724	B cell mediated immunity	2	0.65%
GO:0042110	T cell activation	2	0.65%
GO:0042590	Antigen presentation, exogenous antigen via MHC classI	2	0.65%
GO:0006629	Lipid metabolism	2	0.65%
GO:0016064	Humoral defense mechanism (sensu Vertebrata)	1	0.32%
GO:0008286	Insulin receptor signalling pathway	1	0.32%
GO:0042562	Hormone binding	1	0.32%
GO:0051249	Regulation of lymphocyte activation	1	0.32%
GO:0046651	Lymphocyte proliferation	1	0.32%
GO:0042288	MHC class I protein binding	1	0.32%
GO:0046879	Hormone secretion	1	0.32%
GO:0005764	Lysosome	1	0.32%
GO:0042287	MHC protein binding	1	0.32%
GO:0005768	Endosome	1	0.32%
GO:0007155	Cell adhesion	1	0.32%
GO:0014065	Phosphoinositide 3-kinase cascade	1	0.32%
GO:0005773	Vacuole	1	0.32%
	Total	320	100.00%

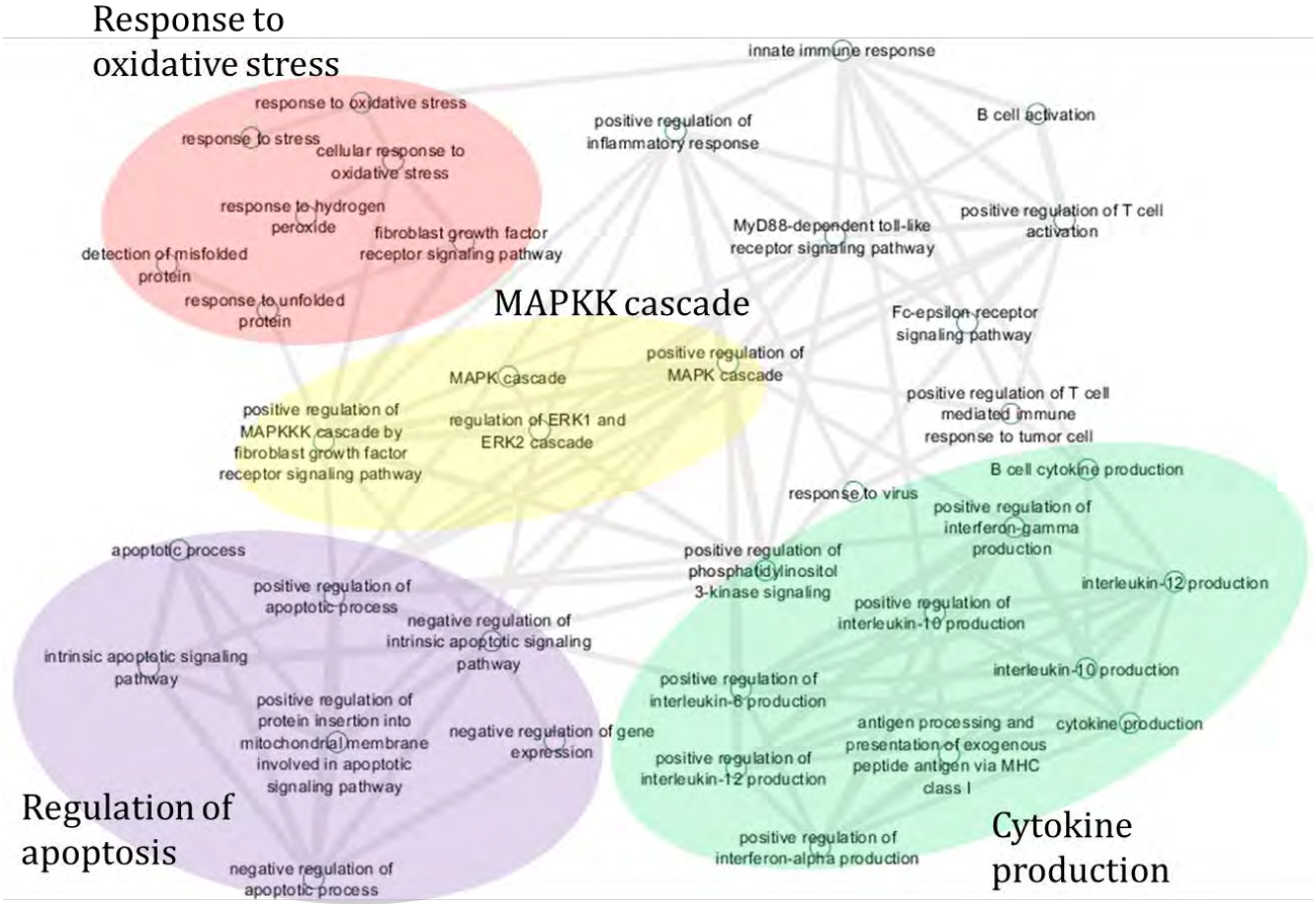

Figure 3.3 Functional network map of the cluster-representative GO terms retrieved following immune-related GO classification of the co-expressed *H. midae* haemocyte proteins identified in cluster B. Each node corresponds to a summarised, single representative GO term for all related sibling and child terms. Highly similar GO terms are linked by edges in the graph where the line width indicates the degree of similarity. Significant and related regions have been marked with background colours and labels to describe the main functions pertaining to that group.

Table 3.4 Functional mapping of the 75 GO terms assigned to *H. midae* haemocyte proteins identified in cluster C to 108 of the "immune class" ancestor terms by single count occurrence.

GO Term	Definition	No of counts	Fraction
GO:0008152	Metabolism	8	61.54%
GO:0019538	Protein metabolism	2	15.38%
GO:0006950	Stress response	2	15.38%
GO:0009056	Catabolism	1	7.69%
	Total	13	100.00%

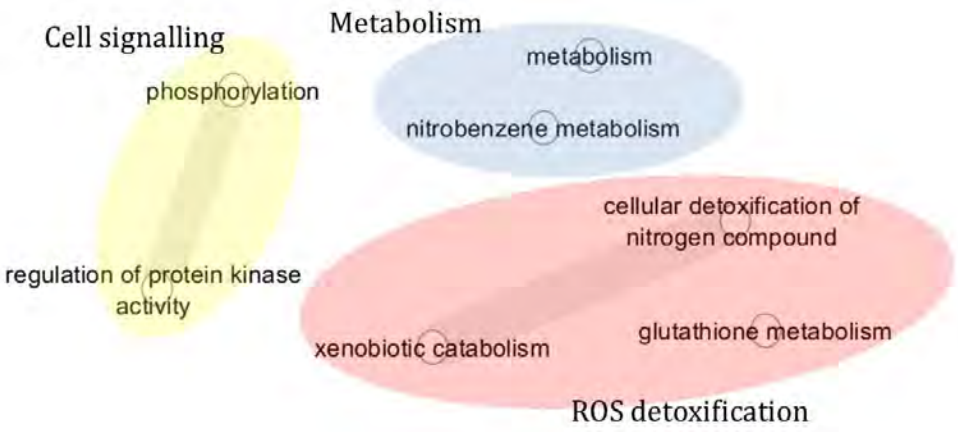

Figure 3.4 Functional network map of the cluster-representative GO terms retrieved following immune-related GO classification of the co-expressed *H. midae* haemocyte proteins identified in cluster C. Each node corresponds to a summarised, single representative GO term for all related sibling and child terms. Highly similar GO terms are linked by edges in the graph where the line width indicates the degree of similarity. Significant and related regions have been marked with background colours and labels to describe the main functions pertaining to that group.

3.3.3 Validation of differentially expressed proteins by western blot analysis

To validate the iTRAQ quantitation data, four proteins were selected for western blot analysis. In this study, temporal expression of allograft inflammatory factor-1 (AIF), calreticulin (CRT), isocitrate dehydrogenase (IDH) and glutathione-S-transferase (GST) was investigated in *H. midae* haemocytes following bacterial-challenge. The polyclonal anti-AIF antibody detected two protein bands on the western blot: a band at the predicted size of 15 kDa, which matched the iTRAQ-expression data but was only detected in two biological replicates, and a strongly expressed 52 kDa band which was reproducibly detected in all three replicates and thus measured for densitometric analysis (Figure 3.5A). Western blot analysis with the anti-CRT antibody detected two clear bands (Figure 3.5B), one of which (51.5 kDa) was similar to the predicted band size (Table 3.5). The anti-IDH antibody detected two protein bands, one with a molecular weight of 162 kDa band (reproducibly detected in all three biological replicates) and a 39 kDa band which was only detected in two replicates (Figure 3.5C). The anti-GST antibody detected a single reproducible band at 87.8 kDa which is approximately 63 kDa larger than expected (Figure 3.5D).

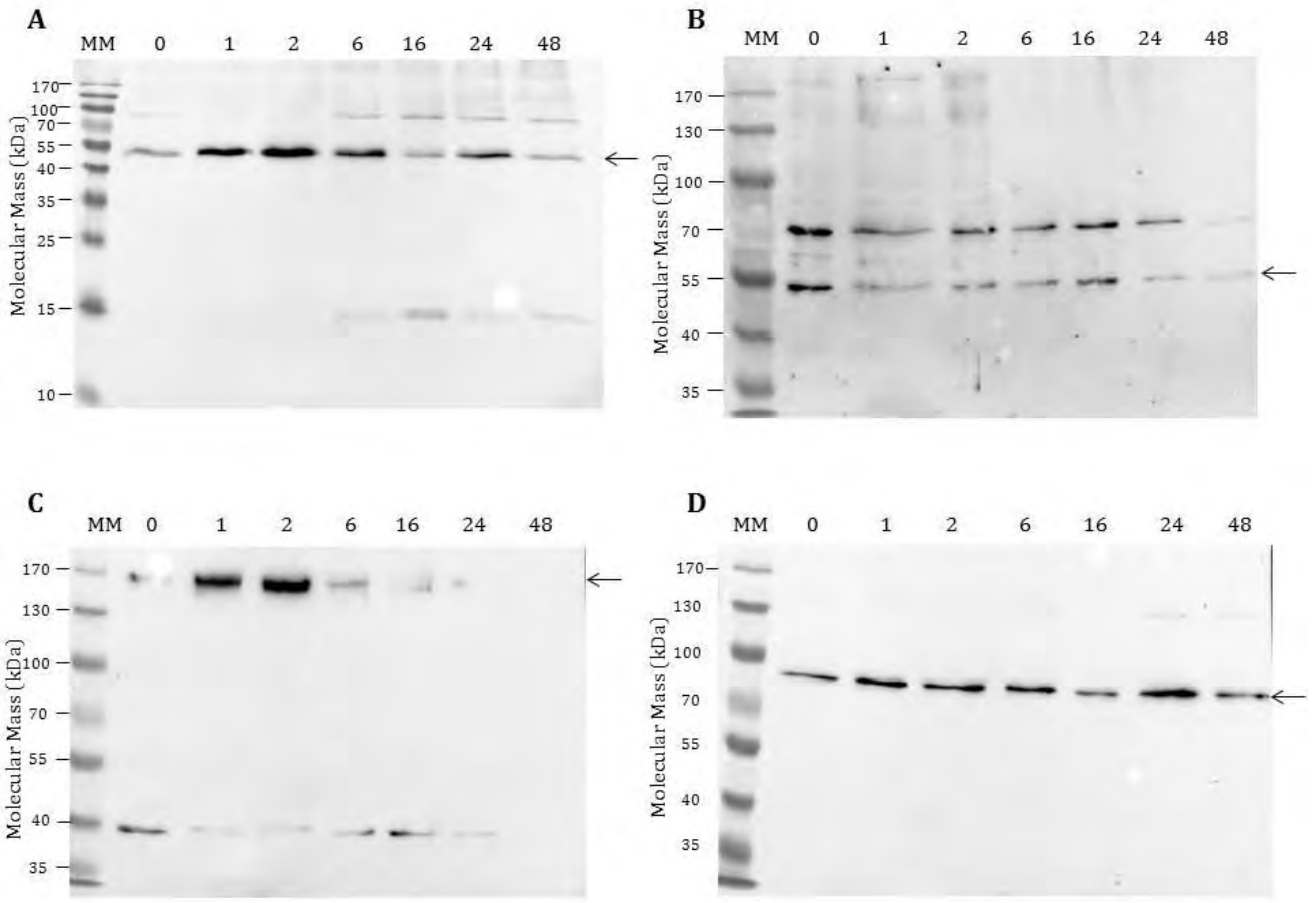

Figure 3.5 Representative images of the western blot analysis of (A) allograft inflammatory factor-1, (B) calreticulin, (C) isocitrate dehydrogenase and (D) glutathione-S-transferase in haemocytes following bacterial-challenge in *H. midae*. MM: PageRuler™ prestained protein ladder (Fermentas). Lanes 2-8: Total soluble protein isolated from haemocytes sampled from bacterial-challenged *H. midae* at 0 (control), 1, 2, 6, 16, 24 and 48 hours p.i. The arrows indicate the band that was measured for densitometric analysis.

Table 3.5 The predicted band sizes according to the UniProt entry for each protein selected for validation compared to the observed measured band size detected by western blot analysis.

Protein Probed	Predicted band size (kDa)	Measured band size (kDa)
AIF	15.6	±52.0
CRT	48.2	51.5
IDH	50.9	162.0
GST	24.6	87.8

In agreement with the iTRAQ data, western blot analysis showed that three of the proteins are indeed differentially expressed in *H. midae* haemocytes. Figure 3.6 shows the densitometric analysis of the relative expression of AIF, CRT, IDH and GST at various times post-injection with heat-killed *Vibrio anguillarum*. Compared to the unchallenged control, up-regulated expression of AIF and IDH and down-regulation of CRT was detected (Figure 3.6), whilst GST expression remained largely unchanged. These expression trends are similar to the protein expression values obtained with iTRAQ, although certain differences were identified which may be attributed to differences between the observed measured band size detected by western blot and the predicted band size according to the UniProt entry as identified by iTRAQ (Table 3.5).

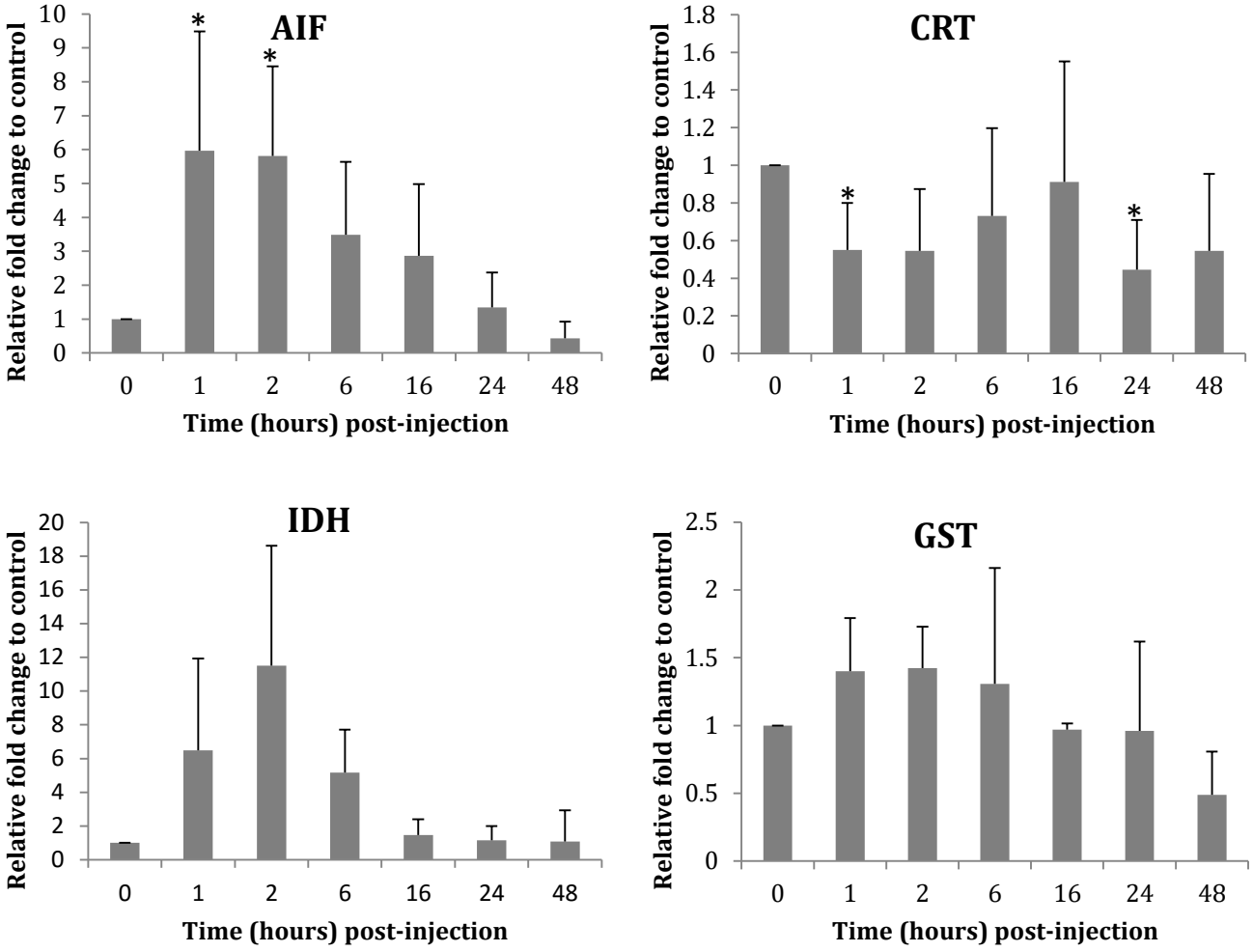

Figure 3.6 Densitometric analysis of the relative protein expression of allograft inflammatory factor-1 (AIF), calreticulin (CRT), isocitrate dehydrogenase (IDH) and glutathione-S-transferase (GST) normalized to β-actin expression and the unchallenged control. Equal amounts of total soluble protein isolated from haemocytes sampled at 0 (control), 1, 2, 6, 16, 24 and 48 hours post-injection following bacterial-challenge in *H. midae* were separated by SDS PAGE and processed for western blot analysis. Data represents the mean (±) standard error (n=3). Statistical significance is indicated by an asterisk (*) above the bars as calculated by one-way ANOVA (P <0.05).

3.4 Discussion

Improving our understanding of the abalone immune response is paramount to controlling and managing disease outbreaks on farms. A high throughput, quantitative proteomic analysis combined with bioinformatics can be used to generate a deeper understanding of important molecular pathways involved in the immune response of these commercially valuable molluscs. The resulting networks generated in this study enabled the identification of key regulatory pathways and proteins involved in disease-related activities. Ultimately, this information may lead to the discovery and development of diagnostic markers, which may be used for improved disease management and targeted therapeutic treatment.

3.4.1 Hierarchical clustering and functional annotation of protein expression profiles from iTRAQ analysis

A measurable change in protein expression following immune stimulation can reflect a shift in biological processes as circulating haemocytes respond to invading pathogens. Since iTRAQ-based datasets contain quantitative information, the induced molecular mechanisms underlying the *H. midae* immune response can be investigated through global expression analysis and functional characterisation. From a temporal perspective, significant up- and down-regulated protein clusters reflected a shift in expression of the abalone haemocyte proteome from an early (1 and 2 hours p.i.) to a late phase (48 hours p.i.) response to bacterial-challenge (Figure 3.1). To simplify functional analysis of each cluster, GO terms were consolidated to generate a small set of representative, major immune-class GO terms (Shiel et al., 2014). Functional analysis of the immune-related proteins provided insight into the regulated molecular processes occurring in *H. midae* haemocytes. These results show the sequential activation of immune responses including phagocytosis, respiratory burst, apoptosis and ROS detoxification processes. Specifically, the data presented herein implicate calcium and cAMP signalling as central players in the signal transduction cascades initiating immune responses in *H. midae*. These results are in agreement with previous large-scale abalone genomic studies (Wang et al., 2008; De Zoysa et al., 2012; De Zoysa et al., 2011a) and targeted proteomic investigations conducted in other marine invertebrates that have

implicated similar biological processes of the innate immune response, whilst providing additional information on novel proteins previously unknown in abalone immune pathways.

Fc-gamma receptor signalling pathway

The recognition of foreign particles is one of the earliest events of the innate defence response, which ultimately results in activation of immune responses such as phagocytosis (Beutler, 2004; Mogensen, 2009). In this study, immune responses involving "Fc-gamma receptor signalling pathway involved in phagocytosis" was identified as an early response to bacterial challenge (Figure 3.2). The actin remodelling that occurs during phagocytosis is associated with activation of Rho GTPase signalling pathways which triggers actin reassembly and membrane ruffling (Chimini & Chavrier, 2000). In this study, HCA indicates the early involvement of the extensively studied GTPase Cdc42 protein, which has been implicated in regulating signalling pathways that control various functions including FcR-mediated phagocytosis in leukocytes (Swanson & Hoppe, 2004; Jaumouillé & Grinstein, 2011). Interestingly, there are reports that certain pathogenic bacteria are able to regulate the host's Rho GTPases, such as Cdc42, as a means of avoiding phagocytosis by immune cells (Aderem, 2003). However, cdc42 has not been characterised in marine invertebrates. These results suggest that FcR-related proteins such as Cdc42 are induced early in *H. midae* haemocytes following bacterial-challenge and consequently, their role in mediating phagocytosis via FcR-mediated signalling pathways should be investigated further.

Mammalian signalling pathways regulating phagocytosis are well understood, specifically those associated with Fc, Toll-like, complement and lectin receptors (Aderem & Underhill, 1999; Humphries & Yoshino, 2003). These have been shown to be conserved in insect haemocytes although the expression of the associated signalling molecules show divergence from mammalian systems (Marmaras & Lampropoulou, 2009). Molluscan haemocyte cellular receptors and their associated signalling pathways are still under investigation, but research in this area has demonstrated the involvement of homologous receptor molecules and their ability to transduce ligand-mediated intracellular signalling (Humphries & Yoshino, 2003; Kletsas et al., 1998; Lebel et al., 1996; Ottaviani et al., 1995). However, less is known regarding molluscan

Fc-receptors (FcRs). FcRs are some of the most extensively studied phagocytic receptors in vertebrates and have well-defined roles within the immune system (Nimmerjahn & Ravetch, 2008; Jaumouillé & Grinstein, 2011). They form part of the immunoreceptor class of tyrosine kinases (Swanson & Hoppe, 2004) and their role in invertebrate signalling has been mostly derived from insect models (Marmaras & Lampropoulou, 2009). FcRs bind to the Fc portion of immunoglobulins, initiating a series of signalling cascades involved in the reorganisation of the actin cytoskeleton into a phagosome (Garcia-Garcia & Rosales, 2002). Although molluscan immunoglobulin-like proteins are under reported, molecules belonging to the immunoglobulin super family (IgSF) have been identified in certain invertebrate species (Benian et al., 1989; Hoek et al., 1996; Lanz-Mendoza et al, 1996; Zhang et al., 2004). The early cytoskeletal rearrangement necessary for phagocytosis may be further supported by the presence of ATP-dependent motor protein non-muscle myosin II in the up-regulated cluster.

Metabolism

The prevalence of metabolism-related GO terms in all three clusters (Tables 3.2-3.4) may be attributed to the three root classes of "molecular function", "biological processes" and "cellular component", being grouped together during immune-class classification (Hu et al., 2008). Since there may be overlap between parental terms from each category, terms belonging to the metabolism category may be over-inflated; a factor that should be taken into account when interpreting results. Nonetheless, the presence of energy and metabolism proteins, such as ATP synthase and glucose-6-phosphate dehydrogenases, in the three clusters is not surprising. Haemocytes require a regular supply of energy to maintain cellular functions in addition to carrying out immune-related processes (Coyne, 2011). The bioenergetic activity of immune cells undergoes drastic changes upon activation and requires specific changes in metabolic activity to meet these requirements (Krauss et al., 2001). Functional analysis shows a strong indication of such regulation, particularly early post-challenge.

The early induction of immunologic events such as cell signalling, migration, phagocytosis and endocytosis are all energy demanding mechanisms that require drastic changes in metabolism to accommodate this demand (Kominsky et al., 2010; Krauss et al., 2001). This change may be reflected in Cluster A, where metabolism terms

suggest strong regulation of the energy storage metabolite ATP (adenosine triphosphate) as reflected by the number of important proteins involved in ATP synthesis present in this cluster (Figure 3.2). This includes vacuolar H^+ATPase (V-ATPase), the beta subunit of mitochondrial ATP synthase, arginine kinase, glyceraldehyde-3-phosphate dehydrogenase, ATP binding cassette transporter subfamily and Gap A protein. The molluscan studies that have been conducted to elucidate the effects of abiotic stressors, particularly toxicological studies, reflect the importance of ATP in the immune response (Dondero et al., 2006; Kingtong et al., 2007; Zhou et al., 2010). Indeed, regulation of ATP following bacterial challenge is supported by studies conducted in *M. galloprovincialis* and *C. gigas,* which showed similar fluctuations in ATP levels (Ji et al., 2013; Huvet et al., 2004). Furthermore, the defence response of molluscs has been shown to be severely inhibited as a consequence of depleted energy reserves (Delaporte et al., 2006; Hannam et al., 2010; Li et al., 2010). This effect has been directly linked to inhibited phagocytosis, in which ATP plays vital roles in F-actin polymerization and ATP-driven motility of the motor protein myosin (Bearer, 1998; Xufeng et al., 2000).

Cell signalling

In addition to providing energy for anabolic reactions, ATP regulates a number of important molecular processes by acting as a coenzyme in the functionality of many proteins and enzymes (Chauhan et al., 2009; Woolner & Bement, 2009) and mediating important signalling events (Hardie et al., 2003; Krauss et al., 2001; TranVan Nhieu et al., 2004). The recognition of invading pathogens is associated with the activation of numerous convergent cell signalling pathways, which are responsible for mediating downstream immune cellular responses such as phagocytosis and inflammation (Beutler, 2004). In mussels, studies investigating the induction of immune responses have suggested the involvement of p38 MAPK, JNK, ERK, NF-kappaB, PKC, cAMP/PKA, ROS and NO signalling (Koutsogiannaki & Kaloyianni, 2010). In abalone, signalling studies have focussed primarily on cytokine signalling (De Zoysa et al., 2010; Wang et al., 2008) and far less is understood regarding other signalling pathways. However, certain studies suggest similar involvement of the p38 MAPK pathway, ROS signalling

and the Rel/NF-kappa B signal transduction pathway (De Zoysa et al., 2010d; De Zoysa et al., 2011; Jiang & Wu, 2007; Travers et al., 2009).

Results from this study agree with these investigations, reflecting a similar involvement of some of these pathways in the immune response of *H. midae.* Functional analysis identified a number of proteins involved in the regulation of nitric oxide production (Figure 3.2), regulation of the MAPK/ERK cascade (Figure 3.3), cytokine production (Figure 3.3) and late induction of protein kinase activity (Figure 3.4). The results suggest a temporal sequence for the signal transduction cascade in *H. midae,* where Ca^{2+} and cAMP signalling pathways initiate the activation of downstream signal transduction pathways.

cAMP and calcium signalling

Pattern recognition proteins (PRR) trigger an early response that involves an influx of cytosolic calcium (Ca^{2+}) and the subsequent activation of protein-kinase and lipid-kinase driven cascades (Canesi et al., 2006). Although these signalling cascades have been extensively studied in mammalian cells, similar invertebrate pathways remain to be extensively clarified (Canesi et al., 2006; Humphries & Yoshino, 2003). Ca^{2+} and cAMP are the two most pervasive intracellular messengers, occurring ubiquitously in virtually all organisms and playing a principal role in mediating a wide range of important cellular functions via activation of these cascades (Hofer, 2012). More importantly, Ca^{2+} and cAMP signalling pathways have been linked to the regulation of immune responses in mammalian cells (Racioppi & Means, 2008; Racioppi & Means, 2012; TranVan Nhieu et al., 2004), which appears to be conserved in invertebrates (Engelmann et al., 2011). Although Ca^{2+} signalling has been linked to phagocytosis in marine invertebrates (Aton et al., 2006; Yuan et al., 2001; Ballarin et al., 1997; Seastone et al., 1999), the biological role of Ca^{2+} and cAMP signalling has not been extensively studied in gastropods and bivalves (Aton et al., 2006). Results from this study may provide information on the regulation of these pathways, particularly from an activation perspective.

In this study, numerous G protein coupled receptors (GPCRs), as well as adenylate cyclase, were present in both clusters A and B, which may suggest their involvement in

the production of Ca^{2+} and cAMP in initiating the immune response in *H. midae* haemocytes. The principal route for cAMP generation occurs primarily through activated alpha units of GPCRs which bind to and activate adenylate cyclase, catalysing the conversion of ATP into the secondary messenger cAMP (Antoni, 2000). In contrast, calcium signals may be elicited via several different signals, including GPCRs. Studies have shown highly coordinated interplay between both messengers, displaying intertwined temporal and causal interactions of reciprocal regulation (Borodinsky & Spitzer, 2006; Hofer, 2012). The results from this study may provide supporting evidence linking these two signalling messengers as they both appear to be regulated early post-challenge, however further research would be required to establish the causal relationship of both these signals in *H. midae*.

One of the most important features of the secondary messenger signalling system is the coupling of messengers to protein kinase cascades, which amplifies the signal by serially phosphorylating target kinases (Alberts et al., 2002). The Ca^{2+}-binding messenger protein calmodulin (CaM) is one of the most important Ca^{2+} transducers and mediates several vital biological processes via interaction with a number of target enzymes, ion channels and proteins (Racioppi & Means, 2008; Soderling, 1999). One of which, calmodulin-dependent protein kinase (CAMK), represents a multifunctional phosphorylation enzyme that activates the CaM kinase cascade and has been shown to regulate the activity of proteins involved in pivotal roles in the immune response and inflammation in vertebrates (Zhang et al., 2011). This includes the secretion of cytokines (Pan et al., 2004; Racioppi & Means, 2008) and regulation of immune functions by the early transcription factor cAMP response element-binding protein (CREB) (Bachère et al., 2004; Canesi et al., 2006; Zhu & Wu, 2008). Far less information regarding the role of CaM in mediating immune responses in marine invertebrates is available, however it has been identified as down-regulated in haemocytes from *P. monodon* following bacterial-challenge (Somboonwiwat et al., 2010). Since both CaM and CaMK were identified as significantly up-regulated in response to bacterial-challenge (Chapter 2), it is reasonable to conclude that Ca^{2+} signalling represents important signalling events in the immune response of *H. midae*, occurring via CaM/CAMK cascades.

Analogous to the allosteric activation of CaM by Ca^{2+}, cAMP exerts its signal by activating cAMP-dependent protein kinase (PKA) (Alberts et al., 2002). cAMP activates PKA by binding to the R subunits and thus, releases the C subunits which phosphorylate a number of target enzymes, ion channels and chromosomal proteins (Baillie et al., 2005). The statistically significant regulation of PKA in this study supports the importance of cAMP signalling in the immune response of *H. midae,* which is consistent with studies conducted in other marine invertebrates (Bardales et al., 2004; Cao et al., 2004; Sossin & Abrams, 2009). However, the molecular and biological role of cAMP/PKA signalling in abalone remains to be established. Vertebrate studies have demonstrated the involvement of PKA in the regulation of important immune-related signalling pathways including CREB (Dash et al., 1991; Delghandi et al., 2005) and the PKC signalling system (Chio, 2004). PKA signalling has also been linked to regulation of phagocytosis in human neutrophils (Ydrenius et al., 2000) although certain studies report conflicting effects (Brooks & Dunphy, 2005). In marine invertebrates, PKA activity has been linked to catecholamine production (Cao et al., 2004; Malagoli et al., 2000), however its role in other immune-related activities such as phagocytosis remains to be comprehensively elucidated. Studies conducted in *C. gigas* haemocytes implicate the cAMP/PKA pathway in the modulation of phagocytosis (Lacoste et al., 2001), however this effect is contrasted in *L. stagnalis* haemocytes (Plows et al., 2006). Inhibition of PKA had a minimal effect on the phagocytic activity, suggesting it may not play a role in regulating phagocytosis in *L. stagnalis.* The authors hypothesize that PKA signalling in phagocytosis may not have been evolutionarily conserved and furthermore, may be influenced by the phagocytic target (Plows et al., 2006).

Regulation of Ca^{2+}/CAMK and cAMP/PKA signalling pathways has been linked to MAPK/ERK activation (Duca et al., 2005; Plows et al., 2004), which have been shown to play important roles in the immune response (Racioppi & Means, 2008; Delghandi et al., 2005). Furthermore, results from the HCA conducted in this study could provide insight into a number of proteins that may be involved in the activation of MAPK signalling. This includes the 14-3-3 protein, serine threonine protein phosphatase, nucleoside diaphosphate (NDP) kinase, leucine-rich repeat receptor tyrosine kinase, members of the Rho GTPase family and an abundance of proteins involved in the regulation of G protein-coupled receptor (GPCR) signalling. These proteins may be of functional

significance in regulating important signalling processes in *H. midae*, particularly the prevalence of GPCR signalling observed in this functional analysis. In addition to its cAMP and Ca^{2+} signal generating role, GPCR signalling modulates important immune functions by acting as a GTPase activating protein (De Vries et al., 2000). One of the most important functions of GTPases is the activation of MAPKs (Marinissen & Gutkind, 2001) and the results of this study suggest that they are active in *H. midae* haemocytes.

The MAPK signal transduction pathway is ubiquitous in eukaryotes and is one of the most evolutionarily conserved signalling pathways of the immune response (Zhang & Dong, 2005). It is associated with the regulation of a number of cellular and biological processes including cell growth, differentiation, host-parasite interactions and apoptosis (Cowan & Storey, 2003; Seger & Krebs, 1995). The modulation of MAPK signalling has been reported in a number of marine invertebrate haemocyte types following immune stimulation and inhibition studies, suggesting a similar role in regulating immune system processes such as phagocytosis (Canesi et al., 2002a; Hatanaka et al., 2009; Iakovleva et al., 2006; Plows et al., 2004; Travers et al., 2009). However, much of the work that has been conducted on invertebrate MAPK signalling has focussed on the p38 MAPK pathway (Travers et al., 2009; Canesi et al., 2002b) and further research is required regarding other MAPKs. Future studies should aim to establish the biological role of MAPK signalling in *H. midae* haemocytes and the molecular constituents making up this response.

Downstream targets of activated MAPKs include cytosolic compounds, cytoskeletal proteins and nuclear proteins such as transcription factors (Cowan & Storey, 2003; Plows et al., 2004). Furthermore, numerous substrates that are phosphorylated by ERK MAPKs have been shown to be involved in a number of immune-related responses (Roux & Blenis, 2004). Specifically in invertebrates, the inhibition of ERK in haemocytes from *Biomphalaria glabrata*, *L. stagnalis* and *M. galloprovincialis* significantly reduced NO, H_2O_2 production, haemocyte motility and phagocytosis (García-García et al., 2008; Zelck et al., 2007). Increased activity of MAPK/ ERK pathways has also been shown to be involved in the up-regulation of various inflammatory genes, including inducible nitric oxide and inflammatory cytokines (Ridley et al., 1998; Larsen et al., 1998; Vanden Berghe et al., 1998; Kaminska, 2005).

In this study, regulation of nitric oxide synthesis was identified as responding early to bacterial-challenge (Figure 3.2). Following the engulfment of foreign particles, reactive oxygen species and nitrogen intermediates (ROI & RNI) are produced to kill the pathogen in a process known as respiratory (or oxidative) burst (Stuart & Ezekowitz 2005). The production of ROS and RNI serves a dual role in the innate immune response, not only acting directly as antimicrobial agents, but as important signalling molecules in the activation and regulation of host defences (Fialkow et al., 2007). Specifically, nitric oxide (NO) is an ancestral intra- and inter-cellular signalling molecule which has numerous molecular targets in invertebrate and vertebrate species (Conte & Ottaviani, 1995; Franchini et al., 1995; Palumbo, 2005). NO signalling in invertebrates has been shown to play multiple biological roles related to feeding, defence, metamorphosis, haemocyte aggregation and response to environmental stress (Palumbo 2005). In the immune response, NO signalling has been linked to various important signalling pathways primarily involved in regulating phagocytosis and inflammatory responses (Cirino et al., 2003; Franchini et al., 1995; Palumbo, 2005).

NO is generated by the enzyme nitric oxide synthase (NOS), which occurs as three isoforms in mammals (Conte & Ottaviani, 1995; Palumbo, 2005). Although these have been shown to be conserved in invertebrates (Palumbo, 2005; Gourdon et al., 2001; Conte & Ottaviani, 1995) little is known about the inducing pathways of gastropod NO biosynthesis. In mammals, calmodulin (CaM) has been shown to play a key role in NO synthesis, whereby an influx of intracellular calcium causes CaM to bind to NOS, facilitating the flow of electrons from the NADPH reductase domain to the haem in the oxygenase domain (Förstermann & Sessa, 2012). Although Ca^{2+}/calmodulin-dependent activation of NOS has been demonstrated in haemocytes of the freshwater snail and *Drosophila* cell lines (Conte & Ottaviani, 1995; Regulski & Tully, 1995), this has yet to be demonstrated in gastropods. Since calmodulin was identified as significantly up-regulated in response to bacterial-challenge, it would be beneficial to establish whether calmodulin-dependent activation of NOS occurs in *H. midae* haemocytes.

The copper-containing protein haemocyanin is an interesting target of NO signalling that has been reported in a few invertebrate species (Palumbo, 2005; Torres & Wilson, 1999; Tahon et al., 1989). Cluster A included a large number of haemocyanin proteins,

representing 66% of the total haemocyanin proteins identified in this study. The biological role of haemocyanin in invertebrate immunity has gained interest in the last decade (Coates & Nairn, 2014) as it appears to have multiple immune functionalities besides its role as an oxygen carrier. This includes anti-microbial and -viral activity (Lee et al., 2003; Lei et al., 2008), ROS production (Jiang et al., 2007) and prophenoloxidase (proPO) system activation (Coates & Nairn, 2013; Decker & Rimke, 1998; Decker et al., 2001; Siddiqui et al., 2006). The proPO cascade is an important component of the humoral immune response and plays a crucial role in non-self-recognition and cellular melanotic encapsulation of foreign organisms (Pang et al., 2014). Early induction of both NO signalling and numerous haemocyanin proteins reflects their important functional involvement in the immune response of *H. midae* haemocytes and consequently, their interaction and participation in immune related processes such as phagocytosis warrant further attention.

Response to oxidative stress and ROS detoxification

The accumulation of free radicals generated during the respiratory burst may be toxic to surrounding tissues, resulting in a phenomenon called oxidative stress (Apel & Hirt 2004). Functional analysis revealed several proteins involved in the regulation of oxidative stress which is consistent with increased ROS formation associated with endocytosis (Canesi et al., 2010). Induction of genes and proteins in response to oxidative stress following immune challenge is supported by studies conducted in other marine organisms (De Zoysa et al., 2011a; De Zoysa et al., 2011b; Tomanek, 2011; Wang et al., 2010). One of the effects of oxidative stress is the degradation and oxidation of enzymes and proteins (Matés, 2000) which is reflected in the detection of misfolded proteins and the unfolded protein response (Figure 3.2). Heat shock proteins (HSPs) constitute important intra-cellular molecular chaperones that assist in the detection and folding of misfolded proteins during periods of stress (Feder & Hofmann, 1999). In this study, there were four heat shock proteins present in cluster B identified as HSP 71, 84 kDa HSP, HSP cognate 70 and HSP 60, which may reflect their role in the response to oxidative stress in *H. midae*. Moreover, certain HSPs have been shown to regulate the immune response of certain invertebrate species (Zhao & Jones, 2012) and this immune-related activity may be analogous in *H. midae* haemocytes.

Detection of the oxidative stress response in *H. midae* haemocytes is further supported by the presence of members of the anti-oxidant system identified in both clusters A and B (Figure 3.2 and 3.3). This includes metabolic processes involved in gluconeogenesis, glutathione and glucose 6-phosphate metabolism (Appendix B.2.3). Gluconeogenesis is a pathway that generates glucose from non-carbohydrate carbon sources and thus, may play a role in maintaining glucose levels during periods of stress and increased energy requirements (Yoon et al., 2001). Specifically, the identified enzyme glyceraldehyde-3-phosphate dehydrogenase (GAPDH) plays an important role in both glycolysis and gluconeogenesis by reversibly catalysing the oxidation and phosphorylation of glyceraldehyde-3-phosphate to 1,3-bisphosphoglycerate (Sirover, 1999). Glucose 6-phosphate and glutathione metabolism are both integral detoxification processes, providing NADPH for reductive detoxifying reactions (Maeng et al., 2004).

The identification of the phase II detoxification enzyme, glutathione-S-transferase (GST), further indicates cellular detoxification processes of nitrogen compounds. GST catalyses conjugation of the reduced form of glutathione to numerous xenobiotic substrates (Hayes et al., 2005). GSTs involvement as an important detoxification enzyme is consistent with studies conducted in *H. diversicolor* that show increased mRNA levels of the sigma class GST in haemocytes following bacterial challenge at 3 and 48 hours post challenge (Ren et al., 2009). A number of different GSTs were identified in this study (Figure 3.3) which may suggest the regulation of different GST classes over time in response to a bacterial challenge. GSTs represent a large group of detoxification enzymes, grouped into two major super families. These may be further divided into numerous classes displaying distinct catalytic activities depending on the inducing substrate (Hayes et al., 2005). Since this may be of functional significance, further studies characterising the different GST classes in *H. midae*, as well as the mechanisms by which the different isoforms regulate their involvement in ROS detoxification at various times post-challenge, would greatly enhance our understanding of their functional role in *H. midae* haemocytes.

Regulation of apoptosis

In molluscan systems, the signalling pathways underlying the regulation of apoptosis may be orchestrated via numerous apoptotic signalling pathways (Sokolova, 2009). This

study provides an insight into the putative involvement of certain molecules in the regulation of apoptosis in *H. midae*, including several calreticulin proteins, gelsolin, annexin, cAMP, nitric oxide and thioredoxin peroxidase. Calreticulin (CRT) has been identified as an important signal molecule of immunogenic apoptosis in cancer research, as high levels of CRT exposed on cell surfaces have been shown to induce apoptosis (Obeid et al., 2007; Panaretakis et al., 2009). Although increased CRT expression following immune stimulation is well documented in marine invertebrates (Chen et al., 2011; Dheilly et al., 2011; Huan et al., 2011; Meng et al., 2014; Tomanek, 2011), its role in mediating apoptosis has not yet been explored. Gelsolin and annexin, known cytoskeletal remodelling proteins, have also been shown to be involved in the regulation of apoptosis and inflammation (Arur et al., 2003; Kusano et al., 2000; Sun et al., 1999). However this effect has yet to be demonstrated in marine invertebrates.

Another key effector of molluscan apoptosis is cyclic AMP (cAMP) which functions as either a pro- or anti-apoptotic molecule (Sokolova 2009). Inhibition of adenylate cyclase in *C. gigas* haemocytes has been shown to promote apoptosis (Lacoste et al., 2002). The down-regulation of adenylate cyclase (Figure 3.3) may indeed confirm induced apoptosis in *H. midae* haemocytes. Although nitric oxide has also been shown to modulate apoptosis (Buttke & Sandstrom, 1994; Kannan & Jain, 2000), this effect has only been demonstrated in one molluscan species (Gifondorwa & Leise, 2006). Thioredoxin peroxidase (TPx) has been identified as a novel inhibitor of apoptosis in Molt-4 leukaemia cells by protecting cells from apoptosis in response to ROS (Zhang et al., 1997). The late up-regulated expression of TPx in this study may suggest ROS-induced apoptosis in *H. midae*. Future work investigating the regulation of apoptosis in *H. midae* should focus on the joint response of these proteins to bacterial-challenge, as apoptosis regulation is most likely due to the combined interaction of these apoptosis-related proteins.

Protein synthesis-related GO terms

All three clusters included a high representation of protein synthesis GO terms (Figure 3.2, Appendix B.2.2 and Figure 3.4) which may be indicative of high translation rates and induction of the unfolded protein response. Alterations in protein turnover in immune cells has been suggested as a potential indicator of immunological activation (Januszkiewicz et al., 2002; Januszkiewicz et al., 2006). Indeed, changes in protein synthesis in immune-challenged invertebrates has been reported in several studies (Ji et al., 2013; Nair et al., 2005; Zhang et al., 2014). The immunologic events that have been described in this study are all protein demanding processes. Thus, the presence of numerous ribosomal proteins, chaperonins, ubiquitins and critical enzymes involved in protein folding, recruitment and translation across all three clusters may reflect the translational load required during immune-related processes in *H. midae* haemocytes.

The functional clustering analysis performed in this study enabled a comprehensive insight into the molecular mechanisms underlying the immune response of *H. midae* haemocytes. In agreement with previous studies, these results demonstrated the sequential induction of immune responses spanning phagocytosis, numerous cell signalling events, cytokine production, ROS production, response to oxidative stress, ROS detoxification and the regulation of apoptosis. Network modelling provided an integrated view of the putative biological processes occurring in response to immune stimulation, which demonstrates the complex mechanisms used by haemocytes to conduct and coordinate the immune response. Although functional bioinformatics analysis hypothesizes the involvement of these proteins in the aforementioned molecular pathways and immune-related biological processes, future studies are required to functionally characterise the role of these proteins in immune processes in *H. midae*.

3.4.2 Validation of differentially expressed proteins by western blot analysis

Although iTRAQ LC-MS/MS proteomics is becoming increasingly reliable and reproducible, validation of proteomic data using an alternate molecular method is an important step to verify the true expression of proteins in the cell. Western blot hybridization was used to validate differential expression of proteins identified by iTRAQ analysis. Due to a lack of available antibodies to *H. midae* proteins, commercial human antibodies to protein homologues that possess a high sequence similarity to the abalone protein sequences acquired from the iTRAQ study were used for validation. Four of the statistically significantly changing proteins identified in the bacterial-challenge abalone group were selected for validation.

Allograft inflammatory factor-1

The predicted size of AIF is approximately 15.608 kDa and most of the invertebrate AIF family proteins reflect a similar range in size (De Zoysa et al., 2010a; Li et al., 2013; Wang et al., 2013; Zhang et al., 2011). In this study, an immunoreactive band corresponding to approximately 15 kDa reflected the AIF iTRAQ expression profile (Table 2.4); that is, down-regulation at 1 and 2 hours p.i. and up-regulation at 48 hours p.i. However, since expression was only detected in two biological replicates, the intensity of the reproducibly changing 52 kDa band was measured instead. The identification of a larger AIF band has been reported in a study observing AIF distribution in Creutzfeldt-Jakob disease brains. Here, the authors observed the presence of a prominent 50 kDa band rather than the expected 17 kDa band (Deininger et al., 2003). By treating the protein samples with strong chaotropic agents; 8M urea and β-mercaptoethanol and 6M urea SDS PAGE, the complete diminution of the 50 kDa band into the predicted size of 17 kDa was observed. Furthermore, LC-MS analysis of both the 17 kDa and the 50 kDa band confirmed the identity of AIF in both bands (Deininger et al., 2003). Thus, it was concluded that AIF exists primarily as a trimer *in vivo*. Identical subunits may explain the expression patterns exhibited in this study whereby the 52 kDa band was strongly expressed at the onset of the immune response and the 15 kDa band appeared late post-challenge (Figure 3.5A). A possible mechanism of action may be the formation of a functional AIF trimer, followed by degradation of this complex late post-challenge.

Since inflammation is one of the first responses following pathogen exposure (Gouw et al., 2005; Medzhitov, 2008) and AIF has been shown to be a pro-inflammatory cytokine (Zhao et al., 2013), the rapid induction of this protein in haemocytes is not surprising. To date, the marine invertebrate studies investigating AIF expression have concentrated on transcriptional characterisation (Li et al., 2013; Xu et al., 2014; Zhang et al., 2011) and the protein response of AIF has not been explored. Analysis of AIF mRNA levels in *Haliotis discus discus* following bacterial challenge shows sustained up-regulation in circulating haemocytes from 3-24 hours post-challenge (De Zoysa et al., 2010a). Conversely in *V. philippinarum* haemocytes, AIF mRNA levels were initially down-regulated in the first 12 hours post-infection, followed by a significant increase from 48 to 96 hours p.i. (Zhang et al., 2011). AIF mRNA in haemocytes from *C. gigas* levels only increased at 24 hours following LPS challenge (Zhang et al., 2013). However, it was shown that AIF mRNA levels increased as early as 3 hours following exposure to the viral mimic, polyinosinic-polycytidylic acid (Zhang et al., 2013), suggesting the response of AIF may be target-dependent. Nevertheless, the strong up-regulation of AIF displayed in this study confirms its regulation in *H. midae* haemocytes and suggests it plays an important immune role in *H. midae*.

Calreticulin

Western blot analysis detected a significant reduction in the relative protein expression of CRT at 1 and 24 hours p.i. (Figure 3.6), confirming the down-regulated expression pattern observed by iTRAQ analysis (Table 2.4). Calreticulin has been identified as a calcium binding chaperone protein involved in the folding of newly synthesized and misfolded proteins, as well as regulating calcium homeostasis and apoptosis (Kawabe & Yokoyama, 2010; Michalak et al., 1999). Down-regulation of CRT in *H. midae* haemocytes may indicate endoplasmic reticulum (ER) stress and the unfolded protein response, as well as diminished intracellular Ca^{2+} stores and induction of apoptosis. The role of calreticulin in mediating the proposed biological processes should be investigated in *H. midae* haemocytes with specific attention to its role in mediating apoptosis.

Isocitrate dehydrogenase (NADP)

Western blot analysis of IDH relative expression revealed two immunoreactive bands, a reproducibly changing band of approximately 160 kDa and a 40 kDa band detected in two biological replicates (Figure 3.5C). The larger band displayed consistent and strong up-regulated expression at 1 and 2 hours p.i., although it was not found to be statistically significant (Figure 3.6). Conversely, the smaller 40 kDa band (Figure 3.5C) reflected the down-regulated pattern observed by iTRAQ analysis (Table 2.4). These differences may be attributed to the presence of IDH isozymes in *H. midae* haemocytes. There exists three distinct IDH isozymes in eukaryotes which differ in subunit structure, cellular location and coenzyme specificity and which may either function as monomers, homodimers or multimers (Steen et al., 2001). In mammals, IDH functions as a heterotetramer consisting of four 40 kDa subunits present in a ratio of 2:1:1 (Ehrlich et al., 1981; Kim et al., 1999). This may explain the expression patterns observed in this study, whereby the functional 160 kDa heterotetramer was present at the onset of immune stimulation and the dissociated 40 kDa subunits appeared later post-injection. Since the protein identity assigned by PEAKS comprises 8% coverage of the identified peptides (Table 2.2), it is highly probable that a different IDH isozyme or subunit isozyme was identified by iTRAQ.

Glutathione-S-transferase

The antibody used to validate the expression of GST by western blot failed to detect a band of the correct size. Instead of the predicted size of 24.5 kDa, an immunoreactive band of approximately 87.8 kDa was detected (Figure 3.6D). According to iTRAQ analysis, GST isoform 1 was down-regulated at 1 and 2 hours p.i. and up-regulated at 48 hours p.i. (Table 2.4). There was no detectable change in the relative expression of GST following bacterial-challenge according to western blot analysis (Figure 3.5). Part of the difficulty of characterising GSTs is the sheer number of classes that exist of this protein, with 14 different classes having been described (Wan et al., 2008). Subsequent analysis by two-dimensional (2-D) western blot indicated the presence of multiple protein spots (Appendix B.4) which could be indicative of multiple GST isoforms or non-specific antibody binding to other proteins. Since the coverage for the identified peptides was 13% (Table 2.2) and the antibody used in this study was raised to human GST, it is

highly likely that either multiple GST isoforms or a different GST was measured by western blotting. Further characterisation of GST isoforms and their involvement in *H. midae* haemocytes is required.

Orthogonal validation of iTRAQ-derived data is an important step in any large-scale proteomic experiment and western blotting proved to be a partially successful strategy in this study. Although antibodies were acquired with a high sequence similarity to the proteins under investigation, the use of antibodies raised to proteins from a different organism presented numerous challenges. Whilst quantification by western blotting is considered an established and accepted "gold standard" practice, inherent characteristics of the technique can result in poor cross-validation of results (Aebersold et al., 2013). Indeed, discrepancies between observed and theoretical molecular weights of proteins have been reported in proteomic studies (Kling & Förlin, 2009). Since western blotting is dependent on the specificity of an antibody and the binding of an antigen to a target protein, multiple isoforms and issues with epitope occlusion and cross reactivity are difficult to control (Aebersold et al., 2013). This could result in large deviations from iTRAQ-derived quantitation, which is able to discriminate between isoforms and different phosphorylation status (Yates et al., 2009). Additionally, SDS-resistant multimer formation has been described previously (Coling et al., 2007; Crago & Koronakis, 1998; Oh et al., 1997) which would result in higher molecular weights derived from SDS-PAGE. Thus, identification and quantification of protein expression data acquired from the iTRAQ analysis cannot be rejected solely on the basis of discrepancies between predicted and observed molecular weights on a western blot. One of the outcomes of the validation portion of this study was the presence of multimer complexes that were difficult to resolve, even in the presence of the reducing agents included in the lysis buffer used in this study. Although unsuitable for LC-MS/MS, the use of strong chaotropic agents may be used to elute complex formation (Deininger et al., 2003). However, sample preparation for western blot analysis was kept as close to that used for the iTRAQ samples as far as possible since the point of validating iTRAQ data was to confirm protein expression under similar experimental conditions,. Nevertheless, due to the inherent difference between peptide preparation for LC-MS/MS and protein preparation for SDS-PAGE, inconsistencies between the two

experiments may be expected (Aebersold et al., 2013). Although validation with suitable antibodies, as was demonstrated with the calreticulin expression analysis, proved successful, the use of antibodies raised to abalone proteins should circumvent many of the abovementioned issues. Alternatively, MS-based validation such as selected reaction monitoring (SRM) assays or real-time PCR using degenerate primers to the peptide sequence could be used in the future to validate iTRAQ-derived expression profiles.

3.4.3 Concluding remarks and future work

Despite the constraints of working with a non-model organism, iTRAQ-based profiling has proved to be an excellent tool for investigating proteome changes associated with the immune response in *H. midae* haemocytes. Investigating the protein dynamics of pathophysiological processes through global expression analysis and immune-related functional characterisation allowed for an integrated view of the coordinated action of multiple proteins in the immune response of *H. midae* haemocytes. The change to an immunologically activated state alters the haemocyte proteome, involving a range of molecular and biological processes. Although functional roles have been postulated for the identified proteins, future studies will be required to functionally characterise their role in the proposed molecular pathways. *H. midae* haemocytes appear to respond rapidly to an immune challenge via a concerted, coordinated host response spanning nitric oxide synthesis, cytokine secretion, phagocytosis, endocytosis, regulation of apoptosis and numerous proteins synthesis and energy metabolism alterations, all under the modulation of several important signalling pathways. Particularly, cAMP and calcium signalling are at the apex of the signalling cascades and their regulatory mechanisms and downstream targets merit further enquiry. The narrow range of the time points investigated in this study makes it difficult to assign absolute time responses to these proteins, as temporal up- and down-regulated expression patterns observed during iTRAQ analysis only provide a “snap shot” of the proteome changes. Future work should focus on a targeted approach using a broad temporal range, as well as focussing on potential protein-protein interactions to elucidate mechanistic action. Western blot analysis has already revealed the rapid and prolonged response of certain proteins and the putative formation of complexes. The continuous expansion of protein

databases will markedly improve future proteomic studies attempting to characterise these changes.

CHAPTER 4

CHARACTERIZATION OF A PUTATIVE ALLOGRAFT INFLAMMATORY FACTOR PROTEIN IN *H. MIDAE*

CONTENTS

4.1 Introduction

The inflammatory response is an important component of innate immunity and one of the first responders to infection, acting to eliminate invading microorganisms and damaged tissue in an attempt to restore homeostasis (Ottaviani & Franceschi, 1998; Libby, 2007). The inflammatory and stress responses regulate a host of defence mechanisms, orchestrated in a sequential manner by regulatory signalling molecules such as pro-inflammatory cytokines and chemokines (Gouwy et al., 2005; Hanada & Yoshimura, 2002). These molecular signals bind to surface membrane receptors on immune cells, to initiate a signal transduction cascade that regulates cellular processes such as cellular motility, endocytosis, cytotoxic responses and apoptosis (Humphries & Yoshino, 2003; Canesi et al., 2006; De Vico & Carella, 2012). One such signalling molecule, allograft inflammatory factor-1 (AIF) has been identified as an important modulator of inflammatory and immune responses in both vertebrates and invertebrates (Wang et al., 2013). In the present study, AIF was established to be differentially expressed in haemocytes isolated from bacterial-challenged *H. midae* (Chapters 2 and 3). Further characterisation of the biological role of AIF in *H. midae* haemocytes would help improve our understanding of signalling molecules involved in the immune response of this abalone.

AIF is an interferon (IFN)-γ-inducible Ca^{2+}-binding cytokine (Deininger et al., 2002; Zhao et al., 2013). It was first described in rat allografts undergoing chronic rejection and has been demonstrated to be involved in macrophage activation in mammals (Mishima et al., 2008; Ohsawa et al., 2000; Utans et al., 1995; Yang et al., 2005). There are increasing reports of AIF's involvement in not only the inflammatory response (Hecker et al., 1999; Jia et al., 2007), but key host immune-related reactions (Liu et al., 2007). In vertebrate species, AIF has been shown to increase the expression of both cytokines and chemokines (Del Galdo & Jiménez, 2007; Kimura et al., 2007; Liu et al., 2007; Autieri, 1996) as well as inducible nitric oxide synthase (Huang et al., 2011; Yang et al., 2005). AIF has also been found to promote cell migration in macrophages (Zhao et al., 2013; Utans et al., 1995; Mishima et al., 2008; Ohsawa et al., 2000) and vascular smooth muscle cells (VSMCs) (Autieri et al., 2003). Similar immune modulating roles

are predicted for AIF in abalone since the protein shows a high level of structural domain conservation with homologs in other species (Deininger et al., 2002).

To date, transcriptional studies of AIF in invertebrates have indicated similar functional roles in immunity and inflammation. The AIF gene has been cloned from sponge (Kruse et al., 1999), manila clam (Zhang et al., 2011a), pacific oyster (Zhang et al., 2013), disc abalone (De Zoysa et al., 2010a), zhikong scallop (Wang et al., 2013), pearl oyster (Li et al., 2013a) and more recently, the sea cucumber (Ji et al., 2014). AIF displays constitutive expression in most tissue types but significant up-regulation in haemocytes, gills and coelomocytes upon bacterial challenge (De Zoysa et al., 2010a; Ji et al., 2014; Li et al., 2013a; Wang et al., 2013; Zhang et al., 2011a; Zhang et al., 2013). The response of the AIF-encoding gene in the aforementioned organisms appears to be fairly rapid and shows sustained expression from 3-24 hours post-challenge. Functional characterisation of AIF in the pacific oyster showed that recombinant AIF significantly enhanced mRNA expression levels of a number of inflammatory cytokines in haemocytes and stimulated the phagocytic activity of granulocytes (Zhang et al., 2013). These findings were similar to vertebrate studies, which together, suggest that AIF may act as an acute response protein in invertebrates, involved in haemocyte activation and early cytokine induction (Del Galdo & Jiménez, 2007). The functional role of AIF in haemocyte phagocytosis does however remain to be clarified.

One of the most important aspects of the phagocytic process is the remodelling of the actin cytoskeleton, which is critical for motility and cell extension (May & Machesky, 2001). Cellular actin can be present in two forms, either as monomeric, globular actin (G-actin) which can polymerise to form double stranded, filamentous actin (F-actin), responsible for higher order structures such as stress fibres and lamellipodia (Hooper & Thuma, 2005; Dominguez & Holmes, 2011). An interesting association has been observed between endogenous AIF and F-actin in macrophages and vascular smooth muscle cells (VSMCs), which have shown binding and colocalization *in vitro* (Ohsawa et al., 2000; Autieri et al., 2003). In stimulated VSMCs, AIF dissociates from larger F-actin bundles and translocates to the lamellipodia (Autieri et al., 2003). Conversely, AIF in macrophages shows increased colocalization with F-actin in membrane ruffles upon stimulation (Ohsawa et al., 2000). These results suggest that there is a functional

interaction between AIF and F-actin, and while the mechanisms of action are not yet fully understood, it is thought that calcium signalling may play a role in this association (Autieri & Chen, 2005).

Although there is some evidence that AIF activates phagocytosis in invertebrates (Zhang et al., 2013), functional characterization of AIF in haemocyte activation has not been explored. Understanding this interaction may infer its role in *H. midae* haemocytes and provide new insight into the cell signalling events that occur during haemocyte activation in invertebrates. Thus, the effect of AIF in *H. midae* haemocytes was investigated in this study to attempt to elucidate the functional role AIF may play in haemocyte phagocytosis.

4.1.1 Aims of this chapter

The inflammatory response is an important component of the host's immune response, regulated through a large consortium of mediators which together, form an intricate and complex regulatory network. Cytokines play a prominent role in this regulation and the interferon (IFN)-γ-inducible Ca^{2+}-binding cytokine allograft inflammatory factor-1 (AIF) has been shown to be critically involved in the activation of inflammation (Zhao et al., 2013). Since AIF was identified as differentially expressed in *H. midae* haemocytes following bacterial-challenge (Chapter 2 and 3), a similar functional role in the immune response of *H. midae* is postulated. Thus, the aim of this chapter was to characterise a putative AIF molecule in *H. midae* to investigate the functional biological role of this protein in haemocytes.

The first objective of this chapter was to establish an *in vitro* system using cultured haemocytes so as to investigate the functional role of AIF. Therefore, the temporal expression of AIF that was observed *in vivo* (Chapter 3) was confirmed by challenging cultured *H. midae* haemocytes with a bacterial pathogen and monitoring AIF expression by western blot hybridization. The second objective of this study was to investigate the biological role of AIF in *H. midae* haemocytes. Since previously published studies have demonstrated that AIF plays a role in macrophage and granulocyte activation, a similar function is hypothesized in *H. midae* haemocytes. To test this hypothesis, the effect of

inhibiting AIF on the phagocytic capability of *H. midae* haemocytes was investigated. Finally, the functional interaction of AIF with F-actin that has been reported in macrophages and VSMCs (Autieri et al., 2003; Ohsawa et al., 2000) was investigated using the *in vitro* system and immunofluorescent imaging to further infer the mechanistic action of AIF in activating haemocyte phagocytosis.

4.2 Materials and methods

All media and solutions used in this study are listed in Appendix A

4.2.1 I*n vitro* bacterial challenge and AIF expression

4.2.1.1 *In vitro* tissue culture of *H. midae* haemocytes

Haemolymph was isolated from healthy, unchallenged *H. midae* via the pedal sinus (section 2.2.3) and pooled (500 µL per animal; n = 6) and the concentration of haemocytes determined (section 2.2.4). Haemolymph at a concentration of 1×10^6 cells/ml was seeded onto 35 × 10 mm tissue culture dishes (Nunclon™ Delta Surface, Nunc™) and left in a dark, moistened chamber for 30 min at 18 ^{0}C to allow the haemocytes to settle and attach to the surface. Excess haemolymph was aspirated and the adhered cells washed twice with 1 ml phosphate buffered saline solution (PBS, Appendix A.2.1.2). A 1 ml portion of Hanks M-199 media (Gibco®) modified with the addition of supplementary salt solution (Suja & Dharmaraj, 2005, Appendix A.2.5.1), Amphotericin B (Sigma®, Appendix A.2.5.2) and Penicillin G/Streptomycin G (Invitrogen™) was added to each well (MHBSS, Appendix A.2.5.3). The cultures were subsequently incubated in a dark, moist chamber at 18 ^{0}C. Culture medium was replaced every second day. Cultured haemocytes were allowed to acclimate for two days prior to initiating the bacterial-challenge trials.

4.2.1.2 *In vitro* bacterial-challenge

Bacterial-challenge trials were performed by adding 100 µL heat-killed *V. anguillarum* (1×10^8 cells/ml) (section 2.2.2) to each well containing monolayers of *H. midae* haemocytes (section 4.2.1.1). Protein samples were destructively collected (section 4.2.1.3) at 0 (control), 15, 30, 60, 90 and 120 min post-challenge and total soluble protein isolated following haemocyte lysis (section 4.2.1.3). The control group included haemocytes that were sampled immediately after the addition of bacteria as a time zero control. In order to collect sufficient protein for western blotting, duplicate wells were included for each time point. This trial was repeated in three independent experiments.

4.2.1.3 Total soluble protein isolation and western blot analysis

Following bacterial-challenge (section 4.2.1.2), haemocytes were lysed and total protein was isolated at 0, 15, 30, 60, 90 and 120 minutes post-challenge. Excess culture medium was aspirated and the haemocytes were rinsed twice with 1 ml PBS (Appendix A.2.1.2) prior to adding 100 µL of lysis buffer (Appendix A.2.2.1) to the well. Cells and cell lysate were harvested by perpendicular strokes across the diameter of the well using a 25 cm cell scraper (Greiner Bio-One). The cell lysate from duplicate wells was aspirated and pooled in a microfuge tube. Cell debris was collected by centrifugation at 8000 $\times g$ for 30 min at 4 ^{0}C to replicate the protein isolation conditions from the iTRAQ experiment (section 2.2.7.11), and the supernatant transferred to a fresh microfuge tube. Protein concentration was determined using a NanoDrop™ 2000 (Thermo Scientific) machine using A280 absorbance measurements. Total soluble protein was fractionated on a 15% SDS-PAGE (section 3.1.3.2) and transferred onto nitrocellulose membrane (section 3.1.3.3) prior to densitometric analysis (section 3.1.3.4).

4.2.2 AIF effect on phagocytosis in *H. midae* haemocytes

4.2.2.1 Antagonist *in vitro* treatment

The anti-inflammatory drug sodium salicylate has been used in several studies to inhibit the expression of AIF (Yang et al., 2005; Watano et al., 2001; Lemay et al., 1999). To prepare slides for the phagocytosis assay (section 4.2.2.2), glass coverslips were washed twice for 30 min in 3.2% (*v/v*) hydrochloric acid and rinsed with distilled water. These were then placed at the bottom of 6-well tissue culture plates prior to seeding with cultured *H. midae* haemocytes (section 4.2.1.1). Three groups were included in this assay: (1) an unchallenged control group (-ve control), (2) haemocytes challenged with *V. anguillarum* (+ve control) and (3) haemocytes pre-treated with sodium salicylate and challenged with *V. anguillarum* (inhibited). Haemocytes from the inhibited group were pre-treated for 2 hours with 1 mM (*w/v*) sodium salicylate (Appendix A.2.5.4) prior to bacterial-challenge. The bacterial-challenge was conducted as described above (section 4.2.1.2) and haemocytes sampled at 2 hours post-challenge since this was when the highest expression of AIF was detected (Figure 4.1). Coverslips containing haemocytes from the –ve control group were sampled immediately after the addition of bacteria. All

experimental groups were treated and challenged in a time staggered manner in order to sample all the coverslips for the phagocytosis assay at the same time. Each group was assayed in duplicate and three independent experiments were carried out for statistical purposes.

4.2.2.2 Evaluation of AIF inhibition by western blot analysis

In order to confirm down-regulation of AIF in the inhibited group, additional haemocytes were prepared for western blot analysis. Here, haemocytes subjected to a bacterial-challenge (+ve control) and those pre-treated with sodium salicylate (inhibited) were sampled at 2 hours post-challenge. This was followed by protein isolation and western blot analysis (Section 4.2.1.3). Total protein concentration was quantified by PonceauS stain and used for normalization.

4.2.2.3 Phagocytosis assay

The coverslips containing the –ve control, +ve control and inhibited haemocytes were prepared for the phagocytosis assay by removing excess culture medium and rinsing the coverslips twice with ice-cold PBS (Appendix A.2.1.2) before adding 100 µL of fluorescein isothiocyanate isomer-1 (FITC isomer-1) labelled *V. anguillarum* 5676 (1×10^8 cells/ml)(Appendix A.2.6.1). Coverslips were incubated in the dark at room temperature (RT) for 20 min followed by two PBS washes. Cells were then fixed with 150 µL of ice-cold methanol (5 min, RT). The methanol was subsequently removed by washing twice with ice-cold PBS before adding 100 µL ethidium bromide (100 µg/ml, Appendix A.2.6.2) to each coverslip and incubating (1 min, RT). Excess ethidium bromide was rinsed off with ice-cold PBS. The percentage of phagocytic cells was counted using an inverted fluorescent microscope (Nikon Inverted Microscope DIAPHOT-TMD containing a Nikon EPI-Fluorescent attachment TMD-EF) at 400X magnification using a 510 nm excitation filter. Images were captured using an AxioCam (Zeiss) camera with the corresponding software AxioVision AC version 4.4.

Haemocytes that contained more than three FITC-labelled *V. anguillarum* were considered to be phagocytic cells. Each duplicate group was counted twice. The percentage of phagocytosing haemocytes was determined from a total count of 200 randomly selected haemocytes. Statistical significance was calculated using a one-factor ANOVA with posthoc pairwise comparison.

4.2.3 Cellular location of AIF in *H. midae* haemocytes and colocalization of AIF with F-actin

4.2.3.1 Slide preparation for confocal imaging

Acid-washed coverslips were placed at the bottom of the 6-well plates prior to seeding with cultured *H. midae* haemocytes (section 4.2.1). Here, four groups were examined: control haemocytes, bacterial-challenged haemocytes examined at 15 min and 2 hours post-challenge (section 4.2.2.1) and sodium salicylate treated haemocytes challenged with *V. anguillarum* and examined at 2 hours post-challenge (section 4.2.3.1). In order to establish background interference levels prior to imaging, two control coverslips were prepared, one with no staining and one treated with secondary antibody only. Each group was prepared in duplicate and the experiment repeated a total of three independent times for statistical purposes.

Coverslips were rinsed twice with 2 ml of PBS prior to fixing the cells with 2% (*w/v*) paraformaldehyde (Appendix A.2.7.1) by incubating the coverslips at room temperature for 10 min in a fume hood. Coverslips were subsequently washed twice with PBS and the cells permeabilized with 0.5% (*v/v*) Triton X-100 (Appendix A.2.7.2) by incubating the coverslips in an ice-water bath for 10 min. In order to reduce non-specific staining, the coverslips were washed a further two times with PBS and blocked with 5% (*w/v*) bovine serum albumin (BSA) (blocking solution, Appendix A.2.7.3) for one hour at room temperature. Coverslips were rinsed once with PBS and the cells stained with 200 µL primary anti-AIF (Separations PA5-27436) antibody (1:100 in blocking solution). These were incubated overnight in a sealed humidified chamber at 4^0C. Following incubation, coverslips were placed back in the 6-well plates and rinsed with three consecutive 10 min PBS washes. The cells were then stained with 200 µL secondary antibody conjugated to fluorophores (anti-rabbit Alexa Fluor® 488; 1:500 in blocking solution) and incubated for one hour in the dark, at room temperature. F-actin staining was performed by adding 200 µL Rhodamine Phalloidin (Cytoskeleton, Inc.) at a concentration of 100 nM (Appendix A.2.7.4). The coverslips were incubated in the dark for one hour at room temperature. Coverslips were then rinsed once with PBS and counterstained with two ml Hoechst Nuclear stain prepared from a working stock solution (0.5 µg/ml in PBS) and diluted to a final concentration of 1:5000. Coverslips

were incubated for 10 min at room temperature followed by a final PBS rinse. Coverslips were mounted onto microscope slides using Mowiol mounting medium containing *n*-propylgallate as an anti-fading agent and stored in the dark at 4^0C until viewing.

4.2.3.2 Confocal imaging

Confocal microscopy was performed with a Zeiss Axiovert 200M LSM 150 Meta NLO Confocal Microscope using the 40 X oil immersion objective. A multitrack configuration using the 488 nm (Argon laser) for Alexa 488, 561 nm (Solid state laser) for Rhodamine Phalloidin and 750 nm (MaiTai two photon laser) for Hoechst nuclear stain excitation lines were employed to minimise bleed through between fluorophores. Emission filters were 500-550 nm band pass (BP), 575-630 nm BP and 390-465 nm BP for Alexa 488, Rhodamine Phalloidin and Hoechst nuclear stain, respectively. The photomultiplier gain and offset were adjusted to exclude any background fluorescence emitted by the cells and fluorophores. Three different fields of view from three independent experiments were collected for each sample. All imaging parameters were kept the same for all data acquisitions in order to not affect pixel intensity for co-localization analysis. The single label control samples were used to set appropriate crosshair threshold values which were kept constant for the analysis of all double-label experimental samples.

4.2.3.3 Colocalization analysis

In order to explore the potential functional relationship between AIF and F-actin, the acquired confocal images were analysed for colocalization with the Carl Zeiss ZEN software (version 2009) using Mander's correlation and overlap coefficients (Manders et al., 1993; Costes et al., 2004) for the two fluorophores. Threshold values were set as 31 and 30 for the red and green channels respectively. Three fields of view were analysed for each experimental group (n = 3 with 3-15 cells on each) and the average calculated for each biological repeat. Statistical analysis was performed using one-way ANOVA pairwise multiple comparison (Holm-Sidak method) and significance set $P < 0.05$. Co-localization analysis was conducted on both the entire population of pixels and a defined region of interest (ROI) to cross-examine both methods. Since there appeared to be no significant difference between the two methods, overlapping coefficients for the entire population of pixels was used.

4.3 Results

4.3.1 *In vitro* bacterial challenge and AIF expression

The temporal expression of AIF was investigated in cultured *H. midae* haemocytes to determine the response time of this protein to an *in vitro* bacterial-challenge. Total soluble protein was isolated from haemocytes collected at 0, 15, 30, 60, 90 and 120 min post-challenge and analysed by western blot (Figure 4.1). AIF expression was observed as early as 15 min post-challenge, reaching a maximal level at 120 min post-challenge (Figure 4.1B). These results are consistent with the time-dependent expression of AIF observed *in vivo* following bacterial-challenge (Figure 3.1).

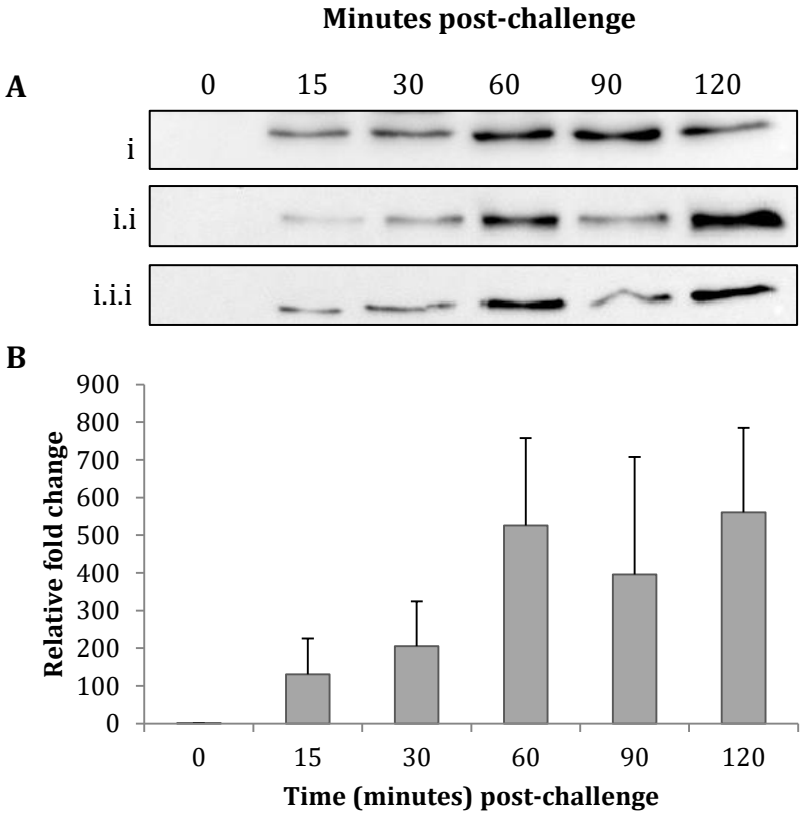

Figure 4.1 (**A**) Western blot and (**B**) densitometric analysis of the temporal expression of allograft inflammatory factor in cultured *H. midae* haemocytes sampled at 0, 15, 30, 60, 90 and 120 minutes post bacterial-challenge. i-i.i.i represents three experimental replicates. Error bars represent the mean (±) standard error (n = 3).

4.3.2 AIF effect on phagocytosis in *H. midae* haemocytes

To investigate whether enhanced AIF expression modulates the phagocytic activity of *H. midae* haemocytes, AIF-inhibited cultured haemocytes were examined for incorporation of FITC-labelled *V. anguillarum* in comparison to positive and negative controls. Since AIF expression appeared to be at its highest 120 min post-challenge (Figure 4.1B), the effect of the AIF antagonist on haemocyte activity was examined at this time point.

Western blot analysis confirmed the inhibitory action of sodium salicylate on AIF expression as seen by the lack of up-regulated AIF expression following bacterial-challenge (Figure 4.2A). Furthermore, total protein concentration as quantified by PonceauS stain during normalization showed that there were not any differences in total protein expression across treatments. A consequence of inhibiting AIF expression in haemocytes was a statistically significant decrease in phagocytic activity when compared to positive and negative controls (Figure 4.2B). The ability of haemocytes to phagocytose *V. anguillarum* was confirmed by immunofluorescence microscopy (Figure 4.2C).

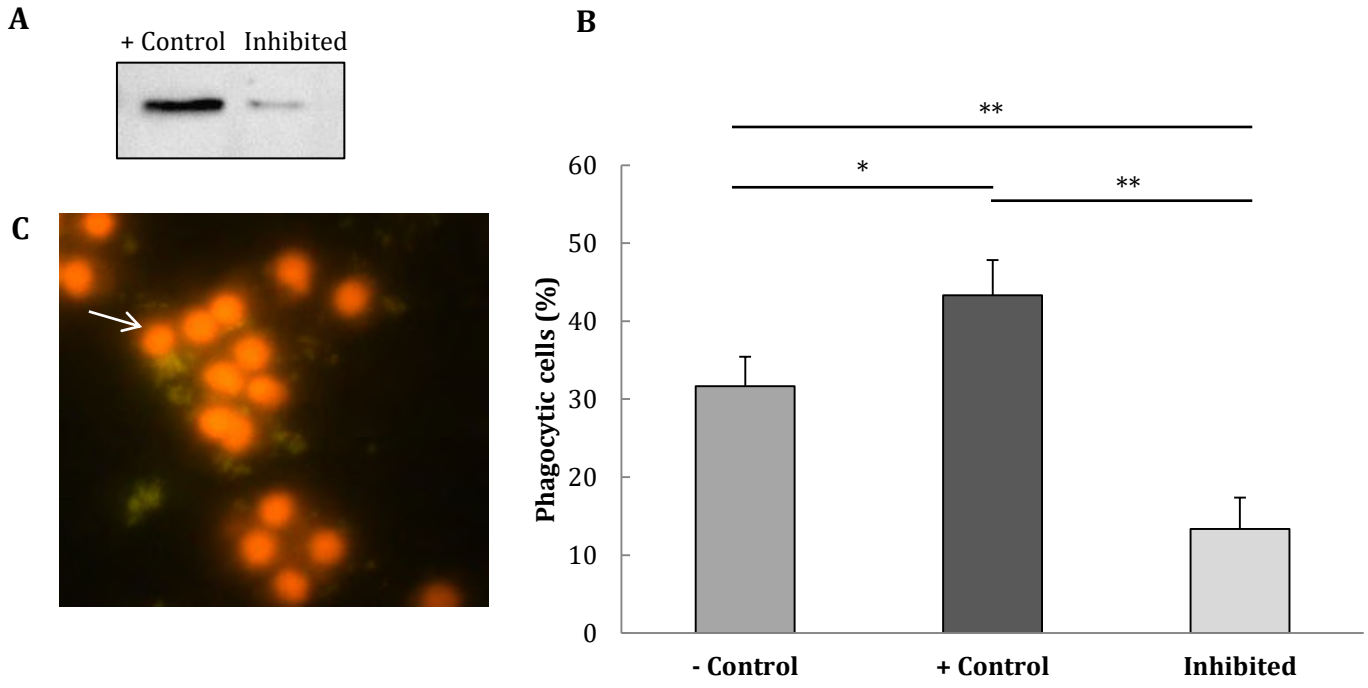

Figure 4.2 (**A**) Western blot showing down-regulation of AIF in the sodium salicylate pre-treated group (inhibited) compared to the positive control (bacterial-challenged). (**B**) Effect of the AIF antagonist sodium salicylate, on the phagocytic activity of *H. midae* haemocytes compared to the negative (unchallenged) and positive controls. Error bars represent the mean (±) standard error (n = 3). Statistical significance was calculated using a one way ANOVA with posthoc comparison (where * is $P \leq 0.01$ and ** is $P \leq 0.001$). (**C**) Representative image (400X magnification), obtained from the positive control group, showing *H. midae* haemocytes phagocytosing *V. anguillarum* (white arrow).

4.3.3 Cellular location of AIF in *H. midae* haemocytes and colocalization of AIF with F-actin

The cellular location of AIF and its colocalization with F-actin was investigated in cultured *H. midae* haemocytes. Unchallenged cells displayed endogenous AIF expression that colocalizes with F-actin (Figure 4.3A). Upon bacterial-challenge, colocalization with F-actin decreased at 15 min post-challenge (Figure 4.3B) with the lowest overlapping coefficient occurring at 2 hours post-challenge (Figure 4.3C). Bacterial-challenged haemocytes in which AIF was inhibited did not display decreased colocalization but rather, resembled unchallenged cells (Figure 4.3D). In addition, many of the inhibited cells exhibited a contracted morphology with little to no lamellipodia extensions (Figure 4.3D). By contrast, bacterial-challenged cells displayed a large number of extensions, particularly at 15 min post-challenge (white arrows, Figure 4.3B). There was a statistically significant difference in AIF and F-actin colocalization between the control and 2 hour post-challenge cells and between the 2 hour post-challenge and the inhibited cells (Figure 4.4).

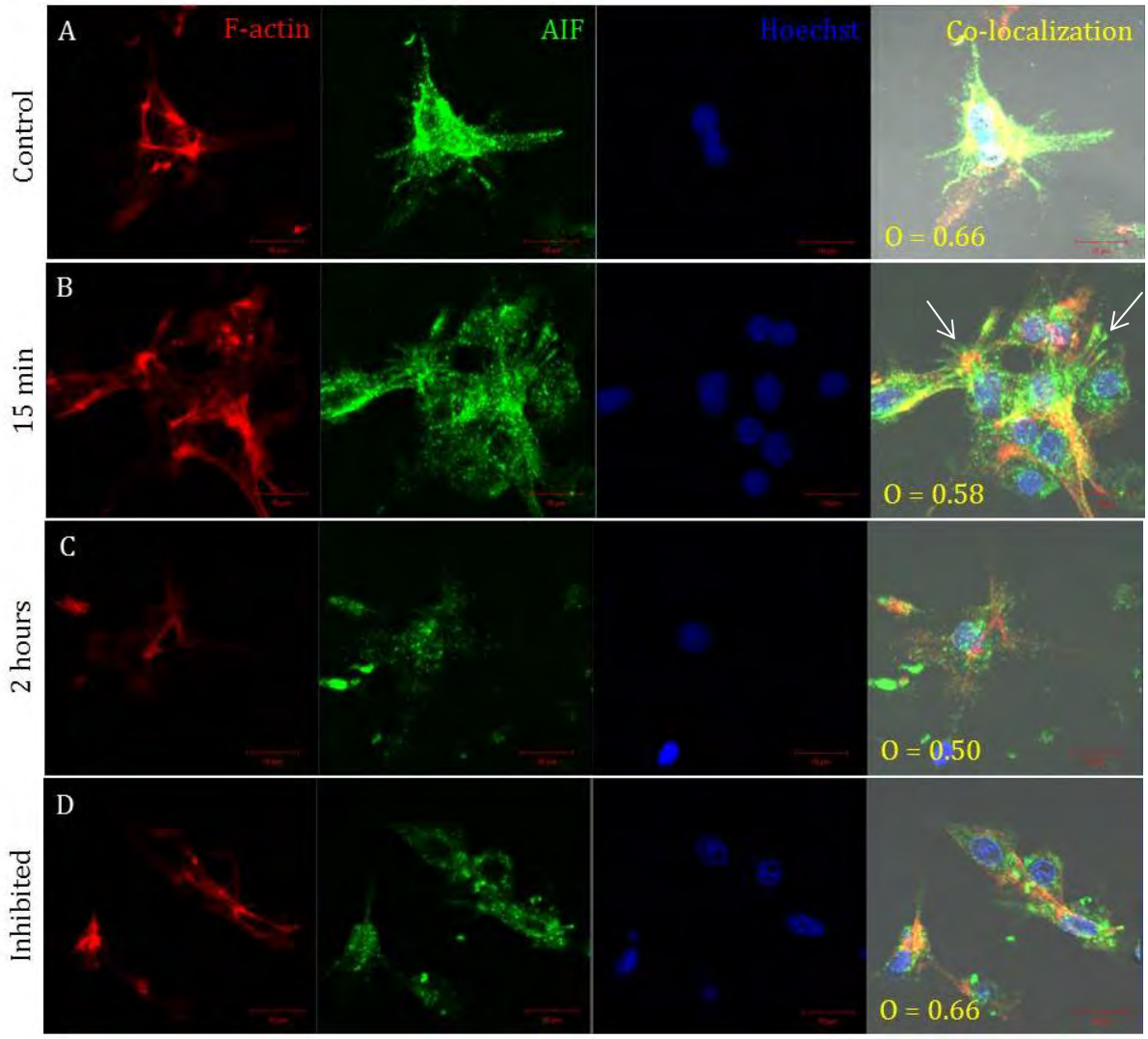

Figure 4.3 Immunofluorescent imaging and colocalization analysis of allograft inflammatory factor-1 (AIF) and filamentous actin (F-actin) in cultured *H. midae* haemocytes. (**A-D**) Representative images showing split channels for F-actin (red), AIF (green), Hoechst nuclear stain (blue) and merged images (yellow). Haemocytes challenged with *Vibrio anguillarum* and analysed at (A) 0 (control), (B) 15 minutes and (C) 2 hours post-challenge, whilst the (D) inhibited groups were pre-treated with sodium salicylate for 2 hours prior to bacterial-challenge and analysed at 2 hours post-challenge. Mander's Overlap coefficient (O) calculated from three independent replicate experiments each containing three different fields of view; values range from 0 to 1 where 1 indicates perfectly colocalized pixels. Scale bar = 10 µm, white arrows indicate lamellipodia extensions.

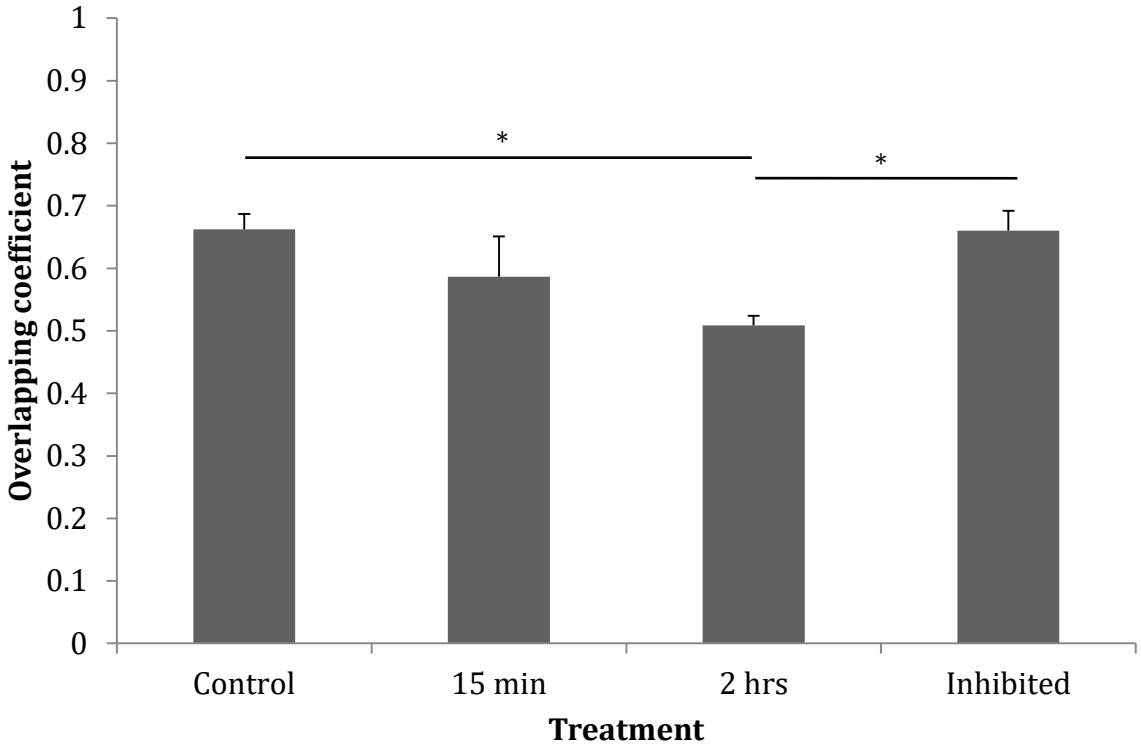

Figure 4.4 Statistical analysis of colocalization between AIF and F-actin in cultured *H. midae* haemocytes following bacterial-challenge at 0 min (control), 15 min and 2 hours post-challenge. The inhibited cells were pre-treated with sodium salicylate prior to bacterial-challenge and analysed at 2 hours post-challenge. Error bars represent the mean (±) standard error (n = 3) where each replicate experimental sample contained three different fields of view (n = 3 with 3-15 cells on each). Statistical significance was calculated using one-way ANOVA pairwise multiple comparison (Holm-Sidak method) and significance set $P < 0.05$ (where * is $P \leq 0.01$).

4.4 Discussion

Allograft inflammatory factor-1 (AIF) has been identified as an important modulator of diverse inflammatory pathological processes and key immune responses in vertebrate species (Deininger et al., 2002; Zhao et al., 2013). The high sequence similarity across different species suggests evolutionary functional conservation of this protein (Deininger et al., 2002) although its function in the innate immune system remains to be clarified (Li et al., 2013). Genetic studies conducted in a variety of invertebrate species have demonstrated that AIF is transcribed at high levels in haemocytes and coelomocytes following microbial stimuli (De Zoysa et al., 2010; Ji et al., 2014; Kruse et al., 1999; Li et al., 2013; Wang et al., 2013; Zhang et al., 2011b; Zhang et al., 2013). Furthermore, studies conducted in the pacific oyster observed that recombinant AIF stimulates phagocytosis in granulocytes (Zhang et al., 2013) suggesting a functional role in haemocyte phagocytosis. This is similar to vertebrate studies showing augmented macrophage phagocytic activity as a result of AIF over-expression (Ohsawa et al., 2000; Autieri et al., 2003). Taken together, these results suggest a conserved evolutionary role for AIF as a fundamental component of the inflammatory and immune response. It is therefore reasonable to hypothesize that AIF may play a key role in regulating haemocyte activity in *H. midae*. To date, the functional role of invertebrate AIF in immune activation of haemocytes remains obscure.

AIF was found to respond to a bacterial-challenge in *H. midae* haemocytes (Chapter 2) and its expression confirmed *in vivo* by western blot analysis (Chapter 3). To confirm and further explore the response of AIF *in vitro*, bacterial-challenge trials were conducted on cultured *H. midae* haemocytes. The response of AIF *in vitro* is comparable to the *in vivo* bacterial-challenge trials with a similar time-dependent up-regulation of the relative expression of AIF following bacterial-challenge (Figure 4.1). AIF induction was observed as early as 15 min post-challenge and persisted throughout the assessed time course (Figure 4.1). This protein is interesting in view of its rapid activation which suggests a critical role in haemocyte stimulation. This is consistent with the idea that AIF functions as an early cytokine inducer and important modulator of the immune response (Autieri, 1996; Deininger et al., 2002; Xu et al., 2014; Zhang et al., 2013).

Since haemocytes are the first line of defence during infection, a rapid response is critical to combat invading pathogens. To date, there have been no proteomic studies on the temporal expression of AIF in invertebrates but studies on transcriptional regulation in *H. discus discus* demonstrated up-regulation of AIF transcripts in circulating haemocytes from 3-24 hours following bacterial-challenge (De Zoysa, Nikapitiya et al., 2010a). The up-regulated and sustained expression of AIF transcripts in bacterial-challenged invertebrate species is mirrored in other studies (Ji et al., 2014; Kruse et al., 1999; Li et al., 2013; Wang et al., 2013; Zhang et al., 2011b; Zhang et al., 2013). This study showed that AIF protein expression significantly increases following bacterial challenge, which correlates well with the earlier transcription studies. Although the protein response was identified as early as 15 min post-challenge *in vitro*, early induction of this protein should be further explored *in vivo*. Nonetheless, the comparable expression profile observed in this study demonstrates that *H. midae* haemocytes cultured *in vitro* provide a suitable model for short term functionality studies, similar to published reports of *in vitro* haemocyte studies conducted in other marine organisms (Jose et al., 2010; Mortensen & Glette, 1996; O'Neill et al., 2013; Rinkevich, 2005; Villena, 2003).

Previous studies have shown that AIF plays a central role in mammalian cell migration and phagocytosis (Mishima et al., 2008; Utans et al., 1995; Yang et al., 2005; Ohsawa et al., 2000; Autieri & Chen, 2005), with a similar effect demonstrated with regard to the phagocytic capability of *C. gigas* granulocytes (Zhang et al., 2013). As such, the effect of AIF expression on *H. midae* haemocyte phagocytosis was investigated. Although sodium salicylate has been used in studies to study the effects of inhibiting AIF (Yang et al., 2005; Lemay et al., 1999; Wantano et al., 2001), the specificity of this drug cannot be exclusively determined to be AIF-specific. Studies have shown that sodium salicylate treatment down-regulates AIF mRNA in macrophages and has a mild suppressive action on certain cytokines, however inflammatory proteins such as Nf-κB were shown not to be affected (Yang et al., 2005; Lemay et al., 1999). Thus, functional mechanisms cannot be conclusively determined without the use of recombinant AIF protein to stimulate haemocytes, or using gene-knockdown assays. Nevertheless, quantitation of total protein expression by PonceauS stain during the normalization of western blot

expression data showed that there was not a broad decrease in protein expression in the inhibited treatment group. This indicated that sodium salicylate did not have a depressive action on total protein expression and that a fair level of functional inference may still be achieved from these results.

Increased AIF expression, as a result of bacterial infection, was found to enhance the phagocytic ability of haemocytes *in vitro* (Figure 4.2B). Inhibiting AIF expression significantly decreased phagocytic activity, resulting in fewer phagocytosed cells in the inhibited group (Figure 4.2B). Down-regulation of AIF expression was confirmed by western blot which indicated that pre-treatment with the anti-inflammatory drug sodium salicylate supressed up-regulated expression of AIF when the haemocytes were challenged with a bacterial-pathogen. Although the limitations of using sodium salicylate reduces the functional analysis that may be achieved, these findings are consistent with studies with mammalian cells (Mishima et al., 2008; Utans et al., 1995; Yang et al., 2005; Ohsawa et al., 2000; Autieri & Chen, 2005) and *C. gigas* (Zhang et al., 2013), thus indirectly supporting the hypothesis that AIF plays a similar functional role in *H. midae* haemocyte phagocytosis.

The functional role by which AIF induces haemocyte phagocytosis remains to be clarified further. The induction mechanisms of phagocytosis are varied and complex, as numerous receptors and signalling molecules can be induced, oftentimes in a parallel fashion, depending on the target and its location (Underhill & Goodridge, 2012; Underhill & Ozinsky, 2002). Traditionally, phagocytosis and the activation of pro-inflammatory signals were considered separate events. However, it is now well established that phagocytic-associated responses are either pro- or anti-inflammatory (García-García & Rosales, 2000). A number of phagocytic receptors that are actively recruited to phagosomes, such as Toll-like receptors (TLRs) and dectin-1, are now known to also trigger the inflammatory response (Aderem, 2003; Kawai & Akira, 2011; Underhill & Ozinsky, 2002). Combinatorial signalling between multiple receptors has been shown to result in qualitatively different inflammatory responses (Gantner et al., 2003), further compounding the complexity of cell signalling during phagocytosis. There is a clear functional relationship that exists between phagocytosis and the inflammatory response as common signalling molecules can be attributed to both processes (Underhill & Ozinsky, 2002). Identification of binding and interacting

partners can often offer insight into the function of proteins. Thus, the mechanism by which AIF mediates cell movement was investigated by studying whether intracellular colocalization occurs between AIF and F-actin in cultured haemocytes.

Visualising colocalization through merging of red and green channels (giving rise to yellow) can be ambiguous and limited, since generation of yellow spots is highly dependent on the signal intensity obtained from each channel (Dunn et al., 2011). Instead, calculating the proportion of colocalized pixels from overlapping coefficients using either Pearson's correlation coefficient or Mander's coefficient is the most commonly used method to perform quantitative colocalization analysis (Costes et al., 2004). In this study, the use of overlapping coefficient according to Mander's (Manders et al., 1993) was used for colocalization analysis since it indicates actual overlap of the signals and is considered more biologically relevant (Costes et al., 2004). The values of this coefficient range from 0 to 1, where a value of 0.5 implies that 50% of both selected channels colocalize. Values ranging from 0.6 to 1 indicate colocalization (Zinchuk & Zinchuk, 2008), where a value of 1 represents perfectly colocalized pixels. One limitation of this method is that measurements are affected by the ratio of pixels between channels, which may result in lowered overlap coefficient values (Dunn et al., 2011).

In the absence of bacterial-challenge, endogenously expressed AIF displayed a diffuse, cytoplasmic presence and colocalized with F-actin bundles (Figure 4.3A), which correlated well with what has been observed in other cellular systems (Ohsawa et al., 2000; Autieri et al., 2003). Stimulation of haemocytes by bacterial-challenge resulted in disruption of the AIF and F-actin association and an increase in cell extension, particularly evident at 15 min post-challenge (Figure 4.3B). The overlapping coefficient decreased significantly over time in the challenged cells, with the lowest coefficient observed at 2 hours post-challenge (Figure 4.3C). This effect was attenuated in cells that had been pre-treated with sodium salicylate (Figure 4.3D). These results are consistent with colocalization studies conducted in VSMCs that showed decreased colocalization with F-actin following stimulation (Autieri et al., 2003), although direct translocation of AIF into lamellipodia was not observed in *H. midae* haemocytes. The reason for this difference is unclear, but it may be due to differences between vertebrate and invertebrate cellular systems.

The functional association of AIF with F-actin is thought to result from calcium binding (Ohsawa et al., 2000). AIF is structurally comprised of three parts, the N- and C-terminal regions and a partially conserved EF-hand calcium binding domain (Deininger et al., 2002). Macrophage AIF mutants carrying deletions at either the N- and C-terminal regions or in the EF-hand calcium-binding domain exhibited inhibited membrane ruffle and phagocytic cup formation, suggesting that calcium signalling is a regulator of AIF and that binding is necessary for AIF to function (Ohsawa et al., 2000). Calcium signalling is believed to be a major regulator of cytoskeletal rearrangement, while initiation of phagocytosis and actin polymerization is associated with a rapid flux in the cytosolic calcium concentration (TranVan Nhieu et al., 2004). Many actin-binding proteins dissociate from F-actin in the presence of calcium (Autieri et al., 2003), and AIF may be responding in a similar manner. Since calcium binding is thought to cause a conformational change that is critical in AIF-mediated events (Autieri & Chen, 2005), it may be responsible for F-actin binding observed in *H. midae* haemocytes. Indeed, a number of regulatory molecules involved in calcium signalling were identified as differentially expressed by iTRAQ analysis which further supports this notion, although further characterisation is required. Deconvoluting the associated molecular signals involved in the inflammatory signalling cascade that occurs during immune stimulation remains a challenge due to the complexity of the system under observation. AIF has been shown to interact with numerous signalling molecules and transcription factors, as well as containing a number of theoretical binding sites (Zhao et al., 2013). Thus, these molecular associations should be investigated to confirm their action in *H. midae* haemocytes and further our understanding of inflammatory signalling in invertebrates. Results from this study provide some insight into potential functional mechanisms of AIF's involvement in activating the phagocytic function of *H. midae* haemocytes via an F-actin interaction.

4.4.1 Concluding remarks and future work

The molecular characterization of the protein allograft inflammatory factor in invertebrate marine species remains to be clarified and until now, only transcriptional studies had been conducted. Understanding the functional role of inflammatory molecules in haemocytes is a key step in elucidating the complex and multifarious signal transduction events that occur during haemocyte phagocytosis and activation of the innate immune response. This study aimed to characterise a putative AIF protein in *H. midae* haemocytes and has demonstrated its association with haemocyte phagocytosis.

Although the mechanisms of action of AIF are not well understood, a functional interaction with F-actin was identified upon bacterial stimulation. One of the challenges of elucidating signalling pathways is the complex role of signalling molecules and interacting partners. There are numerous AIF-binding proteins that have been reported in vertebrate species and the corresponding homologues should therefore be explored in *H. midae* haemocytes in order to further understand the mechanistic action of AIF in haemocytes. There are reports in mammalian systems that calcium binding may play a role in this regard, and since calcium signalling was identified as differentially regulated during iTRAQ-profiling, investigating this relationship could further our understanding of the signalling molecules involved in inflammation and immune regulation in *H. midae* haemocytes.

CHAPTER 5
CONCLUSIONS AND FUTURE PROSPECTS

South African land-based aquaculture of the abalone species *H. midae* has grown significantly since it began in the early 1990s, with annual production reaching 1036 tons by 2012 (Aquaculture yearbook South Africa, 2012). It therefore represents a vital economic sector for South Africa which is currently one of the largest producers of abalone worldwide. However, the reoccurrence of disease outbreaks has had a severe and detrimental impact on the abalone aquaculture industry, resulting in large-scale economic loss (Lafferty et al., 2014). Mitigating and controlling infections in aquacultured abalone requires an intricate understanding of the molecular mechanisms underlying the innate immune response of these commercially valuable molluscs. Unfortunately, research in this area is severely lacking. Much of the work conducted in the field of marine invertebrate immunology has focussed on other marine organisms. Consequently, the pathophysiology of disease in *H. midae* remains poorly understood. The recent advancements made in quantitative mass spectrometry-based proteomics now allow a systems-wide analysis of global proteome changes under different conditions. This approach offers a powerful tool for elucidating the functional and biochemical pathways of the immune response. Thus, this study set out to investigate changes in global protein expression in *H. midae* haemocytes to determine how these are modulated in response to a bacterial challenge. A comparative, shotgun approach in combination with isobaric tagging for relative and absolute quantification (iTRAQ)-LC-MS/MS was used. Through this approach, this study addressed the following objectives: i) quantitatively profile protein expression in *H. midae* haemocytes to identify proteins that are differentially regulated following immune stimulation using iTRAQ-based LC-MS/MS proteomics, ii) elucidate the molecular pathways modulating the immune response of *H. midae* and establish the pathophysiological mechanisms underlying temporal regulation of innate immune system of abalone, iii) validate and functionally characterise a potential molecular indicator of health in *H. midae* haemocytes to establish its relevance as a suitable biomarker candidate in abalone aquaculture.

This study represents the first comprehensive analysis of the haemocyte proteome of *H. midae* in response to immune stimulation. The main empirical findings of this study

have been summarised within the respective experimental chapters (Chapters 2-4). The data presented provides qualitative and quantitative information regarding the haemocyte proteome of *H. midae* and an overview of the molecular pathways and biological processes modulated in response to a bacterial-challenge. Over 100 proteins were identified and quantified in bacterial-challenged haemocytes, 16 of which were found to have significantly altered expression, fulfilling the first objective of this study. The second objective was satisfied through clustering and functional bioinformatics analysis of the immune-related biological processes of the identified proteins. This provided insight into the molecular mechanisms underlying the innate immune response. The network modelling conducted in this study implicates some of these proteins in key processes of innate immunity and in conjunction with results obtained from other marine invertebrate studies, a classical induction of innate immune responses in *H. midae* haemocytes can be observed. The hypothesized cellular processes and molecular pathways are summarised in Figure 5.1, as well as the putative involvement of proteins identified as significantly changing (metabolic processes have not been included).

Overall, this study demonstrates the intertwined nature of the innate immune response and may provide targets for future investigations in the search for appropriate biomarker candidates. The putative participation of the identified proteins in the proposed molecular pathways has been discussed extensively in Chapter 3, along with the studies corroborating their involvement in marine invertebrate immune processes. The results indicate a complex and multifaceted response to bacterial challenge in *H. midae,* implicating the coordinated response of multiple signalling pathways. Results show that calcium and cAMP signalling pathways control the majority of signalling pathways regulated in *H. midae* and exert immune responses via activation of MAPK signalling cascades. Distinct biological processes were shown to be temporally regulated in response to bacterial challenge. This includes early up-regulation of proteins involved in phagocytosis, nitric oxide production and ATP-synthesis, whilst down-regulated responses predominantly included proteins involved in the regulation of apoptosis. The late up-regulated response primarily involved protein kinase activity and detoxification processes.

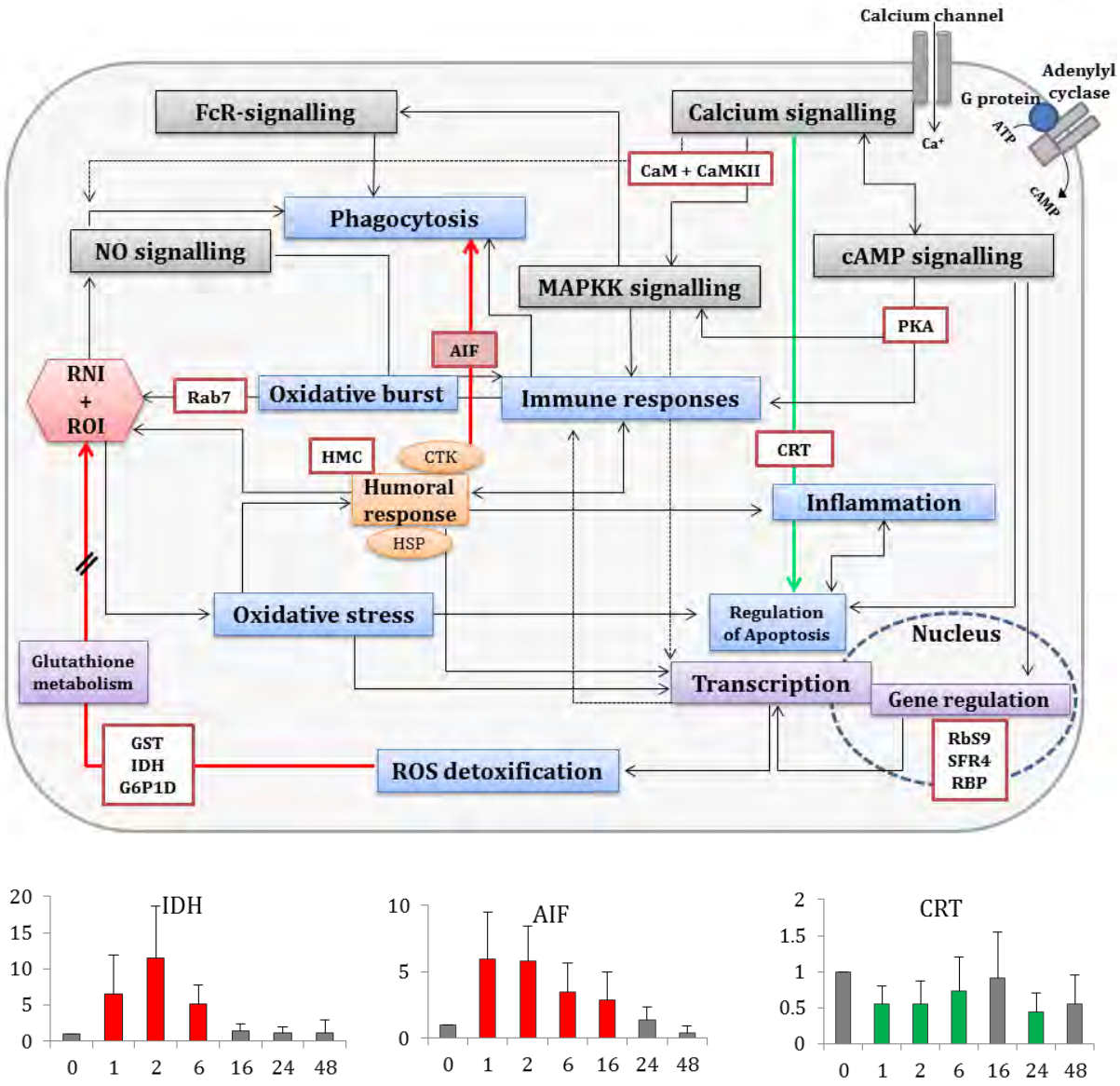

Figure 5.1 Schematic diagram of the hypothesized immune response and pathways induced in response to bacterial-challenge in *H. midae*. The proteins that were identified as statistically significantly changing are shown in red boxes. The secondary messengers, calcium (Ca^{2+}) and cAMP, activate signalling cascades involving calmodulin (CaM), calmodulin-dependent protein kinase (CaMKII) and cAMP-dependent protein kinase (PKA) as regulatory molecules. Subsequent activation of the MAPKK signalling pathways regulates immune responses including phagocytosis and oxidative burst, potentially involving the small GTPase Rab7 as a regulator of endocytosis. Furthermore, MAPK activation regulates the production of reactive oxygen and nitrogen intermediates (ROI & RNI), humoral factors including cytokines (CTK) such as allograft inflammatory factor (AIF), heat shock proteins (HSP) and haemocyanin(s) (HMC). Oxidative stress induces ROS detoxification processes that involve the detoxification enzymes glutathione-S-transferase (GST), NADP-dependent isocitrate dehydrogenase (IDH) and glucose-6-phosphate-1-dehydrogenase (G6P1D). Oxidative stress and inflammation trigger apoptosis, which may be regulated via calreticulin (CRT) through calcium binding. These cellular events are under the influence of various gene regulation and transcription events which may involve ribosomal proteins S9 (RbS9), splicing factor arginine/serine-rich 4 (SFR4) and RNA binding protein (RBP). The validated protein expression changes of IDH, AIF and CRT are shown in the histograms with up- and down-regulation in red and green respectively, corresponding to the respective pathways on the diagram. The shaded AIF box indicates that the involvement of this protein in phagocytosis has been confirmed.

Although participation of the identified proteins in the proposed molecular pathways have been deduced through network modelling of known biological processes, their role in *H. midae* haemocytes needs to be established through lab-based experimentation. The validation portion of this study confirmed the differential expression of NADP-dependent isocitrate dehydrogenase (IDH), calreticulin (CRT) and allograft inflammatory factor (AIF) in response to bacterial-challenge in *H. midae* haemocytes (Chapter 3). Moreover, functional characterisation of a putative allograft inflammatory factor supported its functional involvement in phagocytosis (Chapter 4).

The few large-scale published studies that investigated immune-related gene expression in abalone complement this study and the proposed interaction network. Changes in gene expression following bacterial challenge indicate a comparable involvement of cellular metabolic processes, biogenesis, signal transduction and immune-related defences in *H. diversicolor* haemocytes (Wang et al., 2008). Similarly, microarray analysis of gene expression changes in the gill and digestive tract tissue of *H. discus disc*us after bacterial-challenge identified the involvement of immune-relevant genes such as transcription factors, inflammatory cytokines, antioxidant enzymes, apoptosis and IFN-regulatory genes (De Zoysa et al., 2011ab). This response was also reported in the gills and haemocytes of *H. discus discus* following viral haemorrhagic septicaemia virus challenge (De Zoysa et al., 2012). More recently, a study investigating *Vibrio harveyi* infection in *H. tuberculata* demonstrated a similar early induction of an immune response based on a number of immune-relevant genes such as glutamine synthase, Rel/NF-κB and ferritin (Cardinaud et al., 2015).

These results highlight the complementary nature of proteomic, genomic and transcriptomic studies which, when combined, may be used to generate a more complete picture of the molecular constituents of the innate immune response of marine molluscs. The results presented herein describe known biological processes of the innate immune response, whilst providing new insights into the proteomic regulation of the *H. midae* immune response. Thus, the proposed pathways that have been summarised in this study should be used as a platform for further investigation. The identification of molecular indicators of health in *H. midae* will hinge on future functional characterisation of the proteins that show critical involvement in the immune response of *H. midae*. Characterisation of a putative AIF in Chapter 4 already

demonstrates the importance of targeted studies to identify suitable biomarker candidates. Bacterial-challenge in *H. midae* elicits a strong and sustained up-regulation of AIF expression which was shown to be correlated with an increase in phagocytosis. Thus, this protein may be of significance as a potential molecular indicator of health in aquacultured abalone. However, future studies must focus on multiple stresses to establish the relevance of AIF as a specific disease biomarker (see: Limitations of the study and recommendations for future research). Results from this study have provided several avenues for further investigation.

Specifically, given that cell signalling pathways of marine invertebrates are still under investigation, the prevalence of signalling-related proteins involved in calcium, cAMP and MAPK signalling in this study provide attractive potential targets. For example, it has been suggested that pathogenic *Vibrio* are able to evade the abalone's immune response by modifying the p38 MAPK signalling pathways in *H. tuberculata* (Travers et al., 2009). Therefore, a comprehensive understanding of the key players responsible for the MAPK signal response is critical for combating pathogen infections in abalone. However, invertebrate signalling pathways remain multivariate in different organisms. For instance, characterisation of PKA in invertebrates has indicated conflicting and often contradictory patterns of regulation (Cao et al., 2004; Plows et al., 2006; Sossin & Abrams, 2009). In this study, significant differential regulation of PKA in response to bacterial challenge suggests PKA may be of functional significance in the immune response of *H. midae*. Therefore, characterisation of this signalling protein in *H. midae* would be highly beneficial towards understanding the multiplicity of MAPK regulation in different marine molluscs. The mechanism of NO signalling equally warrants further attention in *H. midae,* as evidence suggests it may play important signalling roles in numerous invertebrate immune-related activities, including reciprocal MAPK regulation (Förstermann & Sessa, 2012; Palumbo, 2005). Clarifying MAPK regulation in abalone may also provide exciting avenues for therapeutic strategies for controlling disease-related inflammation in abalone. Although inflammation is a crucial component of the immune response, chronic inflammation as a result of increased stress may have a significant impact on the health of animals. Already, the inhibition of members of the p38 MAPK family has proven successful in treating inflammatory conditions in

vertebrate models (Kaminska, 2005; Kumar et al., 2003). This may be a promising avenue to decrease stress-related negative effects in abalone aquaculture.

Other notable candidates for future research are members of the haemocyanin family. Haemocyanin has already been found to play a number of important roles in immune-related processes such as possessing phenoloxidase activity, anti-viral and anti-microbial properties, participating in the synthesis of ROS and functioning as a precursor of antimicrobial peptides (Coates & Nairn, 2014). A putative antimicrobial region has recently been identified in *H. tuberculata* haemocyanin (Zhuang et al., 2015), suggesting its involvement in equally important immune-related processes in the abalone immune response. Data from this study supports this view as numerous haemocyanin proteins were found to cluster together in the early response to bacterial challenge. Thus, abalone haemocyanin proteins need to be characterised and their role in the abalone immune response clarified.

From a physiological standpoint, this study may reflect the progression of stress in *H. midae* and how infection by bacterial pathogens may affect physiological functions. It is well established that up-regulation of the immune response is costly to the host, both from a metabolic and protein perspective, due to the redistribution of energy resources to immune-related metabolic processes (Lochmiller & Deerenberg, 2000, Stone et al., 2014). This study showed that energy metabolism was altered at every level of the immune response, reflecting the bioenergetic cost of inducing cellular stress responses in *H. midae* haemocytes.

Immune challenge elicited significant alterations in the metabolic priorities of the haemocytes. The pathways identified in this study include complex mechanisms for regulating and maintaining energy reserves. Shifts in energy metabolism in response to infection have been demonstrated in *H. tuberculata* and *H. diversicolor* (Travers et al., 2010; Wang et al., 2008), however the exact mechanisms of this regulation have not been elucidated. There appears to be a close link between disease resistance and energy metabolism in abalone as differences in the regulation of metabolism have been shown in resistant and susceptible individuals (Travers et al., 2010). Thus, temporal regulation of distinct metabolic processes may provide insight into this mode of regulation. This information could be used to further understand the relationship between disease and

metabolism. It has been recognized that poor diet may lead to immunosuppression in animals, rendering them highly susceptible to infection by pathogenic organisms (Lochmiller & Deerenberg, 2000). Furthermore, up-regulation of immune responses leads to significantly increased gluconeogenesis rates which may lead to a severe breakdown of proteins, carbohydrates and lipids in the host (Lochmiller & Deerenberg, 2000). Consequently, these considerations should be taken into account when implementing disease control strategies in aquaculture. For example, dietary changes may accommodate nutritional requirements of farmed abalone in response to anticipated environmental changes (seasonal fluctuations linked to disease outbreaks). Ideally, a probiotic feed that enhances the immune response, whilst meeting the nutritional requirements during periods of stress, could ensure a primed immune response in aquacultured abalone (Lange et al., 2014).

Furthermore, data obtained from this study shows regulation of apoptotic processes in response to bacterial challenge, which may be of functional significance in understanding the pathophysiology of disease in *H. midae*. Pathogenic organisms have been shown to modulate the host's apoptotic signals in eukaryotic cells as an escape mechanism from the immune system (Favaloro et al., 2012). Similarly, defective regulatory mechanisms of apoptosis in vertebrates often result in disease (Rudin & Thompson, 1997). Although the exact inducing mechanisms of apoptosis regulation remain to be clarified, an important role for calreticulin (CRT) has been suggested in vertebrate models (Obeid et al., 2007; Tarr et al., 2010). The significant reduction in CRT expression in response to bacterial challenge observed in this study may be of importance. Thus, functional characterisation of this protein would be highly beneficial to clarify its biological role in *H. midae*.

Limitations of the study and recommendations for future research

One of the limiting factors of this study is the strict filtering that was conducted during iTRAQ analysis, which resulted in a large portion of potentially relevant proteins being omitted from the final identification list. This stringent approach was deemed necessary since iTRAQ investigations in non-model organisms are limited and a cautious approach was chosen to ensure maximum confidence in the protein identifications made in this study. However, the protein identifications that were omitted from the final merged list could be used to conduct further bioinformatics analyses which could provide additional quantitative proteomic information. Furthermore, the lack of available abalone genome sequences resulted in many peptide spectrums remaining unidentified. Thus, as more invertebrate genomic sequences become available, the MS/MS spectra generated from this study should be re-analysed against the updated database to identify uncharacterised proteins and increase the number of protein identifications. This may reveal more proteins involved in immune processes which could be used in conjunction with targeted studies to provide the "missing pieces" of the molecular pathways under investigation and thus, enhance the proposed pathway model.

Another limitation of this study is the narrow time frame that was investigated during iTRAQ analysis. To increase identification confidence and strengthen the statistical validity of this study, the 8-plex iTRAQ system was used to include a greater number of biological repeats at the expense of including more time points. Although an early and late response was identified, the time points chosen were not broad enough to provide definitive temporal responses for the identified proteins. Thus, up- or down-regulation of these pathways cannot be conclusively established until orthogonal validation is conducted. As was shown in the validation portion of this study, conflicting expression patterns may arise. Thus, targeted experiments are vital in delineating these immune-related pathways comprehensively. The data presented here should be viewed as a "snapshot" of the haemocyte proteome which provides an overview of the potential molecules and pathways expressed in response to bacterial challenge at a specific moment in time. Many of the upstream proteins, specifically early response elements such as cytokines and recognition particles, may not have been identified owing to the

narrow time range used. One of the outcomes of the validation portion of this study demonstrated that the immune response may be induced as early as one hour post-challenge and in some instances, as early as 15 minutes. Thus, future studies investigating these pathways must include appropriate time points when investigating these molecular pathways, particularly with regard to pathways that are thought to respond early in the challenge.

Live bacterial challenge trials could not be used due to the flow-through circulation system at the research facility which cycles water from the aquarium back into the ocean. Whilst the study showed that the injection of heat killed *Vibrio* clearly induced an immune response in *H. midae*, it would be beneficial for targeted studies to investigate immune responses using live bacteria to simulate a typical infection progression. It is likely that the response of these pathways will be modulated differently in terms of temporal regulation. This is an important consideration if effective biomarkers are to be developed that can make precise predictions of disease progression in animals. Furthermore, future studies should focus on multiple-stress responses in *H. midae*. This may provide a compound view of the effects of disease, thermal and movement stress on the health of *H. midae,* as well as provide predictive enhancements of probiotic treatments. Additionally, since different tissues have been shown to respond differently to stress challenges, the regulation of protein expression in different abalone tissue types (gills, epipodia and digestive gland) would be beneficial.

Another important consideration for future research is the lack of suitable antibodies for characterising proteomic changes. In this study, the use of polyclonal antibodies raised to human proteins presented numerous problems owing to a lack of specificity. Additionally, certain commercial antibody suppliers do not disclose the peptide antigen sequence to which polyclonal antisera are raised, making it difficult to determine whether the antibody will bind to the target molecule. Consequently, antibodies raised to *H. midae* proteins would be preferable for characterisation and functional studies.

This proteomic investigation of the innate immune response of *H. midae* haemocytes has successfully addressed the objectives of the study. The data presented provide an insight into the proteins which are differentially regulated in response to a bacterial-challenge. This has allowed to us to gain insight into the molecular pathways involved in innate immunity and create an integrated picture of these networks and pathways. To the best of our knowledge, this is the first study using iTRAQ-based proteome profiling to investigate global protein expression changes in response to a bacterial-challenge in an abalone species. In so doing, this research has contributed to the broader knowledge of the innate immune response of marine invertebrates. Further research targeted at individual proteins will uncover the mechanistic and functional roles of these proteins in the proposed molecular pathways, furthering our understanding of the pathophysiology of disease in *H. midae*.

APPENDIX A
MEDIA AND SOLUTIONS
CONTENTS

For the preparation of all media, solutions and buffers, glassware was washed in distilled water (dH_2O) and autoclaved at 121 ^{0}C for 40 min prior to use. dH_2O was purified using a Milli-RO Plus (Millipore) water purification system. To sterilise purified water (dH_2O), dH_2O was autoclaved at 121 ^{0}C for 40 min before use. Ultrapure water for all MS-based experiments was obtained by further purifying dH_2O using a Milli-Q Plus (Millipore) water purification system. After preparation, all media, solutions and buffers were autoclaved at 121 ^{0}C for 40 min, before being stored at room temperature, unless otherwise stated.

A.1 Media

A.1.1 Sterile Sea Salts (SSS)

3.0 % (*w/v*) Sodium chloride (NaCl)

0.23 % (*w/v*) Magnesium chloride ($MgCl_2$)

0.03 % (*w/v*) Potassium chloride (KCl)

Make in distilled water. Autoclave.

A.1.2 Tryptic soy broth (TSB)

2.0 % (*w/v*) Peptone

0.25 % (w/v) D-glucose ($C_6H_{12}O_6$)

0.5 % (*w/v*) NaCl

0.25 % (*w/v*) Dipotassium hydrogen orthophosphate (K_2HPO_4)

Make in distilled water. Adjust pH to 7.3 and autoclave.

A.1.3 Tryptic soy agar (TSA)

2.0 % (*w/v*) Peptone

0.25 % (*w/v*) $C_6H_{12}O_6$

0.5 % (*w/v*) NaCl

0.25 % (*w/v*) K_2HPO_4

2.0 % (*w/v*) Agar

Make in distilled water. Adjust pH to 7.3 and autoclave.

A.2 Solutions

A.2.1 General Solutions

A.2.1.1 Alsever's Fixative Solution

0.1 M (*w/v*) $C_6H_{12}O_6$ (Saarchem)

0.03 M (*w/v*) Sodium citrate ($C_6H_5Na_3O_7.2H_2O$) (Saarchem)

0.5 M (*w/v*) EDTA (Sigma)

0.38 M (*w/v*) NaCl

4.4% (*v/v*) Formaldehyde (HCHO) (Saarchem)

Make in distilled water. Adjust pH to 7.5, autoclave and store at 4^0C.

A.2.1.2 Phosphate Buffered Saline Stock Solution (10 ×)

1.37M (*w/v*) NaCl

27mM (*w/v*) KCl

100mM (*w/v*) Disodium phosphate (Na_2HPO_4)

18 mM (*w/v*) Monopotassium phosphate (KH_2PO_4)

Make in distilled water. Adjust pH to 7.4 and autoclave. Dilute 10 × stock solution to 1 × working concentration (PBS) in dH_2O.

A.2.2 Solutions for iTRAQ

All solutions for MS were made up in Ultrapure water. All glassware was washed thoroughly in 70% acetonitrile and rinsed with Ultrapure water.

A.2.2.1 Lysis Buffer

1% (*w/v*) Sodium dodecyl sulphate (SDS) (Merck)

0.5 M (*v/v*) Triethylammonium bicarbonate (TEAB) (Sigma)

Make up fresh in Ultrapure water before every use. Do not autoclave.

A.2.2.2 50mM Tris (2-carboxyethyl) phosphine stock solution (TCEP)

50 mM (*w/v*) Tris (2-carboxyethyl) phosphine (Sigma)

Make up in Ultrapure water. Do not autoclave. Aliquot into sterile microfuge tubes and store at -20^0C. Stock solution (50mM TCEP) diluted in the final protein volume sample (will vary between samples), to yield a final working concentration of 5mM TCEP.

A.2.2.3 UT Buffer

8 M Urea (*w/v*) (Sigma)

0.5 M (*v/v*) TEAB

Make up fresh in Ultrapure water before every use. Do not autoclave.

A.2.2.4 200 mM s-methylmethanethiosulfonate (MMTS)

1M (*w/v*) s-methylmethanethiosulfonate (Fluka)

Make up in 100% isopropanol (MS-grade, Fluka). Do not autoclave. Aliquot out into 20 µL fractions into sterile microfuge tubes and store at -20^{0}C. Dilute to 200mM working concentration with 100% isopropanol immediately prior to use.

A.2.2.5 Trypsin Gold

2 µg.µL^{-1} Trypsin Gold (Promega, Product Code: PRV5280)

Reconstitute lyophilised powder in 50mM (*v/v*) acetic acid and aliquot into sterile microfuge tubes. Store at -80^{0}C. Thaw on ice.

A.2.3 Solutions for Pierce BCA protein assay

A.2.3.1 Bovine Serum Albumin (BSA) (2 mg/ml^{-1})

2 mg/mL^{-1} BSA (Roche)

Make up in 10% (*v/v*) lysis buffer (Appendix 2.2.1), do not autoclave. Aliquot into sterile microfuge tubes and store at -20^{0}C.

A.2.4 Solutions for SDS PAGE and Western blot analysis

A.2.4.1 Stock solutions for the preparation of SDS PAGE gels

A.2.4.1.1 40% (*v/v*) acrylamide (Sigma-Aldrich)

Reconstitute lyophilized powder in dH2O and filter sterilise. Store at 4 °C.

A.2.4.1.2 4 × Tris-HCl/SDS (pH 6.8)

0.5M (*w/v*) Tris (hydroxymethyl)aminomethane (Sigma-Aldrich)

0.4% (*w/v*) SDS

Dissolve solutes in 0.6 of the final volume of sterile dH2O, adjust the pH to 6.8, then make up to final volume. Do not autoclave. Filter sterilise and store at 4 °C.

A.2.4.1.3 10% Ammonium persulfate

10% (*w/v*) AMPS (Promega)

Prepare in dH_2O, do not autoclave. Filter sterilise and store at 4 °C. Make up fresh every two weeks.

A.2.4.1.4 4 × Tris-HCl/SDS (pH 8.8)

1M (*w/v*) Tris
0.4% (*w/v*) SDS

Dissolve solutes in 0.6 of the final volume of sterile dH2O, adjust the pH to 8.8, then make up to final volume. Do not autoclave. Filter sterilise and store at 4 °C.

A.2.4.1.5 5 × Protein sample application buffer (SAB)

250 mM Tris-Cl pH 6.8 (Prepared from 1M stock solution, Appendix A.2.4.1.6)
500 mM (*w/v*) dithiothreitol (DTT)
10% (*w/v*) SDS
0.5% (*w/v*) bromophenol blue,
67% (*v/v*) glycerol

Prepare in dH_2O, do not autoclave. Store at -20^0C.

A.2.4.1.6 1 M Tris (hydroxymethyl) aminomethane-hydrochloric acid (Tris-HCl) pH 6.8

1M (*w/v*) Tris

Dissolve Tris in 0.6 volume of the dH_2O. Adjust the pH to 6.8, then make up to final volume. Do not autoclave. Filter sterilise and store at 4 °C.

A.2.4.1.7 SDS PAGE running buffer (5 ×)

125 mM (*w/v*) Tris
0.96 M (*w/v*) Glycine (Saarchem)
17 mM (*w/v*) SDS
Prepare in dH_2O, do not autoclave. Store at 4^0C.

A.2.4.2 Stock solutions for western blot analysis

A.2.4.2.1 Towbin buffer

25 mM (*w/v*) Tris,
192 mM (*w/v*) glycine
20% (*v/v*) methanol
Prepare in dH_2O, do not autoclave. Store at 4^0C.

A.2.4.2.2 Ponceau S stain

0.1 % (*w/v*) Ponceau S (Sigma)
5 % (*v/v*) Glacial acetic acid
Prepare in dH_2O, do not autoclave. Store at RT. Light sensitive. Re-useable

A.2.4.2.3 Tris-buffered saline stock solution (10 ×)

0.5 M (*w/v*) Tris,
1.5 M (*w/v*) NaCl,
Dissolve solutes in 0.6 volume of the dH_2O. Adjust the pH to 7.4, then make up to final volume. Do not autoclave and store at RT. Dilute 10 × stock solution to 1 × working concentration (TBS) in dH_2O.

A.2.4.2.4 Blocking buffer

5 % (*w/v*) skim milk powder
Make up fresh before every use in 1 × TBS (Appendix A.2.4.2.3).

A.2.5 Solutions for *In vitro* haemocyte culturing

A.2.5.1 Supplementary Salts Stock Solution

1.75 M (*w/v*) NaCl
24 mM (*w/v*) KCl
46 mM (*w/v*) $CaCl_2$
124 mM (*w/v*) $MgCl_2$
138 mM (*w/v*) $MgSO_4$
Make up in distilled water and autoclave twice. Store at room temperature.

A.2.5.2 Amphotericin B Stock solution

Amphotericin B (Sigma) 0.25 mg/mL
Dilute to a 0.1 mg/mL stock solution and store at -20 ^{0}C. Light sensitive.

A.2.5.3 Modified Hank's M-199 balanced salt solution (MHBSS)

0.322% (*w/v;* final concentration) Medium-199 (Gibco)
12.5 mL Supplementary Salts Stock Solution
500 µL Penicillin G-Streptomycin (Invitrogen)
50 µL Amphotericin B Stock solution

Make up in distilled water to a final 50 mL volume, filter sterilise (0.22 µm filter) and store at 4^{0}C. Make up fresh every week. Light sensitive.

A.2.5.4 1 M sodium salicylate stock solution

1 M (*w/v*) sodium salicylate (Sigma)

Prepare 1 mL of stock solution in MHBSS (Appendix A2.5.3) and store at 4^{0}C for up to two weeks. Dilute to final working concentration (1 mM) immediately before use in MHBSS.

A.2.6 Solutions for Phagocytosis Assay

A.2.6.1 FITC-labelled Vibrio anguillarum 5676

Grow *Vibrio anguillarum* 5676 (Section 2.2.2) for 18 hours in TSB, heat-kill at 65^{0}C for 5 minutes and dilute to a final concentration of 1×10^8 cells/ml. Collect the cells via centrifugation at 13 000 X *g* for 10 minutes at 4°C and then wash the cells twice with 1 × PBS. Resuspend pelleted cells in 10ml 0.1M $NaHCO_3$ pH 9 with 1 X PBS containing 0.1mg/ml fluorescin 5-isothiocyanate (FITC) Isomer 1 (Sigma-Aldrich). Incubate the cells whilst shaking overnight (~16 hours), in the dark, at room temperature. Thereafter, collect the cells by centrifugation at 13 000 X *g* for 1 minutes at 4°C, and subsequently resuspend in 1 × PBS.

A.2.6.2 Ethidium Bromide

100 µg/ml (*w/v*) ethidium bromide (Sigma)

Make up in 1 × PBS (Appendix A.2.1.2). Store at RT.

A.2.7 Solutions for Confocal Imaging

A.2.7.1 2% Paraformaldehyde

Preparation of 2% (*w/v*) paraformaldehyde (Sigma Aldrich #30525-89-4) in 100 ml PBS:

In a fume hood, heat 80 mL of 1 × PBS (Appendix A.2.1.2) on a heated stirring plate to 70 ^{0}C (do not let solution boil). Add 2 grams paraformaldehyde powder (weighed out in fume hood) and allow to dissolve by stirring until the solution turns clear (approximately 30 min). It may be necessary to add a few drops of 1M NaOH to the solution to become completely clear. Allow to cool to room temperature and adjust the pH to 7.4 (using pH strips). Make up to final 100 mL volume with more PBS.

Filter sterilize and store at 4^{0}C up to 2 weeks. Light sensitive.

A.2.7.2 0.5% Triton X-100

0.5 % (*v/v*) Triton-X

Make up in PBS (Appendix A.2.1.2).

A.2.7.3 Blocking Solution

5% (*w/v*) bovine serum albumin (BSA, Roche)

Make up fresh before every use in PBS (Appendix A.2.1.2).

A.2.7.4 100 nM Rhodamine phalloidin

Reconstitute Rhodamine phalloidin (Cytoskeleton, Cat. # PHDR1) in 100% methanol to a final 14 µM stock concentration. Aliquot into 50 µL amounts and store at -20^{0}C (up to 6 months). Light sensitive. Dilute to 100 nM working stock with PBS immediately prior to use.

Appendix B

SUPPLEMENTARY DATA

CONTENTS

B.1

Chapter 2 Supplementary information

B.1.1 Number of proteins identified in bacterial-challenged and mock-infected iTRAQ

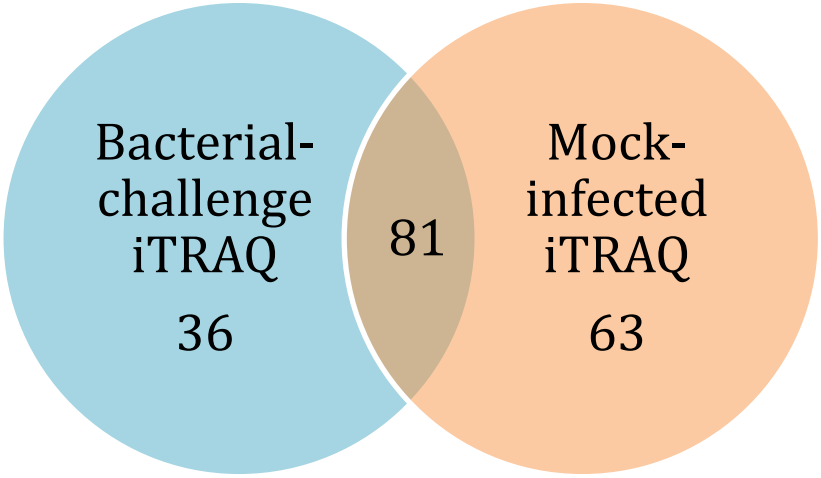

B.1.2 Common proteins found in both treatment groups (bacterial-challenge & mock-infected)

Protein description	
14-3-3 protein	Heat shock inducible protein 70
40S ribosomal protein S18	Heat shock protein 60
40S ribosomal protein S8	Haemocyanin (Frag)
60S acidic ribosomal protein P0 (Frag)	Haemocyanin alphaD-sbu
60S acidic ribosomal protein P2	Haemocyanin beta-sbu
84kDa heat shock protein	Haemocyanin fg (Frag)
Actin	Haemocyanin isoform 1 (Frag)
Actin depolymerisation factor/cofilin	Haemocyanin sbu 1
Adenosylhomocysteinase	Haemocyanin type 2 protein (Frag)
ADP/ATP carrier protein (Frag)	Histone variant H2A.X
ADP-ribosylation factor 2	Myosin VI (Fragment)
Allograft inflammatory factor (Frag)	Nonmuscle myosin II (Fragment)
ATP synthase subunit alpha	Non-muscle myosin II heavy chain
ATP-binding cassette transporter sub-fam A	Nucleoside diphosphate kinase
ATP-dependent RNA helicase DDX5	Omega class glutathione-S-transferase 1
Bone morphogenic protein type 2 receptor	Peptidyl-prolyl cis-trans isomerase
Calmodulin-dependent protein kinase (Frag)	Peroxidase
Calreticulin	PL10-like protein
Calreticulin	Proteasome subunit alpha type
Calreticulin	Protein disulfide isomerase
Cdc42	Psmc6 protein
Chaperonin containing T-complex polypeptide sbu	Putative polyadenylate-binding protein 1 Frag
Chaperonin containing tcp1	Putative RNA-binding protein
Elongation factor 1-alpha	Pyruvate kinase
Elongation factor-2 (Frag)	RAB protein
Fascin (Frag)	Raminin receptor
Gelsolin	Ran-1-prov protein
Glucose-6-phosphate 1-dehydrogenase	Ras-related protein Rab-1A
Glucose-regulated protein 94	Ribosomal protein l
Glutathione-S-transferase	Ribosomal protein L17A (Frag)
Glutathione-S-transferase isoform	Ribosomal protein S14
Glutathione-S-transferase isoform 1	Ribosomal protein S20
Glyceraldehyde-3-phosphate dehydrogenase	Ribosomal protein S5
Glyceraldehyde-3-phosphate dehydrogenase	Serine/threonine-protein phosphatase
Guanine nucleotide-binding protein G alpha sbu	Splicing factor arginine/serine-rich 4
Guanine nucleotide-binding protein G(o) sbu α	Thioredoxin peroxidase 1
Guanine nucleotide-binding protein G(o) sbu α	Transgelin
Guanine nucleotide-binding protein G(s) sbu α	Triosephosphate isomerase (Frag)
H2 protein (Frag)	Twitchin
Haemocyanin	Vacuolar H+-ATPase (Frag)
Heat shock cognate protein 70	Voltage-dependent anion channel 2-like prot.

B.2

Chapter 3 Supplementary information

B.2.1 Cluster B deleted protein GO term entries:

Fibroblast-related nodes
Response to cocaine
Response to estrogen
Axon guidance
Histamine secretion from mast cells

B.2.2 Cluster B cytoscape deleted protein translation network

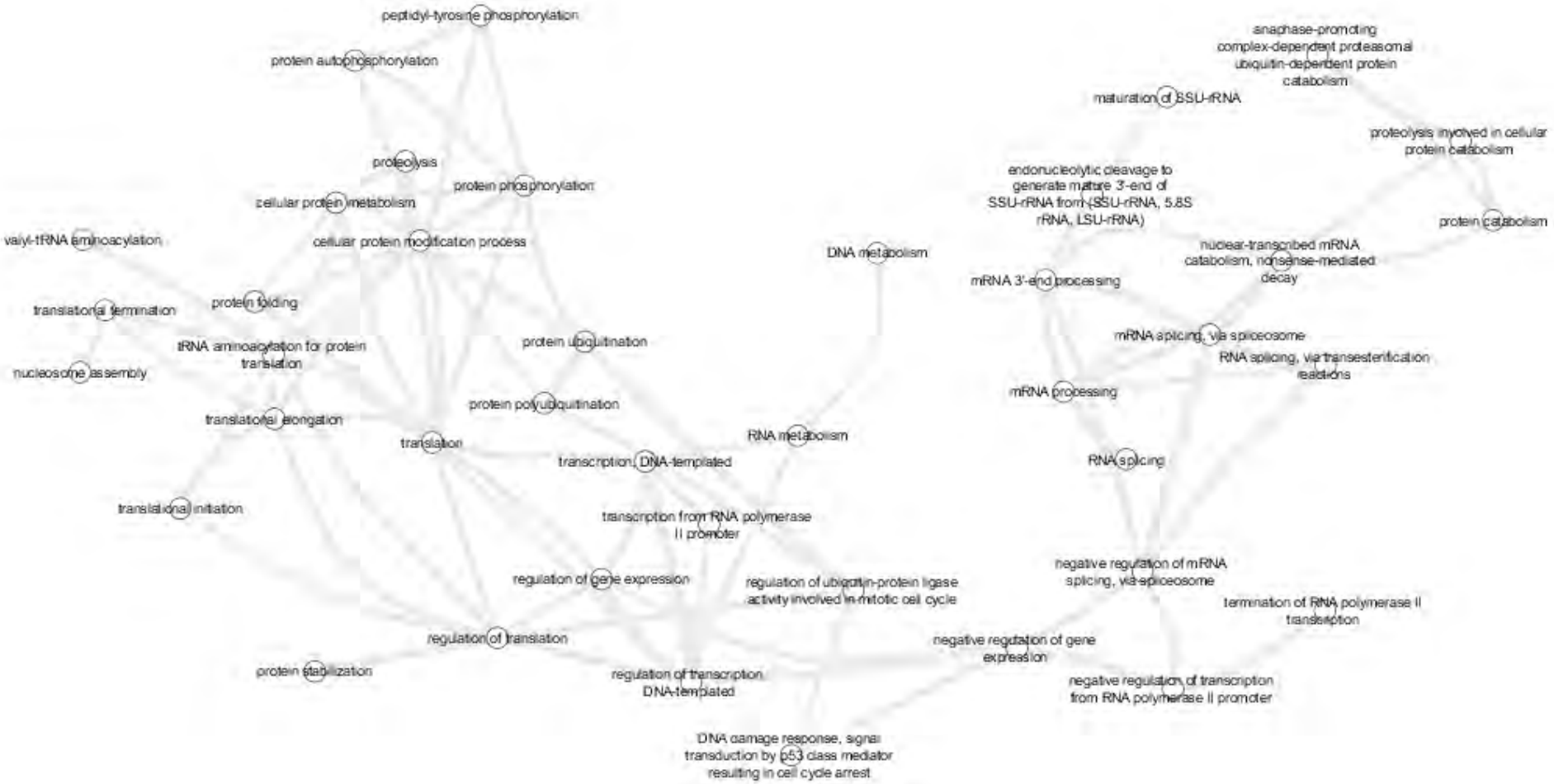

B.2.3 Cluster B metabolism network

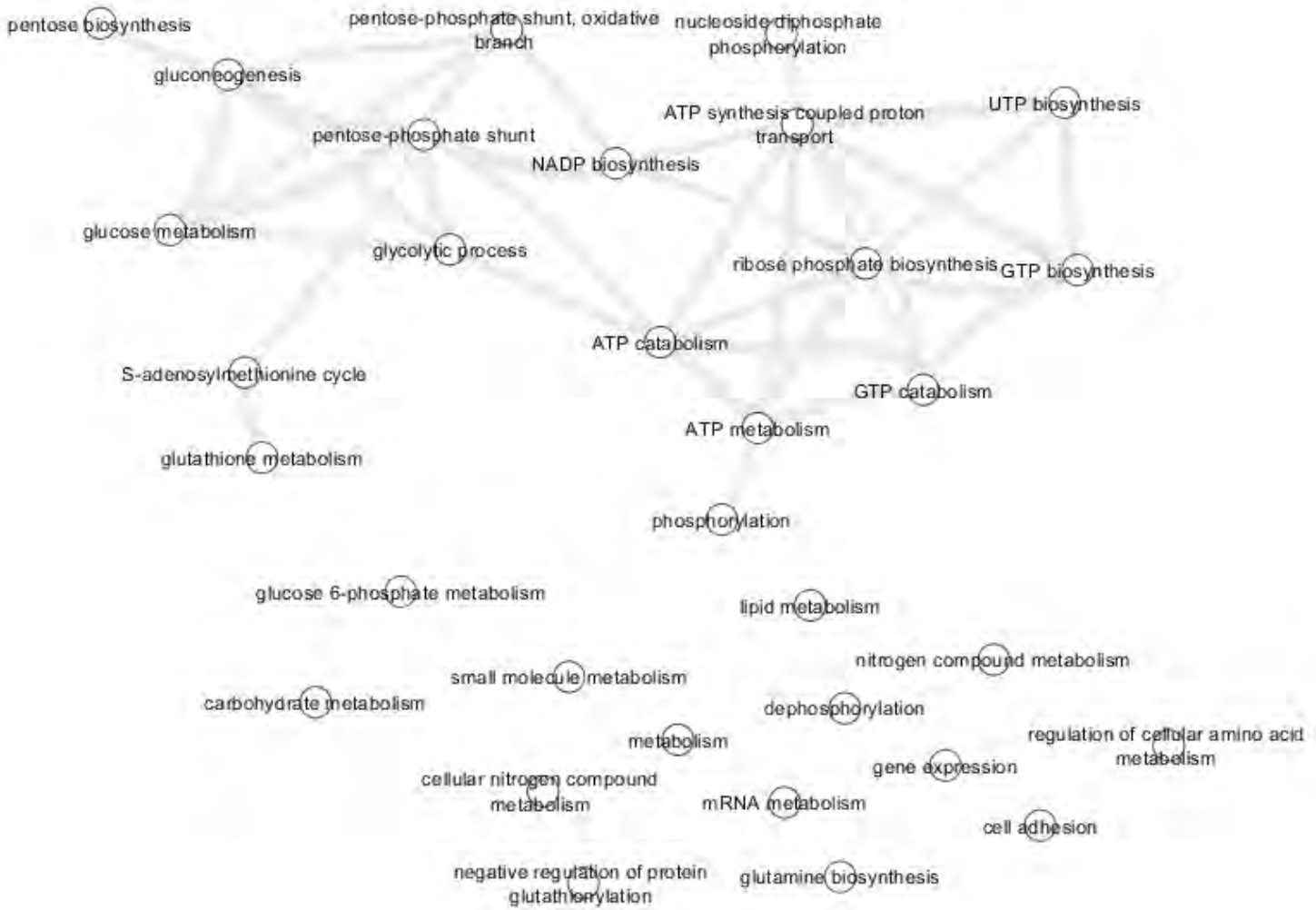

B.2.4 Biological replicate western blots (left) and Ponceau S stain (right)

Allograft inflammatory factor-1

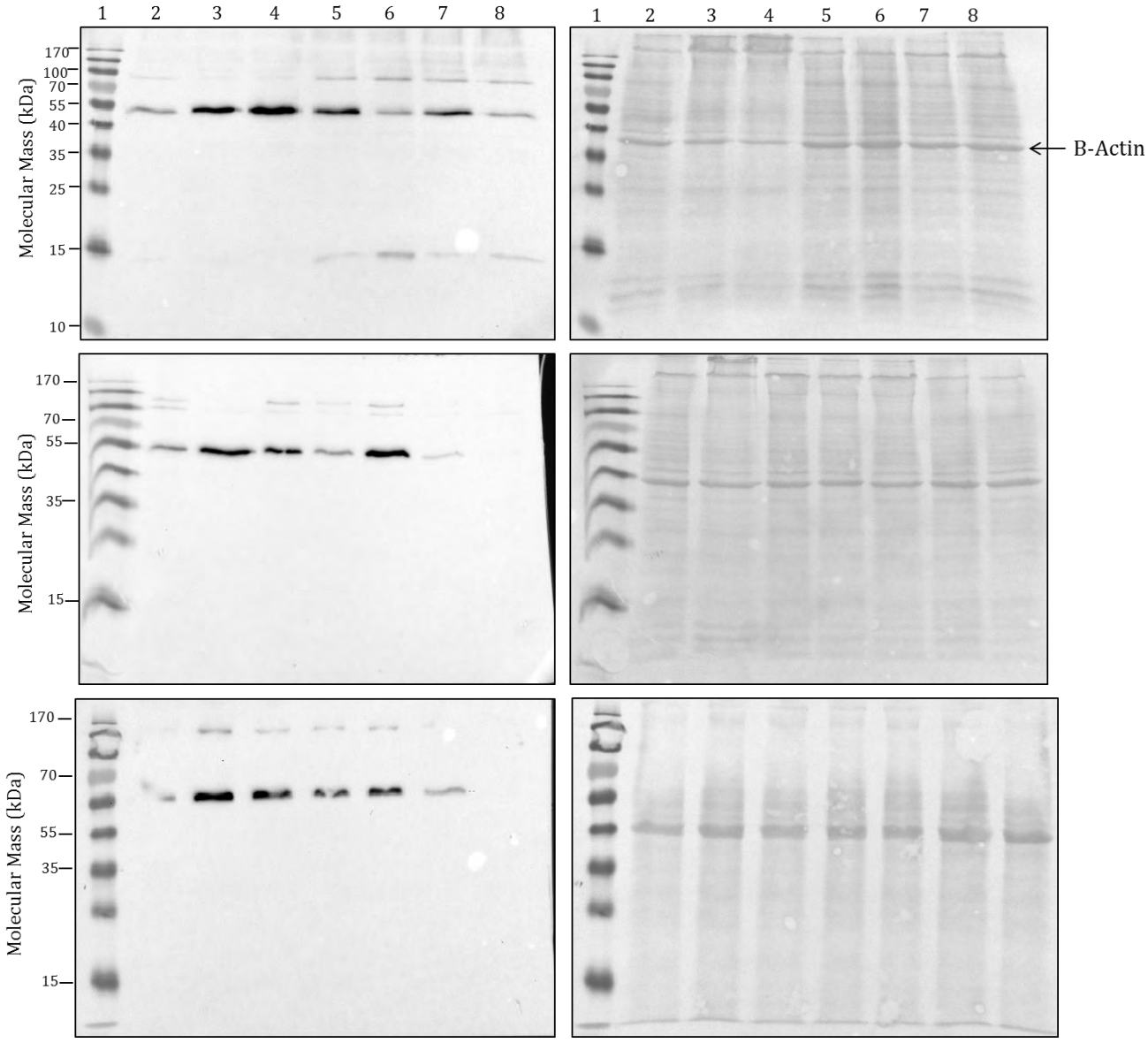

Calreticulin

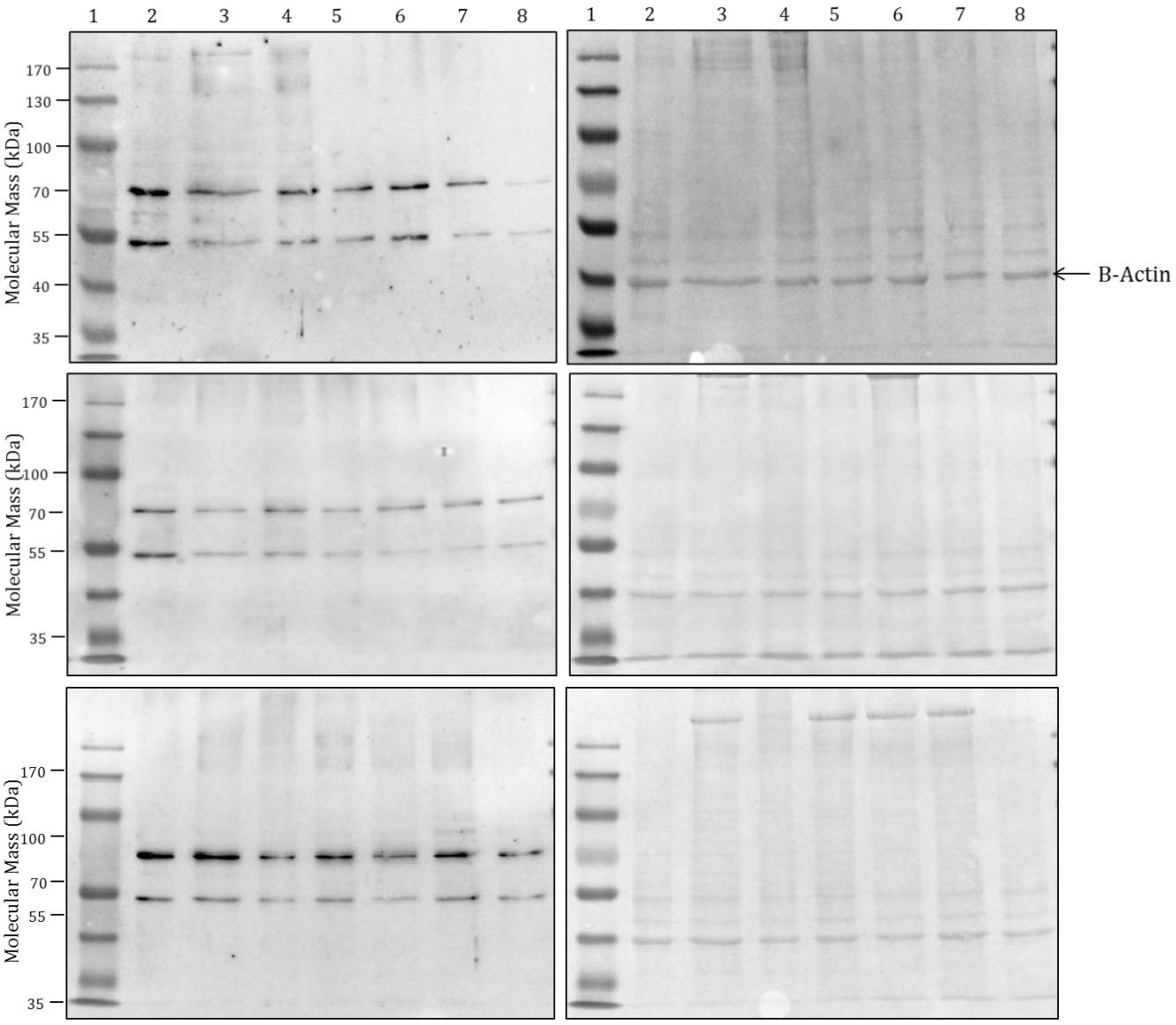

NADP-dependent isocitrate dehydrogenase

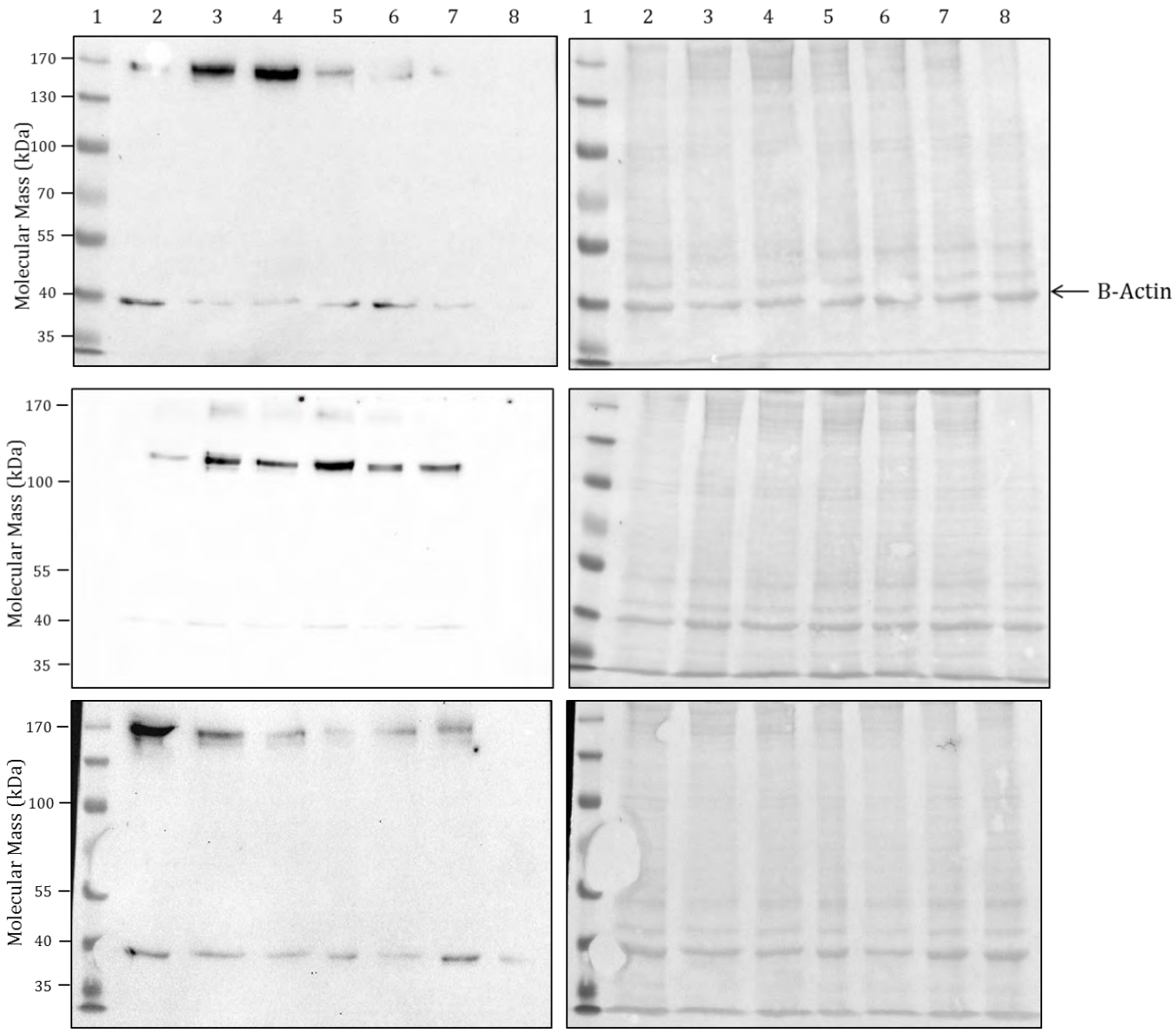

Glutathione-S-transferase

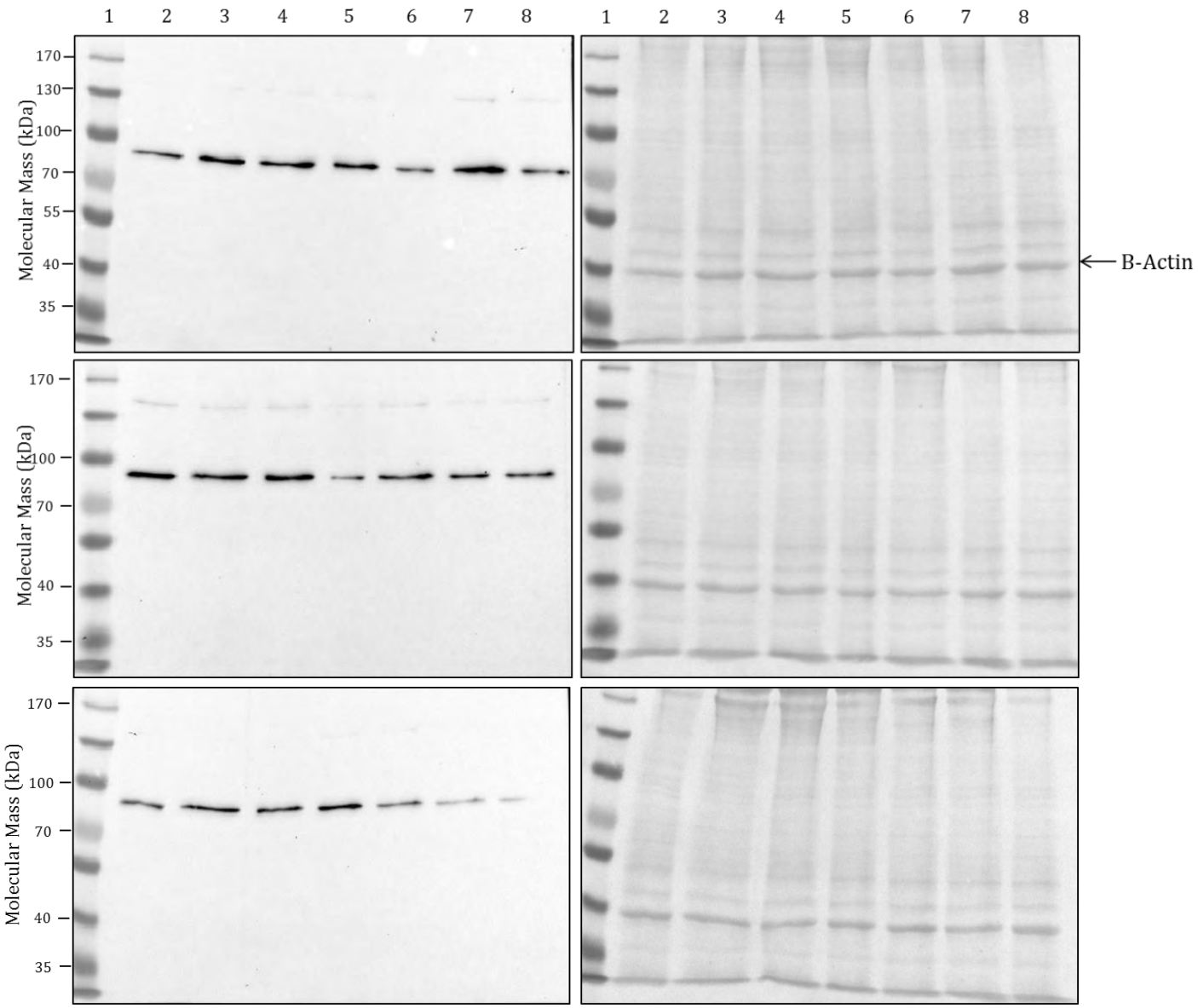

B.2.5 GST 2D-western blot

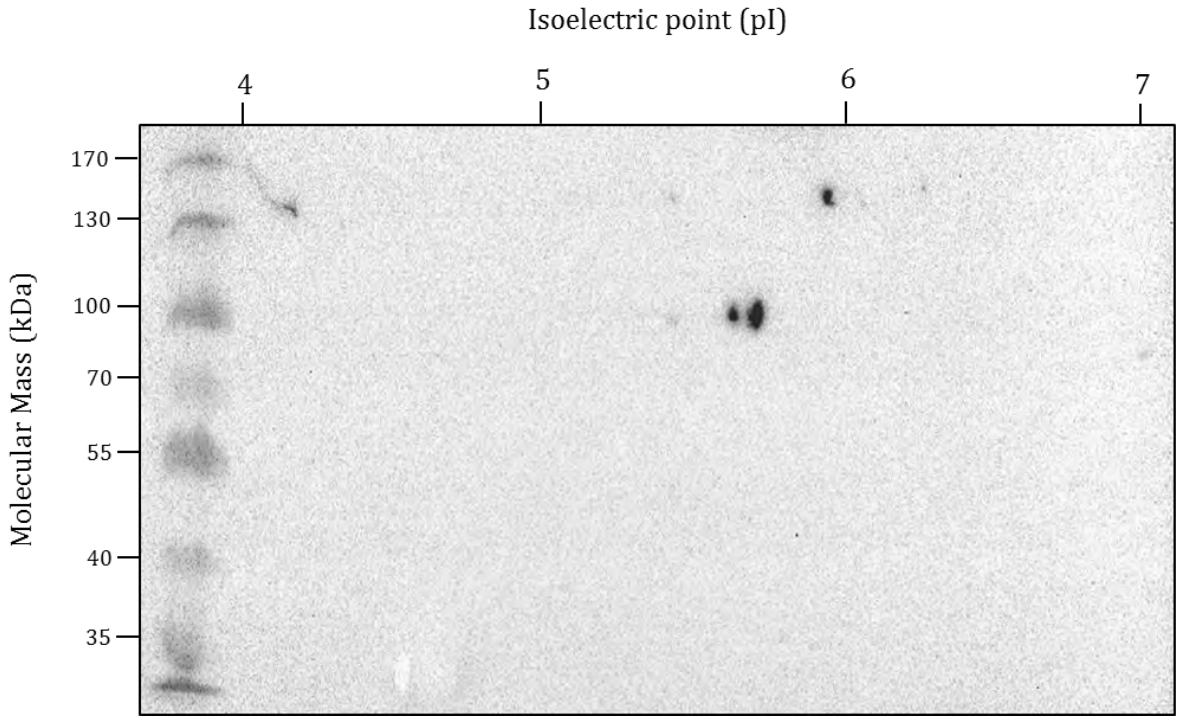

B.3

Chapter 4 Supplementary information

B.3.1 *In vitro* western blots (biological replicates)

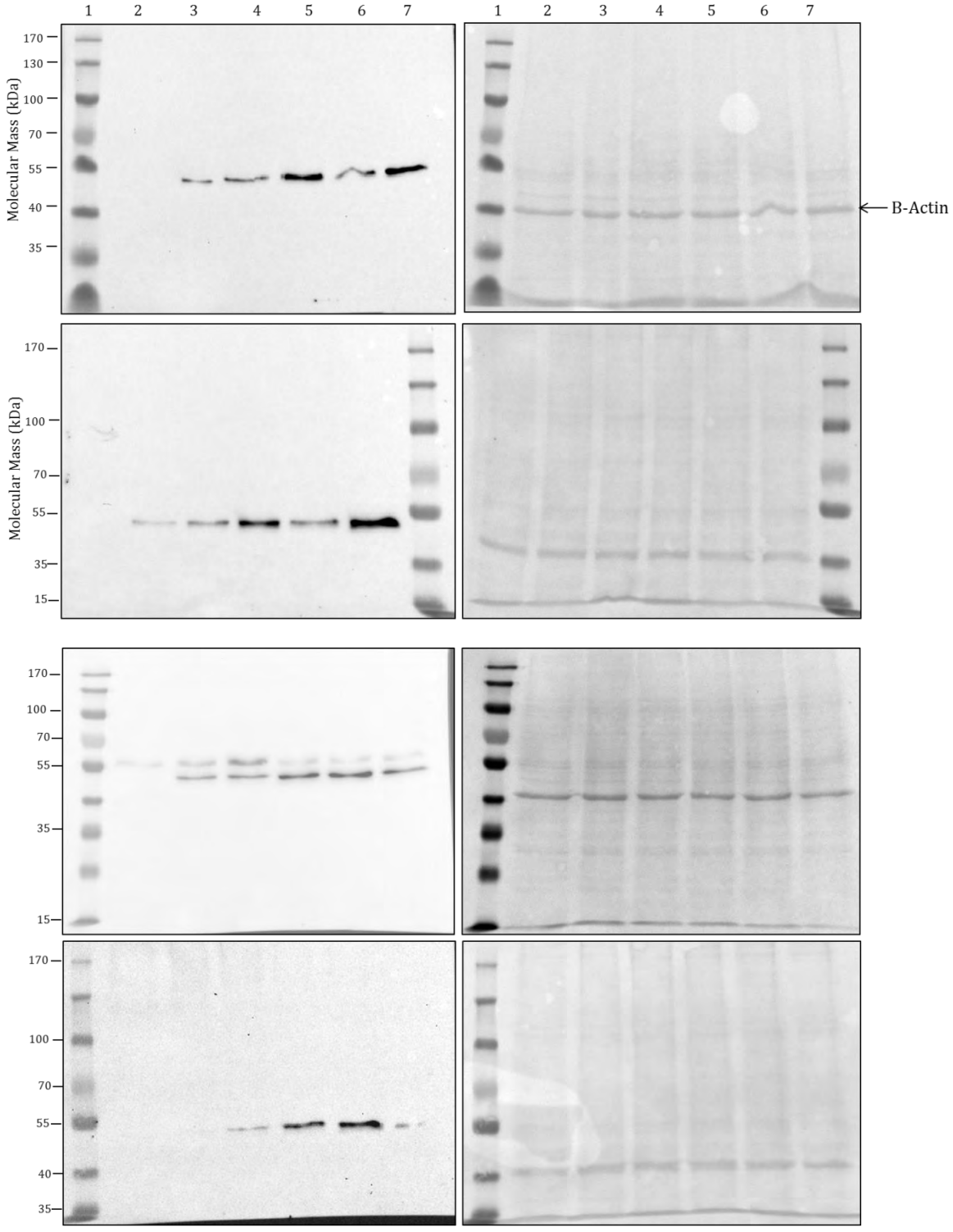

B.3.2 Antagonist western blots

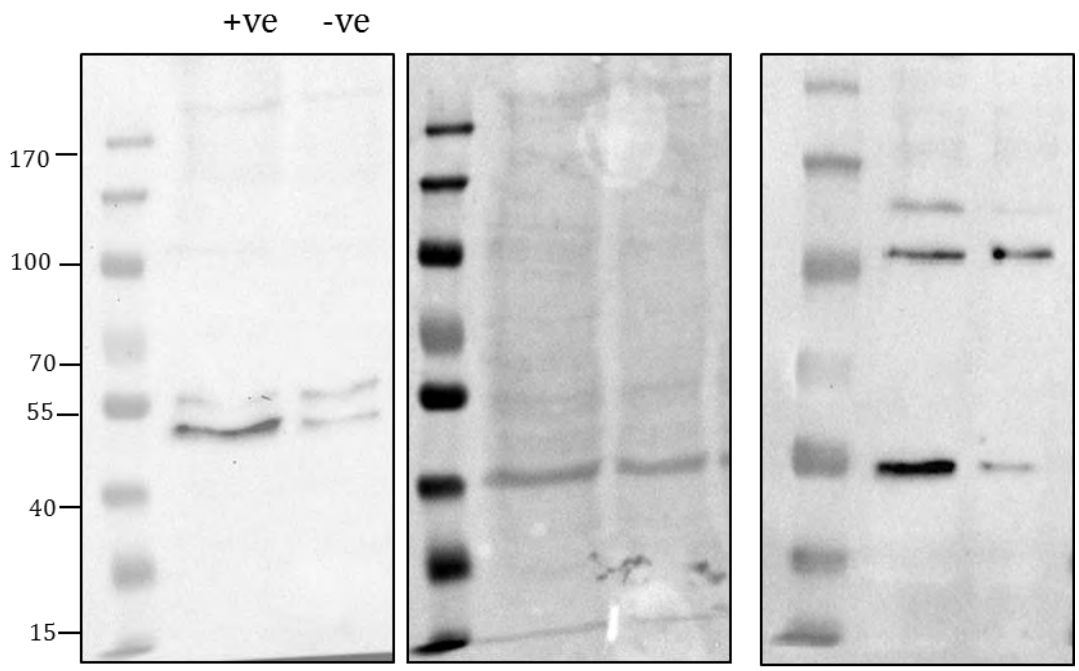

B.3.4 Phagocytosis assay all biological repeats

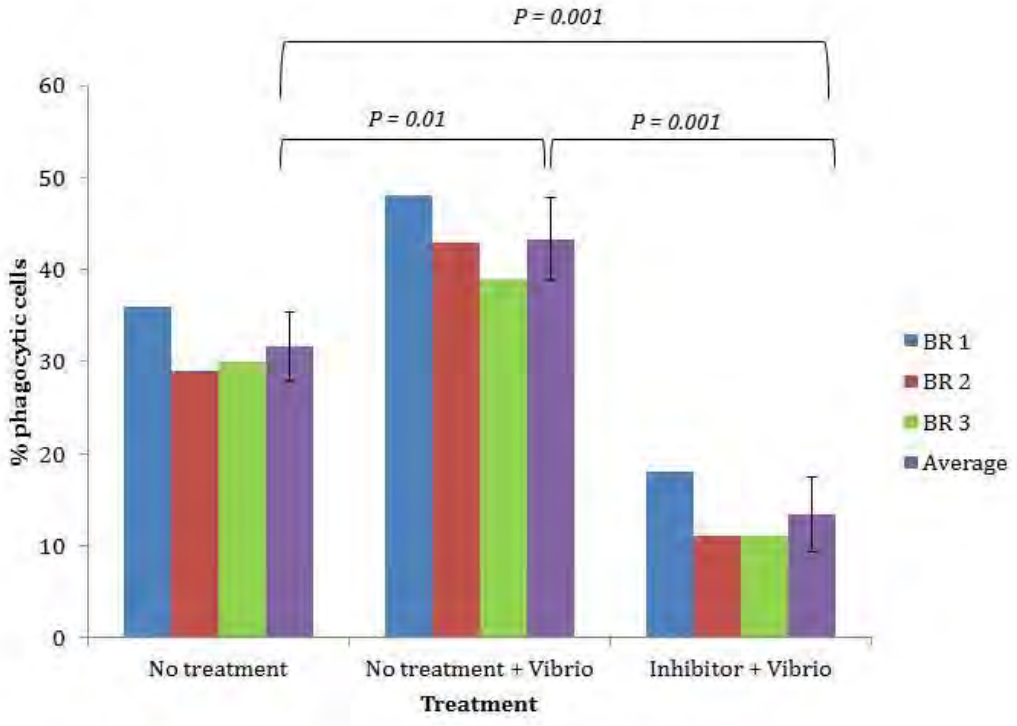

APPENDIX C

LITERATURE CITED

Adamo, S.A., 2012. The effects of the stress response on immune function in invertebrates: An evolutionary perspective on an ancient connection. Hormones and Behavior, 62(3), pp.324–330.

Aderem, A., 2003. Phagocytosis and the inflammatory response. The Journal of infectious diseases, 187 Suppl(Suppl 2), pp.S340–S345.

Aderem, A. & Underhill, D.M., 1999. Mechanisms of phagocytosis in macrophages. Annual review of immunology, 17, pp.593–623.

Aebersold, R., Burlingame, A.L. & Bradshaw, R.A., 2013. Western Blots vs. SRM Assays: Time to turn the tables? Molecular & cellular proteomics : MCP, pp.2381–2382.

Aggarwal, K., Choe, L.H. & Lee, K.H., 2006. Shotgun proteomics using the iTRAQ isobaric tags. Briefings in functional genomics & proteomics, 5(2), pp.112–20.

Alberts, B., Johnson, A., Lewis, J., Raff, M., Roberts, K., Walter, P., 2002. Molecular Biology of the Cell 4th Edition, New York. Garland Science.

Alexandratos, N. & Bruinsma, J., 2012. World agriculture towards 2030/2050: the 2012 revision, Rome.

Antoni, F.A., 2000. Molecular diversity of cyclic AMP signalling. Frontiers in neuroendocrinology, 21(2), pp.103–32.

Apel, K. & Hirt, H., 2004. Reactive oxygen species: metabolism, oxidative stress, and signal transduction. Annual review of plant biology, 55, pp.373–99.

Arechavala-Lopez, P., Sanchez-Jerez, P., Bayle-Sempere, J. T., Uglem, I. & Mladineo, I. l., 2013. Reared fish, farmed escapees and wild fish stocks - A triangle of pathogen transmission of concern to Mediterranean aquaculture management. Aquaculture Environment Interactions, 3(2), pp.153–161.

Arur, S., Uche, U.E., Rezaul, K., Fong, M., Scranton, V., Cowan, A.E., Mohler, W., Han, D. K., 2003. Annexin I is an endogenous ligand that mediates apoptotic cell engulfment. Developmental Cell, 4(4), pp.587–598.

Aton, E., Renault, T., Gagnaire, B., Thomas-Guyon, H., Cognard, C. & Imbert, N., 2006. A flow cytometric approach to study intracellular-free $^{Ca2+}$ in *Crassostrea gigas* haemocytes. Fish and Shellfish Immunology, 20(4), pp.493–502.

Autieri, M. V, 1996. cDNA Cloning of Human Allograft Inflammatory Factor-1 : Tissue Distribution , Cytokine Induction , and mRNA Expression in Injured Rat Carotid Arteries. Biochemical and biophysical research communications, 228(1), pp.29–37.

Autieri, M. V & Chen, X., 2005. The ability of AIF-1 to activate human vascular smooth muscle cells is lost by mutations in the EF-hand calcium-binding region. Experimental cell research, 307(1), pp.204–11.

Autieri, M. V, Kelemen, S.E. & Wendt, K.W., 2003. AIF-1 is an actin-polymerizing and Rac1-activating protein that promotes vascular smooth muscle cell migration. Circulation research, 92(10), pp.1107–14.

Bachère, E., Gueguen, Y., Gonzalez, M., de Lorgeril, J., Garnier, J. & Romestand, Bernard., 2004. Insights into the anti-microbial defense of marine invertebrates: the *penaeid* shrimps and the oyster *Crassostrea gigas*. Immunological reviews, 198, pp.149–168.

Baillie, G.S., Scott, J.D. & Houslay, M.D., 2005. Compartmentalisation of phosphodiesterases and protein kinase A: opposites attract. FEBS letters, 579(15), pp.3264–70.

Balcázar, J.L., de Blas, I., Ruiz-Zarzuela, I., Cunningham, D., Vendrell, D. & Múzquiz, José Luis., 2006. The role of probiotics in aquaculture. Veterinary microbiology, 114(3-4), pp.173–86.

Ballarin, L., Cima, F. & Sabbadin, A., 1997. Calcium homeostasis and yeast phagocytosis in hemocytes of the colonial ascidian *Botryllus schlosseri*. Comparative Biochemistry and Physiology - A Physiology, 118(1), pp.153–158.

Bao, Y., Li, L., Wu, Q. & Zhang, G., 2009. Cloning, characterization, and expression analysis of extracellular copper/zinc superoxide dismutase gene from bay scallop *Argopecten irradians*. Fish & shellfish immunology, 27, pp.17–25.

Barcia, R., Ramos-martinez, J.I. & Ramos-martinez, J.I., 2008. Effects of interleukin-2 on nitric oxide production in molluscan innate immunity. Invertebrate survival journal, 5, pp.43–49.

Bardales, J.R., Díaz-Enrich, M.J., Ibarguren, I. & Villamarín, J Antonio., 2004. Isoforms of cAMP-dependent protein kinase in the bivalve mollusk *Mytilus galloprovincialis*: activation by cyclic nucleotides and effect of temperature. Archives of biochemistry and biophysics, 432(1), pp.71–8.

Bédouet, L., Marie, A., Berland, S., Marie, B., Auzoux-Bordenave, S., Marin, F. & Milet, Christian., 2012. Proteomic Strategy for Identifying Mollusc Shell Proteins Using Mild Chemical Degradation and Trypsin Digestion of Insoluble Organic Shell Matrix: A Pilot Study on Haliotis tuberculata. Marine Biotechnology, 14(4), pp.446–458.

Behar, S., Martin, C.J., Booty, M.G., Nishimura, T., Zhao, X., Gan, H., Divangahi, M. & Remold, HG., 2011. Apoptosis is an innate defense function of macrophages against *Mycobacterium tuberculosis*. Mucosal Immunology, 4(3), pp.279–287.

Benian, G.M., Kiff, J.E., Neckelmann, N., Moerman, D.G. & Waterston, R H., 1989. Sequence of an unusually large protein implicated in regulation of myosin activity in *C. elegans*. Nature, 342(6245), pp.45–50.

Bensmail, H. & Haoudi, A., 2005. Data mining in genomics and proteomics. Journal of biomedicine & biotechnology, 2005(2), pp.63–4.

Vanden Berghe, W., Plaisance, S., Boone, E., De Bosscher, K., Schmitz, M.L., Fiers, W. & Haegeman, G., 1998. p38 and extracellular signal-regulated kinase mitogen-activated protein kinase pathways are required for nuclear factor-kappaB p65 transactivation mediated by tumor necrosis factor. The Journal of biological chemistry, 273(6), pp.3285–3290.

Berthelot, K., Muldoon, M., Rajkowitsch, L., Hughes, J. & McCarthy, John E. G.., 2004. Dynamics and processivity of 40S ribosome scanning on mRNA in yeast. Molecular Microbiology, 51(4), pp.987–1001.

Beutler, B., 2004. Innate immunity: An overview. Molecular Immunology, 40, pp.845–859.

Birge, R.B. & Ucker, D.S., 2008. Innate apoptotic immunity: the calming touch of death. Cell death and differentiation, 15, pp.1096–1102.

Boehm, A.M., Pütz, S., Altenhöfer, D., Sickmann, A. & Falk, M., 2007. Precise protein quantification based on peptide quantification using iTRAQ. BMC Bioinformatics, 8(1), p.214.

Boman, H.G., 1998. Gene-encoded peptide antibiotics and the concept of innate immunity: An update review. Scandinavian Journal of Immunology, 48(1), pp.15–25.

Bondad-Reantaso, M.G., Subasinghe, R.P., Arthur, J.R., Ogawa, K., Chinabut, S., Adlard, R., Tan, Z. & Shariff, M., 2005. Disease and health management in Asian aquaculture. Veterinary parasitology, 132(3-4), pp.249–72.

Borodinsky, L.N. & Spitzer, N.C., 2006. Second messenger pas de deux: the coordinated dance between calcium and cAMP. Science's STKE : signal transduction knowledge environment, 2006, p.pe22.

Boutet, I., Jollivet, D., Shillito, B., Moraga, D. & Tanguy, A., 2009. Molecular identification of differentially regulated genes in the hydrothermal-vent species *Bathymodiolus thermophilus* and *Paralvinella pandorae* in response to temperature. BMC genomics, 10, p.222.

Bower, S.M., McGladdery, S.E. & Price, I.M., 1994. Synopsis of infectious diseases and parasites of commercially exploited shellfish. Annual Review of Fish Diseases, 4, pp.1–199.

Braid, B.A., Moore, J.D., Robbins, T.T., Hedrick, R.P., Tjeerdema, R.S. & Friedman, C S., 2005. Health and survival of red abalone, *Haliotis rufescens*, under varying temperature, food supply, and exposure to the agent of withering syndrome. Journal of invertebrate pathology, 89(3), pp.219–31.

Bricknell, I., Bowden, T.J., Verner-Jeffreys, D.W., Bruno, D.W., Sheilds, R.J. & Ellis, A.E., 2000. Susceptibility of juvenile and sub-adult Atlantic halibut (*Hippoglossus hippoglossus L.*) to infection by *Vibrio anguillarum* and efficacy of protection induced by vaccination. Fish & Shellfish Immunology, 10(4), pp.319–327.

Brooks, C.L. & Dunphy, G.B., 2005. Protein kinase A affects Galleria mellonella (Insecta: *Lepidoptera*) larval haemocyte non-self responses. Immunology and Cell Biology, 83(2), pp.150–159.

Bucci, C., Thomsen, P., Nicoziani, P., McCarthy, J. & van Deurs, B., 2000. Rab7: a key to lysosome biogenesis. Molecular biology of the cell, 11(2), pp.467–80.

Buttke, T.M. & Sandstrom, P.A., 1994. Oxidative stress as a mediator of apoptosis. Immunology today, 15(1), pp.7–10.

Canesi, L., Gallo, G., Gavioli, M. & Pruzzo, C., 2002a. Bacteria-hemocyte interactions and phagocytosis in marine bivalves. Microscopy research and technique, 57(6), pp.469–76.

Canesi, L., Betti, M., Ciacci, C., Scarpato, A., Citterio, B., Pruzzo, C. & Gallo, G., 2002b. Signaling pathways involved in the physiological response of mussel hemocytes to bacterial challenge: the role of stress-activated p38 MAP kinases. Developmental and comparative immunology, 26(4), pp.325–34.

Canesi, L., Betti, M., Ciacci, C., Lorusso, L.C., Pruzzo, C. & Gallo, G., 2006a. Cell signalling in the immune response of mussel hemocytes. Invertebrate survival journal,3, pp.40–49.

Canesi, L., Barmo, C., Fabbri, R., Ciacci, C., Vergani, L., Roch, P. & Gallo, G., 2010. Effects of vibrio challenge on digestive gland biomarkers and antioxidant gene expression in *Mytilus galloprovincialis*. Comparative biochemistry and physiology. Toxicology & pharmacology : CBP, 152(3), pp.399–406.

Cao, A., Martinez, J.I.R. & Barcia, R., 2004. Implication of PKA and PKC in the activation of the haemocytes of *Mytilus galloprovincialis* Lmk. by LPS and IL-2. Molecular Immunology, 41(1), pp.45–52.

Cao, S.S. & Kaufman, R.J., 2012. Unfolded protein response. Current biology : CB, 22(16), pp.R622–6.

Cardinaud, M., Dheilly, N.M., Huchette, S., Moraga, D. & Paillard, C., 2015. The early stages of the immune response of the European abalone *Haliotis tuberculata* to a *Vibrio harveyi* infection. Developmental & Comparative Immunology.

Carr, S., Aebersold, R., Baldwin, M., Burlingame, A., Clauser, K. & Nesvizhskii, A., 2004. The need for guidelines in publication of peptide and protein identification data: Working Group on Publication Guidelines for Peptide and Protein Identification Data. Molecular & cellular proteomics : MCP, 3(6), pp.531–3.

Chan, Q.W.T., Howes, C.G. & Foster, L.J., 2006. Quantitative comparison of caste differences in honeybee hemolymph. Molecular & cellular proteomics : MCP, 5(12), pp.2252–62.

Chang, P.H., Kuo, S.T., Lai, S.H., Yang, H.S., Ting, Y.Y., Hsu, C.L. & Chen, Hon Cheng., 2005. Herpes-like virus infection causing mortality of cultured abalone *Haliotis diversicolor supertexta* in Taiwan. Diseases of aquatic organisms, 65(1), pp.23–7.

Chatterjee, S. & Haldar, S., 2012. Vibrio Related Diseases in Aquaculture and Development of Rapid and Accurate Identification Methods. Journal Marine Science Research & Development, 002, pp.1–7.

Chauhan, J.S., Mishra, N.K. & Raghava, G.P.S., 2009. Identification of ATP binding residues of a protein from its primary sequence. BMC bioinformatics, 10, p.434.

Chen, C.-H. & Chen, J.-H., 2007. Adenosine receptor-like molecules and related signaling transduction pathways regulate hemocyte adhesion in abalone (*Haliotis diversicolor*). <I>The FASEB Journal</I>, 21(6).

Chen, G., Zhang, C., Li, C., Wang, C., Xu, Z. & Yan, P., 2011. Haemocyte protein expression profiling of scallop *Chlamys farreri* response to acute viral necrosis virus (AVNV) infection. Developmental and comparative immunology, 35(11), pp.1135–45.

Chen, H., Mai, K., Zhang, W., Liufu, Z., Xu, W. & Tan, Beiping., 2005. Effects of dietary pyridoxine on immune responses in abalone, *Haliotis discus hannai* Ino. Fish & shellfish immunology, 19, pp.241–252.

Chen, L.M., Tran, B.N., Lin, Q., Lim, T.K., Wang, F. & Hew, C.-L., 2008. iTRAQ analysis of Singapore grouper iridovirus infection in a grouper embryonic cell line. The Journal of general virology, 89(Pt 11), pp.2869–76.

Cheng, W., Hsiao, I.-S., Hsu, C.-H., et al., 2004a. Change in water temperature on the immune response of Taiwan abalone *Haliotis diversicolor supertexta* and its susceptibility to *Vibrio parahaemolyticus*. Fish & shellfish immunology, 17(3), pp.235–43.

Cheng, W., Hsiao, I.-S. & Chen, J.-C., 2004b. Effect of nitrite on immune response of Taiwan abalone *Haliotis diversicolor supertexta* and its susceptibility to *Vibrio parahaemolyticus*. Diseases of aquatic organisms, 60(2), pp.157–64.

Cheng, W., Juang, F.-M. & Chen, J.-C., 2004. The immune response of Taiwan abalone *Haliotis diversicolor supertexta* and its susceptibility to *Vibrio parahaemolyticus* at different salinity levels. Fish & shellfish immunology, 16(3), pp.295–306.

Cheresh, D. A., Leng, J. & Klemke, R.L., 1999. Regulation of cell contraction and membrane ruffling by distinct signals in migratory cells. The Journal of cell biology, 146(5), pp.1107–16.

Chimini, G. & Chavrier, P., 2000. Function of Rho family proteins in actin dynamics during phagocytosis and engulfment. Nature cell biology, 2(10), pp.E191–6.

Chong, P.K., Gan, C.S., Pham, T.K. & Wright, P.C., 2006. Isobaric Tags for Relative and Absolute Quantitation (iTRAQ) Reproducibility : Implication of Multiple Injections research articles. Journal of proteome research, 5, pp.1232–1240.

Chongsatja, P.-O., Bourchookarn, A., Lo, C.F., Thongboonkerd, V. & Krittanai, C., 2007. Proteomic analysis of differentially expressed proteins in *Penaeus vannamei* hemocytes upon Taura syndrome virus infection. Proteomics, 7(19), pp.3592–601.

Chuaqui, R.F., Bonner, R.F., Best, C.J.M., Gillespie, J.W., Flaig, M.J., Hewitt, S.M., Phillips, J.L., Krizman, D.B., Tangrea, M.A., Ahram, M., Linehan, W.M., Knezevic, V. & Emmert-Buck, M.R., 2002. Post-analysis follow-up and validation of microarray experiments. Nature genetics, 32 Suppl(december), pp.509–14.

Cirino, G., Fiorucci, S. & Sessa, W.C., 2003. Endothelial nitric oxide synthase : the Cinderella of inflammation ? Trends in Pharmacological Sciences, 24(2), pp.91–95.

Coates, C.J. & Nairn, J., 2014. Diverse immune functions of hemocyanins. Developmental and comparative immunology, 45(1), pp.43–55.

Coates, C.J. & Nairn, J., 2013. Hemocyanin-derived phenoloxidase activity : A contributing factor to hyperpigmentation in *Nephrops norvegicus*. Food Chemistry, 140(1-2), pp.361–369.

Colasanti, M. & Venturini, G., 1998. Nitric oxide in invertebrates. Molecular neurobiology, 17, pp.157–174.

Coling, D.E., Ding, D., Young, R., Lis, M., Stofko, E., Blumenthal, K.M. & Salvi, R.J., 2007. Proteomic analysis of cisplatin-induced cochlear damage: methods and early changes in protein expression. Hearing research, 226(1-2), pp.140–56.

Conesa, A., Götz, S., García-Gómez, J.M., Terol, J., Talón, M. & Robles, M., 2005. Blast2GO: a universal tool for annotation, visualization and analysis in functional genomics research. Bioinformatics (Oxford, England), 21(18), pp.3674–6.

Cong, Y.-S., Fan, E. & Wang, E., 2006. Simultaneous proteomic profiling of four different growth states of human fibroblasts, using amine-reactive isobaric tagging reagents and tandem mass spectrometry. Mechanisms of ageing and development, 127(4), pp.332–43.

Conte, A. & Ottaviani, E., 1995. Nitric oxide synthase activity in molluscan hemocytes. FEBS Letters, 365(2-3), pp.120–124.

Cook, P.A. & Gordon, R.H., 2010. World abalone supply, markets and pricing. Journal of shellfish research, 29(3), pp.569–571.

Costa, M.M., Prado-Alvarez, M., Gestal, C., Li, H., Roch, P., Novoa, B. & Figueras, A., 2009. Functional and molecular immune response of Mediterranean mussel (*Mytilus galloprovincialis*) haemocytes against pathogen-associated molecular patterns and bacteria. Fish & Shellfish Immunology, 26(3), pp.515–523.

Costes, S.V., Daelemans, D., Cho, E.H., Dobbin, Z., Pavlakis, G. & Lockett, S., 2004. Automatic and quantitative measurement of protein-protein colocalization in live cells. Biophysical journal, 86(6), pp.3993–4003.

Cottrell, J.S., 2011. Protein identification using MS/MS data. Journal of proteomics, 74(10), pp.1842–51.

Cowan, K.J. & Storey, K.B., 2003. Mitogen-activated protein kinases: new signalling pathways functioning in cellular responses to environmental stress. The Journal of experimental biology, 206, pp.1107–1115.

Cox, J. & Mann, M., 2007. Is proteomics the new genomics? Cell, 130(3), pp.395–8.

Coyne, V.E., 2011. The importance of ATP in the immune system of molluscs. Invertebrate Survival Journal, 8, pp.48–55.

Crago, A. & Koronakis, V., 1998. *Salmonella* InvG forms a ring-like multimer that requires the InvH lipoprotein for outer membrane localization. Molecular microbiology, 30, pp.47–56.

Dang, V. T., Speck, P. & Benkendorff, K., 2012. Influence of elevated temperatures on the antiviral and antibacterial immune response of abalone, Haliotis rubra. Fish and Shellfish Immunology, 32: 732-740.

Dang, V.T., Benkendorff, K., Corbeil, S., Williams, L.M., Hoad, J., Crane, Mark S.J. & Speck, Peter., 2013. Immunological changes in response to herpesvirus infection in abalone *Haliotis laevigata* and *Haliotis rubra* hybrids. Fish and Shellfish Immunology, 34(2), pp.688–691.

Dang, V.T., Speck, P., Doroudi, M., Smith, B. & Benkendorff, K., 2011. Variation in the antiviral and antibacterial activity of abalone *Haliotis laevigata, H.* rubra and their hybrid in South Australia. Aquaculture, 315(3-4), pp.242–249.

Davies, S.P., Reddy, H., Caivano, M. & Cohen, P., 2000. Specificity and mechanism of action of some commonly used protein kinase inhibitors. The Biochemical journal, 351, pp.95–105.

Decker, H., Ryan, M., Jaenicke, E. & Terwilliger, N., 2001. SDS-induced phenoloxidase activity of hemocyanins from *Limulus polyphemus*, *Eurypelma californicum*, and *Cancer magister*. The Journal of biological chemistry, 276(21), pp.17796–9.

Decker, H. & Rimke, T., 1998. Tarantula Hemocyanin Shows Phenoloxidase Activity. Journal of Biological Chemistry, 273(40), pp.25889–25892.

Deininger, M.H. et al., 2003. The allograft inflammatory factor-1 in Creutzfeldt-Jakob disease brains. Neuropathology and applied neurobiology, 29(4), pp.389–99.

Deininger, M.H., Meyermann, R. & Schluesener, H.J., 2002. The allograft inflammatory factor-1 family of proteins. FEBS letters, 514(2-3), pp.115–21.

Delaporte, M., Soudant, P., Lambert, C., Moal, J., Pouvreau, S. & Samain, J. F., 2006. Impact of food availability on energy storage and defense related hemocyte parameters of the Pacific oyster *Crassostrea gigas* during an experimental reproductive cycle. Aquaculture, 254(1-4), pp.571–582.

Delghandi, M.P., Johannessen, M. & Moens, U., 2005. The cAMP signalling pathway activates CREB through PKA, p38 and MSK1 in NIH 3T3 cells. Cellular signalling, 17(11), pp.1343–51.

Deng, W., Wang, Y., Liu, Z., Cheng, H. & Xue, Y., 2014. HemI: a toolkit for illustrating heatmaps. PloS one, 9(11), p.e111988.

Aquaculture and economic development, Fisheries branch, Department of agriculture, forestry and fisheries, 2012. Aquaculture yearbook 2012 South Africa.

Destoumieux-Garzón, D., Saulnier, D., Garnier, J., Jouffrey, C., Bulet, P. & Bachère, E., 2001. Crustacean immunity. Antifungal peptides are generated from the C terminus of shrimp hemocyanin in response to microbial challenge. The Journal of biological chemistry, 276(50), pp.47070–7.

Devasagayam, T.P., Tilak, J.C., Boloor, K.K., Sane, K.S., Ghaskadbi, S.S. & Lele, R.D., 2004. Free radicals and antioxidants in human health: current status and future prospects. The Journal of the Association of Physicians of India, 52(October), pp.794–804.

Dhar, A.K., Dettori, A., Roux, M.M., Klimpel, K.R. & Read, B., 2003. Identification of differentially expressed genes in shrimp (*Penaeus stylirostris*) infected with White spot syndrome virus by cDNA microarrays. Archives of virology, pp.2381–2396.

Dheilly, N.M., Haynes, P.A., Bove, U., Nair, S.V. & Raftos, D.A., 2011. Comparative proteomic analysis of a sea urchin (*Heliocidaris erythrogramma*) antibacterial response revealed the involvement of apextrin and calreticulin. Journal of invertebrate pathology, 106(2), pp.223–9.

Dheilly, N.M., Raftos, D.A., Haynes, P.A., Smith, L.C. & Nair, S.V., 2013. Shotgun proteomics of coelomic fluid from the purple sea urchin, *Strongylocentrotus purpuratus*. Developmental and comparative immunology, 40(1), pp.35–50.

Dimmer, E.C., Huntley, R.P., Barrell, D.G., Binns, D., Draghici, S., Camon, E.B., Hubank, M., Talmud, P.J., Apweiler, R. & Lovering, R.C., 2008. The Gene Ontology - Providing a Functional Role in Proteomic Studies. Proteomics, 8(23-24).

Dixon, M.G., Hecht, T. & Brandt, C.R., 1991. Identification and treatment of a *Clostridium* and *Vibrio* infection in South African abalone, *Haliotis midae L*. Journal of Fish Diseases, 14(6), pp.693–695.

Dominguez, R. & Holmes, K.C., 2011. Actin structure and function. Annual review of biophysics, 40(3), pp.169–86.

Donaghy, L., Hong, H.K., Lambert, C., Park, H.S., Shim, W.J. & Choi, K.S., 2010. First characterisation of the populations and immune-related activities of hemocytes from two edible gastropod species, the disk abalone, *Haliotis discus discus* and the spiny top shell*, Turbo cornutus*. Fish & shellfish immunology, 28(1), pp.87–97.

Donaghy, L., Kim, B.-K., Hong, H.-K., Park, H.-S. & Choi, K.-S., 2009. Flow cytometry studies on the populations and immune parameters of the hemocytes of the Suminoe oyster, *Crassostrea ariakensis*. Fish & shellfish immunology, 27(2), pp.296–301.

Donaghy, L., Lambert, C., Choi, K.-S. & Soudant, P., 2009. Hemocytes of the carpet shell clam (*Ruditapes decussatus*) and the Manila clam (*Ruditapes philippinarum*): Current knowledge and future prospects. Aquaculture, 297(1-4), pp.10–24.

Dondero, F., Dagnino, A., Jonsson, H., Caprì, F., Gastaldi, L. & Viarengo, A., 2006. Assessing the occurrence of a stress syndrome in mussels (*Mytilus edulis*) using a combined biomarker/gene expression approach. Aquatic toxicology, 78 Suppl 1, pp.S13–24.

Duca, L., Lambert, E., Debret, R., Rothhut, B., Blanchevoye, C., Hornebeck, W., Martiny, L. & Debelle, L.L., 2005. Elastin Peptides Activate Extracellular Signal-Regulated Kinase 1 / 2 via a Ras-Independent Mechanism Requiring Both p110 γ / Raf-1 and Protein Kinase A / B-Raf Signaling in Human Skin Fibroblasts. Molecular pharmacology, 67(4), pp.1315–1324.

Dunn, K.W., Kamocka, M.M. & McDonald, J.H., 2011. A practical guide to evaluating colocalization in biological microscopy. American journal of physiology. Cell physiology, 300(4), pp.C723–42.

Ehrlich, R.S., Hayman, S., Ramachandran, N. & Colman, R.F., 1981. Re-evaluation of molecular weight of pig heart NAD-specific isocitrate dehydrogenase. The Journal of biological chemistry, 256(20), pp.10560–4.

Elias, J.E. & Gygi, S.P., 2010. Proteome Bioinformatics. Methods molecular biology,, 604(5), pp.1–16.

Ellis, R.P., Parry, H., Spicer, J. I., Hutchinson, T. H., Pipe, R. K. & Widdicombe, S.., 2011. Immunological function in marine invertebrates: Responses to environmental perturbation. Fish and Shellfish Immunology, 30(6), pp.1209–1222.

Engelmann, P., Opper, B. & Németh, P., 2011. Interactions of intracellular calcium and immune response in earthworms. , pp.78–84.

Ernoult, E., Bourreau, A., Gamelin, E. & Guette, C., 2010. A Proteomic Approach for Plasma Biomarker Discovery with iTRAQ Labelling and OFFGEL Fractionation. Journal of biomedicine biotechnology, 2010, p.927917.

Evans, C., Noirel, J., Ow, S.Y., Salim, M., Pereira-Medrano, A.G., Couto, N., Pandhal, J., Smith, D., Pham, T.K., Karunakaran, E., Zou, X., Biggs, C.A. & Wright, P.C., 2012. An insight into iTRAQ: where do we stand now? Analytical and bioanalytical chemistry, 404(4), pp.1011–27.

Favaloro, B., Allocati, N., Graziano, V., Di Ilio, C. & De Laurenzi, V., 2012. Role of apoptosis in disease. Aging, 4(5), pp.330–349.

Feder, M.E. & Hofmann, G.E., 1999. Heat-shock proteins, molecular chaperones, and the stress response: evolutionary and ecological physiology. Annual review of physiology, 61, pp.243–82.

Feng, Y., Press, B. & Wandinger-Ness, a, 1995. Rab 7: an important regulator of late endocytic membrane traffic. The Journal of cell biology, 131(6 Pt 1), pp.1435–52.

Fialkow, L., Wang, Y. & Downey, G.P., 2007. Reactive oxygen and nitrogen species as signalling molecules regulating neutrophil function. Free Radical Biology and Medicine, 42, pp.153–164.

Fong, C.C., Shi, Y.F., Yu, W.K., Wei, F., van de Merwe, J.P., Chan, A.K.Y., Ye, R., Au, D.W.T., Wu, R.S.S. & Yang, M.S., 2014. iTRAQ-based proteomic profiling of the marine medaka (*Oryzias melastigma*) gonad exposed to BDE-47. Marine pollution bulletin.

Förstermann, U. & Sessa, W.C., 2012. Nitric oxide synthases: Regulation and function. European Heart Journal, 33, pp.829–837.

Franchini, A., Fontanili, P. & Ottaviani, E., 1995. Invertebrate immunocytes: relationship between phagocytosis and nitric oxide production. Comparative Biochemistry and Physiology Part B: Biochemistry and Molecular Biology, 110(2), pp.403–407.

Fukushi, S., Okada, M., Stahl, J., Kageyama, T., Hoshino, F.B. & Katayama, K., 2001. Ribosomal protein S5 interacts with the internal ribosomal entry site of hepatitis C virus. The Journal of biological chemistry, 276(24), pp.20824–6.

Fuller, H.R. & Morris, G.E., 2012. Quantitative Proteomics Using iTRAQ Labelling and Mass Spectrometry. Science and Technology, pp.347–362.

Del Galdo, F. & Jiménez, S.A, 2007. T cells expressing allograft inflammatory factor 1 display increased chemotaxis and induce a profibrotic phenotype in normal fibroblasts in vitro. Arthritis and rheumatism, 56(10), pp.3478–88.

Gan, C.S., Chong, P.K., Pham, T.K. & Wright, P.C., 2007. Technical , Experimental , and Biological Variations in Isobaric Tags for Relative and Absolute Quantitation (iTRAQ) research articles. Journal of Proteome Research, pp.821–827.

García-García, E., Prado-Alvarez, M., Novoa, B., Figueras, A., Rosales, C., Prado-Álvarez, M., Novoa, B., Figueras, A. & Rosales, C., 2008. Immune responses of mussel hemocyte subpopulations are differentially regulated by enzymes of the PI 3-K, PKC, and ERK kinase families. Developmental and Comparative Immunology, 32, pp.637–653.

Garcia-Garcia, E. & Rosales, C., 2002. Signal transduction during Fc receptor-mediated phagocytosis. J. Leukoc. Biol., 72(6), pp.1092–1108.

Garcia-Reyero, N. & Perkins, E.J., 2011. Systems biology: leading the revolution in ecotoxicology. Environmental toxicology and chemistry / SETAC, 30(2), pp.265–73.

Ghazalpour, A., Bennett, B., Petyuk, V.A., Orozco, L., Hagopian, R., Mungrue, I.N., Farber, C.R., Sinsheimer, J., Kang, H.M., Furlotte, N., Park, C.C., Wen, P.-Z., Brewer, H., Weitz, K., Camp, D.G., Pan, C., Yordanova, R., Neuhaus, I., Tilford, C., Siemers, N., Gargalovic, P., Eskin, E., Kirchgessner, T., Smith, D.J., Smith, R.D. & Lusis, A.J., 2011. Comparative analysis of proteome and transcriptome variation in mouse. PLoS genetics, 7(6), p.e1001393.

Ghosh, J., Lun, C.M., Majeske, A.J., Sacchi, S., Schrankel, C.S. & Smith, L.C., 2011. Invertebrate immune diversity. Developmental and Comparative Immunology, 35(9), pp.959–974.

Gifondorwa, D.J. & Leise, E.M., 2006. Programmed cell death in the apical ganglion during larval metamorphosis of the marine mollusc *Ilyanassa obsoleta*. Biological Bulletin, 210(2), pp.109–120.

Goedken, M. & De Guise, S., 2004. Flow cytometry as a tool to quantify oyster defence mechanisms. Fish & shellfish immunology, 16(4), pp.539–52.

Gopalakrishnan, S., Huang, W.-B., Wang, Q.-W.,Wu, M.-Li., Liu, J. & Wang, K.-J., 2011. Effects of tributyltin and benzo[a]pyrene on the immune-associated activities of hemocytes and recovery responses in the gastropod abalone, *Haliotis diversicolor*. Comparative biochemistry and physiology. Toxicology & pharmacology : CBP, 154(2), pp.120–8.

Gordon, H.R. & Cook, P.A., 2013. World abalone supply, markets, and pricing: 2011 Update. Journal of Shellfish Research, 32(1):5-7.

Götz, S., García-Gómez, J.M., Terol, J., Williams, T.D., Nagaraj, S.H., Nueda, M.J., Robles, M., Talón, M., Dopazo, J. & Conesa, A., 2008. High-throughput functional annotation and data mining with the Blast2GO suite. Nucleic acids research, 36(10), pp.3420–35.

Gourdon, I., Guérin, M.C., Torreilles, J. & Roch, P., 2001. Nitric oxide generation by hemocytes of the mussel *Mytilus galloprovincialis*. Nitric oxide : biology and chemistry / official journal of the Nitric Oxide Society, 5(1), pp.1–6.

Gouwy, M., Struyf, S., Proost, P. & Van Damme, Jo., 2005. Synergy in cytokine and chemokine networks amplifies the inflammatory response. Cytokine & growth factor reviews, 16(6), pp.561–80.

Greenberg, S., 1995. Signal transduction of phagocytosis. Trends in cell biology, 5(3), pp.93–9.

Habermann, B., Oegema, J., Sunyaev, S. & Shevchenko, Andrej., 2004. The power and the limitations of cross-species protein identification by mass spectrometry-driven sequence similarity searches. Molecular & cellular proteomics : MCP, 3(3), pp.238–49.

Hanada, T. & Yoshimura, A., 2002. Regulation of cytokine signalling and inflammation. Cytokine & Growth Factor Reviews, 13(4-5), pp.413–421.

Hancock, R.E. & Scott, M.G., 2000. The role of antimicrobial peptides in animal defences. Proceedings of the National Academy of Sciences of the United States of America, 97(16), pp.8856–8861.

Hannam, M.L., Bamber, S.D., Galloway, T.S., John Moody, A. & Jones, M.B., 2010. Functional immune response in *Pecten maximus*: Combined effects of a pathogen-associated molecular pattern and PAH exposure. Fish and Shellfish Immunology, 28(1), pp.249–252.

Hardie, D.G., Scott, J.W., Pan, D.A. & Hudson, E.R., 2003. Management of cellular energy by the AMP-activated protein kinase system. FEBS Letters, 546(1), pp.113–120.

Hatanaka, R., Sekine, Y., Hayakawa, T., Takeda, K. & Ichijo, H., 2009. Signalling pathways in invertebrate immune and stress response. Invertebrate Survival Journal, pp.32–43.

Hauck, M. & Sweijd, N.A., 1999. A case study of abalone poaching in South Africa and its impact on fisheries management. Journal of marine science, 56, pp.1024–1032.

Hayes, J.D., Flanagan, J.U. & Jowsey, I.R., 2005. Glutathione transferases. Annual review of pharmacology and toxicology, 45, pp.51–88.

Haynes, C. & Iakoucheva, L.M., 2006. Serine/arginine-rich splicing factors belong to a class of intrinsically disordered proteins. Nucleic acids research, 34(1), pp.305–12.

Hecker, M., Cattaruzza, M. & Wagner, A.H., 1999. Regulation of Inducible Nitric Oxide Synthase Gene Expression in Vascular Smooth Muscle Cells. General Pharmacology: The Vascular System, 32(1), pp.9–16.

Hill, E.G., Schwacke, J.H., Comte-walters, S., Slate, E.H., Oberg, A.L., Eckel-Passow, J.E., Therneau, T.M. & Schey, K.L., 2008. A Statistical Model for iTRAQ Data Analysis research articles. Journal of Proteome Research, pp.3091–3101.

Hoek, R.M., Smit, A.B., Frings, H., Vink, J.M., De Jong-Brink, M. & Geraerts, W.P.M., 1996. A new Ig-superfamily member, molluscan defence molecule (MDM) from *Lymnaea stagnalis*, is down-regulated during parasitosis. European Journal of Immunology, 26(4), pp.939–944.

Hofer, A.M., 2012. Interactions between calcium and cAMP signaling. Current medicinal chemistry, 19, pp.5768–73.

Hooper, C., Day, R., Slocombe, R., Benkendorff, K., Handlinger, J. 2014. "Histopathology and haemolymph biochemistry following anaesthesia and movement in farmed Australian abalone (Haliotis rubra Haliotis laevigata). Journal of Aquaculture , 422-423:202 - 210 .

Hooper, C., Day, R., Slocombe, R., Benkendorff, K. & Handlinger, J., 2011. Effect of movement stress on immune function in farmed Australian abalone (hybrid *Haliotis laevigata* and *Haliotis rubra*). Aquaculture, 315(3-4), pp.348–354.

Hooper, C., Slocombe, R., Day, R. & Crawford, S., 2012. Leucopenia associated with abalone viral ganglioneuritis. Australian veterinary journal, 90(1-2), pp.24–8.

Hooper, C., Day, R., Slocombe, R., Handlinger, J. & Benkendorff, K, 2007. Stress and immune responses in abalone: limitations in current knowledge and investigative methods based on other models. Fish & shellfish immunology, 22(4), pp.363–79.

Hooper, S.L. & Thuma, J.B., 2005. Invertebrate muscles: muscle specific genes and proteins. Physiological reviews, 85(3), pp.1001–60.

Hu, Z.-L., Bao, J. & Reecy, J., 2008. CateGOrizer: A Web-Based Program to Batch Analyze Gene Ontology Classification Categories. Online Journal of Bioinformatics, pp.108–112.

Huan, P., Wang, H. & Liu, B., 2011. Comparative proteomic analysis of challenged Zhikong scallop (*Chlamys farreri*): a new insight into the anti-*Vibrio* immune response of marine bivalves. Fish & shellfish immunology, 31(6), pp.1186–92.

Huang, C.Y., Liu, P.C. & Lee, K.K., 2001. Withering syndrome of the small abalone, *Haliotis diversicolor supertexta*, is caused by *Vibrio parahaemolyticus* and associated with thermal induction. Zeitschrift für Naturforschung. C, Journal of biosciences, 56(9-10), pp.898–901.

Huang, W. B., Ren, H.L., Gopalakrishnan, S., Xu, D.D., Qiao, K. & Wang, K.J., 2010. First molecular cloning of a molluscan caspase from variously colored abalone (*Haliotis diversicolor*) and gene expression analysis with bacterial challenge. Fish and Shellfish Immunology, 28(4), pp.587–595.

Huang, X., Zhao, Y., Jia, S., Yan, D. & Chen, Z., 2011. Effects of daintain/AIF-1 on β cell dysfunction in INS-1 cells. Bioscience, biotechnology, and biochemistry, 75(9), pp.1842–4.

Humphries, J.E. & Yoshino, T.P., 2003. Cellular Receptors and Signal Transduction in Molluscan Hemocytes : Connections with the Innate Immune System of Vertebrates 1. Integrative and comparative biology, 43, pp.305–312.

Huvet, A., Herpin, A., Dégremont, L., Labreuche, Y., Samain, J.-F. & Cunningham, C., 2004. The identification of genes from the oyster *Crassostrea gigas* that are differentially expressed in progeny exhibiting opposed susceptibility to summer mortality. Gene, 343(1), pp.211–20.

Iakovleva, N. V., Gorbushin, A.M. & Storey, K.B., 2006. Modulation of mitogen-activated protein kinases (MAPK) activity in response to different immune stimuli in haemocytes of the common periwinkle *Littorina littorea*. Fish and Shellfish Immunology, 21, pp.315–324.

Ivarsson, Y., Mackey, A.J., Edalat, M., Pearson, W.R. & Mannervik, B., 2003. Identification of residues in glutathione transferase capable of driving functional diversification in evolution. A novel approach to protein redesign. The Journal of biological chemistry, 278(10), pp.8733–8.

Izawa, S., Izawa, S., Maeda, K., Miki, T., Mano, J., Inoue, Y. & Kimura, A., 1998. Importance of glucose-6-phosphate dehydrogenase in the adaptive response to hydrogen peroxide in *Saccharomyces cerevisiae*. Journal of biochemistry, 330, pp.811–817.

Jagtap, P., Michailidis, G., Zielke, R., Walker, A.K., Patel, N., Strahler, J.R., Driks, A., Andrews, P.C. & Maddock, J.R., 2006. Early events of *Bacillus anthracis* germination identified by time-course quantitative proteomics. Proteomics, 6(19), pp.5199–211.

Janeway, C.A. & Medzhitov, R., 2002. Innate immune recognition. Annual review of immunology, 20(2), pp.197–216.

Januszkiewicz, A., Loré, K., Essén, P., Andersson, B., Mcnurlan, M.A., Garlick, P. J., Ringdén, O., Andersson, J. & Wernerman, J., 2002. Response of in vivo protein synthesis in T lymphocytes and leucocytes to an endotoxin challenge in healthy volunteers. Clinical and Experimental Immunology, 130, pp.263–270.

Januszkiewicz, A., Rooyackers, O. & Wernerman, J., 2006. Quantitative in vivo Protein Synthesis as a Measure of Immune Function. Yearbook of Intensive Care and Emergency Medicine, Volume 2006, pp 52-67

Jaumouillé, V. & Grinstein, S., 2011. Receptor mobility, the cytoskeleton, and particle binding during phagocytosis. Current opinion in cell biology, 23(1), pp.22–9.

Ji, C., Wu, H., Wei, L., Zhao, J., Wang, Q. & Lu, Hongjian., 2013. Responses of *Mytilus galloprovincialis* to bacterial challenges by metabolomics and proteomics. Fish and Shellfish Immunology, 35(2), pp.489–498.

Ji, N., Chang, Y., Zhao, C., Pang, Z. & He, Z., 2014. Cloning and gene expression of allograft inflammatory factor-1 (AIF-1) provide new insights into injury and bacteria response of the sea cucumber *Apostichopus japonicus* (Selenka, 1867). Fish & shellfish immunology, 38(2), pp.400–5.

Jia, J., Zhao, Y.-F. & Zhao, J.-H., 2007. Potential roles of allograft inflammatory factor-1 in the pathogenesis of hemangiomas. Medical hypotheses, 68(2), pp.288–90.

Jiang, N., Tan, N.S., Ho, B., Ding, J.L., 2007. Respiratory protein-generated reactive oxygen species as an antimicrobial strategy. Nature immunology, 8(10), pp.1114–22.

Jiang, Y.S. & Wu, X.Z., 2007. Characterization of a Rel\NF-kappa B hornologue in a gastropod abalone, *Haliotis diversicolor supertexta*. Developmental and Comparative Immunology, 31(2), pp.121–131.

Johnson, D.A., Akamine, P., Radzio-Andzelm, E., Madhusudan, M. & Taylor, S.S., 2001. Dynamics of cAMP-dependent protein kinase. Chemical reviews, 101(8), pp.2243–70.

Jose, S., Mohandas, A., Philip, R. & Bright Singh, I.S., 2010. Primary hemocyte culture of *Penaeus monodon* as an in vitro model for white spot syndrome virus titration, viral and immune related gene expression and cytotoxicity assays. Journal of invertebrate pathology, 105(3), pp.312–21.

Jurgen, F., Valerio, M., Roberto, R., Paolo, S.G. & Marta, M., 2011. 2-DE proteomic analysis of HSP70 in mollusc *Chamelea gallina*. Fish & shellfish immunology, 30(2), pp.739–43.

Kaminska, B., 2005. MAPK signalling pathways as molecular targets for anti-inflammatory therapy - From molecular mechanisms to therapeutic benefits. Biochimica et Biophysica Acta - Proteins and Proteomics, 1754, pp.253–262.

Kannan, K. & Jain, S., 2000. Oxidative stress and apoptosis. Pathophysiology : the official journal of the International Society for Pathophysiology / ISP, 7(27), pp.153–163.

Karp, N.A. & Lilley, K.S., 2007. Design and analysis issues in quantitative proteomics studies. Proteomics, 7 Suppl 1, pp.42–50.

Karp, N.A., Huber, W., Sadowski, P.G., Charles, P.D., Hester, S.V. & Lilley, K.S., 2010. Addressing Accuracy and Precision Issues in iTRAQ Quantitation. Molecular cellular proteomics MCP, 9(9), pp.1885–1897.

Kawabe, S. & Yokoyama, Y., 2010. Molecular cloning of calnexin and calreticulin in the Pacific oyster *Crassostrea gigas* and its expression in response to air exposure. Marine genomics, 3(1), pp.19–27.

Kemp, I.K. & Coyne, V.E., 2011. Identification and characterisation of the Mpeg1 homologue in the South African abalone, *Haliotis midae*. Fish & shellfish immunology, 31(6), pp.754–64.

Kesarcodi-Watson, A., Kaspar, H., Lategan, M. J. & Gibson, Lewis., 2008. Probiotics in aquaculture: The need, principles and mechanisms of action and screening processes. Aquaculture, 274(1), pp.1–14.

Keshamouni, V.G., Michailidis, G., Grasso, C.S., Anthwal, S., Strahler, J.R., Walker, A., Arenberg, D.A., Reddy, R.C., Akulapalli, S., Thannickal, V.J., Standiford, T.J., Andrews, P.C. & Omenn, Gilbert S., 2006. Differential Protein Expression Profiling by iTRAQ - 2DLC - MS / MS of Lung Cancer Cells Undergoing Epithelial-Mesenchymal Transition Reveals a Migratory / Invasive Phenotype research articles. , pp.1143–1154.

Kim, Y.-O., Kim, Y.-O., Koh, H.-J., Kim, S.-H., Jo, S.-H., Huh, J.-W., Jeong, K.-S., Lee, I. J., Song, B. J. & Huh, T.-L., 1999. Identification and Functional Characterization of a Novel, Tissue-specific NAD+-dependent Isocitrate Dehydrogenase Subunit Isoform. Journal of Biological Chemistry, 274(52), pp.36866–36875.

Kimura, M., Kawahito, Y., Obayashi, H., Ohta, M., Hara, H., Adachi, T., Tokunaga, D., Hojo, T., Hamaguchi, M., Omoto, A., Ishino, H., Wada, M., Kohno, M., Tsubouchi, Y. & Yoshikawa, T., 2007. A Critical Role for Allograft Inflammatory Factor-1 in the Pathogenesis of Rheumatoid Arthritis. The Journal of Immunology, 178(5), pp.3316–3322.

Kingtong, S., Chitramvong, Y. & Janvilisri, T., 2007. ATP-binding cassette multidrug transporters in Indian-rock oyster *Saccostrea forskali* and their role in the export of an environmental organic pollutant tributyltin. Aquatic toxicology (Amsterdam, Netherlands), 85(2), pp.124–32.

Kletsas, D., Sassi, D., Franchini, A. & Ottaviani, E., 1998. PDGF and TGF-beta induce cell shape changes in invertebrate immunocytes via specific cell surface receptors. European Journal of Cell Biology, 75(4), pp.362–366.

Kling, P. & Förlin, L., 2009. Proteomic studies in zebrafish liver cells exposed to the brominated flame retardants HBCD and TBBPA. Ecotoxicology and environmental safety, 72(7), pp.1985–93.

Kolega, J. & Taylor, D.L., 1993. Gradients in the concentration and assembly of myosin II in living fibroblasts during locomotion and fiber transport. Molecular biology of the cell, 4(8), pp.819–36.

Kominsky, D.J., Campbell, E.L. & Colgan, S.P., 2010. Metabolic shifts in immunity and inflammation. Journal of immunology (Baltimore, Md. : 1950), 184(8), pp.4062–4068.

Koutsogiannaki, S. & Kaloyianni, M., 2010. Signalling molecules involved in immune responses in mussels. Invertebrate survival journal, 7(1), pp.11–21.

Krauss, S., Brand, M.D. & Buttgereit, F., 2001. Signalling takes a breath-new quantitative perspectives on bioenergetics and signal transduction. Immunity, 15(4), pp.497–502.

Kruse, M., Steffen, R., Batel, R., Müller, I.M. & Müller, W E., 1999. Differential expression of allograft inflammatory factor 1 and of glutathione peroxidase during auto- and allograft response in marine sponges. Journal of cell science, 112(2), pp.4305–13.

Kumar, C. & Mann, M., 2009. Bioinformatics analysis of mass spectrometry-based proteomics data sets. FEBS letters, 583(11), pp.1703–12.

Kumar, S., Boehm, J. & Lee, J.C., 2003. p38 MAP kinases: key signalling molecules as therapeutic targets for inflammatory diseases. Nature reviews. Drug discovery, 2(9), pp.717–726.

Kusano, H., Shimizu, S., Koya, R.C., Fujita, H., Kamada, S., Kuzumaki, N. & Tsujimoto, Yoshihide., 2000. Human gelsolin prevents apoptosis by inhibiting apoptotic mitochondrial changes via closing VDAC. Oncogene, 19, pp.4807-4814.

Labreuche, Y., Lambert, C., Soudant, P., Boulo, V., Huvet, A. & Nicolas, J.L., 2006. Cellular and molecular hemocyte responses of the Pacific oyster, *Crassostrea gigas*, following bacterial infection with *Vibrio aestuarianus* strain 01/32. Microbes and Infection, 8, pp.2715–2724.

Lacoste, A., Malham, S.K., Cueff, A. & Poulet, S.A., 2001. Noradrenaline modulates oyster hemocyte phagocytosis via a beta-adrenergic receptor-cAMP signaling pathway. General and comparative endocrinology, 122(3), pp.252–9.

Lacoste, A., Cueff, A. & Poulet, S.A., 2002. P35-sensitive caspases, MAP kinases and Rho modulate beta-adrenergic induction of apoptosis in mollusc immune cells. Journal of cell science, 115(Pt 4), pp.761–8.

Lafferty, K. D., Harvell, D., Conrad, J. M., Friedman, C. S., Kent, M. L., Kuris, A. M, Powell, E. N., Rondeau, D. & Saksida, S. M., 2014. Infectious diseases affect marine fisheries and aquaculture economics. Annual Review of Marine Science, Vol. 7: 471-496.

Lafferty, K.D. & Kuris, A.M., 1993. Mass mortality of abalone *Haliotis cracherodii* on the California Channel Islands: tests of epidemiological hypotheses. , 96, pp.239–248.

Lange, B., Currie, K., Howarth, G. S. & Stone. D.A.J., 2014. Grape seed extract and dried macroalgae, Ulva lactuca Linnaeus, improve survival of greenlip abalone, Haliotis

laevigata Donovan, at high water temperature. Journal of Aquaculture 433, 348-360.

Lanz-Mendoza, H., Bettencourt, R., Fabbri, M. & Faye, I., 1996. Regulation of the insect immune response: the effect of hemolin on cellular immune mechanisms. Cellular immunology, 169(1), pp.47–54.

Larsen, C.M., Wadt, K.A., Juhl, L.F., Andersen, H.U., Karlsen, A.E., Su, M.S., Seedorf, K., Shapiro, L., Dinarello, C. & Mandrup-Poulsen, T., 1998. Interleukin-1beta-induced rat pancreatic islet nitric oxide synthesis requires both the p38 and extracellular signal-regulated kinase 1/2 mitogen-activated protein kinases. The Journal of biological chemistry, 273(24), pp.15294–15300.

Lebel, J.M., Giard, W., Favrel, P. & Boucaud-Camou, E., 1996. Effects of different vertebrate growth factors on primary cultures of hemocytes from the gastropod mollusc, *Haliotis tuberculata*. Biology of the Cell, 86(1), pp.67–72.

Lee, K.-K., Liu, P.-C. & Huang, C.-Y., 2003. *Vibrio parahaemolyticus* infectious for both humans and edible mollusk abalone. Microbes and infection / Institut Pasteur, 5(6), pp.481–5.

Lee, M.-H. & Schedl, T., 2006. RNA-binding proteins. WormBook, ed. The C. elegans Research Community, WormBook.

Lee, S.M., Koh, H.-J., Park, D.-C., Song, B.J., Huh, T.-L., Park, J.-W., 2002. Cytosolic NADP +-dependent isocitrate dehydrogenase status modulates oxidative damage to cells. Free Radical Biology and Medicine, 32(11), pp.1185–1196.

Lee, S.Y., Lee, B.L. & Söderhäll, K., 2003. Processing of an antibacterial peptide from hemocyanin of the freshwater crayfish *Pacifastacus leniusculus*. The Journal of biological chemistry, 278(10), pp.7927–33.

Lee, Y., De Zoysa, M., Whang, I., Lee, S., Kim, Y., Oh, C., Choi, C.Y., Yeo, S.Y. & Lee, J., 2011. Molluscan death effector domain (DED)-containing caspase-8 gene from disk abalone (*Haliotis discus discus*): Molecular characterization and expression analysis. Fish and Shellfish Immunology, 30(2), pp.480–487.

Lei, K., Li, Fang., Zhang, M., Yang, H., Luo, T. & Xu, X., 2008. Difference between hemocyanin subunits from shrimp *Penaeus japonicus* in anti-WSSV defense. Developmental and comparative immunology, 32(7), pp.808–13.

Lemay,S., Lebedeva, T. V & Singh, A. J., 1999. Inhibition of cytokine gene expression by sodium salicylate in a macrophage cell line through an NF-κB-Independent Mechanism. Clinical Diagnostic Laboratory Immunology, 6(4): 567–572.

Li, H., Parisi, M.G., Parrinello, N., Cammarata, M. & Roch, P., 2011. Molluscan antimicrobial peptides, a review from activity-based evidences to computer-assisted sequences. Isj-Invertebrate Survival Journal, 8, pp.85–97.

Li, J., Chen, J., Zhang, Y. & Yu, Z., 2013. Expression of allograft inflammatory factor-1 (AIF-1) in response to bacterial challenge and tissue injury in the pearl oyster, *Pinctada martensii*. Fish & shellfish immunology, 34(1), pp.365–71.

Li, Y., Qin, J.G., Li, X. & Benkendorff, K., 2010. Assessment of metabolic and immune changes in postspawning Pacific oyster *Crassostrea gigas*: Identification of a critical period of vulnerability after spawning. Aquaculture Research, 41(9).

Li, Y., Qin, J.G., Abbott, C.A., Li, X. & Benkendorff, K., 2007a. Synergistic impacts of heat shock and spawning on the physiology and immune health of *Crassostrea gigas*: an explanation for summer mortality in Pacific oysters. American journal of physiology. Regulatory, integrative and comparative physiology, 293(6), pp.R2353–62.

Li, Z., Lin, Q., Chen, J., Wu, J.L., Lim, T.K., Loh, S.S., Tang, X. & Hew, C.-L., 2007b. Shotgun identification of the structural proteome of shrimp white spot syndrome virus and iTRAQ differentiation of envelope and nucleocapsid subproteomes. Molecular & cellular proteomics : MCP, 6(9), pp.1609–20.

Libby, P., 2007. Inflammatory Mechanisms : The Molecular Basis of Inflammation and Disease. Nutrition reviews, 65(12), pp. 140-146.

Lindstro, M.S. & Zhang, Y., 2008. Ribosomal Protein S9 Is a Novel B23 / NPM-binding Protein Required for Normal Cell Proliferation. The journal of biological chemistry, 283, pp.15568–15576.

Liu, C.-H., Tseng, M.-C. & Cheng, W., 2007. Identification and cloning of the antioxidant enzyme, glutathione peroxidase, of white shrimp, *Litopenaeus vannamei*, and its expression following *Vibrio alginolyticus* infection. Fish & shellfish immunology, 23, pp.34–45.

Liu, G., Ma, H., Jiang, L. & Zhao, Y., 2007. Allograft inflammatory factor-1 and its immune regulation. Autoimmunity, 40(March), pp.95–102.

Liu, P.C., Chen, Y.C. & Lee, K.K., 2001. Pathogenicity of *Vibrio alginolyticus* isolated from diseased small abalone *Haliotis diversicolor supertexta*. Microbios, 104(408), pp.71–7.

Liu, Y., Tam, N.F.Y., Guan, Y., Yasojima, M., Zhou, J., Gao, B., 2011. Acute toxicity of nonylphenols and bisphenol A to the embryonic development of the abalone *Haliotis diversicolor supertexta*. Ecotoxicology, 20(6), pp.1233–1245.

Lochmiller, R.L. & Deerenberg, C., 2000. Trade-Offs in Evolutionary Immunology: Just What Is the Cost of Immunity? Oikos, 88(1), pp.87–98.

Lopez-Cotes, L. Castro, D., Navas, J.I. & Borrego, J.J., 1999. Phagocytic and chemotactic responses of manila and carpet shell clam haemocytes against *Vibrio tapetis* , the causative agent of brown ring disease. Fish and Shellfish Immunology, 9, pp.543–555.

Lü, A., Hu, X., Wang, Y., Shen, X., Li, X., Zhu, A., Tian, J., Ming, Q. & Feng, Z., 2014. iTRAQ analysis of gill proteins from the zebrafish (*Danio rerio*) infected with *Aeromonas hydrophila*. Fish & shellfish immunology, 36(1), pp.229–39.

Luciani, M.F. & Chimini, G., 1996. The ATP binding cassette transporter ABC1, is required for the engulfment of corpses generated by apoptotic cell death. The EMBO journal, 15(2), pp.226–35.

Lundberg, E., Fagerberg, L., Klevebring, D., Matic, I., Geiger, T., Cox, J., Algenäs, C., Lundeberg, J., Mann, M. & Uhlen, M., 2010. Defining the transcriptome and proteome in three functionally different human cell lines. Molecular systems biology, 6(450), p.450.

Luzio, J.P., Pryor, P.R. & Bright, N.A., 2007. Lysosomes: fusion and function. Nature reviews. Molecular cell biology, 8(8), pp.622–32.

Ma, B., Zhang, K., Hendrie, C., Liang, C., Li, M., Doherty-Kirby, A. & Lajoie, G., 2003. PEAKS: powerful software for peptide de novo sequencing by tandem mass spectrometry. Rapid communications in mass spectrometry : RCM, 17(20), pp.2337–42.

Maeng, O., Kim, Y.C., Shin, H.-J., Lee, J.-O., Huh, T.-L., Kang, K.-i., Kim, Y. S., Paik, S.-G. & Lee, H., 2004. Cytosolic NADP(+)-dependent isocitrate dehydrogenase protects macrophages from LPS-induced nitric oxide and reactive oxygen species. Biochemical and biophysical research communications, 317(2), pp.558–64.

Malagoli, D., Franchini, A. & Ottaviani, E., 2000. Synergistic role of cAMP and IP(3) in corticotropin-releasing hormone-induced cell shape changes in invertebrate immunocytes. Peptides, 21(2), pp.175–82.

Maldonado-Aguayo, W., Lafarga-De la Cruz, F. & Gallardo-Escárate, C., 2015. Identification and expression of antioxidant and immune defense genes in the surf clam *Mesodesma donacium* challenged with Vibrio anguillarum. Marine Genomics, 19, pp.65–73.

Malham, S.K., Lacoste, A., Gélébart, F., Cueff, A. & Poulet, S.A., 2003. Evidence for a direct link between stress and immunity in the mollusc *Haliotis tuberculata*. Journal of experimental zoology. Part A, Comparative experimental biology, 295(2), pp.136–44.

Mallick, P. & Kuster, B., 2010. Proteomics: a pragmatic perspective. Nature biotechnology, 28(7), pp.695–709.

Manders, E.M., Verbeek, F. & Aten, J., 1993. Measurement of co-localization of objects in dual-colour confocal images. Journal of Microscopy, 169(3), pp.375–382.

Marie, B., Marie, A., Jackson, D.J., Dubost, L., Degnan, B.M., Milet, C. & Marin, F., 2010. Proteomic analysis of the organic matrix of the abalone *Haliotis asinina* calcified shell. Proteome Science, 8(1), p.54.

Marinissen, M.J. & Gutkind, J.S., 2001. G-protein-coupled receptors and signalling networks: Emerging paradigms. Trends in Pharmacological Sciences, 22(7), pp.368–376.

Marmaras, V.J. & Lampropoulou, M., 2009. Regulators and signalling in insect haemocyte immunity. Cellular signalling, 21(2), pp.186–95.

Martello, L.B. & Tjeerdema, R.S., 2001. Combined effects of pentachlorophenol and salinity stress on chemiluminescence activity in two species of abalone. Aquatic Toxicology, 51(3), pp.351–362.

Martyniuk, C.J., Alvarez, S. & Denslow, N.D., 2012. DIGE and iTRAQ as biomarker discovery tools in aquatic toxicology. Ecotoxicology and environmental safety, 76(2), pp.3–10.

Matés, J.M., 2000. Effects of antioxidant enzymes in the molecular control of reactive oxygen species toxicology. Toxicology, 153(1-3), pp.83–104.

Mavrouli, M.D., Tsakas, S., Theodorou, G.L., Lampropoulou, M. & Marmaras, V.J., 2005. MAP kinases mediate phagocytosis and melanization via prophenoloxidase activation in medfly hemocytes. Biochimica et Biophysica Acta (BBA) - Molecular Cell Research, 1744(2), pp.145–156.

May, R.C. & Machesky, L.M., 2001. Phagocytosis and the actin cytoskeleton. Journal of cell science, 114(Pt 6), pp.1061–77.

McDonagh, B. & Sheehan, D., 2006. Redox proteomics in the blue mussel *Mytilus edulis*: carbonylation is not a pre-requisite for ubiquitination in acute free radical-mediated oxidative stress. Aquatic toxicology (Amsterdam, Netherlands), 79(4), pp.325–33.

McDonagh, B., Tyther, R. & Sheehan, D., 2006. Redox proteomics in the mussel, *Mytilus edulis*. Marine environmental research, 62 Suppl, pp.S101–4.

Medzhitov, R., 2008. Origin and physiological roles of inflammation. Nature, 454(7203), pp.428–35.

Mehta, T.S., Zakharkin, S.O., Gadbury, G.L. & Allison, D.B., 2006. Epistemological issues in omics and high-dimensional biology: give the people what they want. Physiological genomics, 28(1), pp.24–32.

Meissner, F. & Mann, M., 2014. Quantitative shotgun proteomics: considerations for a high-quality workflow in immunology. Nature immunology, 15(2), pp.112–7.

Meng, Q., Hou, L., Zhao, Y., Huang, X., Huang, Y., Xia, S., Gu, W. & Wang, W., 2014. iTRAQ-based proteomic study of the effects of *Spiroplasma eriocheiris* on Chinese mitten crab *Eriocheir sinensis* hemocytes. Fish & shellfish immunology, 40(1), pp.182–9.

Meunier, B., Dumas, E., Piec, I., Béchet, D., Hébraud, M. & Hocquette, J.-F., 2007. Assessment of hierarchical clustering methodologies for proteomic data mining. Journal of proteome research, 6(1), pp.358–66.

Mialhe, E., Bachère, E., Boulo, V. & Cadoret, J.P., 1995. Strategy for research and international cooperation in marine invertebrate pathology, immunology and genetics. Aquaculture, 132(1-2), pp.33–41.

Michalak, M., Corbett, E.F., Mesaeli, N., Nakamura, K. & Opas, M., 1999. Calreticulin: one protein, one gene, many functions. The Biochemical journal, 344 Pt 2, pp.281–92.

Mishima, T., Iwabuchi, K., Fujii, S., Tanaka, S.-Y., Ogura, H., Watano-Miyata, K., Ishimori, N., Andoh, Y., Nakai, Y., Iwabuchi, C., Ato, M., Kitabatake, A., Tsutsui, H. & Onoé, K., 2008. Allograft inflammatory factor-1 augments macrophage phagocytotic activity and accelerates the progression of atherosclerosis in ApoE-/- mice. International journal of molecular medicine, 21(2), pp.181–7.

Mitta, G., Vandenbulcke, F. & Roch, P., 2000. Original involvement of antimicrobial peptides in mussel innate immunity. FEBS Letters, 486, pp.185–190.

Mogensen, T.H., 2009. Pathogen recognition and inflammatory signaling in innate immune defenses. Clinical microbiology reviews, 22(2), pp.240–73.

Molloy, M.P., Brzezinski, E.E., Hang, J., McDowell, M.T. & VanBogelen, R. A., 2003. Overcoming technical variation and biological variation in quantitative proteomics. Proteomics, 3(10), pp.1912–9.

Mortensen, S. & Glette, J., 1996. Phagocytic activity of scallop (*Pecten maximus*) haemocytes maintained in vitro. Fish & Shellfish Immunology, 6(2), pp.111–121.

Mouton, A. & Gummow, B., 2011. The occurrence of gut associated parasites in the South African abalone, *Haliotis midae*, in Western Cape aquaculture facilities. Aquaculture, 313(1-4), pp.1–6.

Muralidharan, S., Thompson, E., Raftos, D., Birch, G. & Haynes, P.A., 2012. Quantitative proteomics of heavy metal stress responses in Sydney rock oysters. Proteomics, 12(6), pp.906–21.

Murray, A.G. & Peeler, E.J., 2005. A framework for understanding the potential for emerging diseases in aquaculture. In Preventive Veterinary Medicine. pp. 223–235.

Nair, S. V., Del Valle, H., Gross, P.S., Terwilliger, D.P. & Smith, L.C., 2005. Macroarray analysis of coelomocyte gene expression in response to LPS in the sea urchin. Identification of unexpected immune diversity in an invertebrate. Physiological genomics, 22(1), pp.33–47.

Nappi, A.J. & Ottaviani, E., 2000. Cytotoxicity and cytotoxic molecules in invertebrates. BioEssays, 22, pp.469–480.

United Nations, department of economic and social affairs, population division, 2004. WORLD POPULATION TO 2300. UN Doc ST/ESA/SER.A/236.

Nicolas, J.L., Basuyaux, O., Mazurié, J. & Thébault, A., 2002. *Vibrio carchariae*, a pathogen of the abalone *Haliotis tuberculata*. Diseases of aquatic organisms, 50(1), pp.35–43.

Nimmerjahn, F. & Ravetch, J. V, 2008. Fcgamma receptors as regulators of immune responses. Nature reviews. Immunology, 8(1), pp.34–47.

Novas, A., Cao, A., Barcia, R. & Ramos-Martinez, J.I., 2004. Nitric oxide release by hemocytes of the mussel *Mytilus galloprovincialis* Lmk was provoked by interleukin-2 but not by lipopolysaccharide. The International Journal of Biochemistry & Cell Biology, 36(3), pp.390–394.

O'Neill, M., Gaume, B., Denis, F. & Auzoux-Bordenave, S., 2013. Expression of biomineralisation genes in tissues and cultured cells of the abalone *Haliotis tuberculata*. Cytotechnology, 65(5), pp.737–47.

Obeid, M., Panaretakis, T., Tesniere, A., Joza, N., Tufi, R., Apetoh, L., Ghiringhelli, F., Zitvogel, L. & Kroemer, G., 2007. Leveraging the immune system during chemotherapy: Moving calreticulin to the cell surface converts apoptotic death from "silent" to immunogenic. Cancer Research, 67(17), pp.7941–7944.

Oberg, A.L., Mahoney, D.W., Eckel-passow, J.E., Malone, C.J., Wolfinger, R.D., Hill, E.G., Cooper, L.T., Onuma, O.K., Spiro, C., Therneau, T.M., Bergen, H.R. & Iii, O., 2008. Statistical Analysis of Relative Labelled Mass Spectrometry Data from Complex Samples Using ANOVA research articles. Journal of Proteome Research, pp.225–233.

Oh, E.-S., Woods, A. & Couchman, J.R., 1997. Multimerization of the Cytoplasmic Domain of Syndecan-4 Is Required for Its Ability to Activate Protein Kinase C. Journal of Biological Chemistry, 272(18), pp.11805–11811.

Ohsawa, K., Imai, Y., Kanazawa, H., Sasaki, Y. & Kohsaka, S., 2000. Involvement of Iba1 in membrane ruffling and phagocytosis of macrophages/microglia. Journal of cell science, 113 (Pt 1, pp.3073–84.

Otero-González, A.J., Magalhães, B.S., Garcia-Villarino, M., López-Abarrategui, C., Sousa, D.A., Dias, S.C. & Franco, O.L., 2010. Antimicrobial peptides from marine invertebrates as a new frontier for microbial infection control. The FASEB journal : official publication of the Federation of American Societies for Experimental Biology, 24, pp.1320–1334.

Ottaviani, E., Franchini, A., Malagoli, D. & Genedani, S., 2000. Immunomodulation by recombinant human interleukin-8 and its signal transduction pathways in invertebrate hemocytes. Cellular and molecular life sciences : CMLS, 57(3), pp.506–13.

Ottaviani, E., Caselgrandi, E. & Franceschi, C., 1995. Cytokines and evolution: in vitro effects of IL-1 alpha, IL-1 beta, TNF-alpha and TNF-beta on an ancestral type of stress response. Biochemical and biophysical research communications, 207(1), pp.288–292.

Ottaviani, E., Caselgrandi, E. & Kletsas, D., 1998. The CRH-ACTH-biogenic amine axis in invertebrate immunocytes activated by PDGF and TGF-β. FEBS Letters, 427, pp.255–258.

Ottaviani, E. & Franceschi, C., 1998. A new theory on the common evolutionary origin of natural immunity, inflammation and stress response: the invertebrate phagocytic immunocyte as an eye-witness. Domestic animal endocrinology, 15(5), pp.291–6.

Ottaviani, E. & Franceschi, C., 1997. The invertebrate phagocytic immunocyte: Clues to a common evolution of immune and neuroendocrine systems. Immunology Today, 18, pp.169–174.

Ottaviani, E. & Franceschi, C., 1996. The neuroimmunology of stress from invertebrates to man. Progress in Neurobiology, 48, pp.421–440.

Ottaviani, E., Malagoli, D. & Franceschi, C., 2007. Common evolutionary origin of the immune and neuroendocrine systems: from morphological and functional evidence to in silico approaches. Trends in immunology, 28(11), pp.497–502.

Ow, S.Y., Salim, M., Noirel, J., Evans, C., Rehman, I. & Wright, P.C., 2009. iTRAQ Underestimation in Simple and Complex Mixtures : " The Good , the Bad and the Ugly " research articles. Journal of Proteome Research, pp.5347–5355.

Ow, S.Y., Salim, M., Noirel, J., Evans, C. & Wright, P.C., 2011. Minimising iTRAQ ratio compression through understanding LC-MS elution dependence and high-resolution HILIC fractionation. Proteomics, 11(11), pp.2341–6.

Paillard, C., Le Roux, F. & Borrego, J.J., 2004. Bacterial disease in marine bivalves, a review of recent studies: Trends and evolution. Aquatic Living Resources, 17(4), pp.477–498.

Palmer, M.R., Mcdowall, M.H., Stewart, L., Ouaddi, A., Maccoss, M.J. & Swanson, W. J., 2013. Mass spectrometry and next-generation sequencing reveal an abundant and rapidly evolving abalone sperm protein. Molecular Reproduction and Development, 80(6), pp.460–465.

Palumbo, A., 2005. Nitric oxide in marine invertebrates: a comparative perspective. Comparative biochemistry and physiology. Part A, Molecular & integrative physiology, 142(2), pp.241–8.

Pan, F., Ye, Z., Cheng, L. & Liu, J.O., 2004. Myocyte enhancer factor 2 mediates calcium-dependent transcription of the interleukin-2 gene in T lymphocytes: a calcium signalling module that is distinct from but collaborates with the nuclear factor of

activated T cells (NFAT). The Journal of biological chemistry, 279(15), pp.14477–80.

Pan, Z.-C., He, J.-G., Weng, S.-P., Yin, Z.-X., Fu, X.-Z. & Li, S.-D., 2008. Changes in mortality and immunological variables of *Litopenaeus vannamei* parents and their filial families infected with white spot syndrome under different experimental conditions. Fish & shellfish immunology, 25(5), pp.459–71.

Panaretakis, T., Kepp, O., Brockmeier, U., Tesniere, A., Bjorklund, A.-C.,Chapman, D.C., Durchschlag, M., Joza, N., Pierron, G., van Endert, P., Yuan, J., Zitvogel, L., Madeo, F., Williams, D.B. & Kroemer, G., 2009. Mechanisms of pre-apoptotic calreticulin exposure in immunogenic cell death. The EMBO journal, 28(5), pp.578–590.

Pang, Z., Kim, S.-K., Yu, J. & Jang, I.-K., 2014. Distinct regulation patterns of the two prophenoloxidase activating enzymes corresponding to bacteria challenge and their compensatory over expression feature in white shrimp (*Litopenaeus vannamei*). Fish & shellfish immunology, 39(2), pp.158–67.

Pipe, R. & Coles, J., 1995. Environmental contaminants influencing immune function in marine bivalve molluscs. Fish & Shellfish Immunology, 5(8), pp.581–595.

Pitcher, G.C., Franco, J.M., Doucette, G.J., Powell, C.L. & Mouton, A., 2001. Paralytic shellfish poisoning in the abalone *Haliotis midae* on the West Coast of South Africa. Journal of Shellfish Research, 20(2), pp.895–904.

Plows, L.D., Cook, R.T., Davies, A.J. & Walker, A.J., 2004. Activation of extracellular-signal regulated kinase is required for phagocytosis by *Lymnaea stagnalis* haemocytes. Biochimica et biophysica acta, 1692(1), pp.25–33.

Plows, L.D., Cook, R.T., Davies, A.J. & Walker, A.J., 2006. Phagocytosis by *Lymnaea stagnalis* haemocytes: a potential role for phosphatidylinositol 3-kinase but not protein kinase A. Journal of invertebrate pathology, 91(1), pp.74–7.

Pontén, F., Gry, M., Fagerberg, L., Lundberg, E., Asplund, A., Berglund, L., Oksvold, P., Björling, E., Hober, S., Kampf, C., Navani, S., Nilsson, P., Ottosson, J., Persson, A., Wernérus, H., Wester, K. & Uhlén, M., 2009. A global view of protein expression in human cells, tissues, and organs. Molecular systems biology, 5(337), p.337.

Poteryaev, D., Fares, H., Bowerman, B. & Spang, A., 2007. *Caenorhabditis elegans* SAND-1 is essential for RAB-7 function in endosomal traffic. The EMBO journal, 26(2), pp.301–12.

Racioppi, L. et al., 2012. Calcium / Calmodulin-dependent Protein Kinase Kinase 2 Regulates Macrophage-mediated Inflammatory Responses. Journal of Biological Chemistry, 287(14), pp.11579–11591.

Racioppi, L. & Means, A.R., 2012. Calcium / Calmodulin-dependent Protein Kinase Kinase 2 : Roles in Signalling and Pathophysiology. Journal of Biological Chemistry, 287(38), pp.31658–31665.

Racioppi, L. & Means, A.R., 2008. Calcium/calmodulin-dependent kinase IV in immune and inflammatory responses: novel routes for an ancient traveller. Trends in immunology, 29(12), pp.600–7.

Raemaekers, S., Hauck, M., Bürgener, M., Mackenzie, A., Maharaj, G., Plagányi, É.E. & Britz, P.J., 2011. Review of the causes of the rise of the illegal South African abalone fishery and consequent closure of the rights-based fishery. Ocean and Coastal Management, 54(6), pp.433–445.

Regulski, M. & Tully, T., 1995. Molecular and biochemical characterization of dNOS: a *Drosophila* Ca^{2+}/calmodulin-dependent nitric oxide synthase. Proceedings of the National Academy of Sciences of the United States of America, 92, pp.9072–9076.

Ren, H.-L., Xu, D.-D., Gopalakrishnan, S., Qiao, K., Huang, W.-B. & Wang, K.-J., 2009. Gene cloning of a sigma class glutathione S-transferase from abalone (*Haliotis diversicolor*) and expression analysis upon bacterial challenge. Developmental and comparative immunology, 33(9), pp.980–90.

Rho, S.-C., You, S.-Y., Kim, Y.-S. & Hwang, D.-H., 2008. From proteomics toward systems biology: integration of different types of proteomics data into network models. BMB Reports, 41(3), pp.184–193.

Ridley, S.H., Dean, J.L.E., Sarsfield, S.J., Brook, M., Clark, A.R. & Saklatvala, J., 1998. A p38 MAP kinase inhibitor regulates stability of interleukin-1-induced cyclooxygenase-2 mRNA. FEBS Letters, 439, pp.75–80.

Rinkevich, B., 2005. Marine invertebrate cell cultures: new millennium trends. Marine biotechnology (New York, N.Y.), 7(5), pp.429–39.

Rivero, A., 2006. Nitric oxide: an antiparasitic molecule of invertebrates. Trends in Parasitology, 22(5), pp.219–225.

Rodrigues, P.M., Silva, T., Dias, J. & Jessen, F., 2012. PROTEOMICS in aquaculture: applications and trends. Journal of proteomics, 75(14), pp.4325–45.

Roux, P.P. & Blenis, J., 2004. ERK and p38 MAPK-Activated Protein Kinases : a Family of Protein Kinases with Diverse Biological Functions. Microbiology and molecular biology reviews : MMBR, 68(2), pp.320–344.

Rudin, C.M. & Thompson, C.B., 1997. Apoptosis and disease: regulation and clinical relevance of programmed cell death. Annual review of medicine, 48, pp.267–281.

Rufino-Palomares, E. Reyes-Zurita, F., Fuentes-Almagro, C.A., de la Higuera, M., Lupiáñez, J.A. & Peragón., 2011. Proteomics in the liver of gilthead sea bream (*Sparus aurata*) to elucidate the cellular response induced by the intake of maslinic acid. Proteomics, 11(16), pp.3312–25.

Sabidó, E., Selevsek, N. & Aebersold, R., 2011. Mass spectrometry-based proteomics for systems biology. Current opinion in biotechnology, 23, pp.1–7.

Sahaphong, S., Linthong, V., Wanichanon, C., Riengrojpitak, S., Kangwanrangsan, N., Viyanant, V., Upatham, E. S., Pumthong, T., Chansue, N., Sobhon, P. & Cook, P. A., 2001. Morphofunctional study of the hemocytes of *Haliotis asinina*. Journal of shellfish research, 20 (2), pp. 711–716.

Sales, J. & Britz, P.J., 2001. Research on abalone (*Haliotis midae L.*) cultivation in South Africa. Aquaculture Research, 32(11), pp.863–874.

Salzet, M., 2000. Invertebrate molecular neuroimmune processes. Brain Research Reviews, 34, pp.69–79.

Savitski, M.M., Mathieson, T., Zinn, N., Sweetman, G., Doce, C., Becher, I., Pachl, F., Kuster, B. & Bantsche, M., 2013. Measuring and Managing Ratio Compression for Accurate iTRAQ/ TMT Quantification. Journal of proteome research, 12, pp.3586-3598.

Sawabe, T., Inoue, S., Fukui, Y., Yoshie, K., Nishihara, Y. & Miura, H., 2007. Mass mortalities of Japanese abalone *Haliotis discus hannai* caused by *Vibrio harveyi* infection. Microbes and environment, 22(3), pp.300–308.

Schiess, R., Wollscheid, B. & Aebersold, R., 2009. Targeted proteomic strategy for clinical biomarker discovery. Molecular oncology, 3(1), pp.33–44.

Schwarz, S., Kehrenberg, C. & Walsh, T.R., 2001. Use of antimicrobial agents in veterinary medicine and food animal production. International journal of antimicrobial agents, 17(6), pp.431–7.

Seastone, D.J., Zhang, L., Buczynski, G., Rebstein, P., Weeks, G., Spiegelman, G. & Cardelli, J., 1999. The small Mr Ras-like GTPase Rap1 and the phospholipase C pathway act to regulate phagocytosis in *Dictyostelium discoideum*. Molecular biology of the cell, 10(2), pp.393–406.

Seger, R. & Krebs, E.G., 1995. The MAPK signaling cascade. FASEB journal : official publication of the Federation of American Societies for Experimental Biology, 9, pp.726–35.

Shevchenko, A., Sunyaev, S., Loboda, A., Bork, P., Ens, W. & Standing, K G., 2001. Charting the proteomes of organisms with unsequenced genomes by MALDI-quadrupole time-of-flight mass spectrometry and BLAST homology searching. Analytical chemistry, 73(9), pp.1917–26.

Shiel, B.P. Hall, N.E., Cooke, I.R., Robinson, N.A. & Strugnell, J.M., 2014. De Novo Characterisation of the Greenlip Abalone Transcriptome (*Haliotis laevigata*) with a Focus on the Heat Shock Protein 70 (HSP70) Family. Marine Biotechnology, 70, pp.23–32.

Siddiqui, N.I., Akosung, R.F. & Gielens, C., 2006. Location of intrinsic and inducible phenoloxidase activity in molluscan hemocyanin. Biochemical and biophysical research communications, 348(3), pp.1138–44.

Sindermann, C.J., 1984. Disease in marine aquaculture. Helgoländer Meeresuntersuchungen, 37(1-4), pp.505–530.

Sirover, M.A., 1999. New insights into an old protein: the functional diversity of mammalian glyceraldehyde-3-phosphate dehydrogenase. Biochimica et biophysica acta, 1432, pp.159–184.

Slattery, M. et al., 2012. Marine Proteomics: A Critical Assessment of an Emerging Technology. Journal of natural products, 75 (10), pp 1833–1877.

Smoot, M.E. et al., 2011. Cytoscape 2.8: new features for data integration and network visualization. Bioinformatics (Oxford, England), 27(3), pp.431–2.

Snyder, M.J., Girvetz, E. & Mulder, E.P., 2001. Induction of marine mollusc stress proteins by chemical or physical stress. Archives of environmental contamination and toxicology, 41(1), pp.22–9.

Soderhall, K., 1999. Cell adhesion molecules and antioxidative enzymes in a crustacean, possible role in immunity. Aquaculture, 172, pp.111–123.

Soderling, T.R., 1999. The Ca-calmodulin-dependent protein kinase cascade. Trends in biochemical sciences, 24(2), pp.232–236.

Sokolova, I., 2009. Apoptosis in molluscan immune defense. Invertebrate Survival Journal, 6, pp.49–58.

Somboonwiwat, K., Chaikeeratisak, V., Wang, H.-C., Fang Lo, C. & Tassanakajon, A., 2010. Proteomic analysis of differentially expressed proteins in *Penaeus monodon* hemocytes after *Vibrio harveyi* infection. Proteome science, 8, p.39.

Song, X., Bandow, J., Sherman, J., Baker, J.D., Brown, P.W., Mcdowell, M.T. & Molloy, M.P., 2008. iTRAQ Experimental Design for Plasma Biomarker Discovery research articles. Journal of Proteome Research, pp.2952–2958.

Song, Y.-L., Yu, C.-I., Lien, T.-W., Huang, C.-C. & Lin, M.-N., 2003. Haemolymph parameters of Pacific white shrimp (*Litopenaeus vannamei*) infected with Taura syndrome virus. Fish & Shellfish Immunology, 14(4), pp.317–331.

Sossin, W.S. & Abrams, T.W., 2009. Evolutionary conservation of the signaling proteins upstream of cyclic AMP-dependent kinase and protein kinase C in gastropod mollusks. Brain, behavior and evolution, 74(3), pp.191–205.

Sperstad, S. V., Haug, T., Blencke, H.M., Styrvold, O.B., Li, C. & Stensvåg, K., 2011. Antimicrobial peptides from marine invertebrates: Challenges and perspectives in marine antimicrobial peptide discovery. Biotechnology Advances, 29(5), pp.519–530.

Standing, K., 2003. Peptide and protein de novo sequencing by mass spectrometry. Current Opinion in Structural Biology, 13(5), pp.595–601.

Steen, I.H., Madern, D., Karlström, M., Lien, T., Ladenstein, R. & Birkeland, N.K., 2001. Comparison of isocitrate dehydrogenase from three hyperthermophiles reveals differences in thermostability, cofactor specificity, oligomeric state, and phylogenetic affiliation. The Journal of biological chemistry, 276(47), pp.43924–31.

Stefano, G.B., Cadet, P. & Scharrer, B., 1989. Stimulatory effects of opioid neuropeptides on locomotory activity and conformational changes in invertebrate and human immunocytes: evidence for a subtype of delta receptor. Proceedings of the National Academy of Sciences of the United States of America, 86, pp.6307–6311.

Stone, D. A. J., Bansemer, M. S., , Lange, B., Schaefer, E. N., Howarth, G. S., Harris, J. O., 2014. Dietary intervention improves the survival of cultured greenlip abalone (Haliotis laevigata Donovan) at high water temperature. Journal of Aquaculture, Volume 430, 230–240.

Stone, D. A. J., Harris, J. O., Wang, H., Mercer, G. J., Schaefer, E. N. & Bansemer, M. S., 2013. Dietary protein level and water temperature interactions for greenlip abalone Haliotis laevigata. Journal of Shellfish Research, 32(1):119-130.

Stuart, L.M. & Ezekowitz, R.A.B., 2005. Phagocytosis: elegant complexity. Immunity, 22(5), pp.539–50.

Suja, C.P. & Dharmaraj, S., 2005. In vitro culture of mantle tissue of the abalone *Haliotis varia Linnaeus*. Tissue & cell, 37(1), pp.1–10.

Sun, H.Q., Yamamoto, M., Yin, H.L. & Mejillano, M., 1999. Gelsolin, a multifunctional actin regulatory protein. The journal of biological chemistry, 274 (47), pp.33179-33182.

Supek, F., Bošnjak, M., Škunca, N. & Šmuc, T., 2011. REVIGO summarizes and visualizes long lists of gene ontology terms. PloS one, 6(7), p.e21800.

Swanson, J.A. & Hoppe, A.D., 2004. The coordination of signalling during Fc receptor-mediated phagocytosis. Journal of leukocyte biology, 76, pp.1093–1103.

Tahon, J.P., Gielens, C., Vinckier, C., Witters, R., De Ley, M., Préaux, G. & Lontie, R., 1989. The reaction of nitrogen monoxide with the haemocyanins of the crayfish *Astacus leptodactylus* and the snail *Helix pomatia*. The Biochemical journal, 262, pp.253–260.

Tiscar, P.G. & Mosca, F., 2004. Defense mechanisms in farmed marine molluscs. Veterinary research communications, 28 Suppl 1, pp.57–62.

Tomanek, L., 2011. Environmental Proteomics: Changes in the Proteome of Marine Organisms in Response to Environmental Stress, Pollutants, Infection, Symbiosis, and Development. Annual Review of Marine Science, 3(1), pp.373–399.

Tomanek, L., 2014. Proteomics to study adaptations in marine organisms to environmental stress. Journal of proteomics, 105C, pp.92–106.

Torreilles, J., Guérin, M.C. & Roch, P., 1996. Reactive oxygen species and defense mechanisms in marine bivalves. Comptes rendus de l'Académie des sciences. Série III, Sciences de la vie, 319(3), pp.209–18.

Torres, J. & Wilson, M.T., 1999. The reactions of copper proteins with nitric oxide. Biochimica et Biophysica Acta - Bioenergetics, 1411, pp.310–322.

Torres, M.A., Jones, J.D.G. & Dangl, J.L., 2006. Reactive Oxygen Species Signalling in Response to Pathogens 1. Plant physiology, 141, pp.373–378.

TranVan Nhieu, G., Clair, C., Grompone, G. & Sansonetti, P., 2004. Calcium signalling during cell interactions with bacterial pathogens. Biology of the cell, 96(1), pp.93–101.

Travers, M.-A., Meistertzheim, A.-L., Cardinaud, M., Friedman, C.S., Huchette, S., Moraga, D. & Paillard, C., 2010. Gene expression patterns of abalone, *Haliotis tuberculata*, during successive infections by the pathogen *Vibrio harveyi*. Journal of invertebrate pathology, 105(3), pp.289–97.

Travers, M.-A., Mirella da Silva, P., Le Goïc, N., Marie, D., Donval, A., Huchette, S., Koken, M. & Paillard, C., 2008. Morphologic, cytometric and functional characterisation of abalone (*Haliotis tuberculata*) haemocytes. Fish & shellfish immunology, 24(4), pp.400–11.

Travers, M.-A., Le Bouffant, R., Friedman, C.S., Buzin, F., Cougard, B., Huchette, S., Koken, M. & Paillard, C., 2009. Pathogenic *Vibrio harveyi*, in contrast to non-pathogenic strains, intervenes with the p38 MAPK pathway to avoid an abalone haemocyte immune response. Journal of cellular biochemistry, 106(1), pp.152–60.

Travers, M.-A., Le Goïc, N., Huchette, S., Koken, M. & Paillard, C., 2008. Summer immune depression associated with increased susceptibility of the European abalone, *Haliotis tuberculata* to *Vibrio harveyi* infection. Fish & shellfish immunology, 25(6), pp.800–8.

Troell, M., Robertson-Andersson, D., Anderson, R., Bolton, J., Maneveldt, G., Halling, C. & Probyn, T., 2006. Abalone farming in South Africa: An overview with perspectives on kelp resources, abalone feed, potential for on-farm seaweed production and socio-economic importance. Aquaculture, 257(1-4), pp.266–281.

Unwin, R.D., Smith, D.L., Blinco, D., Wilson, C.L., Miller, C.J., Evans, C.A., Jaworska, E., Baldwin, S.A., Barnes, K., Pierce, A., Spooncer, E. & Whetton, A.D., 2006. Quantitative proteomics reveals posttranslational control as a regulatory factor in primary hematopoietic stem cells. , 107(12), pp.4687–4694.

Utans, U., Arceci, R.J., Yamashita, Y., Russell, M.E., 1995. Cloning and characterization of allograft inflammatory factor-1: a novel macrophage factor identified in rat cardiac allografts with chronic rejection. The Journal of clinical investigation, 95(6), pp.2954–62.

De Vico, G. & Carella, F., 2012. Morphological features of the inflammatory response in molluscs. Research in veterinary science, 93(3), pp.1109–15.

Villena, A.J., 2003. Applications and needs of fish and shellfish cell culture for disease control in aquaculture. Reviews in fish biology and fisheries, 13, pp.111–140.

De Vries, L., Zheng, B., Fischer, T., Elenko, E. & Farquhar, M.G., 2000. The regulator of G protein signaling family. Annual review of pharmacology and toxicology, 40(1), pp.235–71.

Walker, A.J. & Plows, L.D., 2003. Bacterial lipopolysaccharide modulates Protein Kinase C signalling in *Lymnaea stagnalis* haemocytes. Biology of the Cell, 95(8), pp.527–533.

Wan, Q., Whang, I. & Lee, J., 2008. Comparative Biochemistry and Physiology, Part B Molecular characterization of mu class glutathione-S-transferase from disk abalone (*Haliotis discus discus*), a potential biomarker of endocrine-disrupting chemicals. Construction, 150, pp.187–199.

Wang, H.-C., Leu, J.-H., Kou, G.-H., Wang, A. H.-J. & Lo, C.-F., 2007. Protein expression profiling of the shrimp cellular response to white spot syndrome virus infection. Developmental and comparative immunology, 31(7), pp.672–686.

Wang, J., Zhang, H., Wang, L., Qui, L., Yue, F., Yang, C. & Song, L., 2013. Molecular cloning and transcriptional regulation of an allograft inflammatory factor-1 (AIF-1) in Zhikong scallop *Chlamys farreri*. Gene, 530(2), pp.178–84.

Wang, K.-J., Ren, H.-L., Xu, D.-D., Cai., L. & Yang, M., 2008. Identification of the up-regulated expression genes in hemocytes of variously colored abalone (*Haliotis diversicolor* Reeve, 1846) challenged with bacteria. Developmental and comparative immunology, 32(11), pp.1326–47.

Wang, S., Peatman, E., Liu, H., Bushek, D., Ford, S.E., Kucuktas, H., Quilang, J., Li, P., Wallace, R., Wang, W., Guo, X. & Liu, Z., 2010. Microarray analysis of gene expression in eastern oyster (*Crassostrea virginica*) reveals a novel combination of antimicrobial and oxidative stress host responses after dermo (*Perkinsus marinus*) challenge. Fish & shellfish immunology, 29(6), pp.921–9.

Warren, C.M., Geenen, D.L., Helseth, D.L., Xu, H. & Solaro, R.J., 2010. Sub-proteomic fractionation, iTRAQ, and OFFGEL-LC-MS/MS approaches to cardiac proteomics. Journal of proteomics, 73(8), pp.1551–61.

Watano K., Iwabuchi, K., Fujii, S., Ishimori, N., Mitsuhashi, S., Ato, M., Kitabatake, A. & Onoé, K., 2001. Allograft inflammatory factor-1 augments production of interleukin-6, -10 and -12 by a mouse macrophage line. Journal of Immunology, 104(3):307-16.

Welter, B.H., Laughlin, R.C. & Temesvari, L. A, 2002. Characterization of a Rab7-like GTPase, EhRab7: a marker for the early stages of endocytosis in *Entamoeba histolytica*. Molecular and biochemical parasitology, 121(2), pp.254–64.

Wenner, B.R. & Lynn, B.C., 2004. Factors that affect ion trap data-dependent MS/MS in proteomics. Journal of the American Society for Mass Spectrometry, 15(2), pp.150–7.

Wilson, M.R., 1998. Apoptotic signal transduction: emerging pathways. Biochemistry and cell biology, 76(4), pp.573–582.

De Winter, P., Rayne, R.C. & Coast, G.M., 2007. The effects of intracellular signalling pathway inhibitors on phagocytosis by haemocytes of *Manduca sexta*. Journal of insect physiology, 53(10), pp.975–82.

Wiśniewski, J.R., Zougman, A., Nagaraj, N. & Mann, M., 2009. Universal sample preparation method for proteome analysis. Nature methods, 6(5), pp.359–62.

Woolner, S. & Bement, W.M., 2009. Unconventional myosins acting unconventionally. Trends in cell biology, 19(6), pp.245–52.

Wright, P.C., Noirel, J., Ow, S.-Y. & Fazeli, A., 2012. A review of current proteomics technologies with a survey on their widespread use in reproductive biology investigations. Theriogenology, 77(4), pp.738–765.e52.

Wu, J., Lin, Q., Lim, T.K., Liu, T. & Hiu, C.-L., 2007. White spot syndrome virus proteins and differentially expressed host proteins identified in shrimp epithelium by shotgun proteomics and cleavable isotope-coded affinity tag. Journal of virology, 81(21), pp.11681–11689.

Wu, W.W., Wang, G., Baek, S.J. & Shen, R.-F., 2006. Comparative Study of Three Proteomic Quantitative Methods , DIGE , cICAT , and iTRAQ , Using 2D Gel- or LC - MALDI TOF / TOF. Journal of proteome research, 5, pp.651–658.

Xu, C. & Ma, B., 2006. Software for computational peptide identification from MS-MS data. Drug discovery today, 11(13-14), pp.595–600.

Xu, T., Xi, J., Zhu, B., Liu, X. & Wu, X., 2014. Allograft inflammatory factor 1 functions as a pro-inflammatory cytokine in the oyster, *Crassostrea ariakensis*. PloS one, 9(4), p.e95859.

Yang, C., He, Z. & Yu, W., 2009. Comparison of public peak detection algorithms for MALDI mass spectrometry data analysis. BMC bioinformatics, 10, p.4.

Yang, H., Zheng, Q.-Y., Li, E.-Q., Zhu, S.-G. & Zhou, X.-W., 2004. Molecular cloning, expression and characterization of glutathione S-transferase from *Mytilus edulis*. Comparative biochemistry and physiology. Part B, Biochemistry & molecular biology, 139(2), pp.175–82.

Yang, Z.F., Ho, D.W., Lau, C.K., Lam, C.T., Lum, C.T., Poon, R.T.P. & Fan, S.T., 2005. Allograft inflammatory factor-1 (AIF-1) is crucial for the survival and pro-inflammatory activity of macrophages. International immunology, 17(11), pp.1391–7.

Yates, J.R., Ruse, C.I. & Nakorchevsky, A., 2009. Proteomics by mass spectrometry: approaches, advances, and applications. Annual review of biomedical engineering, 11(c), pp.49–79.

Ydrenius, L. Majeed, M., Rasmusson, B.J., Stendahl, O. & Särndahl, E., 2000. Activation of cAMP-dependent protein kinase is necessary for actin rearrangements in human neutrophils during phagocytosis. Journal of leukocyte biology, 67(4), pp.520–528.

Yoon, J.C. Puigserver, P., Chen, G., Donovan, J., Wu, Z., Rhee, J., Adelmant, G., Stafford, J., Kahn, C.R., Granner, D.K., Newgard, C.B. & Spiegelman, B.M., 2001. Control of hepatic gluconeogenesis through the transcriptional coactivator PGC-1. Nature, 413(6852), pp.131–8.

Yuan, A, Siu, C.H. & Chia, C.P., 2001. Calcium requirement for efficient phagocytosis by *Dictyostelium discoideum*. Cell calcium, 29(4), pp.229–238.

Zak, D.E., Tam, V.C. & Aderem, A., 2014. Systems-level analysis of innate immunity. Annual review of immunology, 32, pp.547–77.

Zelck, U.E., Gege, B.E. & Schmid, S., 2007. Specific inhibitors of mitogen-activated protein kinase and PI3-K pathways impair immune responses by hemocytes of trematode intermediate host snails. Developmental and comparative immunology, 31(4), pp.321–31.

Zhang, J., Xin, L., Shan, B., Chen, W., Xie, M., Yuen, D., Zhang, W., Zhang, Z., Lajoie, G. & Ma, B., 2012. PEAKS DB: de novo sequencing assisted database search for sensitive and accurate peptide identification. Molecular & cellular proteomics : MCP, 11(4), p.M111.010587.

Zhang, J., Li, F., Jiang, H., Yu, Y., Liu, C., Li, S., Wang, B. &Xiang, J., 2010. Proteomic analysis of differentially expressed proteins in lymphoid organ of *Fenneropenaeus chinensis* response to *Vibrio anguillarum* stimulation. Fish and Shellfish Immunology, 29(2), pp.186–194.

Zhang, L., Zhao, J., Li, C., Su, X., Chen, A., Li, T. & Qin, S., 2011. Cloning and characterization of allograft inflammatory factor-1 (AIF-1) from Manila clam *Venerupis philippinarum*. Fish & shellfish immunology, 30(1), pp.148–53.

Zhang, P., Li, C., Zhang, P., Jin, C., Pan, D. & Bao, Y., 2014. ITRAQ-based proteomics reveals novel members involved in pathogen challenge in sea cucumber *Apostichopus japonicus*. PLoS ONE, 9(6), p.e100492.

Zhang, P., Liu, B., Kang, S.W., Seo, M.S., Rhee, S.G. & Obeid, L.M., 1997. Thioredoxin peroxidase is a novel inhibitor of apoptosis with a mechanism distinct from that of Bcl-2. Journal of Biological Chemistry, 272, pp.30615–30618.

Zhang, X., Guo, L., Collage, R.D., Stripay, J.L., Tsung, A., Lee, J.S. & Rosengart, M.R., 2011. Calcium/calmodulin-dependent protein kinase (CaMK) Ialpha mediates the macrophage inflammatory response to sepsis. Journal of leukocyte biology, 90(2), pp.249–61.

Zhang, Y., Li, J., Yu, F., He, X. & Yu, Z., 2013. Allograft inflammatory factor-1 stimulates hemocyte immune activation by enhancing phagocytosis and expression of inflammatory cytokines in *Crassostrea gigas.* Fish and Shellfish Immunology, 34(5), pp.1071–1077.

Zhang, Y., Wang, S. & Peng, X., 2004. Identification of a type of human IgG-like protein in shrimp *Penaeus vannamei* by mass spectrometry. Journal of Experimental Marine Biology and Ecology, 301(1), pp.39–54.

Zhang, Y.L. & Dong, C., 2005. MAP kinases in immune responses. Cellular & molecular immunology, 2(1), pp.20–27.

Zhao, L. & Jones, W.A., 2012. Expression of heat shock protein genes in insect stress responses. Invertebrate Survival Journal, 9, pp.93–101.

Zhao, Y.-Y., Yan, D.-J. & Chen, Z.-W., 2013. Role of AIF-1 in the regulation of inflammatory activation and diverse disease processes. Cellular immunology, 284(1-2), pp.75–83.

Zhou, J., Cai, Z.-H., Li, L., Gao, Y.-F. & Hutchison, T.H., 2010. A proteomics based approach to assessing the toxicity of bisphenol A and diallyl phthalate to the abalone (*Haliotis diversicolor supertexta*). Chemosphere, 79(5), pp.595–604.

Zhu, B. & Wu, X., 2008. Characterization and function of CREB homologue from *Crassostrea ariakensis* stimulated by rickettsia-like organism. Developmental and comparative immunology, 32(12), pp.1572–81.

Zhuang, J. Coates, C.J., Zhu, H., Zhu, P., Wu, Z. & Xie, L., 2015. Identification of candidate antimicrobial peptides derived from abalone hemocyanin. Developmental & Comparative Immunology, 49(1), pp.96–102.

Zieske, L.R., 2006. A perspective on the use of iTRAQ reagent technology for protein complex and profiling studies. Journal of experimental botany, 57(7), pp.1501–8.

Zinchuk, V. & Zinchuk, O., 2008. Quantitative colocalization analysis of confocal fluorescence microscopy images. Current protocols in cell biology. 39:4.19:4.19.1–4.19.16

De Zoysa, M., Nikapitiya, C., Moon, D.O., Whang, I., Kim, G.I. & Lee, J., 2009a. A novel Fas ligand in mollusk abalone: Molecular characterization, immune responses and biological activity of the recombinant protein. Fish and Shellfish Immunology, 27, pp.423–432.

De Zoysa, M., Nikapitiya, C., Whang, I., Lee, J. & Lee, J., 2009b. Abhisin: a potential antimicrobial peptide derived from histone H2A of disk abalone (*Haliotis discus discus*). Fish & shellfish immunology, 27(5), pp.639–46.

De Zoysa, M., Jung, S. & Lee, J., 2009c. First molluscan TNF-α homologue of the TNF superfamily in disk abalone: Molecular characterization and expression analysis. Fish and Shellfish Immunology, 26, pp.625–631.

De Zoysa, M., Nikapitiya, C., Kim, Y., Oh, C., Kang, D., Whang, I., Kim, S., Lee, J. J., Choi, C. Y. & Lee, J. J., 2010a. Allograft inflammatory factor-1 in disk abalone *(Haliotis discus discus*): Molecular cloning, transcriptional regulation against immune challenge and tissue injury.pdf. Fish & shellfish immunology, 29(2), pp.319–326.

De Zoysa, M., Whang, I., Lee, Y., Lee, S., Lee, J., Lee, J., 2010b. Defensin from disk abalone *Haliotis discus discus*: molecular cloning, sequence characterization and immune response against bacterial infection. Fish & shellfish immunology, 28, pp.261–266.

De Zoysa, M., Nikapitiya, C., Lee, Y., Lee, S., Oh, C., Whang, I., Yeo, S., Choi, C.Y., Lee, J., 2010c. First molluscan transcription factor activator protein-1 (Ap-1) member from disk abalone and its expression profiling against immune challenge and tissue injury. Fish & shellfish immunology, 29(6), pp.1028–36.

De Zoysa, M., Nikapitiya, C., Oh, C., Wang, I., Lee, J., Jung, S., Choi, C.Y., Lee, J., 2010d. Molecular evidence for the existence of lipopolysaccharide-induced TNF-alpha factor (LITAF) and Rel/NF-kB pathways in disk abalone (*Haliotis discus discus*). Fish & shellfish immunology, 28(5-6), pp.754–63.

De Zoysa, M. Nikapitiya, C., Oh, C., Whang, I., Shin, H. & Lee, J., 2012. cDNA microarray analysis of disk abalone genes in gills and hemocytes after viral hemorrhagic septicemia virus (VHSV) challenge. Fish & shellfish immunology, 32(6), pp.1205–15.

De Zoysa, M., Nikapitiya, C., Oh, C., Lee, Y., Whang, I., Lee, J.S., Choi, C.Y., Lee, J., 2011a. Microarray analysis of gene expression in disk abalone *Haliotis discus discus* after bacterial challenge. Fish and Shellfish Immunology, 30(2), pp.661–673.

De Zoysa, M., Whang, I., Nikapitiya, C., Oh, C., Choi, C. Y., Lee, J., 2011b. Transcriptional analysis of disk abalone (*Haliotis discus discus*) antioxidant enzymes against marine bacteria and virus challenge. Fish & shellfish immunology, 31(1), pp.155–60.

De Zoysa, M., Pushpamali, W.A., Oh, C., Whang, I., Kim, S.J., Lee, J., 2008. Transcriptional up-regulation of disk abalone selenium dependent glutathione peroxidase by H_2O_2 oxidative stress and *Vibrio alginolyticus* bacterial infection. Fish & shellfish immunology, 25(4), pp.446–57.